IDENTIFICATION AND CHARACTERIZATION OF BRN3A/BRN3B AS DLX HOMEOBOX GENE TRANSCRIPTIONAL TARGETS IN RETINAL DEVELOPMENT

by

Qi Zhang, B. Med

A Thesis submitted to the Faculty of Graduate Studies of

The University of Manitoba

in partial fulfilment of the requirements of the degree of

Doctor of Philosophy (Ph.D.)

Department of Human Anatomy and Cell Science

University of Manitoba

Winnipeg

Table of Contents

List of Figures

List of Tables

Acknowledgements

I finished this section on my way to Toronto, where I am going to start the first step of my new journey. The airplane cabin, 37,000 feet up in the air, is a good place for thinking, but not much else. Looking back, I feel grateful for those wonderful people who shared my laughter and frustration, and supported me along the road.

The first person I would like to thank is my supervisor, Dr. David Eisenstat. I am extremely lucky to have a supervisor like Dr. Eisenstat, a "physician plus scientist". He treated me like a family member, and fully supported me within and outside of the research field. He became my role model and inspired me to pursue an exciting, yet crazy, career as his. Now Dr. Eisenstat is going to start a new chapter in his career. I wish him all the best!

I also thank my advisory committee members, Dr. Jeffrey Wigle, Dr. Hugo Bergen and Dr. Jiming Kong, for their advice and insightful discussions on this project. My thanks also go to the Department of Human Anatomy & Cell Science and the Manitoba Institute of Cell Biology for the academic environment and to the CancerCare Manitoba Foundation and Manitoba Institute of Child Health/Children's Hospital Foundation for their financial support.

I appreciate the help provided by all the Eisenstat lab members. Special thanks go to Vanessa, my little sister, "retina" team-mate and editor. I thank Shunzhen and Mehdi for their technical support; Mario and Jamie, for shouting my name and keeping me alert beside my bench; and my "buddies", Trung and Yongyao, for their friendship within and outside of the lab.

Last but not least, I would like to thank my family. Without their support, this thesis would not exist. I would like to thank my wife, Yuanyuan, for her constant encouragement. Her love is the source of my strength. Wherever life leads me, I feel like home with her by my side. My son, Yifei, has the sweetest voice and smile in the world. They are the best gifts I could ever imagine. I thank my parents, Baoan and Jingmin. They probably couldn't read a single word from this thesis, but they have supported, and will always support me to pursue my dreams, no matter what and where my dreams are.

To my family, I dedicate this thesis.

Abstract

Introduction: The *Dlx1/Dlx2* double knockout mouse has reduced numbers (33% fewer) of retinal ganglion cells (RGC), due to enhanced apoptosis. *Brn3a* and *Brn3b* are closely related members of the Class IV POU-domain gene family, and play functionally interchangeable roles in retinal development. We hypothesized that *Brn3a* and/or *Brn3b* are direct DLX transcriptional targets during retinal development.

Methods: Chromatin immunoprecipitation (ChIP) assays were performed on E16.5 retinas to identify DLX proteins bound to the *Brn3a* or *Brn3b* promoters. Electrophoretic mobility shift assays (EMSA) were used to confirm the specificity of this binding. Luciferase reporter gene assays were performed to confirm the functional significance of DLX binding to the *Brn3 or Brn3ba* promoters *in vitro*. *In utero* retinal electroporation was used to study the effect of DLX gain-of-function on *Brn3a/Brn3b* expression *in vivo*. Compound *Dlx1/Dlx2/Brn3a* and *Dlx1/Dlx2/Brn3b* knockout mice were generated for analysis of retinal phenotypes.

Results: Both DLX1 and DLX2 proteins bound to the *Brn3b* promoter, but only DLX2 bound to the *Brn3a* promoter *in vivo*. Using EMSA, recombinant DLX1 and DLX2 bound to *Brn3b* and specific supershifted bands resulted from the addition of specific DLX1 or DLX2 antibodies; only recombinant DLX2 bound to *Brn3a* and the supershifted band resulted from the addition of DLX2 antibody. Both DLX1 and DLX2 binding to the *Brn3b* promoter activated transcription of a luciferase reporter gene *in vitro*. Only *Dlx2*, but not *Dlx1*, co-transfection with *Brn3a* activated luciferase

reporter gene expression. *In utero* retinal electroporation showed that ectopic DLX2 expression promoted both *Brn3b* and *Brn3a* expression *in vivo*. Loss of *Dlx1/Dlx2* and *Brn3b* resulted in loss of 90% of RGC and increased cholinergic amacrine cell differentiation.

Conclusion: *Brn3b* is transcriptionally regulated by both DLX1 and DLX2, whereas *Brn3a* is only regulated by DLX2 *in vitro* and *in vivo*. *Dlx1/Dlx2* and *Brn3b* play combinatorial roles in retinogenesis.

List of Abbreviations

bHLH	Basic Helix-Loop-Helix
BrdU	5-bromo 2'-deoxyuridine
ChAT	Choline Acetyl Transferase
ChIP	Chromatin Immunoprecipitation
CNS	Central Nervous System
DLL	Distal-less
Dlx	Dlx gene
DLX	Dlx protein
DNA	Deoxyribonucleic Acid
E	Embryonic Day
EMSA	Electrophoretic Mobility Shift Assays
FITC	Fluorescein Isothiocyanate
IF	Immunofluorescence
IHC	Immunohistochemistry
IPL	Inner Plexiform Layer
ISH	In Situ Hybridization
GABA	Gamma-Aminobutyric Acid
GAD	Glutamic Acid Decarboxylase
GCL	Ganglion Cell Layer
gDNA	Genomic Deoxyribonucleic Acid

GFAP	Glial Fibrillary Acidic Protein
GFP	Green Fluorescent Protein
H&E	Hematoxylin and Eosin
kDa	Kilo Dalton
LGE	Lateral Ganglionic Eminence
MGE	Medial Ganglionic Eminence
mRNA	Messenger Ribonucleic Acid
NBL	Neuroblastic layer
ONL	Outer Nuclear Layer
OPL	Outer Plexiform Layer
OR	Ocular Retardation
P	Postnatal Day
PBS	Phosphate Buffered Saline
PFA	Paraformaldehyde
PKC	Protein Kinase C
PNA	Peanut Agglutinin
POU	Pit-Oct-Unc Domain
PL	Photoreceptor Layer
RGC	Retinal Ganglion Cell
RNA	Ribonucleic Acid
RPC	Retinal Progenitor Cell
RPE	Retinal Pigment Epithelium

SC Superior Colliculus

SHH Sonic Hedgehog

TH Tyrosine Hydroxylase

TR Texas Red

TUNEL Terminal Deoxynucleotidyl Transferase Biotin-dUTP Nick End Labeling

μM Micrometer

WT Wild Type

Chapter 1: Introduction

1.1 General introduction: Visual system

An ancient proverb says that “the eyes are the windows to the soul”. From the biological point of view, however, the eye functions as a sophisticated optic device to catch and focus light onto the neural retina. Composed of specialized sensory neurons, the retina is an extension of the central nervous system (CNS), which lines the back of the eye. Through a process known as phototransduction, the retina converts light energy into a neural signal, and relays this signal to the brain via the optic nerve. These retinal inputs are processed by different central visual pathways, and serve various purposes such as one’s visual experience and control of eye movement, pupil size and circadian rhythm (Sung and Chuang 2010).

1.1.1 Retinal anatomy

Compared to other CNS tissues (although derived from the same neural tube origin), the neural retina is relatively simple in terms of both structure and cell diversity. Composed of seven major types of cells, the retina is organized as a laminated structure. The retinal neurons are located in three anatomically distinctive layers: the ganglion cell layer (GCL), inner nuclear layer (INL) and outer nuclear layer (ONL). These three cellular layers are separated by an inner plexiform layer (IPL) and an outer plexiform layer (OPL), which are composed of neural processes and synaptic contacts (Fig. 1). Two types of photoreceptor cells, cones and rods, have

their cell bodies located in the ONL, with their outer segments immediately adjacent to the retinal pigment epithelial layer (RPE). The photoreceptor cell outer segments contain photopigments, and serve as the light detector. This arrangement, therefore, makes it necessary for the light to travel through the entire transparent retina before the photons are detected. The INL contains the cell bodies of three types of interneurons: bipolar cells, amacrine cells and horizontal cells. These interneurons, excitatory or inhibitory, contact other neurons and participate in both the vertical and lateral visual pathways. The synapses formed by photoreceptors and bipolar or horizontal cells take place in the OPL, whereas the synapses between retina ganglion cells (RGC) and bipolar or amacrine cells occur in the IPL. The innermost cellular layer of retina is the GCL, which is comprised of mainly retinal ganglion and displaced amacrine cells. The RGC axons gather at the central optic disc, and exit the eye as the optic nerve (Purves and Williams 2001).

Fig. 1

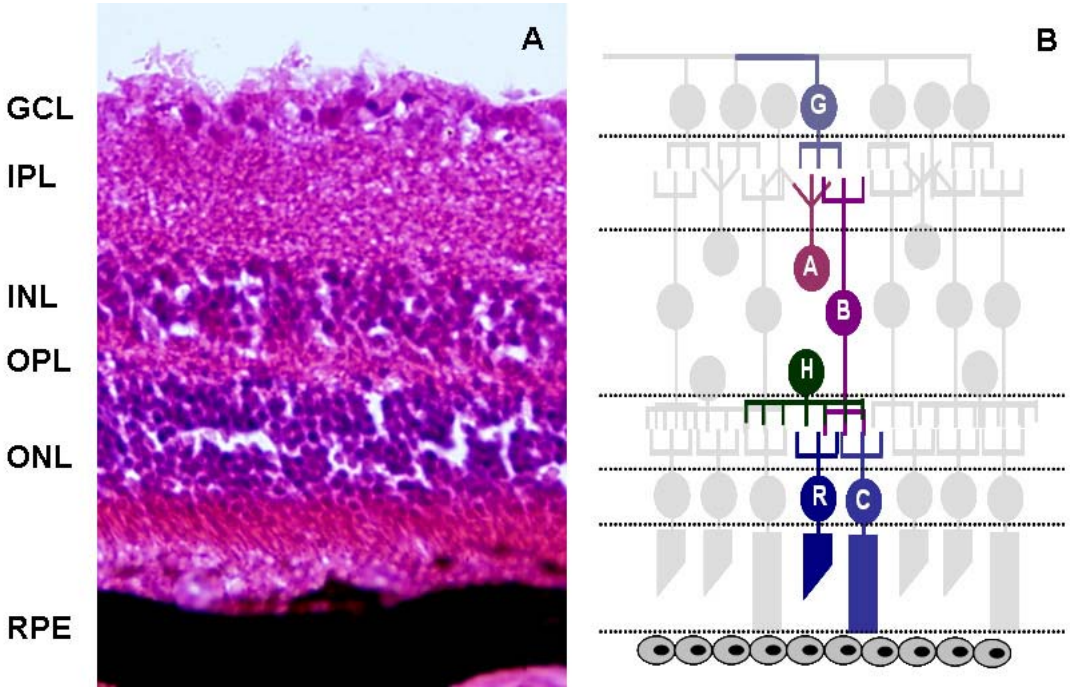

Fig. 1 The retina is organized as a laminated structure. (A) H&E staining of the adult mouse retina. Nuclei of retinal cells are positioned in three distinct layers: GCL, INL and ONL. (B) The cell bodies of retinal ganglion cells and displaced amacrine cells are located in the GCL. Three interneurons, amacrine, bipolar and horizontal cells, are positioned in the INL. Two photoreceptor cells, rods and cones, form the ONL, the outer segments of which are directly adjacent to the RPE. The ganglion cells and amacrine, bipolar cells form synapses in IPL, whereas the photoreceptor cells and horizontal, bipolar cells form synapses in OPL. GCL, ganglion cell layer; IPL, inner plexiform layer; INL, inner nuclear layer; OPL, outer plexiform layer; ONL, outer nuclear layer; RPE, retinal pigment epithelium; A, amacrine; B, bipolar; C, cone; G, ganglion cell; H, horizontal. R, rod.

1.1.2 Photoreceptor cells: cone and rod

Visual perception begins with the photoreceptor cells, where the photon is captured and a phototransduction cascade is initiated. This process occurs in the outer segments of the photoreceptor cells. Based on their distinct structure, the photoreceptor cells are divided into two groups, rods and cones. These two classes of cells contain different types of photopigment molecules, synapse with different interneurons, and are specialized for different types of visual perceptions. The rod photoreceptor cells are very sensitive to light and they mediate vision in dark or dim light. In contrast, cones are less sensitive to light, but are specialized to mediate color vision in bright light with high resolution. There is only one kind of rod photoreceptor cell type in humans, which represents more than 80% of all retinal cells (~124 million in human) (Sung and Chuang 2010). Rods are distributed throughout the ONL, except in the human fovea. The fovea, composed solely of cone photoreceptor cells, is a specialized retinal region that provides the highest visual acuity. Using different photopigment molecules, rods and cones share a very similar phototransduction process. The photopigment in rods is rhodopsin. When a light photon is absorbed by rhodopsin, a series of configurational changes leads to activation of cGMP-mediated intracellular signals. As a result, the cation channels in the outer segments close, the photoreceptor cell membrane hyperpolarizes and the synaptic terminal decreases the release of neurotransmitters (Purves and Williams 2001). This process is different from the depolarization found in most sensory systems' activation. In contrast to rods, there are three different photopigments that function in the three subsets of cones:

blue, green and red cone opsins.

1.1.3 Interneurons: bipolar, horizontal, and amacrine cells

Bipolar cells form synaptic contacts with both photoreceptors and retinal ganglion cells. Through bipolar cells, the photoreceptor cells transmit signals to ganglion cells, which in turn relay this information to the brain. However, the synapses are formed in distinct ways to serve different visual perceptions. For example, in order to maintain the higher resolution of the cone photoreceptor system, each bipolar cell synapses with a single cone in the fovea. This cone-bipolar cell, in turn, connects with one ganglion cell. On the other hand, the rod system is more convergent. One bipolar cell may form synapses with many rods and collect information from those cells. Many rod-bipolar cells will then converge on a single RGC. This arrangement reduces the acuity and resolution of the rod photoreceptor system, but increases the sensitivity to light (Masland 2001; Purves and Williams 2001) . Depending on their response to light stimuli, bipolar cells are further divided into two groups, *on* and *off* bipolar cells, which are depolarized or hyperpolarized by light, respectively. These opposite effects are mediated by their opposite responses to glutamate, the excitatory neurotransmitter released by photoreceptors.

In addition to the vertical pathway formed by the photoreceptor-bipolar-ganglion cell interaction, there are two major lateral pathways modulating retinal activities that are mediated by horizontal and amacrine cells, respectively. Horizontal cells are a small retinal cell population (less than 5% of the

total retinal cells), and only one type of horizontal cell has been identified in the mouse retina. Functioning as inhibitory GABAergic interneurons, most horizontal cells are positioned in the outer INL. Horizontal cells form synaptic contacts with both photoreceptors and bipolar cells, resulting in a complex three-way interaction. It is well accepted that horizontal cells antagonize the signalling between photoreceptors and bipolar cells, through a "center-surround" organization. By directly regulating the neurotransmitter release from photoreceptor terminals to bipolar cells, horizontal circuitry induces opposite light responses between central and surrounding visual pathways, and thus enhances the visual contrast (Masland 2001; Purves and Williams 2001).

The second group of lateral interneurons, amacrine cells, are a much more diverse cell population. There are more than 30 morphologically distinct amacrine subtypes identified so far in the mouse (MacNeil and Masland 1998; Voinescu, Kay et al. 2009). Most of these amacrine cells use GABA or glycine as neurotransmitters. GABAergic and glycinergic amacrine cells are the two major types, representing almost 90% of the total amacrine population. About 8% of amacrine cells are cholinergic interneurons, the majority of which are positioned in the inner INL or GCL. Amacrine cells mainly form synapses with RGC, as well as bipolar cells. The amacrine cells' processes and synapses are located in the IPL. One single amacrine cell can contact multiple ganglion cells, and synchronize their responses to light stimuli (Masland 2001). It is believed that the distinct subtypes of amacrine cells are specialized for their own functions, but few details are known.

1.1.4 Retinal output: retinal ganglion cells

Retinal ganglion cells (RGC) are the only projection or output neurons of the retina. Located in the GCL, RGC receive inputs from bipolar cells. RGC transmit visual information to the brain via their axons, which travel within the optic nerve. A complex computational circuit formed by amacrine cells shapes ganglion cells' light responses. All RGC axons exit the retina through the optic disc, a specialized region in the central retina. The optic disc is considered to be the "blind spot" in the retina due to the lack of photoreceptor cells. The routing of RGC axons is a well regulated and complex process. Different RGC project their axons to different regions of the brain in a very precise manner. This will be described in the following sections.

More than ten classes of RGC can be distinguished by their structure and electrophysiology. The most numerous and most studied types are the *P* ganglion cells and *M* ganglion cells in the monkey retina, which are analogous to the *beta* and *alpha* ganglion cells in the cat retina, respectively. The *P* and *M* ganglion cells are responsible for two parallel visual pathways. *P* cells project their axons to the *parvovcellular layers* located in the dorsal Lateral Geniculate Nucleus (LGN), and are sensitive to colour stimuli. *M* cells are more sensitive to black-white stimuli, and project their axons to the two ventral LGN layers, the *magnaocellular layers*. This difference is explained by the fact that *P* and *M* cells receive visual inputs from different photoreceptor cells (Purves and Williams 2001)

1.2 Development of the visual system

The retina has served as an excellent model to study the development of the CNS. Intensive studies have been performed to improve our understanding of this process. After the specialized eye region is established during organogenesis, a series of developmental events occur, including optic vesicle formation, retinogenesis and axonal pathfinding. These events are precisely regulated by both intrinsic and extrinsic signals.

1.2.1 Early eye formation: optic vesicle and optic cup

The neural retina has long been considered as an accessible part of the brain. Developmentally, like other regions of the CNS, the retina derives from the neural tube. The first morphological sign of the mouse eye is appreciated by embryonic day (E) 8, when the ventral region of the developing forebrain evaginates and forms the optic vesicles. The retinal homeodomain transcription factor *Rx* is essential for this process (Mathers, Grinberg et al. 1997). By expressing patterning genes, the nascent optic vesicle is further divided into the distal-dorsal and proximal-ventral regions, which show distinct developmental potency. The distal portion of the optic vesicle continues to grow and contacts the presumptive lens ectoderm, resulting in the invagination of the lens placode and optic vesicle. A double-layered optic cup is then formed. The inner layer of the optic cup gives rise to the neural retina, while the outer layer develops into the retinal pigment epithelium (RPE). The proximal portion of the optic vesicle becomes the optic fissure, which eventually fuses at the ventral midline.

The coordinated regulation of extrinsic cues and intrinsic signals, which include homeodomain and bHLH transcription factors, controls neural retinal patterning and maintenance. The LIM homeodomain transcription factor *Lhx2* was identified as the early patterning gene in the eye, and is required to initiate retinal and RPE specific gene expression, including *Vsx2/Chx10* and *Mitf*, respectively (Yun, Saijoh et al. 2009). Bone morphogenic protein (BMP) is important for the early steps of retinal development. BMP signalling induces and maintains retinal gene expression in the distal optic vesicle. Deletion of *Bmp7* in the mouse leads to anophthalmia, aplasia of the optic nerve, down-regulated retinal genes, and up-regulated RPE genes including *Mitf* (Morcillo, Martinez-Morales et al. 2006). Mediated by *Vsx2*, the fibroblast growth factor (FGF) signalling pathway also participates in neural retina development (Horsford, Nguyen et al. 2005). Inactivation of FGF signalling at the early optic vesicle stage inhibits *Vsx2* expression and neural retina development in the mouse (Cai, Feng et al. 2010). Conversely, mis-expression of FGF promotes RPE transdifferentiation into fully differentiated retina (Fuhrmann 2010).

1.2.2 Retinal progenitor cells: proliferation and differentiation

The neural retina is initially organized as a single layer of neuroblastic cells, which give rise to multi-potential retinal progenitor cells (RPC), and eventually differentiate into a variety of retinal neurons and Müller glia. During early retinal development, the RPCs expand the pool of progenitors by symmetrical division. This mitotic cell division occurs at the apical retina, and the resulting daughter cells

migrate toward the basal retina. The presence of mitogens and G1 phase proteins is essential for RPCs to continue progressing through the cell cycle. In early G1 phase, the mitogens for RPC progression into the G1 phase include but are not limited to: FGF, epidermal growth factor (EGF) and Hedgehog. Retinoblastoma proteins, Cyclin D1 (CycD1), $p27^{Kip1}$ and $p57^{Kip2}$ are also key regulators for RPCs in G1 phase progression. Disruptions in the expression of these proteins results in defects in RPC proliferation and retinal dysplasia (Levine and Green 2004). Interestingly, $p27^{Kip1}$ and $p57^{Kip2}$ are both expressed by the RPCs in their last cell cycle and also required for appropriate cell cycle exit (Dyer and Cepko 2001). Many transcription factors, especially homeodomain transcription factors including *Pax6* and *Chx10*, play important roles in maintaining the proliferative ability of the RPCs.

At later developmental stages, RPCs start exiting the cell cycle and differentiating into a variety of retinal cell types. The neural retina is then transformed from one layer of RPCs into a laminated multi-layered retina with various cell types. Birth-dating studies among different species show a well conserved timetable of retinogenesis. In the mouse, retinogenesis starts at E10, and finishes at postnatal (P) day 11 (Cepko 1999; Marquardt and Gruss 2002; Harada, Harada et al. 2007; Reese 2011). Among all the retinal cells, RGC are first generated at E11, followed by amacrine cells, horizontal cells and cone photoreceptor cells. With largely overlapping birthdates, the majority of these cells are produced during the embryonic period in the mouse. Although the cone photoreceptors are generated by birth, their outer segments are not fully differentiated until postnatal day 11. Differentiation of rod photoreceptor,

bipolar cells and Müller glia starts in late embryonic stages, but finishes by P14 (Fig. 2). A similar temporal order is followed in human retinogenesis. However, the human retina is fully developed by the 30th gestational week (Fig. 2).

Fig. 2

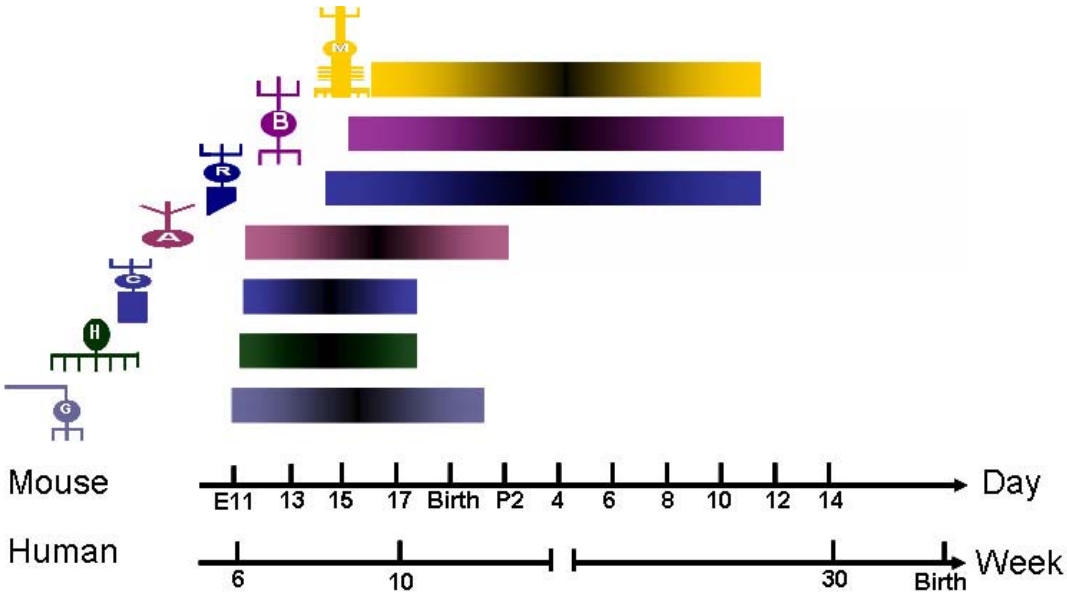
M
B
R
A
C
H
G
Mouse
E11
13
15
17
Birth
P2
4
6
8
10
12
14
Day
Human
6
10
30
Birth
Week

Fig. 2 Retinogenesis follows a conserved temporal order. By E11 in the mouse, the first population of retinal ganglion cells are differentiated, followed by horizontal, amacrine and cone cells. Rod, bipolar and Müller glia cells are among the late born retinal cells. In the mouse, retinogenesis is completed at postnatal day 14. In humans, however, by the 30th gestational week, all the retinal cells are differentiated.

1.2.3 Intrinsic regulation of retinogenesis: overview

A number of transcription factors, including homeodomain and bHLH factors, have been shown to play important roles in retinogenesis. These factors are expressed by subsets of RPCs, post-mitotic precursors, and differentiated retinal neurons during a particular developmental stage. They act to regulate cell fate commitment, neuronal or glial, terminal differentiation and survival. Many gain-of-function and loss-of-function studies on these genes have been performed in mice, chick and other model systems. Altering the function of these genes result in striking retinal phenotypes, varying from lack of specific cell types, cell fate switch, failure to differentiate, to increased cell death. The function of some of these genes will be described in detail in the following sections. Many mutations of these genes have been identified in inherited or congenital human eye disorders.

1.2.4 *Pax6/Pax2*

For more than a decade, *Pax6* has been considered as the "master control gene" in retinogenesis (Gehring and Ikeo 1999). *Pax6* belongs to the *Pax* gene family, with nine family members identified in human and mouse to date. *Pax* genes are characterized by the presence of two conserved motifs, the paired-box and the homeobox, which encode two DNA binding domains, the paired-domain (PD) and the homeodomain (HD) respectively. The homeodomain in all PAX proteins contains a crucial residue, S_{50}, which specifies the HD DNA sequence recognition (Wilson, Guenther et al. 1995). Although both the PD and HD are important for PAX6 function,

it has been shown that the PD is more important for regulating retinogenesis (Punzo, Kurata et al. 2001). The exact functions of these two DNA binding domains await further elucidation.

In the mouse eye, *Pax6* expression is first detected at E8, in the lens, neural retina and RPE. All mitotic RPCs express *Pax6* during retinogenesis. Together with *Sox2, Chx10* and other early retinal TFs, *Pax6* maintains the proliferative status of RPCs. Without the function of *Pax6*, the optic vesicle fails to complete its formation in both mouse and *Drosophila*, thereby leading to the absence of retina and other eye structures (Hill, Favor et al. 1991; Quiring, Walldorf et al. 1994). However, conditional inactivation of *Pax6* after the optic vesicle forms shows decreased RPC mitotic activity, but retinal identity is well maintained. The *Pax6* null RPC displays limited differentiation potential and the mutant retina consists mainly of amacrine interneurons at the expense of other cell types (Marquardt, Ashery-Padan et al. 2001). These results suggest a dual temporal role of *Pax6* in RPC differentiation. The dosage of the *Pax6* gene is also important for eye development. Both under-expression ($Pax6^{Sey/+}$) and over-expression ($PAX77^{+/+}$) of the *Pax6* gene caused a similar eye defect, microphthalmia, although the underlying mechanisms are different. Compared to the lens formation defects found in $Pax6^{Sey/+}$ heterozygotes, extra copies of *Pax6* in mice lead to impaired retinal development at later embryonic stages and severe postnatal retinal degeneration (Manuel, Pratt et al. 2008). Mis-expression of *Pax6* is able to induce ectopic eyes in both vertebrates and *Drosophila* (Chow, Altmann et al. 1999; Zuber, Gestri et al. 2003). A recent study has shown that *Pax6* has different

roles on distinct populations of RPCs located at different retinal regions. In the peripheral retina, *Pax6* inhibits *Crx* expression and is required for neurogenesis; in the central retina, however, *Pax6* is required to maintain the multipotency of RPCs but is dispensable in neurogenesis (Oron-Karni, Farhy et al. 2008). In addition to its function in retinogenesis, *Pax6* is also required for lens development.

Pax2 is the second *Pax* gene family member expressed in the developing eye. *Pax2* expression starts as early as E7.5 and is restricted to the ventral part of the optic vesicle. Shortly after E10, retinal *Pax2* expression is repressed by *Pax6* and *Pax2* expression is limited to the optic stalk, with only minimal overlap with *Pax6* expression in the neural retina. The expression pattern of *Pax2* defines its function in the formation of optic stalk and optic nerve pathfinding (Torres, Gomez-Pardo et al. 1996; Schwarz, Cecconi et al. 2000). PAX2 has a paried domain, but in contrast to PAX6, lacks a homeodomain.

1.2.5 *Rx*

The Retinal homeobox gene (*Rx*) is one of the earliest genes expressed in the optic vesicle and later in the retina. *Rx* expression initiates neuroepithelial evagination in the ventral forebrain, leading to optic vesicle formation. In addition, *Rx* expression induces a network of early retinal genes, including *Pax6*, *Six3* and *Lhx2*, which are responsible for the formation of the optic cup and maintaining the RPCs. As a paired-like homeobox gene, *Rx* has a well conserved gene structure and expression pattern in vertebrate and invertebrate species, including *Xenopus*, mouse and human

(Mathers, Grinberg et al. 1997; Bailey, El-Hodiri et al. 2004). In contrast to the dominant function of the PD in PAX6 during retinogenesis, the HD in RX protein is more important in eye development. Evidence for this role is found in both zebrafish and humans. A mutation in the homeobox motif of the *Rx* gene has no HD in the truncated RX protein, leading to the zebrafish mutation *chokh*, which lacks eye structures (Loosli, Staub et al. 2003). In humans, mutations in the human RX HD causes anophthalmia and sclerocornea (Voronina, Kozhemyakina et al. 2004).

In the mouse, *Rx* expression is first detected in the anterior neural plate at E7.5. After the optic cup is formed at E10, *Rx* is mainly expressed in the retina and ventral forebrain. The dynamic expression of *Rx* in neural retina varies with the extent of retinal development: at E15.5, *Rx* is uniformly expressed in the entire neuroretina; at later embryonic stages this expression is reduced along with the differentiation of RGCs; at postnatal day 6.5, *Rx* is confined to the ONL and INL (Mathers, Grinberg et al. 1997). This expression pattern is also present in the *Xenopus* and chick.

Although *Rx* is not required for the initial activation of *Pax6* in the eye, *Rx* is essential to upregulate and to maintain *Pax6* expression in RPCs. It is believed that *Pax6* is a transcriptional downstream target of *Rx*. In the $Rx^{-/-}$ retina, no *Pax6* expression is detected; on the other hand, *Rx* expression is not significantly changed in the $Pax6^{-/-}$ retina (Mathers, Grinberg et al. 1997; Zhang, Mathers et al. 2000). Not surprisingly, the *Rx* null mouse shows a more severe eye phenotype than the $Pax6^{-/-}$ mutants as *Rx* function is essential for optic vesicle formation, which is the initial stage for eye development.

In addition to their critical role in early eye formation, the *Rx* genes have also been shown to regulate photoreceptor gene expression and photoreceptor cell differentiation. In combination with *Crx* and other TFs, RX binds to the photoreceptor conserved element (PCE-1) and activates the rhodopsin and red cone opsin promoters (Nelson, Park et al. 2009; Pan, Martinez-De Luna et al. 2010).

1.2.6 *Crx and Otx2*

Otx2 and *Crx* are the mammalian orthologs of *Drosophila* orthodenticle (*Otd*), which is a paired homeodomain protein required for the development of anterior brain structures and the eye. The homeodomain of these two proteins has a lysine residue at position 50 (K50), which is critical for DNA binding specificity (Furukawa, Morrow et al. 1997; Hennig, Peng et al. 2008). Both *Otx2* and *Crx* play important roles in the development and maintenance of retinal photoreceptor cells. The homeodomain in these proteins is critical to their function as shown by mutations generated or observed in mouse and humans, respectively.

Evidence shows that *Otx2* is located upstream of *Crx* in the transcriptional regulation network. *Otx2* expression precedes *Crx* in the developing retina. In the mouse, retinal *Otx2* expression is initiated at E11.5, and is increased at E12.5 when *Crx* expression is first detected in the neural retina. At E17.5, *Otx2* expression is dramatically increased in the outer neuroblastic layer (NBL), where *Crx* is expressed robustly and overlaps with *Otx2*. In the absence of *Otx2*, *Crx* expression is almost completely abolished in the retina, as shown in the *Otx2* conditional knockout mouse

model (Nishida, Furukawa et al. 2003). OTX2 regulates *Crx* expression by directly binding to the promoter region and enhancing its promoter activity (Hennig, Peng et al. 2008). In addition, as shown by BrdU incorporation assays, *Crx* expressing cells are generated from *Otx2*-expressing progenitors (Garelli, Rotstein et al. 2006).

Otx2 and *Crx* play redundant but distinct roles in photoreceptor development. *Otx2* is responsible for photoreceptor cell fate commitment, whereas *Crx* regulates photoreceptor terminal differentiation. *Otx2* is expressed in retinal progenitor cells during their final cell cycle, and directs them to a photoreceptor cell fate (Swaroop, Kim et al. 2010). Since the homozygous *Otx2* knock-out mouse is embryonically lethal and lacks rostral brain structures, it becomes difficult to study photoreceptor development using this animal model. A retinal specific *Otx2* conditional knockout mouse was generated and by using this model it was shown that without the *Otx2* transcript, the retinal progenitors switched cell fates from photoreceptors to an amacrine-like cell fate, with the resulting retina missing almost all cone and rod photoreceptor cells. In addition, the loss of bipolar and horizontal cells in the *Otx2* null retina suggests multiple roles of *Otx2* in retinal development (Nishida, Furukawa et al. 2003). On the other hand, *Crx* expressing cells are primarily post-mitotic photoreceptor precursors, with much restricted competence. *Crx* seems to be dispensable in photoreceptor fate commitment, but it is essential for final differentiation and maturation. The *Crx* deficient mouse retina is able to generate both rod and cone photoreceptors, which are comparable to those found in wild-type retinas. However the *Crx* null photoreceptors fail to develop outer segments and

therefore have no detectable phototransduction function (Furukawa, Morrow et al. 1999). *Crx* performs this function by directly binding to the promoter regions of its target photoreceptor genes, and activates their transcription (Peng and Chen 2005). However, the specification of photoreceptor subtypes requires interaction of *Crx* with other TFs and nuclear receptors, including neural retina leucine zipper protein (NRL), NR2E3, RORβ and TRβ2 (Hennig, Peng et al. 2008).

The gene dosage of *Otx2* and *Crx* also play a role in retinal development. *Otx2*$^{+/-}$ mice have multiple eye developmental defects, which varies from microphthalmia, lack of lens to a hyperplastic retina. Heterozygous *Crx* mutant mouse have delayed photoreceptor function development. Over-expression of either *Otx2* or *Crx* alone is sufficient to induce rod photoreceptor differentiation, at the cost of amacrine and Müller glia cells. Compared to *Otx2*, *Crx* over-expression is less potent and does not affect bipolar cells (Furukawa, Morrow et al. 1997; Nishida, Furukawa et al. 2003).

Many human *CRX* or *OTX2* mutations have been identified, the majority of which are located in the homeodomain and therefore alter DNA binding ability. Disorders related to these mutations include autosomal-dominant cone-rod dystrophy, autosomal-dominant retinitis pigmentosa and Leber's congenital amaurosis (Hennig, Peng et al. 2008).

1.2.7 *Chx10*/*Vsx2* and *Vsx1*

Like *Pax6* and *Crx*, *Chx10* is another example of the paired-like homeodomain

(Prd-L HD) transcription factor, which plays major roles in eye development. In addition to the paired homeodomain, CHX10 protein is distinguished by containing one additional conserved region, the CVC domain. This 54-amino acid CVC domain is located immediately adjacent to the C-terminus of the HD, and is named after the identification of ***C****hx10* and three other genes, ***V****sx1/Vsx2* and ***C****eh-10*, which are *Chx10* homologues in goldfish and *C. elegans*, respectively (Levine, Hitchcock et al. 1994; Liu, Chen et al. 1994). Although the function of this CVC domain is not clear, it is reported that the HD and CVC domain are the minimal requirements for *Chx10* to act as a repressor (Dorval, Bobechko et al. 2005). The Prd-L HD:CVC protein can be further classified into two groups, depending on the presence of either the RV region, which is exclusive to *Vsx1* group, or the OAR region specific for *Vsx2* group. *Chx10* and *Ceh-10* belong to the *Vsx2* group, which is highly conserved during evolution. The *Vsx1* group, however, is evolving rapidly. The mouse *Vsx1* and human *VSX1* are only 71% identical overall (Chow, Snow et al. 2001).

Chx10 is expressed in the interneurons of retina, hindbrain and spinal cord. *Chx10* expression in the developing retina is initiated in RPCs by E9.5 (Liu, Chen et al. 1994). It is believed that during optic cup formation, the contact between the optic vesicle and the presumptive lens ectoderm induces *Chx10* expression (Nguyen and Arnheiter 2000). *Chx10* expression is downregulated when the RPCs exit the cell cycle and differentiate (Green, Stubbs et al. 2003). In later retinal development and mature retinas, *Chx10* expression is restricted to the inner nuclear layer, where *Chx10* is particularly expressed in bipolar interneurons and a subset of Müller glia (Liu, Chen

et al. 1994; Rowan and Cepko 2004).

Consistent with the expression pattern, *Chx10* mutant mice show two major phenotypes: defects in RPC proliferation and in bipolar cell differentiation. Ocular retardation (or^J) mice carry a spontaneous mutation with a premature stop codon at the midpoint of *Chx10*, and therefore no CHX10 protein is detected in the $Chx10^{orJ}$ homozygous ($Chx10^{orJ/orJ}$) retina. One notable phenotype observed in the $Chx10^{orJ/orJ}$ retina is the significant reduction of RPC proliferation (up to 83% loss of BrdU incorporation in RPC in the peripheral retina). Studies on the *Chx10* BAC reporter mouse have linked the reduction of RPC proliferation to a retinal pigment epithelium trans-differentiation, with increased expression of *Mitf*, a gene associated with onset and maintenance of pigmentation (Rowan, Chen et al. 2004). A second mechanism involved in the severe RPC loss in $Chx10^{orJ/orJ}$ retina is mediated by cyclin D1. The absence of CHX10 de-represses Kip1, which functions as a negative regulator of cell proliferation in retina (Green, Stubbs et al. 2003). Genetic deletion of *Kip1* on a *Chx10* null background is able to partially rescue RPC proliferation. The second striking phenotype of the $Chx10^{orJ/orJ}$ retina is the complete loss of bipolar cells. Bipolar cells are a late-differentiated population, the majority of which are differentiated postnatally. Despite a near absence of RPCs in the $Chx10^{orJ/orJ}$ retina postnatally, bipolar cell loss is more likely due to the failure of a direct role for *Chx10* in bipolar cell genesis. This idea is supported by the observation that no bipolar cells are detected in the $Chx10^{orJ/orJ}$:$Kip^{-/-}$ retina, in which the progenitor cell numbers are partially increased (Green, Stubbs et al. 2003). In addition, shRNA knockdown of

Chx10 in postnatal retinas dramatically reduces bipolar cell numbers, without influencing RPC proliferation (Livne-Bar, Pacal et al. 2006). It is reported that *Chx10* promotes bipolar cell genesis by repressing photoreceptor gene expression (Dorval, Bobechko et al. 2005). Other phenotypes observed as a result of *Chx10* mutations include microphthalmia in both human and mice, and lack of optic nerves (Burmeister, Novak et al. 1996; Ferda Percin, Ploder et al. 2000).

In contrast to the early embryonic expression of *Chx10/Vsx2* in RPCs, *Vsx1* expression is predominant in the postnatal retina. *In situ* hybridization and *Vsx1*-targeting reporter studies revealed that *Vsx1* expression is initiated within the INL at P5, but not at any earlier stage (Chow, Snow et al. 2001; Chow, Volgyi et al. 2004). By P12, *Vsx1* expression is restricted to the outer layer of the INL, where it is expressed in a subset of cone bipolar cells, but not rod bipolar, amacrine, horizontal neurons or Müller glia (Chow, Snow et al. 2001). Absence of *Vsx1* function in the mouse retina leads to incomplete terminal differentiation of off-cone bipolar cells, and associated defects in retinal function (Chow, Volgyi et al. 2004). However, overall bipolar cell fate specification is not altered, since the expression of pan-bipolar markers *Chx10* and *Ret-B1* continue in the INL of *Vsx1*$^{-/-}$ retinas. No microphthalmia is observed in *Vsx1* mutant mice.

A recent study revealed the regulatory interaction between *Chx10/Vsx2* and *Vsx1*; by binding to an intergenic regulatory element, CHX10 represses *Vsx1* expression in mice and zebrafish (Clark, Yun et al. 2008). *Chx10* expression, however, is normal in *Vsx1* null retinas.

1.2.8 *Prox1*

Prox1, the mouse homologue of *Drosophila* HD gene *prospero*, is expressed in many developing tissues, including the CNS, retina, lens, pancreas, liver, heart and cardinal vein (Oliver, Sosa-Pineda et al. 1993; Wigle, Chowdhury et al. 1999; Dyer, Livesey et al. 2003; Boije, Edqvist et al. 2009). In the developing retina, *Prox1* is expressed by differentiating horizontal and amacrine cells. Without the function of *Prox1*, the retina fails to generate horizontal cells, but produces more late-born cells including rod photoreceptors and Müller glia. In addition, *Prox1*$^{-/-}$ retinal progenitors show defects in exiting the cell cycle (Dyer, Livesey et al. 2003). On the other hand, misexpression of *Prox1* increases horizontal cell production, at the expense of the rods and Müller glia. Evidence shows that *Prox1* is located downstream of *Foxn4* and *Ptf1a*. Both *Foxn4* and *Ptf1a* are expressed prior to *Prox1*, and *Foxn4* and *Ptf1a* expression are essential to initiate *Prox1* expression. There is no *Prox1* expression detected in the retinas of either *Foxn4* or *Ptf1a* null mutant mice (Li, Mo et al. 2004; Fujitani, Fujitani et al. 2006).

1.2.9 *Brn-3* genes

The identification of three mammalian homeodomain coding genes, ***P****it1*, ***O****ct1/Oct2*, and one similar *C. elegans* gene ***U****nc-86* led to the name of a new regulatory gene family, which encodes POU-domain transcription factors. The POU-domain is a bipartite DNA-binding protein domain, which contains a

POU-specific region and a POU-homeodomain region. The class IV POU-domain proteins, BRN3a, BRN3b and BRN3c (*POU4f1*, *POU4f2* and *POU4f3*, respectively) are the homologs of *Unc-86* in C. elegans. *Brn-3* genes are expressed in the embryonic and adult CNS, and are required for sensorineural development and survival.

All three *Brn-3* POU-homeodomain genes are expressed in the developing retina, specifically in postmitotic RGCs (Xiang, Zhou et al. 1995). *Brn3b* expression is first detected in the earliest RGCs at E11.5 in the central inner mouse retina, followed by *Brn3a* and *Brn3c* expression two days later (Xiang, Zhou et al. 1995; Pan, Yang et al. 2005). From E15.5 to adulthood, *Brn3a* and *Brn3b* expression overlaps in 80% of RGCs, which are localized into the GCL. Although these two genes share a similar global expression pattern, their expression patterns are distinct at the cellular level, especially in postnatal stages. *Brn3a* is the predominant factor in P5 retinas, with few RGCs strongly expressing *Brn3b* (Quina, Pak et al. 2005). Only ~15% of RGCs are *Brn3c* expressing (Xiang, Zhou et al. 1995).

The overlapping expression patterns and a similar specific DNA-binding site [(A/G)CTCATTAA(T/C)] of these three *Brn-3* proteins suggest their functional redundancy in retinogenesis. Targeted mutations of *Brn-3* genes in the mice, however, show distinct defects. Of the three mutations of *Brn-3* genes, only the *Brn3b*$^{-/-}$ mouse shows an obvious retinal phenotype. Targeted deletion of *Brn3b* in mice leads to a loss of 60-80% of RGCs in adult retinas, depending on the mouse strain (Erkman, McEvilly et al. 1996; Gan, Xiang et al. 1996). This RGC loss is due to enhanced

apoptosis after E15.5, but not to defects of initial cell fate specification or migration. *Brn3b* is also required for RGC axon pathfinding and fasciculation (Erkman, Yates et al. 2000). *Brn3a* null mutants die at birth, with loss of the dorsal root ganglion and trigeminal neurons (Erkman, McEvilly et al. 1996; Xiang, Gan et al. 1996). *Brn3c*$^{-/-}$ mice display deficits in balance and complete deafness, which are attributed to loss of vestibular and auditory hair cells (Erkman, McEvilly et al. 1996; Xiang, Gan et al. 1997). Neither *Brn3a* nor *Brn3c* mutants show obvious defects in retinal development.

Brn3a and *Brn3c* are identified as downstream targets of *Brn3b* in retinogenesis, and there is reduced *Brn3a* expression in *Brn3b* mutants (Erkman, McEvilly et al. 1996). Despite the dominant roles of *Brn3b* in retinal development, several independent research groups have reported that all three *Brn-3* genes are functionally equivalent in retinogenesis. Over-expression of *Brn3a*, *Brn3b* or *Brn3c* in chick retinal progenitors exerts a similar effect in promoting RGC differentiation (Liu, Khare et al. 2000). Knocking-in the *Brn3a* coding sequence into a *Brn3b* null background mouse rescues RGC from apoptosis and restores RGC axonal pathfinding (Pan, Yang et al. 2005).

A recent study has shown that conditional deletion of *Brn3a* alters RGC dendritic stratification without influencing RGC axon central projections. However, conditional *Brn3b* knockout mice show reduced RGCs numbers, loss of axonal projections to the medial terminal nuclei (MTN) and lateral terminal nuclei (LTN) and corresponding visual sensory defects (Badea, Cahill et al. 2009).

Brn3b is reported as a downstream target of *Atoh*7 (*Math*5), a basic helix-loop-helix (bHLH) transcription factor. The *Atoh7-Brn3b* regulation pathway also promotes RGC differentiation by repressing a group of retinal development genes, including *Dlx1/Dlx2*, *Otx2* and *Crx*, based on microarray data (Qiu, Jiang et al. 2008).

1.2.10 *Dlx* genes

Distal-less (Dll) is required for *Drosophila* limb development. *Dlx* genes are the orthologs of *Dll* in vertebrates. There are six *Dlx* genes identified in mice, which are arranged into three bigenic clusters (*Dlx1/Dlx2*, *Dlx5/Dlx6*, and *Dlx3/Dlx7*), and are localized on mouse chromosomes 2, 6 and 11, respectively (Ghanem, Jarinova et al. 2003). Within the intergenic regions of *Dlx1/2* and *Dlx5/6*, several *cis*-acting regulators have been characterized, including *I12a* and *I12b* between the *Dlx1* and *Dlx2* genes, and *I56i* and *I56ii* separating *Dlx5* and *Dlx6* genes (Poitras, Ghanem et al. 2007). Two conserved enhancer elements, URE1 and URE2, have also been found in the 5' flanking region of *Dlx1* (Hamilton, Woo et al. 2005)(Du, Ekker and Eisenstat unpublished). These *cis*-acting elements are important for cross-regulatory interactions between the *Dlx* genes. One example is that DLX1 and DLX2 regulate *Dlx5/Dlx6* expression by acting on *I56i* (Zhou, Le et al. 2004). Of these six *Dlx* genes, *Dlx1*, *Dlx2*, *Dlx5* and *Dlx6* are expressed in the developing forbrain, in different, but temporally and spatially overlapping patterns. *Dlx1* and *Dlx2* genes play important roles in the differentiation and migration of GABAergic interneurons (Panganiban and Rubenstein 2002; Wigle and Eisenstat 2008).

Dlx1 and *Dlx2* were first detected in the retinal neuroepithelium at E12.5, including mitotic cells adjacent to the ophthalmic ventricle (Eisenstat, Liu et al. 1999). Our recent study reported DLX2 immunostaining at E11.5 retina, where DLX2 expression shows a clear high-dorsal-to-low-ventral expression pattern (de Melo, Zhou et al. 2008). At E13.5, both DLX1 and DLX2 are expressed throughout the retina, with boundaries at the peripheral and central inner retina. Interestingly, other homeobox genes important for retinal development are expressed in a nearly complementary manner to DLX2 at this stage. At E13.5, the highest level of PAX6 expression is observed in the most peripheral retina and BRN3b is expressed in the inner central retina, where DLX2 is absent. About 22.5% of total retinal cells are DLX2-expressing at E13.5. The proportion of DLX2 expressing cells in the total population declines during retinal development. By E18.5, DLX1 and DLX2 expression are highly restricted to the GCL and the inner part of the NBL of the retina, where they are co-expressed with markers for RGC, amacrine and horizontal cells. DLX1 expression resembles DLX2 in embryonic retina, but decreases dramatically after birth and is not easily detected in adult retina. However, DLX2 is robustly expressed in the GCL and INL throughout adulthood (de Melo, Qiu et al. 2003).

Although the role of *Dlx* genes in forebrain development is well reported, very few studies have described *Dlx* gene function in retina development. Homozygous deletion of *Dlx1* and *Dlx2* is perinatally lethal, and leads to a 33% reduction of RGC number, due to enhanced apoptosis of late-born RGCs (de Melo, Du et al. 2005). *TrkB*, a receptor for brain derived neurotrophic factor (BDNF) mediated signalling, was

identified as a DLX2 downstream target during mouse retinal development and may contribute to RGC survival (de Melo, Zhou et al. 2008). Similar to the *Dlx1/Dlx2* double mutant, mice lacking only *Dlx2* die at birth, but unlike double mutants, no retinal phenotype has been described to date. Although DLX2 is co-expressed with GAD65, GAD67 and GABA in the developing retina, defects in GABAergic interneurons in the DLX1/DLX2 null retinas were not detected (de Melo, Zhang and Eisenstat, unpublished).

The role of *Dlx5* and *Dlx6* genes in retinogenesis is still not clear. *In situ* hybridization revealed *Dlx5* mRNA expression in retinas by E16.5. In P0 and adult retina, *Dlx5* mRNA is co-expressed with DLX2 in the GCL and INL. The *Dlx5/Dlx6* intergenic enhancer (*I56i*) is co-expressed with DLX5, DLX1 and DLX2 in RGC, amacrine and horizontal cells (Zhou, Le et al. 2004). There is no published report regarding the retinal phenotype of *Dlx5/Dlx6* knockout mice.

1.2.11 *Vax* genes

Vax (Ventral anterior homeobox-containing gene) genes are a homeodomain gene subfamily, closely related to the *Emx* and *Not* genes, sharing sequence homology, similar chromosomal location, and expression patterns (Hallonet, Hollemann et al. 1998). Of the two family members reported thus far, *Vax1* is the first one identified, and is named after its highly specialized expression pattern during early neurulation (Ventral anterior homeobox-containing gene) (Hallonet, Hollemann et al. 1998). In the mouse, *Vax1* mRNA is first detected at E8, in the anterior neural ridge and

adjacent ectoderm. During embryogenesis, *Vax1* expression is restricted to the derivatives of these regions, including the basal forebrain, ventral optic vesicle, optic disk, optic stalk and optic chiasm (Hallonet, Hollemann et al. 1998). *Vax1* is essential for the normal development of these structures (Hallonet, Hollemann et al. 1999). The targeted deletion of *Vax1* shows defects in RGC axonogenesis and axonal-glial associations, without influencing expression of *Pax2* and *BF1*. In addition, *Vax1*$^{-/-}$ axons fail to fasciculate and extend toward the hypothalamic midline, leading to an absence of the optic chiasm. These RGC axon pathfinding defects are partially due to the loss of some important axon guidance cues, including *Netrin-1* and *EphB3*, but not *Slit1* (Bertuzzi, Hindges et al. 1999). Another obvious phenotype of *Vax1* mutants is the failure of choroid fissure closure, known as coloboma. *Pax6* and *Rx* are ectopically expressed in the *Vax1* mutant optic nerve. However, *Pax2* expression remains unaffected in the mutants.

The VAX2 homeodomain is identical to that of VAX1, and the *Vax2* gene is tightly linked with *Emx1* in the mouse and human. By E9, *Vax2* transcripts are detected in the ventral optic vesicle, with lower expression in the optic nerve and stalk. Within a very short time period of development, *Vax1* and *Vax2* share overlapping expression patterns in the ventral retina and optic stalk. By E12, *Vax2* expression is restricted to the entire ventral neural retina However, at later embryonic stages, *Vax2* is only detected in ventral RGCs. There is no *Vax2* expression in the adult retina (Barbieri, Lupo et al. 1999; Bertuzzi, Hindges et al. 1999; Hallonet, Hollemann et al. 1999; Mui, Hindges et al. 2002).

Consistent with its predominant ventral retinal expression pattern, *Vax2* plays a major role in ventralizing the embryonic retina. Misexpression of *Vax2* in the dorsal retina is able to alter the expression of the putative dorsal-ventral (DV) marker genes, including upregulation of ventral retinal marker *EphB2/EphB3*, *Pax2* and *Vax2* itself, and down-regulation of the dorsally restricted transcription factor *Tbx5* (Barbieri, Lupo et al. 1999). In addition, ectopic *Vax2* expression in dorsal retina is enough to induce profound axon pathfinding defects of the dorsal RGC (Schulte, Furukawa et al. 1999). In agreement with these *Vax2* gain-of-function studies, the ventral RGC from *Vax2* null mice results in a complete dorsalization. The RGC axons from *Vax2*$^{-/-}$ ventral retina aberrantly projected into the lateral rostral edge of the superior colliculus (SC), together with all the dorsal RGC axons, instead of the medial rostral SC, the destination of all the wild-type ventral RGC axons. The expression of *EphB2*/*EphB3* is absent in the *Vax2*$^{-/-}$ ventral retina. However, the loss of *Vax2* function failed to alter the expression of early regulators of DV polarization, such as *Pax2* and *Tbx5* (Barbieri, Broccoli et al. 2002; Mui, Hindges et al. 2002). Interestingly, although the ipsilateral projecting axons are primarily from the ventral temporal retina, the two independent studies of *Vax2* knockout mice have different conclusions.

Despite the nearly complementary expression patterns of *Vax1* and *Vax2*, these two genes interact and function in concert in retina and optic nerve formation (Mui, Kim et al. 2005). A *Vax1*/*Vax2* double knockout mouse model has been generated and shows a much more severe retinal coloboma whereas mild coloboma is found in the single *Vax2* mutants. Coloboma results in the transformation from optic nerve to a

fully differentiated and well laminated retina. By directly acting on the α-enhancer, VAX1 and VAX2 negatively regulate *Pax6* expression in the optic neuroepithelium. Interestingly, the repression of the *Pax6* transcript in retinal development is closely related to the subcellular location of VAX2. The phosphorylation of Serine-170, which is C-terminal to the VAX2 homeodomain, confines VAX2 into the cytoplasm after E12.5, which in turn, disables the repression of VAX2 on the *Pax6* transcript. By antagonizing Ser 170 phosphorylation, Sonic hedgehog drives VAX2 into the nucleus (Kim and Lemke 2006).

1.2.12 *Islet genes*

ISL1 and ISL2 are a subfamily of LIM homeodomain transcription factors characterized by two zinc-finger motifs (LIM domain) and a homeodomain. Both ISL1 and ISL2 have been shown to play important roles in determining motor neuron subtype identity, their axonal projection patterns and peripheral innervations (Shirasaki and Pfaff 2002). Most of the work has been done in the spinal cord of vertebrate and invertebrate models.

Isl1 and *Isl2* are also expressed in the embryonic and postnatal retina. *Isl2* expression is first detected in the E13 retina, and by E17, almost all the *Isl2* positive cells are RGCs (94%) (Pak, Hindges et al. 2004). *Isl2* is expressed at high levels in the dorsal retina, with weak expression in the ventral-temporal retina. By repressing *Zic2* and *EphB1*, *Isl2* specifies the contralateral projections of RGC axons. In comparison to the specific RGC expression of *Isl2*, *Isl1* expression varies in

embryonic and postnatal retina. Prior to E15.5, Isl1 is predominantly expressed in the RGCs. However, from E15.5 to adulthood, *Isl1* expression is detected in RGCs, amacrine cells and bipolar cells (Elshatory, Deng et al. 2007). Recent work has shown that under the regulation of ATOH7 (formerly MATH5), *Isl1* defines a distinct but overlapping sub-population of RGCs with *Brn3b* (Mu, Fu et al. 2008; Pan, Deng et al. 2008)

1.2.13 Basic helix-loop-helix genes

In addition to the key roles of HD TFs on retinal development, another group of TFs, the basic helix-loop-helix (bHLH) family, are also critical to this process, especially with respect to the commitment of retinal progenitor cells to a specific retinal neuron fate. These bHLH TFs were first identified in the *Drosophila*, and named as "proneural" TFs, due to their functions in initiating the development of neuronal lineage and in the inhibition of a glial fate (Bertrand, Castro et al. 2002). Two distinct bHLH proneural gene families are isolated in *Drosophila*, namely *achaete-scute* complex (*as-c*) genes and *atonal* (*ato*) genes. These proneural TFs are characterized by the presence of a bHLH domain, a specialized motif responsible for protein dimerization and DNA binding. Most of the proneural proteins form heterodimers with E proteins (*Daughterless* in *Drosophila* and E12 or E47 in vertebrate), and activate their target genes' expression. The E-box, a conserved DNA motif (CANNTG) located in the regulatory regions of the target genes, is recognized by bHLH proteins and required for bHLH heterodimers (Powell and Jarman 2008).

The mouse *as-c* orthologues include *Mash1* and *Mash2*. The mouse *ato* family has two family members, *Math1* and *Math5*. A third distinct bHLH gene family found in mouse are the *ato*-related genes, which, as the name suggests, is related to *ato* genes, but has family specific residues in their bHLH domain. In the mouse, the *NeuroD*, *Neurogenin* (Ngn) and *Olig* subfamilies belong to this third group (Bertrand, Castro et al. 2002). Many of these bHLH proneural genes have been identified and investigated in the developing mouse retina, namely *Mash1, Math3, Math5* and *NeuroD*. The exact function of these bHLH genes in retinogenesis is not clear, but elegant studies with mutational analysis and ectopic gene expression have shed some light on this question.

1.2.14 *Math5* is required for RGC development

Among the earliest bHLH proneural genes expressed in the retina, the *Math5* transcript is first detected at E11 in the mouse retina, and coincides with the differentiation of the RGCs (Brown, Kanekar et al. 1998). Homozygous mice for *Math5* mutations demonstrate dramatic RGC loss, which varies from 80% RGC loss to complete RGC absence depending on the strain, and increased amacrine and cone photoreceptor cells. Over-expression of *Math5* promotes RGC production (Brown, Kanekar et al. 1998; Brown, Patel et al. 2001; Liu, Mo et al. 2001; Wang, Kim et al. 2001). Emerging evidence suggests that *Math5* promotes RGC development by induction of a cascade of RGC-differentiation genes, but not by *Math5* itself. *Math5* expression in the developing retina is transient and does not overlap with the

differentiated RGCs. At E13.5, *Math5* mRNA is expressed throughout the mouse retina, with the exception of the inner central regions where the differentiated RGCs are located. *Math5* expression is dramatically down-regulated at E16.5. At E18.5, *Math5* is confined to the region closest to ciliary margin, where the mitotically active progenitors are located. In the adult retina, no *Math5* is detected (Fig. 13) (Brown, Kanekar et al. 1998). As mentioned above, the POU-HD TFs *Brn3a* and *Brn3b* are among the most important regulators of RGC differentiation and survival. *Brn3b* expression is regulated by *Math5*. *Isl-1* is another downstream target of *Math5* and defines a distinct but overlapping sub-population of RGCs with *Brn3b.* This suggests that *Math5* regulates distinct branches of the gene regulatory network responsible for RGC development (Mu, Fu et al. 2005; Mu, Fu et al. 2008; Pan, Deng et al. 2008).

In addition, *Math5* is not a RGC specific TF, since the retinal progenitor cells of *Math5* origin have multiple competencies and differentiate into RGCs and other retinal neurons, including amacrine, horizontal and photoreceptor cells (Yang, Ding et al. 2003; Feng, Xie et al. 2010). This notion is further supported by *ath5* misexpression studies. In a developmental stage-dependent manner, the misexpression of *ath5* in cultured chick retinal cells can promote both RGC and photoreceptor production. A gene regulatory pathway, "*ath5* → *NeuroD* → photoreceptor genes", is proposed to be involved in this process (Ma, Yan et al. 2004). *Math5* is also required for retinal progenitor cell cycle progression (Le, Wroblewski et al. 2006).

1.2.15 *NeuroD* is required for amacrine and photoreceptor cells development

NeuroD expressing cells in E18.5 retinas are organized into two groups. Cells located in the outermost region of the NBL express *NeuroD* robustly. Scattered *NeuroD* positive cells are also detected in the inner layer of NBL, but not in GCL at this developmental stage (Fig. 15). The outermost *NeuroD* expressing cells represent developing cones and rods, whereas the cells located at the inner NBL are amacrine cells. Early *NeuroD* expression is scattered in the central retina at E10.5 in the mouse embryo (Pennesi, Cho et al. 2003). Interestingly, very few *NeuroD* expressing cells are mitotically active and thus are co-labelled with BrdU at E14.5, suggesting that *NeuroD* is primarily expressed in post-mitotic cells in the developing mouse retina (Liu, Etter et al. 2008). In contrast to mice, in the fish and chick retinas, *NeuroD* is expressed in proliferating progenitors, as well as post-mitotic amacrine and photoreceptors (Yan and Wang 2004; Ochocinska and Hitchcock 2009).

Depending upon the genetic background, the homozygous *NeuroD* mutant mice show different survival rates, from death at P5 to adulthood. Therefore, the analyses of developing retina are carried out differently. Using retinal explant cultures, Morrow and colleagues showed that deletion of *NeuroD* resulted in decreased photoreceptor cell numbers, delayed amacrine cell differentiation, and increased bipolar interneurons and Müller glial cells (Morrow, Furukawa et al. 1999). For the *NeuroD* deficient mice that survived to adulthood, electroretinograms (ERGs) were carried out, showing that by 9 months, no functioning ERG could be detected in the *NeuroD* null retinas. This could be attributed to significant photoreceptor cell loss, shortened outer segments on

the remaining photoreceptors and defective photoreceptor survival in the *NeuroD* mutant retina. However, no other retinal neurons or glia are affected by the loss of *NeuroD* (Pennesi, Cho et al. 2003). Similar loss-of-function studies have been performed on chick embryos, which showed similar results: loss of *NeuroD* function leads specifically to photoreceptor deficiency, but does not affect other retinal cells (Yan and Wang 2004). A series of double bHLH genes knock-out studies have been carried out, namely double knock-out of *ash1/neuroD*, *ath3/neuroD*, *ngn2/neuroD*, *ash1/ngn2*, and *ash1/ath3*. However, in terms of photoreceptor cell loss, no difference was found between either of these double knock-outs and the *NeuroD* single mutants. These data suggest that among the tested bHLH genes, *NeuroD* plays key roles in photoreceptor cell differentiation (Akagi, Inoue et al. 2004). A recent study has shown that by regulating cell cycle control genes, *NeuroD* promotes the exit of photoreceptor progenitors from the cell cycle (Ochocinska and Hitchcock 2009).

Mis-expression of *NeuroD* alone is sufficient to promote photoreceptor cell genesis in both chick and mouse. In addition, retrovirus driven *NeuroD* expression is able to induce retinal pigment epithelial cell transdifferentiation toward photoreceptor cells (Yan and Wang 1998; Inoue, Hojo et al. 2002).

Besides the regulation of photoreceptor development and survival, *NeuroD* is believed to play a role in amacrine cell differentiation. The *NeuroD*$^{-/-}$ retinal explant shows delayed amacrine cell differentiation. Forced expression of *NeuroD* in rat retinal progenitors promotes amacrine cell production at the expense of bipolar cells (Morrow, Furukawa et al. 1999). The *ath3/neuroD* double null retina has no amacrine

cell differentiation (Inoue, Hojo et al. 2002). However, more evidence is needed to establish a clear relation between *NeuroD* and amacrine cell development.

Although many bHLH proneural TFs have demonstrated specialized functions in retinal cell development, their regulation of target genes is modified by the developmental context, both temporally and spatially. Replacing the *Math5* locus with *NeuroD1* leads to ectopic *NeuroD1* expression, which resembles endogenous *Math5* expression temporally and spatially. In the absence of *Math5*, ectopic *NeuroD1* partially assumed the *Math5* role by activating RGC differentiation genes, promoting RGC production and restoring optic nerves (Mao, Wang et al. 2008). Interestingly, under a RGC developmental context, *NeuroD1* promotes RGC differentiation but neither photoreceptor nor amacrine cell differentiation. This suggests that in order to perform their specialized functions, bHLH TFs have to coordinate inputs from other factors, including other co-TFs and extrinsic cues.

1.2.16 bHLH repressors function in maintenance of retinal progenitors

The bHLH factors described above are proneural activators, which regulate the retinal progenitors to exit the cell cycle and promote neuronal differentiation. Antagonistic bHLH genes are also identified in retinogenesis. These gene products form inactive heterodimers with bHLH proneural activators and repress their function. There are two major groups of bHLH repressors: *Id* class repressors lack the basic DNA binding domain; and *Hes/Her*, which encode TF that recognize an N-box (CACNAG) DNA motif, instead of the E-box (Vetter and Brown 2001). Among the

bHLH repressors, *Hes1* and *Hes5* are intensively investigated in the developing retina. Both *Hes1* and *Hes5* are essential effectors for Notch signalling, and are critical to maintain a pool of retinal progenitors. By interacting with neighbouring cells, the retinal progenitor activates its Notch receptor and triggers the downstream signalling cascade, which in turn induces *Hes1* and *Hes5* expression (Hatakeyama and Kageyama 2004). During early eye development, *Hes1* expression is initially detected in the optic vesicle and the optic stalk. Later, *Hes1* is expressed by the retinal progenitors that are restricted in the ventricular zone of the developing retina. The *Hes1* deficient retinal progenitors fail to maintain an adequate level of proliferation, leading to the formation of small eyes, disrupted retinal layers and premature neuronal differentiation. Conversely, retinal progenitors with overexpressed *Hes1* have defects in exiting the cell cycle and differentiation (Tomita, Ishibashi et al. 1996). Although *Hes5* is expressed by the retinal progenitors, deletion of *Hes5* alone has no obvious influence on retinal development. However, *Hes1/Hes5* double null mice have much more severe retinal defects than either *Hes1* or *Hes5* single mutants. The double mutant mice fail to form optic vesicles due to impaired retinal progenitor proliferation (Hatakeyama and Kageyama 2004). These studies suggest that *Hes1* and *Hes5* play a combinatorial role on maintenance of retinal progenitors.

1.2.17 Combinatorial roles of HD and bHLH TFs are required in retinal cell specification

Many retinal cell fates are determined by the combinatorial action of two or

more TFs. One example is the *Chx10*, *Mash1* and *Math3* regulation of bipolar differentiation. As described above, *Chx10* expression is restricted to the developing and mature INL, particularly in bipolar interneurons and a subset of Müller glia. The loss of *Chx10* function leads to complete loss of bipolar cells (Liu, Chen et al. 1994; Rowan and Cepko 2004). However, the ectopic expression of *Chx10* alone induces INL formation and Müller cell differentiation, but not bipolar cells (Hatakeyama, Tomita et al. 2001). The bHLH TFs *Mash1* and *Math3* are transiently expressed in developing bipolar cells. Single mutations of either *Mash1* or *Math3* lead to only modest reduction in bipolar interneuron numbers, whereas the double null mutation of *Mash1* and *Math3* results in a complete loss of bipolar cells and an increase in Müller glia. Misexpression of *Mash1* or *Math3,* either alone or together, promotes the generation of rod photoreceptors instead of bipolar cells (Hatakeyama, Tomita et al. 2001). Thus, neither of *Chx10*, *Mash1* or *Math3* alone is sufficient to specify bipolar differentiation. However, combinatorial misexpression of *Chx10* with either *Mash1* or *Math3* significantly increases bipolar cell production (Hatakeyama, Tomita et al. 2001). These findings suggest that the cooperation of HD factors and bHLH factors is essential for correct retinal cell fate specification.

A similar example is the regulation of *Pax6*, *NeuroD* and *Math3* on amacrine cell specification. Both *NeuroD* and *Math3* are transiently expressed by differentiating amacrine cells. However, besides the delayed amacrine cell development observed in *NeuroD*$^{-/-}$ retinal explants, no amacrine cell loss or morphological changes were found in the single null mutations of either *NeuroD* or *Math3* (Morrow, Furukawa et al.

1999). In contrast, the *NeuroD/Math3* double null mutant retina shows dramatic loss of amacrine cells. Interestingly, compensatory increased RGC production and upregulated *Math5* expression are observed in these double mutants (Inoue, Hojo et al. 2002). The HD TF *Pax6* is also expressed in amacrine cells. The ectopic expression of *Pax6*, *NeuroD* or *Math3* alone is insufficient to induce amacrine cell genesis. Co-expression of *Pax6* with either *NeuroD* or *Math3*, however, is sufficient to significantly promote amacrine cell genesis. In addition, co-expression of *Pax6* and *Math3* can generate horizontal cells (Inoue, Hojo et al. 2002).

1.2.18 Neuronal migration to laminar destinations

After their final mitosis at the ventricular surface, the post-mitotic retinal precursors start to differentiate and migrate at the same time. In contrast to the neocortex, the retinal precursors undergo a short and simple migration before they reach their laminar destination. The cone and rod photoreceptor precursors remain attached to the ventricular retinal surface, even after their final cell cycle. Following a radial process, most of the photoreceptor cells are translocated into the ONL with few in the INL (Spira, Hudy et al. 1984). In comparison to photoreceptors, RGC and retinal interneurons have to travel a longer journey before they arrive at their laminar positions. Nuclear translocation is one of the most common modes of migration used by these retinal neurons. Before RGC fully differentiate, axons of these cells extend across the inner retinal surface and navigate a course into the presumptive optic nerve. The nucleus will subsequently complete translocation to the GCL along this leading

process (McLoon and Barnes 1989; Dunlop 1990). Bipolar cells take a similar means to achieve their final position in the INL. In contrast, amacrine cells are shown to follow local environmental signals, but not any obvious leading processes (Godinho, Mumm et al. 2005). Interestingly, horizontal cells demonstrate a unique migratory behaviour. Under the regulation of *Lim2*, horizontal cells first migrate to the deeper INL, where most amacrine cells are located. A second wave of apical migration re-locates horizontal cells back to the outer INL. Without the function of *Lim2*, horizontal cells fail to migrate back from the deeper INL, and stay among amacrine cells in the inner aspect of the INL. (Edqvist and Hallbook 2004; Poche, Kwan et al. 2007; Boije, Edqvist et al. 2009).

1.2.19 Development of the optic pathway: overview

Before the retinal ganglion cells fully differentiate, their axons start navigating and exit the retina to form an optic nerve. Ganglion cell axonal projections are first detected in the mouse optic chiasm at E14, shortly after the first wave of RGC differentiation. The earliest axons reach their central targets of LGN and SC at E16 in mouse (Godement, Salaun et al. 1984). The optic axonal journey is composed of many critical events. All of the RGC axons must grow toward the optic disc and exit the eye through a tightly bundled optic nerve head. The optic nerve then approaches the optic chiasm, where the majority of axons cross the midline and project to the opposite side of the brain (contralateral projection), whereas a subset of axons remain on the same side (ipsilateral projection). In the mouse, about 3% of the axons, mainly

from the RGCs located at the ventral-temporal retina, are ipsilateral axons. Finally, RGC axons will make connections to the appropriate neurons in their central targets LGN and SC. Numerous molecules function at these pathfinding points to ensure accurate guidance for the ganglion cell axons. Transcription factors are also involved in this process.

1.2.20 RGC axonal growth within the retina

The early generated RGCs are located in the central retina, and the axons of these RGCs extend towards the optic disc. The late-differentiated RGCs are located in more peripheral retinal regions. Their axons travel longer distances from the peripheral retina to the central optic disc than the early generated RGCs. These axons are more likely to fasciculate with the existing axons along their way. L1, an immunoglobulin (Ig) protein, is expressed in these axons and regulates the axon fasciculation. Blockage of L1 function leads to disorganized RGC axonal projection, instead of directed growth within the retina (Brittis, Lemmon et al. 1995). A chondroitin sulphate proteoglycans (CSPG) ring found in the peripheral retina also plays an important role in intraretina axonal guidance (Brittis, Canning et al. 1992). In addition, EphB-ephrinB interactions are required to ensure accurate projection of RGC axons to the optic disc. In the double null mutation of EphB2 and EphB3 retina, RGC axons are defasciculated and miss the optic disc (Birgbauer, Cowan et al. 2000). In normal development, once the RGC axons reach the optic disc, an optic nerve head is formed, which is a netrin protein-dependent process. Netrin-1 is expressed

specifically by the cells surrounding the optic disc. Netrin-1 performs its function by binding to its receptor, deleted in colorectal carcinoma (DCC), which is expressed by RGC axons. Mice with mutations in either netrin-1 or DCC show similar defects of axonal guidance at the optic nerve head, leading to a phenotype of optic nerve hypoplasia (Serafini, Colamarino et al. 1996; Fazeli, Dickinson et al. 1997).

1.2.21 Guidance in the optic nerve

After the RGC axons exit through the optic disc, they travel in a restricted course toward the ventral midline of the diencephalon, where the optic chiasm is formed. A repellent guidance molecule, Sema5A, is expressed by the oligodendroctyes in the optic nerve. It is believed that Sema5A forms a sheath surrounding the optic nerve and prevents the axons from escaping the tight optic nerve bundle (Oster, Bodeker et al. 2003; Goldberg, Vargas et al. 2004). Slit proteins are also expressed around the optic nerve and function to channel axons within the optic pathway (Plump, Erskine et al. 2002; Thompson, Barker et al. 2006).

1.2.22 Optic chiasm formation

Formation of the optic chiasm has been intensively studied. One of the most important pathfinding choices for the RGC axons is whether or not to cross the midline. Sonic hedgehog (SHH) is dynamically expressed along the midline of ventral diencephalon, and is critical for chiasm formation (Trousse, Marti et al. 2001). Through its receptor Boc, SHH repels ipsilateral RGC axons at the midline (Fabre,

Shimogori et al. 2010). Robo/Slit interactions are shown to control where the chiasm is formed. Both Slit1 and Slit2 are expressed near the chiasm and act as a "guardrail" on either side of the midline. Robo2 is expressed by the RGCs and functions as the receptor for Slit signals. A "surround repulsion" model is proposed for Slit functions, in which Slit1 and Slit2 repel axons from either side of the chiasm and keep them on the right track. In the *Slit1/Slit2* double null mouse, RGC axons crossed the midline at a more anterior position, resulting in a second chiasm formation (Plump, Erskine et al. 2002; Rasband, Hardy et al. 2003).

In the mouse, RGCs from the ventral-temporal region of the retina project their axons ipsilaterally. These RGCs express the EphB1 receptor, which interacts with the ephrin-B2 ligand expressed by the radial glia cells located at the midline of the diencephalon. The EphB1-ephrin-B2 interaction is specifically required and provides a repulsive signal to the ipsilateral optic axons, preventing them to cross the optic chiasm (Petros, Shrestha et al. 2009).

Transcription factors play a fundamental role as molecular drivers for growing axons. Zic2, a zinc-finger transcription factor, is expressed transiently by the ipsilaterally projecting RGCs located at the ventral-temporal retina, during the period when uncrossed RGCs traverse the midline. Zic2 regulates EphB1 expression in the developing ventral-temporal retina, and in turn controls the ipsilateral projections through EphB1-ephrinB2 interactions at the midline (Garcia-Frigola, Carreres et al. 2008). Zic2 is regulated by Foxd1, supported by the fact that the null mutation of Foxd1 loses both Zic2 and EphB1 expression in the ventral-temporal retina, leading to

an abnormal optic chiasm (Herrera, Marcus et al. 2004). In contrast, the LIM HD factor Islet-2 marks a distinct population of RGCs from the Zic2/EphB1 group. The Islet-2 expressing RGCs project their axons contralaterally, partially by repressing the ipsilateral pathfinding network Zic2-EphB1 (Pak, Hindges et al. 2004).

By regulating L1 and the guidance cues of SHH, the HD transcription factor *Brn3b* is required to maintain the proper retinal axonal pathfinding at optic chiasm, as well as other points along the retinofugal pathway (Erkman, Yates et al. 2000; Pan, Yang et al. 2005). In addition, other HD transcription factors, *Vax1*, *Vax2* and *Pax2* are also crucial for correct formation of the optic chiasm (Williams, Mason et al. 2004).

1.2.23 Central target projections

After crossing the optic chiasm, RGC axons continue their journey in a tightly bundled optic tract. Slit1 and Slit2 proteins regulate optic tract development by restricting axons in their pathway and preventing axons from penetrating into the telencephalon (Thompson, Barker et al. 2006). A precisely maintained topographic map is developed when RGC axons innervate their visual targets, the lateral geniculate nucleus (LGN) and the superior colliculus (SC) in the mouse. RGC axons from the nasal retina project to the posterior SC, whereas the temporal RGC axons project to the anterior SC. Interactions between Ephs and ephrins play an important role in the development of the topographic map. For example, a high-temporal-to-low-nasal expression gradient of EphA is maintained in the retina, while a high-posterior-to-low-anterior ephrin-A expression gradient is detected in the

SC. Therefore, the axons from the temporal retina express a high level of EphA receptors and respond to the strong repellent signal in the posterior SC by avoiding that region. Disruption of the EphA/EphrinA interaction causes aberrant axonal projection in both LGN and SC (Feldheim, Vanderhaeghen et al. 1998; Frisen, Yates et al. 1998; Clandinin and Feldheim 2009). EphBs are expressed in gradient fashion along the dorsal-ventral axis of retina. EphrinBs are expressed in a complementary manner in the SC, but have an attractive function. Null mutations of either EphB2 or EphB3 show defects in the ventral RGC axons projections (Hindges, McLaughlin et al. 2002).

1.3 *Dlx* genes in the development of forebrain and other organ systems

Besides their roles in retinal development, *Dlx1* and *Dlx2* are well known for promoting differentiation and migration of forebrain GABAergic interneurons. In the developing forebrain, *Dlx1/Dlx2* and *Dlx5/Dlx6* share a distinct but overlapping expression pattern, both temporally and spatially. *Dlx2* expression is initiated first, followed by *Dlx1*, *Dlx5* and lastly *Dlx6* (Eisenstat, Liu et al. 1999; Zerucha and Ekker 2000; Panganiban and Rubenstein 2002). In the E12.5 mouse telencephalon, *Dlx2* is highly expressed in the ventricular zone (VZ) and subventricular zone (SVZ) of the lateral and medial ganglionic eminences (LGE and MGE, respectively). *Dlx1* expression is detected in the VZ, SVZ, as well as the mantle zone (MZ) of the LGE and MGE. *Dlx2* is mainly expressed in the undifferentiated cells, whereas *Dlx5/Dlx6* is primarily expressed in differentiated cells located in the SVZ and MZ (Panganiban

and Rubenstein 2002). These overlapping but different expression patterns suggest the *Dlx* genes have redundant yet distinct functions in the developing forebrain.

The *Dlx1/Dlx2* double null mice die shortly after birth, with a significant loss of GABAergic interneurons in the neocortex, olfactory bulb and hippocampus (Anderson, Eisenstat et al. 1997; Bulfone, Wang et al. 1998; Pleasure, Anderson et al. 2000). Two defects contribute to this GABAergic interneurons loss. Firstly, without *Dlx1/Dlx2* function, the immature interneurons fail to tangentially migrate from the progenitor zone of both the LGE and MGE to their destinations. *Arx*, a homeodomain-containing transcription factor, has been identified as a direct downstream target of DLX2, and contributes to the GABAergic interneuron migration (Colasante, Collombat et al. 2008). Secondly, deleting *Dlx1/Dlx2* gene function alters the GABAergic promoting genes expression, including GAD67 and vGAT, and subsequently fails to specify GABAergic neuron differentiation (Anderson, Mione et al. 1999; Long, Garel et al. 2007). However, only late-born neurons are affected by the loss of *Dlx1/Dlx2*. In the *Dlx1/Dlx2* double mutant mice, GABA is still detected in the subcortical telencephalon (Anderson, Qiu et al. 1997). It is shown that *Mash1* regulates GABAergic interneuron development, through a parallel but overlapping pathway to *Dlx1/Dlx2* (Long, Cobos et al. 2009; Long, Swan et al. 2009). In addition, *Dlx1/Dlx2* inhibits oligodendrocyte development by repressing *Oligo2* expression (Petryniak, Potter et al. 2007). *Dlx1/Dlx2* also regulates neurite morphogenesis by repressing Pak3 (Cobos, Borello et al. 2007).

Despite their redundant roles in promoting the development of GABAergic

interneurons and repressing the formation of oligodendroctyes, *Dlx1* and *Dlx2* also have their own unique functions. *Dlx1* single knockout mice show a selective reduction of some certain subgroups of interneurons. The *Dlx1* single null mice also show decreased postsynaptic inhibition and increased seizures at postnatal stages (Cobos, Calcagnotto et al. 2005). To date, all of the identified DLX1 transcription targets are shared targets for DLX2 including *Neuropilin-2* (*Nrp-2*), *Dlx5/Dlx6* intergenic enhancer (*MI56*) in the forebrain, and *Brn3b* in the retina. However, some gene targets are identified as DLX2-specific in the developing retina, forebrain or branchial arches. These differences suggest some non-overlapping functions between DLX1 and DLX2. For example, although both DLX1 and DLX2 bind directly to *MI56* in the E13 striatum, only DLX2 is immunoprecipitated from developing retinal tissues (Zhou, Le et al. 2004). *Arx* is identified as a direct target of DLX2 in the developing forebrain (Colasante, Collombat et al. 2008). DLX2 is also shown to regulate *Msx2* in the branchial arch development by directly binding to its promoter (Diamond, Amen et al. 2006). In this study, we demonstrated that *Brn3a* is a DLX2 specific transcriptional gene target during retinal development.

Dlx genes also function in branchial arch development. Both *Dlx1* and *Dlx2* are expressed in the proximal branchial arches, and are responsible for patterning this region. The *Dlx3, Dlx4, Dlx5* and *Dlx6* genes also play roles in distal arch development. The *Dlx1/Dlx2* double null mice have severe cleft palate and lack of upper molars (Depew, Simpson et al. 2005). *Dlx5/Dlx6*, on the other hand, biases a lower jaw fate. *Dlx* genes pattern jaw formation through lower or upper jaw-specific

gene networks (Jeong, Li et al. 2008). In addition, *Dlx5* and *Dlx6* are shown to play important roles in the development of bone and cartilage. *Dlx5* promotes osteoblast differentiation by activating *Runx2*, an important TF for osteogenesis (Samee, Geoffroy et al. 2008).

1.4 Epigenetic and post-transcriptional regulation of retinal development

Epigenetic regulation has been reported to be critical for retinogenesis. One important means of epigenetic regulation are microRNAs. MicroRNAs (miRNAs) are endogenous, small, non-coding, regulatory RNAs, ~ 22 nts in size (Carthew and Sontheimer 2009). miRNAs bind to target sites in the 3'-untranslated region (3'-UTR) of mRNAs and negatively regulate gene expression post-transcriptionally, especially in developmental processes and tumorigenesis. Up to date, about 80 miRNAs have been identified in the *Xenopus*, mouse or human retinas (Xu, Witmer et al. 2007). Many of those miRNAs are reported as retinal, or neural specific, and play important roles in neural development. miR-124 is expressed specifically in the developing nervous system and neural retina (Karali, Peluso et al. 2007; Landgraf, Rusu et al. 2007). *Dlx2* was reported as a target of miR-124 in adult subventricular zone (SVZ) neurogenesis (Cheng, Pastrana et al. 2009).

Chapter 2: Research Rationale, Hypothesis and Objectives

Human beings perceive and understand the world around them primarily through visual stimuli. Retinal degeneration and retinal malignancy account for the majority of vision loss diseases, including age-related macular degeneration (ARMD), diabetic retinopathy (DR), and retinoblastoma. Our current knowledge of the genes involved in the processes of neuroretinal proliferation and cell differentiation limits our understanding of retinal development and thus hinders efforts toward prevention and therapies for blindness. The central goal of this proposal is to elucidate the roles of *Dlx* homeobox genes in genetic regulation and determination of retinal cell fate. These studies will provide great insight into the molecular basis for the genesis of specific retinal neurons and may contribute to our understanding of congenital diseases of the retina.

2.1 Research Rationale

The combined influence of extrinsic and intrinsic signals regulates the cell-fate choices of retinal progenitors (Livesey and Cepko 2001). Transcription factors (TFs) act as intrinsic signals and function during different stages of retinogenesis. Although the integrated gene regulatory network is not well established for the terminal differentiation of specific retinal neuronal classes, several important TFs have been identified for RGC differentiation. The bHLH TF, *Atoh*7 (*Math*5), is essential for retinal progenitors to become RGCs (Brown, Patel et al. 2001; Wang, Kim et al. 2001). A POU-homeodomain (POU-HD) TF *Brn*3b (*Pou*4f2), which is genetically downstream of *Atoh*7, is required for the terminal differentiation and survival of the

majority of RGCs, but not for their initial specification (Erkman, McEvilly et al. 1996; Erkman, Yates et al. 2000). *Brn*3b and *Brn*3a (*Pou*4f1) have overlapping yet distinct roles controlling RGC development and function (Badea, Cahill et al. 2009). Recent work has shown that under the regulation of ATOH7, *Isl*1, a LIM-HD TF, defines a distinct but overlapping sub-population of RGCs with *Brn*3b (Mu, Fu et al. 2008; Pan, Deng et al. 2008). This *Atoh*7-*Brn*3b/*Isl*1 pathway appears to determine the fate of a population of early-born RGCs, since a second group of late-born RGCs rely on the Distal-less (*Dll*) homeobox genes *Dlx*1 and *Dlx*2 for terminal differentiation and survival (de Melo, Du et al. 2005; de Melo, Zhou et al. 2008). Retinas from *Dlx*1/*Dlx*2$^{-/-}$ mice demonstrated a 33% reduction of RGC numbers, due to enhanced apoptosis of late-born RGCs. DLX2 and BRN3b are expressed in distinct but partly overlapping regions in the retinal neuroepithelium (de Melo, Qiu et al. 2003).

2.2 Hypotheses

1. *Brn3a* and/or *Brn3b* are direct downstream transcriptional targets of DLX1 and/or DLX2 in retinal development.
2. Absence of *Dlx1/2* and *Brn3b* or *Brn3a* will result in more severe disruptions in retinal development than the single knockouts for these genes.

2.3 Research objectives

1. Use molecular and genetic approaches to establish whether *Brn3a* and/or *Brn3b* are DLX transcriptional targets.
2. Generate a *Dlx1/Dlx2/Brn3b* triple knock-out mouse model to analyse the retinal phenotype.

Chapter 3 Material and Methods

3.1 Animal and Tissue Preparation

All animal protocols in this study were conducted in accordance with the guidelines established by the Canadian Council on Animal Care, the University of Manitoba and the University of Calgary. All wild-type mouse retinal tissues used in chromatin immunoprecipitation and primary retinal cell culture were harvested from the CD-1 strain (Charles River Laboratories, Worcester, MA). *Dlx1/Dlx2* double knockout mice were generated as previously described (Anderson, Eisenstat et al. 1997; Qiu, Bulfone et al. 1997).

Brn3b single knockout mice were provided by Dr. W. Klein from University of Texas M.D. Anderson Cancer Center (Gan, Xiang et al. 1996), and were maintained on a CD1 background. The *Dlx1/Dlx2*$^{+/-}$ *Brn3b*$^{+/-}$ compound heterozygous line was generated by crossing *Dlx1/Dlx2*$^{+/-}$ heterozygotes with *Brn3b*$^{+/-}$ heterozygotes, which are both phenotypically wild-type, and was subsequently used to generate *Dlx1/Dlx2*/*Brn3b* triple homozygous null mice. For comparative studies, all *Dlx1/Dlx2*/*Brn3b* triple knockout mice were paired with *Dlx1/Dlx2*$^{+/-}$*Brn3b*$^{-/-}$ (single knockout), *Dlx1/Dlx2*$^{-/-}$*Brn3b*$^{+/-}$ (double knockout) and *Dlx1/Dlx2*$^{+/-}$*Brn3b*$^{+/-}$ (triple heterozygotes are "wild-type") littermate controls. Genotyping was performed as previously described (Gan, Xiang et al. 1996; Qiu, Bulfone et al. 1997).

Brn3a^{tauLacZ} transgenic reporter mice were a gift from Dr. Eric Turner, University of California San Diego (Quina, Pak et al. 2005).The *Dlx1/Dlx2*$^{+/-}$

Brn3a$^{+/tLacZ}$ compound heterozygous line was generated by crossing *Dlx1/Dlx2*$^{+/-}$ heterozygotes with *Brn3a*$^{+/tLacZ}$ heterozygotes. *Dlx1/Dlx2*/*Brn3a* triple homozygous null mice were generated by mating *Dlx1/Dlx2*$^{+/-}$ *Brn3a*$^{+/tLacZ}$ compound heterozygous. For comparative studies, all *Dlx1/Dlx2*/*Brn3a* triple knockout mice were paired with *Dlx1/Dlx2*$^{+/-}$*Brn3a*$^{tLacZ/tLacZ}$ (single knockout), *Dlx1/Dlx2*$^{-/-}$*Brn3a*$^{+/tLacZ}$ (double knockout) and *Dlx1/Dlx2*$^{+/-}$*Brn3a*$^{+/tLacZ}$ (triple heterozygotes are "wild-type") littermate controls. Genotyping was performed as previously described (Quina, Pak et al. 2005).

Embryonic age was determined by the day of appearance of the vaginal plug (E0.5), as well as overall morphological criteria of the embryos.

For histological staining and immunofluorescence (IF), E18.5 and E16.5 eyes were dissected from embryos, and fixed in freshly made 4% paraformaldehyde (PFA) in phosphate-buffered saline (PBS) for 30 minutes in the cold room (4□ C). E13.5 and E11.5 eyes were left *in situ* prior to brief fixation in freshly made 4% PFA in PBS for 3hrs and 1hr, respectively. P14 and adult eyes were dissected and fixed in 4% freshly made PFA/PBS in the cold room for 1hr. Tissues were then washed with PBS once and transferred to sucrose/PBS gradient series (10% sucrose, 15% sucrose and 20% sucrose) (Sigma, St. Louis, MO). After the sucrose/PBS series, tissues were transferred to a 1:1 mixture of 20% sucrose/ O.C.T. cryo-compound (Sakura Finetek, Torrance, CA) for 30 minutes, and then embedded into O.C.T. Tissues were sectioned coronally at a 12μm thickness on a ThermoShandon Cryotome® cryostat (Thermo Electron Corporation, Waltham, MA). Sections were captured onto Superfrost Plus

slides (Fisher Scientific, Nepean, ON) and stored at –80^{o}C.

For lipophilic dye 1,1'-dioctadecyl-3,3,3',3'-tetramethylindocarbocyanine perchlorate (diI; Molecular Probes, Eugene, OR) labeling, E18.5 embryos were fixed in 4% PFA/PBS for 2 days.

E13.5 and E16.5 *Math5*$^{+/-}$ and *Math5*$^{-/-}$ retinal samples were provided by Dr. Nadean Brown, University of Cincinnati.

Table 1 Knockout mouse lines

Mouse line	**Genetic Strain**	**Provider**	**Reference**
Wild-type	CD-1	Charles River Laboratories, Worcester, MA	de Melo, et al, 2003, de Melo, et al, 2005
Dlx1/Dlx2$^{+/-}$	CD-1	Dr. J. Rubenstein's lab, UCSF	Anderson, Eisenstat et al. 1997
Brn3a$^{+/tLacZ}$	C57/BL6	Dr. E Turner's lab, UCSD	Quina, Pak et al. 2005
Brn3b$^{+/-}$	C57/BL6	Dr. W. Klein's lab, MD Anderson Cancer Centre	Gan, Xiang et al. 1996

3.2 Histological Staining, Immunofluorescence (IF) and immunohistochemistry (IHC)

Frozen sections were allowed to sit at room temperature for 30 mins to air dry, before any histological staining and immunostaining. Histological staining were performed by immersing sections in 0.5% Cresyl Violet dye for two minutes, followed by ddH_2O rinse, graded ethanol wash (50%, 75%, 85%, 95%, 100%, 100% for 2 minutes each), and Xylene twice for 2 minutes each. Slides were air dried in the fumehood and mounted with Permount (Fisher Scientific) and cover slips.

For IF experiments, air-dried sections were placed horizontally in a humidity chamber. 200µl of blocking solution were added to each slide and incubated at room temperature for 2 hours. Primary antibodies were diluted in blocking solution, applied onto slides and incubated overnight at 4^{o}C. Sections were washed in PBS/0.05% Triton X-100 (PBS-T) 3 times for 5 minutes each, and then incubated with secondary antibodies at room temperature for 2 hours. Slides were again washed in PBS-T 3 times for 5mins each, and were mounted using Vectashield fluorescence mounting medium (Vector Laboratories).

For immunohistochemistry (IHC), blocking solution and primary antibodies were applied as described above. Following the third PBS-T washing, slides were then incubated with biotinylated secondary antibodies for 2 hours at room temperature. Sections were again washed with PBS-T 3 times for 5 minutes each. Slides were treated with 0.3% H_2O_2 in PBS for 30 minutes and washed with PBS 3 times for 5 minutes each. Following the final PBS washing, sections were developed using the Vectastain ABC system with DAB substrate reagent (Vector Laboratories, Burlingame, CA).

Negative controls were performed by omitting the primary antibody. For the complete recipe and list of primary and secondary antibodies, refer to Table 1 and to Table 3.

Table 2 Recipe for histological staining and immunostaining solutions

Solution	Recipe
0.5% Cresyl Violet	1 g Cresyl Violet 200ml ddH_2O Stir for about 5hrs in fume hood, till Cresyl Violet dissolves Filter through Whatmann filter #1
Blocking solution (total 100ml)	10 ml 10 X PBS 5 ml horse serum 2 ml 10% Triton X-100 0.2 ml 10% Sodium Azide 100 BSA fraction V ddH_2O to volume 100ml
Washing solution (total 1L)	100ml 10 X PBS 5ml 10% Triton X-100 ddH_2O to volume 1L
4% paraformaldehyde (PFA) (total 50ml)	2 g paraformaldehyde 5 ml 10 X PBS 40 ml ddH_2O 60^oC stir in fume hood, add 5M NaOH till solution clear Adjust PH to 7.2 ddH_2O to volume 50 and filter

Table 3 Primary antibodies used for IHC and IF

Primary Antibody	Dilution	Catalog number and vendor
Rabbit anti-β-Galactosidase	1:5000	A11132, Molecular Probes
Mouse anti-BrdU	1:200	MAB4072, Chemicon, Temecula, CA
Mouse anti-Brn3A	1:100	SC8429, Santa Cruz, Santa Cruz, CA
Goat anti-Brn3B	1:200	SC6026, Santa Cruz, Santa Cruz, CA
Rabbit anti-Caspase3	1:500	9661, Cell Signaling Tech., Beverly, MA
Mouse anti-ChAT	1:100	AB144P, Chemicon, Temecula, CA
Mouse anti-CyclinD1	1:100	2926, Cell Signaling Tech., Beverly, MA
Rabbit anti-DLX1	1:300	Dr. J. Rubenstein, University of California, San Francisco
Rabbit anti-DLX2	1:400	C199 affinity purified, Dr. David Eisenstat, University of Manitoba, MB

Rabbit anti-GABA	1:8000	A2052, Sigma, St. Louis, MO
Rabbit anti-Gad65	1:100	Dev. Studies Hybridoma Bank, University of Iowa
Rabbit anti-Gad67	1:200	MAB5406, Chemicon, Temecula, CA
Rabbit anti-GFAP	1:6000	Dako, Glostrup, Denmark
Goat anti-Glycine transporter (GlyT1)	1:5000	AB1770, Chemicon, Temecula, CA
Mouse anti-ISLET-1	1:600	Dev. Studies Hybridoma Bank, University of Iowa
Mouse anti-NF165	1:50	Dev. Studies Hybridoma Bank, University of Iowa
Rabbit anti-PAX6	1:800	PRB-278P, Covance, Princeton, NJ
Rabbit anti-Phosphohistone H3	1:1000	06-570, Upstate Biochemicals, Charlottesville, VA
Mouse anti-PKC	1:1000	Sigma, St. Louis, MO
Rabbit anti-PROX1	1:500	AB5475, Chemicon, Temecula, CA
Rabbit anti-Recoverin	1:500	AB5585, Chemicon, Temecula, CA
Mouse anti-Rho4D2	1:80	Dr. R Molday, University of British Columbia
Mouse anti-Syntaxin	1:8000	S0664, Sigma, St. Louis, MO
Rabbit anti-Tyrosine Hydroxylase (TH)	1:200	Pel-Freeze, Rogers, AR
Rabbit anti-Tyrosine Hydroxylase (TH)	1:200	AB152, Chemicon, Temecula, CA
Rabbit anti-TRKB	1:200	Santa Cruz, Santa Cruz, CA

Table 4 Secondary antibodies used for IHC and IF

Secondary Antibody	**Dilution**	**Source**
Biotin-SP conjugated goat-anti-rabbit	1:200	Jackson Immunoresearch, West Grove, PA
Biotin-SP conjugated goat anti-mouse	1:200	Jackson Immunoresearch, West Grove, PA
Biotin-SP conjugated rabbit anti-goat	1:200	Jackson Immunoresearch, West Grove, PA
FITC conjugated goat anti-rabbit	1:200	Sigma, St. Louis, MO
Streptavidin conjugated Oregon green-488	1:200	Molecular Probes, Eugene OR
Streptavidin conjugated Texas red	1:200	Vector Laboratories, Burlingame, CA
Texas red conjugated donkey anti-goat	1:200	Jackson Immunoresearch, West Grove, PA

Texas red conjugated donkey anti-mouse	1:200	Jackson Immunoresearch, West Grove, PA
Texas red conjugated donkey anti-rabbit	1:200	Jackson Immunoresearch, West Grove, PA

3.3 *In situ* hybridization (ISH), combined ISH with IF and combined ISH with IHC

A Plasmid vector containing *Math5* cDNA was obtained from Dr. Carol Schuurmans, University of Calgary; vector with *Crx* cDNA was obtained from Dr. Constance Cepko, Harvard Medical School. Plasmids were linearized by restriction enzyme digestion, followed by phenol/chloroform extraction and ethanol precipitation. Linearized plasmid DNA was labelled by digoxigenin (DIG)-UTP, using DIG RNA labeling mix (Roche 11 277 073 910). For microRNA-124 detection, a DIG-labelled LNA (Locked Nucleic Acid) was purchased (5'-DIG-mmu-miR-124, 39452-0, Exiqon, Woburn, MA).

Frozen sections were allowed to sit in room temperature for 30 min to air dry, before *in situ* hybridization. Slides were fixed in freshly made ice-cold 4% PFA for 10 min at room temperature. PBS/DEPC ddH_2O washed twice for 5 min each. Slides were treated with 20μg/ml Proteinase K in PBS/DEPC ddH_2O for 3 min. This Proteinase K step was omitted if performing combined ISH/IF, or ISH/IHC. PBS/DEPC ddH_2O wash for 5 min. Slides were transferred to freshly prepared acetylation solution, and incubated for 10 min at room temperature (see Table 3.4). Sections were refixed in 4% PFA for 5 min, followed by a PBS/DEPC ddH_2O wash 3 times for 5 min each. Tissues were dehydrated in 70% ethanol for 5 min, and 95%

ethanol for 30 sec. Slides were allowed to air dry on a clean paper towel, and were then placed horizontally in a humidity chamber. 200µl hybridization solution was applied on each slide and incubated in a 55^{o}C oven for 1 hr to pre-hybridize. For each slide, 1µl ribo-probe of interest was diluted in 50µl hybridization solution. The hybridization probe mixture was vortexed briefly before denaturing the probe for 5 min at 80 ^{o}C and quickly chilled on ice. After 1 hr pre-hybridization, the hybridization solution was removed and the probe was applied on tissue, covered by pre-cut Parafilm strip. Care was taken to not trap any air bubbles under the Parafilm strip. Slides were placed back to the humidity chamber and incubated in a 55^{o}C oven for 16 hr. After incubation, slides were washed in pre-warmed 5X SSC for about 15 min at 65^{o}C. Parafilm strips will float off. Slides were then placed in pre-warmed washing solution for 30 min at 65^{o}C, with gentle shaking of the Coplin jar at the 15 min time point. Slides were then washed in RNase buffer at 37^{o}C 3 times for 10 min each. Slides were treated with 20µg/ml RNase-A in RNase buffer for 30 min at 37 ^{o}C.

Slides were then washed in RNase buffer (15mins at 37^{o}C), washing solution (twice for 20 min each, at 65^{o}C), 2X SSC (15 min at 37 ^{o}C), 0.1X SSC (15 min at 37 ^{o}C), and finally PBS-T (0.1% Tween-20 in PBS) for 15 min at room temperature. Following these washing steps, slides were again placed horizontally in a humidity chamber and incubated with 10% heat-inactivated horse serum in PBS-T for 1 hr at room temperature. Anti-digoxigenin-alkaline phosphatase (AP) Fab fragments antibody (Roche 11 093 274 910) was diluted in 1% heat-inactivated horse serum in PBS-T (dilution factor 1:2000) as the primary antibody. 200µl of primary antibody

were applied to each slide and incubated at 4 °C for 16 hr. After incubation, primary antibody was removed and slides were treated in NTMT with 0.5mg/ml levamisole 4 times at room temperature, for about 6-8 hrs in total. Slides were placed back into the humidity chamber, and NBT/BCIP was applied (Roche 11 681 451 001) in NTMT without levamisole. Incubation was performed overnight at 4°C, or as required for optimal color development. After incubation, slides were washed in PBS 3 times for 5 min each. When not combining ISH with IF or IHC, dehydration in graded ethanols, immersion in Xylene and mounting with coverslips using Permount was done as described in histological staining (refer to 3.2).

For combined ISH/IF, 200µl blocking solution was applied on each slide after the last PBS wash. Primary and secondary antibodies were applied as described above (refer to 3.2). Slides were washed in PBS (but not PBS-T), and sections were mounted with coverslips using Vectashield fluorescence mounting medium (Vector Laboratories).

For combined ISH/IHC, immunohistochemistry was performed as described above on slides following the last PBS wash.

For microRNA detection, the pre-hybridization and hybridization temperatures were 59°C. The LNA probe was denatured at 70°C. The RNaseA treatment step was omitted on Day 2.

Table 5 Recipe for ISH solutions

Solution	Recipe
Acetylation solution	3ml Triethanolamine (TEA, Fisher) 200ml DEPC ddH_2O Stir and adjust PH to 7.6 with HCL Place slides in stirring TEA, add 3ml acetic anhydride (AcAn, Fisher) Stir for 5mins, and incubate still for 5mins
Hybridization solution (total 10ml, store at room temperature)	5 ml Formamide 1g Dextran Sulfate 200µl 50X Denhardt's solution 250µl 10mg/ml Yeast tRNA 600µl 5M NaCL 200µl 1M Tris-HCL (PH8.0) 100µl 0.5M EDTA 100µl 1M $NaPO_4$ 1ml 10% Sarcosyl 2.56ml DEPC ddH_2O to make total volume 10ml
1M $NaPO_4$, PH7.2 (total 50ml)	3.55g $NaHPO_4$ 3.45g NaH_2PO_4 DEPC ddH_2O to total volume 50ml
RNase Buffer (total 1L)	100ml 5M NaCL 10ml 1M Tris-HCL (PH7.5) 10ml 0.5M EDTA (PH8.0) 880ml DEPC ddH_2O
NTMT (total 200ml)	4ml 5M NaCL 20ml 1M Tris-HCL (PH9.5) 10ml 1M $MgCL_2$ 2ml 10% Tween-20 164ml ddH_2O Before use, add 100mg Levamisole
Washing solution (total 600ml)	60ml 20X SSC 300ml Formamide 240ml ddH_2O

3.4 Anterograde DiI Labeling

For anterograde DiI labelling, with neural retina left *in situ*, the cornea and lens were removed from one eye of the fixed E18.5 embryo. With a fine glass pipette, a crystal of DiI (D3911, Molecular Probes) was positioned to cover the optic disc. The embryos were stored in PBS with 0.02% sodium azide, at 37°C for 2 weeks. For optic chiasm analysis, the labeled brains were removed from the skulls and viewed intact and imaged under an Olympus SZX12 fluorescent stereomicroscope. For assessment of the optic central projections, the labeled brains were embedded subsequently in 3% agarose and sectioned coronally at 100μm on a vibratome. Sections were then mounted on slides using Vectashield and imaged with an Olympus IX81 inverted microscope with Fluoview FV500 confocal laser scanning system (Olympus Optical Co., Tokyo, Japan).

3.5 BrdU Labeling, BrdU Birthdating, and TUNEL Assay

For pulse labeling experiments, BrdU (100μg per gram of animal weight) was injected intraperitoneally (i.p.) to pregnant dams 1 hr before euthanization. For birth-dating experiments, BrdU was injected i.p. to pregnant dams 12, 13, or 16 days after the detection of a vaginal plug, and these animals were sacrificed at E18.5. Sections were then incubated in 50% formamide/2X SSC for 2 hr at 65°C, 2X SSC for 5 min at 65°C, and 2N HCL for 30 min at 37°C, followed by 0.1 M Boric acid (pH8.5) for 10 min at room temperature (RT). Slides were washed in PBS-T 3 times for 5 min each, and blocking solution was applied, then a mouse anti-BrdU antibody (1:200; Chemicon, Temecula, CA) and secondary antibody as described above in 3.2.

TUNEL staining was performed using the In Situ Cell Death Detection Kit, TMR Red (Roche Diagnostics) as per the manufacturer's instructions.

3.6 Retinal Explant Culture

Eyes were dissected from E18.5 *Dlx1/Dlx2*/*Brn3b* triple null embryos and wild-type littermates. Eyes were transferred to a Petri dish, and retinas were dissected from eyes in retinal explant culture media, with the lens and iris *in situ*. Retinas were carefully transferred onto Millicell-CM cell culture inserts with 0.4 μM filters (PICM03050, Millipore) with the lens facing away from the membrane. The lens was dissected out, and all the hyaloid blood vessels were removed. Forceps were used to make three or five cuts on the edge of retina, and the retinas were flattened onto the membrane. Cell culture inserts with retinas were transferred into a 6-well plate and retinas were cultured at 37^{o}C with 5% CO_2 in a humidified incubator. All procedures were performed under sterile conditions. Retinal explant culture media contains 50% high glucose MEM (containing 4.5g/l glucose), 25% Hank's solution, 25% Horse serum, 200μM L-glutamine, 6.75mg/ml glucose, 2.5mM HEPES buffer solution and 1% penicillin/streptomycin. Half of the culture media was replaced with fresh media every other day in cell culture hood. After 7 days incubation, retina explants were fixed in 4% paraformaldehyde for 30 minutes, washed with PBS once and placed in 20% sucrose for 1 hour. Explants were then embedded in O.C.T. compound and sectioned as described above.

3.7 Propidium Iodide (PI) Staining and Cell Cycle Analysis

E16.5 or E18.5 retinas were dissociated into single cell suspensions in 1X PBS and fixed in 70% Ethanol overnight at 4ºC. After washing once in 1X PBS, cells were re-suspended in 250µl PI (50µg/ml) and 1µl RNAse (20µg/ml), and incubated for 15 min at RT. Flow cytometry was performed on a FACSCalibur apparatus (Becton Dickinson), and analyzed using BD CellQuest Pro Version 3.5 software.

3.8 Cell Counting and Statistical Analysis

For quantification of retinal neurons in *Dlx1/Dlx2*$^{-/-}$*Brn3b*$^{-/-}$ triple null retinas, direct cell counts were performed on paired wild-type, *Dlx1/Dlx2*$^{+/-}$*Brn3b*$^{-/-}$ (single knockout, KO)), *Dlx1/Dlx2*$^{-/-}$*Brn3b*$^{+/-}$ (double KO) and *Dlx1/Dlx2*$^{-/-}$*Brn3b*$^{-/-}$ (triple KO) retinas, as described previously (de Melo, Du et al. 2005), with minor modifications. Briefly, tissues were sectioned at 12µm, and slides through widest region of the optic nerve head were used as a centered start point. For E13.5 and E16.5 embryos, the start section and sections 60 and 120µm above and below the start section were used, and for E18.5 embryos, sections 120 and 240 µm above and below the start section were used for IF. Results from five sections were pooled to provide a cell count for each examined eye. For RGCs, BRN3a expressing (BRN3a+) and ISL1+ cells located in the GCL were counted for E16.5 and E18.5 retinas; only ISL1 was used to count RGCs in E13.5 retinas due to the late expression of BRN3a. PAX6+ cells in the inner neuroblastic layer (NBL) but not the GCL or outer NBL, were counted as amacrine cells; Syntaxin+ cells in the GCL were counted as dislocated amacrine cells; and

PROX1+ cells located in the outer NBL were counted as horizontal cells. For BrdU birthdating studies, the BRN3a and BrdU double positive cells represented the RGCs born at the time of BrdU injection; Syntaxin expressing cells in GCL labeled with BrdU represent the dislocated amacrine cells born at the time of the BrdU pulse.

For quantification of amacrine cells in retinal explant, ChAT+ cells were counted on a 500μm long retina explant. 4 sections with 100μm interval were counted and the results were pooled to provide a cell count for each examined eye.

Statistical analyses were performed with SPSS software, and the paired T-test was used to determine statistical significance between sets of cell counting data. Significance was considered for p-values less than 0.05.

3.9 Microscopy and Imaging

Histological images were acquired using an Olympus BX51 microscope with either a SPOT 1.3.0 digital CCD camera (Diagnostic Instruments Inc., Sterling Heights, MI) or an Olympus DP70 digital camera. Fluorescent images were acquired using an Olympus IX81 inverted microscope with a Fluoview FV500 confocal laser scanning system (Olympus Optical Co., Tokyo, Japan). DiI labeled brains were dissected viewed intact and imaged using an Olympus SZX12 fluorescence stereomicroscope equipped with a SPOT 1.3.0 digital camera. Images were processed using Adobe Photoshop 5.5 software (Adobe Systems) for the purposes of presentation.

3.10 Chromatin Immunoprecipitation (ChIP) and Electrophoretic Mobility Shift Assays (EMSA)

E16.5 retina tissues were isolated for ChIP assays under conditions described previously (Zhou, Le et al. 2004; de Melo, Zhou et al. 2008). Oligonucleotide primers used for PCR amplification were designed according to the promoter region of the *Brn*3b gene sequence (MGI 102524). For the primer sets, refer to Table 5. The target region (S4-pro) is 318 bp and located at position 81,326,124-81,326,442, on mouse chromosome 8, within the 5' proximal promoter 2.6 Kbp upstream of the *Brn*3b transcription start site. Genomic DNA derived from the E16.5 mouse embryo tail was used as a positive control. PCR products were separated by 1% agarose gel electrophoresis, visualized by ethidium bromide (EB) gel staining and then purified for TOPO TA cloning (Invitrogen, Burlington, ON) and sequencing confirmation.

For EMSA, we used the same S4-pro region, which was excised from the pCR2.1-TOPO vector (Invitrogen) with EcoRI, and labeled with α-P^{32}-dATP (Perkin Elmer) using the Klenow (large) Fragment of DNA PolI (Invitrogen). The binding reaction mixture contained labeled probes (90,000 cpm), binding buffer (20% glycerol, 5mM $MgCl_2$, 2.5mM EDTA, 2.5mM DTT, 250mM NaCl and 50mM Tris-HCl pH7.5), 1μg poly-dI-dC, and purified recombinant DLX1 or DLX2 protein, and was incubated for 30 min. at RT. 100-fold excess unlabeled probes were used for "cold competition" experiments; rabbit polyclonal DLX1 and DLX2 antibodies were used for "supershift" experiments; and a rabbit polyclonal antibody to mouse immunoglobulin G (Jackson Immunoresearch) was used as an "irrelevant" antibody control.

For EMSA on the Brn3a promoter region, we used 3a-1 region and 3a-3 region. For oligos used for EMSA refer to Table 5.

3.11 Cell Culture and Reporter Gene Assays

The Human Embryonic Kidney cell line-293 (HEK-293) was grown in alpha Dulbecco's Modified Eagle's medium (DMEM) (Gibco) with 10% fetal bovine serum at 37°C with 5% CO_2. 24 hours prior to transfection, cells were seeded at a density of $1x10^7$ per 36 mm^2 dish. Lipofectamine 2000 reagent (Invitrogen) was used to transiently transfect luciferase gene reporter plasmids. Reporter plasmids were constructed by inserting the 318 bp S4-pro fragment into the pGL3-basic vector (Promega). Three putative DLX DNA binding sites (TAAT/ATTA) in S4-pro were deleted respectively by site-directed mutagenesis using the Quick Change Kit (Stratagene). The products of these mutations (Δ1, Δ2 and Δ3) were verified by DNA sequencing. Effector plasmids expressing *Dlx1 and Dlx2* genes were constructed by insertion of a PCR amplified 790 bp *Dlx1* cDNA and 1020 bp *Dlx2* cDNA (provided by Dr. J. Rubenstein, UCSF) into the pcDNA3 vector (Invitrogen). The plasmid pRSV-β-gal (Promega) was co-transfected as an internal control for assessment of transfection efficiency.

3.12 Primary Embryonic Retinal Cell Culture and siRNA Transfection

E14.5 CD-1 mice retinas were dissociated with Accumax (Sigma-Aldrich), and cultured on poly-L-lysine and laminin-coated 6-well plates. Cells were cultured in

DMEM/F12 medium supplemented with HEPES, 0.1% BSA, 1% FBS, N2 and B27 (Invitrogen), at 37^{o}C with 5% CO_2 for 24 hours before interfering RNA (siRNA) transfection. Two duplex siRNAs were designed to target mouse *Dlx*2 coding sequence and a control siRNA was synthesized to scrambled *Dlx*2 coding sequence (Invitrogen). siRNAs were prepared and transfected as previously described (de Melo, Zhou et al. 2008). RNA was isolated 48hrs after transfection.

3.13 Real-time quantitative PCR analysis

RNA was extracted from cultured retinal cells with TRIzol (Invitrogen), and treated with DNase (Sigma) prior to reverse transcription. 1μg RNA was used to synthesize cDNA with SuperScript II reverse transcriptase (Invitrogen). For each sample, 1μl cDNA was then used as a template for *Dlx2*, *Brn3b* and *Gapdh* amplification. Real-time quantitative PCR was performed using the iCycler iQTM Multi-color real-time PCR detection system (Bio-RAD). mRNA copy numbers were calculated utilizing standard curves generated by using plasmids containing the target sequences. *Gapdh* was used as an internal control to normalize *Dlx2* and *Brn3b* mRNA expression levels. Primers used refer to Table 5.

RT-PCR on *Brn3a* transcript was performed as above; for primers refer to Table 5.

Table 6 Primers and Oligonucleotides

Primer	Sequence
ChIP primers	
Brn3b P1S	5’-CCTCCTGCAGAATCTGAAGC-3’
Brn3b P1A	5’-CCGAAGCCATCCCAAGG-3’
Brn3b P2S	5’-GCCAGTCACACATTCACCTTC-3’
Brn3b P2A	5’-GAGGATACTGTTGAACTGACTGG-3’
Brn3b P3S	5’-TCAACAGTATCCTCTCTATTTCATG-3’
Brn3b P3A	5’-GAACTTCTCTTTGTCCCTCCTC-3’
Brn3b P4S	5’-GTTCAGCAGACTGTTGCCAC-3’
Brn3b P4A	5’-TCCTTCCTCACTCAACACTGAG-3’
Brn3b P5S	5’-TCCTTCCTCACTCAACACTGAG-3’
Brn3b P5A	5’-GCCAGTGTCTTGCTGGTCC-3’
Brn3b P6S	5’-GCATGGACCTCGCTAAGG-3’
Brn3b P6A	5’-GGAGACACCGAGCTTCACC-3’
Brn3a S1	5’-CGGTTCTGTGGTTTCCTTTC-3’
Brn3a A1	5’-GCGAGGGACTGGGAAATAGT-3’
Brn3a S2	5’- GGTAGGTGGGTTCGATGAGA-3’
Brn3a A2	5’- CTCTCCTCTCCTCTCCTCTCC-3’
Brn3a S3	5’-TGCAGACCTTCTTGTTGTGC-3’
Brn3a A3	5’-GCTTTGGACCCTTGCTTTTT-3’
Brn3a S4	5’- GCCCTTGATCTGCTGCTACA-3’
Brn3a A4	5’- GCTTTGGACCCTTGCTTTTT-3’
Brn3a S5	5’- GGTGGTGCCTGACACAGTTA-3’
Brn3a A5	5’- AGAAATGCGCTGTGGATGAT-3’
Brn3a S6	5’- AGCGCATTTCTGTGTTGCTA-3’
Brn3a A6	5’- GAAGAAAGCCAGGATGCAAG-3’
Eomesodermin Eo3b007	5’-GACCAACTTGCCACAAAAAACCC-3’
Eomesodermin Eo3b008	5’-CTGAACAGGCTTGCTGCATGCTC-3’
URE2 S	5’-GCCCCGTCTTCCTAAATC-3’
URE2 A	5’-TAACCACCCAAACACCAGT-3’
Dlx1 S	5’-AGGCGGTCTTTAGTTAGG-3’
Dlx1 A	5’-CACTTTGGGGTCTT-3’
I12b S	5’-AGCGGTCCTGTGAGTGGT-3’
I12b A	5’-GGGGGCAGGCATTCA-3’
Dlx2 S	5’-CTGCTCCCAATCTCACTA-3’
Dlx2 A	5’-CCTGCTTTCCCCATAC-3’

EMSA Oligos	
3a1Mtf1S	5’-CCTTTTATTATCACTCTCGAAACCTGGCTATTAAGA-3’
3a1Mtf1A	5’-TCTTAATAGCCAGGTTTCGAGAGTGATAATAAAAGG-3’
Mut13a1Mtf1S	5’-CCTTTTACGATCACTCTCGAAACCTGGCTACGAAGA-3’
Mut13a1Mtf1A	5’-TCTTCGTAGCCAGGTTTCGAGAGTGATCGTAAAAGG-3’
3a1Mtf2S	5’-TTAACAAATTAATTAATCCTAATGAATTAACACTTC-3’
3a1Mtf2A	5’-GAAGTGTTAATTCATTAGGATTAATTAATTTGTTAA-3’
Mut13a1Mtf2S	5’-TTAACAAATCGATCGATCCTCGTGAACGAACACTTC-3’
Mut13a1Mtf2A	5’-GAAGTGTTCGTTCACGAGGATCGATCGATTTGTTAA-3’
3a1Mtf3S	5’-CAGTCCATGAATTAAATTTTCATGCAGTGATTAAAGGCT-3’
3a1Mtf3A	5’-AGCCTTTAATCACTGCATGAAAATTTAATTCATGGACTG-3’
Mut13a1Mtf3S	5’-CAGTCCATGAACGAAATTTTCATGCAGTGACGAAAGGCT-3’
Mut13a1Mtf3A	5’-AGCCTTTCGTCACTGCATGAAAATTTCGTTCATGGACTG-3’
3a1Mtf4S	5’-TTCGTTAAAATTTTATAATAAATCAGGGCAATGTG-3’
3a1Mtf4A	5’-CACATTGCCCTGATTTATTATAAAATTTTAACGAA-3’
Mut13a1Mtf4S	5’-TTCGTTAAAATTTTATCGTAAATCAGGGCAATGTG-3’
Mut13a1Mtf4A	5’-CACATTGCCCTGATTTACGATAAAATTTTAACGAA-3’
RT-PCR Primers	
Brn3bRT-S	5’-GTCGGCAGCCTCCTCTTCTTCTGTG-3’
Brn3bRT-A	5’-GCTTCTCGCGGTGGGATTTCTCAG-3’
Brn3aRT-S	5'-GCA GCG TGA GAA AAT GAA CAA-3’
Brn3aRT-A	5'-CCC CCA AAT GAG AGC AGA AAC-3'
Dlx2RT-S	5’-CCAAACTCAGGTCAAAATCTG-3’
DLX2RT-A	5’-TTAGAAAATCGTCCCCGCG-3’
GAPDH-RT-S	5’-CTCATGACCACAGTCCATGC-3’
GAPDH-RT-A	5’-CACATTGGGGGGTAGGAACAC-3’
Genotyping primers	
DlxNeo-S	5’-TCCAGCCCCTACATCAGTTCC-3’
DlxNeo-A	5’-CTACCCGCTTCCATTGCTCA-3’
Brn3b-S	5’-CGGAGCAGGGCACCTCTCG-3’
Brn3b-A	5’-GGGTTGGAAGACAAGCTCTCCG-3’
Brn3a-S	5’-ACAAGCCGGAGCTCTTCAACGG-3’
Brn3a-A	5’-CAGGATAACGGACAGTCTAAATGA-3’
Dlx1-S	5’-AAGGCGGGGCAGCTCTGGAG-3’

Dlx1-A	5’-AGGGAGACGGGCAGGAAGCG-3’
β-GAL-S	5’-CACAGATGTGGATTGGCGAT-3’
β-GAL-A	5’-CATAATTCAATTCGCGCGTCCC-3’
tLacZ-S	5’-TTCGTCATCGGGTCCAGTCC-3’
tLacZ-A	5’-GATGCGACAGCACCCTTAGTG-3’
Cloning primers	
miR124-S1-SacI	5’-gcgagctcCCCCCTCCCTCTCCCTTCAC-3’
miR124-A1-XhoI	5’-gcctcgagGTTCTCCCGCATCCTTTCGTTT-3’
miR124-S2-SacI	5’-gcgagctcGGATTTCCAAGCTGCACT-3’
miR124-A2-XhoI	5’-gcctcgagCCTCATCTTTTTGTTCTCCTTT-3’
miR124-S5-SacI	5’-gcgagctcTGATCAGGCGCATAGACAG-3’
miR124-A5-XhoI	5’-gcctcgagTAGGAGGGGTGGGTAAGAACTA-3’

3.14 *In utero* electroporation

C57/BL6 mice were intercrossed to generate timed pregnancies for *in utero* electroporation experiments. Embryos were staged using the day of the vaginal plug as embryonic day (E) 0.5. For gain-of-function experiments, *Dlx*2 cDNAs were cloned into pCIG2, an expression vector containing a CMV/β-actin enhancer/promoter and an IRES-mCherry cassette. Endotoxin-free plasmid DNA for electroporation was generated using a column-based purification system (Qiagen; Mississauga, ON). *In utero* electroporation was performed as described (Langevin, Mattar et al. 2007; Mattar, Langevin et al. 2008). Briefly, DNA at a concentration of 3 μg/μl was mixed with Fast Green FCF dye and injected with pulled borosilicate needles and a Femtojet microinjector into the E13.5 or E14.5 retinal region, taking advantage of the pigmented retinal epithelium (RPE) to target injections. Platinum tweezer-style electrodes (Protech; 5mm) and a BTX electroporator were used to apply seven 30 mS pulses of 40 to 60 mV spaced 1S apart. The uterus was replaced in the

maternal body cavity, the peritoneum was sutured and skin stapled and embryos were allowed to develop until E18.5. Electroporated eyes were identified by mCherry epifluorescence and positive retina tissues were prepared and analyzed by immunofluorescence microscopy as mentioned above.

3.15 SDS-PAGE and Western-blot

Protein lystates from E18.5 retina were used for SDS-PAGE. Briefly, retina tissue was dissolved in RIPA solution (1% triton, 158 mM NaCl, 10 mM Tris-HCl ph 7.6, 0.1% SDS, 1% Na-deoxycholate, 1 mM EDTA), with 1X protease inhibitor cocktail and 1 mM PMSF. Protein concentration was measured using the BCA Protein Assay Reagent (ThermoScientific). After boiling protein samples in 1X loading buffer (prepared from 4X SDS Buffer: 0.25M Tris-HCl pH 6.8, 8% SDS, 10% 2-Mercapto-!ethanol, 30% Glycerol, 0.02% Bromophenol blue) for 5 mins, samples were loaded to 12% SDS acrylamide gel, and run for 1.5hr at 140 V at room temperature. Samples were then transferred onto a PVDF membrane at 30V overnight in the cold-room. Primary and secondary antibodies were diluted in 5% milk (1X TBST) for Western blotting. ECL Kit (GE Healthcare Life Sciences) and ECL Plus film (GE Healthcare Life Sciences) were used to detect protein signal.

Chapter 4: Results

4.1 DLX2 and BRN3B expression in the embryonic mouse retina

DLX1 and DLX2 share similar expression profiles in the embryonic retina (de Melo, Qiu et al. 2003). To determine the earliest expression pattern of DLX2 during retinogenesis, we affinity purified specific anti-DLX2 polyclonal antisera (Eisenstat, Liu et al. 1999) for immunofluorescence (IF). Using this purified antibody, DLX2 expression was first detected at E11.5 (de Melo, Zhou et al. 2008), when the earliest postmitotic RGCs begin to differentiate. This is a day earlier than was previously reported (Eisenstat, Liu et al. 1999). A high-dorsal-to-low-ventral expression gradient of DLX2 was observed in the E11.5 retina, although DLX2 was expressed throughout the retina at E13.5 (Fig. 3 A, D). In contrast to the central inner retina restricted expression of BRN3B, DLX2-expressing cells were more dispersed although DLX2 was not expressed in the most peripheral retina. At E11.5, approximately one-third of BRN3B expressing cells co-expressed DLX2 (Fig. 3 C). However, at E13.5, more than 70% of BRN3B immunopositive cells co-expressed DLX2. By this stage, DLX2 expression was well-established in the outer retina (Fig. 3 D-F). In the E16.5 inner neuroretina, almost all BRN3B+ cells co-expressed DLX2 (Fig. 3 G-I). At E18.5, DLX2 continued to be strongly expressed in the neuroblastic layer (NBL), whereas BRN3B expression was localized to the ganglion cell layer (GCL), entirely as a subset of DLX2+ cells (Fig. 3 J-L).

Fig. 3

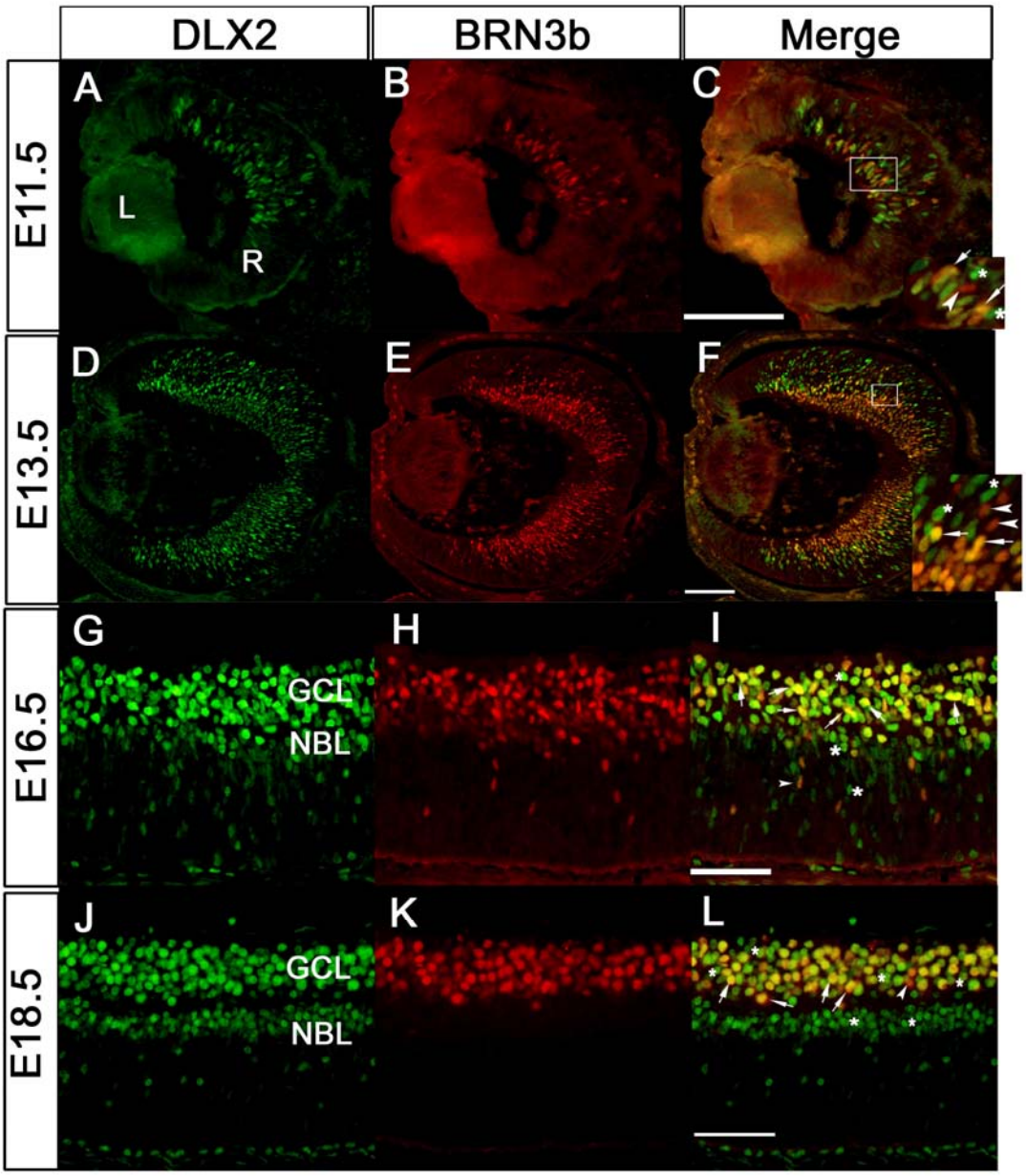
DLX2
BRN3b
Merge
E11.5
E13.5
E16.5
E18.5
A
B
C
D
E
F
G
H
I
J
K
L
L
R
GCL
NBL
GCL
NBL

Fig. 3 DLX2 and BRN3b co-expression pattern from E11.5 to E18.5

(A-C) Both DLX2 and BRN3b are first detected at E11.5, and show a high-dorsal-to-low-ventral expression gradient. DLX2 expression is more dispersed than BRN3b. Only a few double positive cells are located in the central inner retina (arrow), while most cells are either DLX2 (asterisks) or BRN3b (arrow head) single positive. (D-F) In contrast to the restricted central inner expression of BRN3b, DLX2 is expressed throughout the E13.5 retina. More cells are co-labeled by DLX2 and BRN3b (arrow) than in E11.5 retina. (G-I) DLX2 expression is primarily localized to the inner retina at E16.5. Most BRN3b+ cells are in the GCL and co-express DLX2 (arrow). (J-L) At E18.5, DLX2 expression is primarily localized to the GCL and inner NBL, whereas BRN3b is expressed only in the GCL. BRN3b+/DLX2+ cells are observed in the GCL, with very few BRN3b single + cells (arrow head). Some DLX2 single + cells are still distinguished in the GCL and inner NBL (asterisks). R, Retina; L, Lens; GCL, ganglion cell layer; NBL, neuroblastic layer. Scale bar: 50μm.

4.2 Absence of *Dlx*1/*Dlx*2 and *Brn*3b gene function leads to defective retinal ganglion cell genesis

To better understand the role of function of *Dlx*1/*Dlx*2 and *Brn*3b gene in retinal development, we generated *Dlx*1/*Dlx*2 and *Brn*3b triple knockout mice. The *Dlx*1/*Dlx*2/*Brn*3b triple null mice die shortly after birth at P0, and have normally structured eyes with recognizable lamina, a well developed lens, iris, cornea and RPE at E18.5. Previous studies demonstrated that the absence of *Dlx*1/*Dlx*2 leads to a 33% loss of late-born RGCs at E18.5 and the deletion of *Brn3b* causes a 60-70% reduction of RGCs in the mature retina depending upon the background genetic strain. However, neither the *Dlx*1/*Dlx*2 double nor *Brn3b* single knockouts had defects in other retinal cell classes (Erkman, McEvilly et al. 1996; Gan, Xiang et al. 1996; de Melo, Du et al. 2005). With this prior knowledge, we predicted that the triple knockout retina (TKO) would have severe abnormalities in RGC differentiation and survival with a significantly reduced GCL but the remaining RGCs would be positioned normally. Histological analysis demonstrated a thinner *Dlx*1/*Dlx*2/*Brn*3b triple null retina (Fig. 4 D), compared to wild-type. However, this reduced retinal size was not primarily due to the decreased GCL, but to a decreased NBL. Unexpectedly, the *Dlx*1/*Dlx*2/*Brn*3b triple null retina showed only a modestly reduced GCL with well preserved cellularity (Fig. 4 A, D). Second, in the triple null retinas the nascent inner plexiform layer (IPL) separating the GCL and NBL was markedly reduced. In the majority of the triple mutant eyes, the NBL was fused with the GCL (Fig. 4 D boxed). This finding indicates abnormal differentiation of RGC, amacrine or bipolar cells, with fewer

synaptic connections formed. Third, we observed a much thinner optic stalk in sections of *Dlx*1/*Dlx*2/*Brn*3b triple null eyes at E18.5 which is consistent with a reduction in RGC (Fig. 4D).

To assess RGC differentiation, we analysed retinal sections prepared from E18.5 embryos. Antibodies to BRN3A and ISL1 were used as specific RGC markers (Ma, Yan et al. 2004). Although the GCL thickness was only modestly affected by the absence of *Dlx*1/*Dlx*2 and *Brn*3b (Fig. 4 D, Fig. 5D, H), few RGC were detected in the triple mutant retinas (Fig. 5 D, H). Quantification of cell numbers showed a ~95% reduction of BRN3A+RGCs in triple null retinas (78.5±14) compared to wild-type controls (2701±148) ($t=16.19$, $p<0.01$, $n=4$) and a more than 80% loss of ISL1+ cells in triple null retinas ($t=18.37$, $p<0.01$, $n=4$) (Fig. 5 M, N). Not surprisingly, notable decreases of BRN3A+ cells (37%) and ISL1+ cells (40%) were also observed in *Dlx*1/*Dlx*2 double knockout retinas (Fig. 5 C, G, M, N), in agreement with previous studies. However, the loss of RGC numbers in *Brn*3b single knockout retinas (64% of BRN3A cells, 56% of ISL1 cells) at E18.5 (Fig. 5 B, F, M, N), did not reach the 70% loss of mature RGCs previously reported (Erkman, McEvilly et al. 1996; Gan, Xiang et al. 1996; Gan, Wang et al. 1999). To determine whether the loss of *Dlx*1/*Dlx*2 and *Brn*3b affects RGC in early retinal development, we analysed E13.5 and E16.5 embryos. At E16.5, both BRN3A and ISL1 positive RGC numbers were diminished in *Brn3b* single, *Dlx*1/*Dlx*2 double and triple knockout retinas, with the most severe loss evident in *Dlx*1/*Dlx*2/*Brn*3b triple null eyes (data not shown). For E13.5 tissues, we used ISL1 as the RGC marker due to the low expression level of BRN3A. Strikingly,

a marked 82% reduction of ISL1+ expression was observed only in the triple null retinas ($t=9.23$, $p<0.01$, $n=4$), but not in the *Brn*3b single knockout or *Dlx*1/*Dlx*2 double knockout (Fig. 5 I-L, O). A similar reduction in ISL+ RGCs was observed in E12.5 *Dlx*1/*Dlx*2/*Brn*3b triple null retinas (Fig. 6). This result indicates that *Dlx*1/*Dlx*2 and *Brn*3b may have redundant functions during early retinogenesis, since neither knockout mouse alone demonstrated defective early retinal neuronal differentiation.

Fig. 4

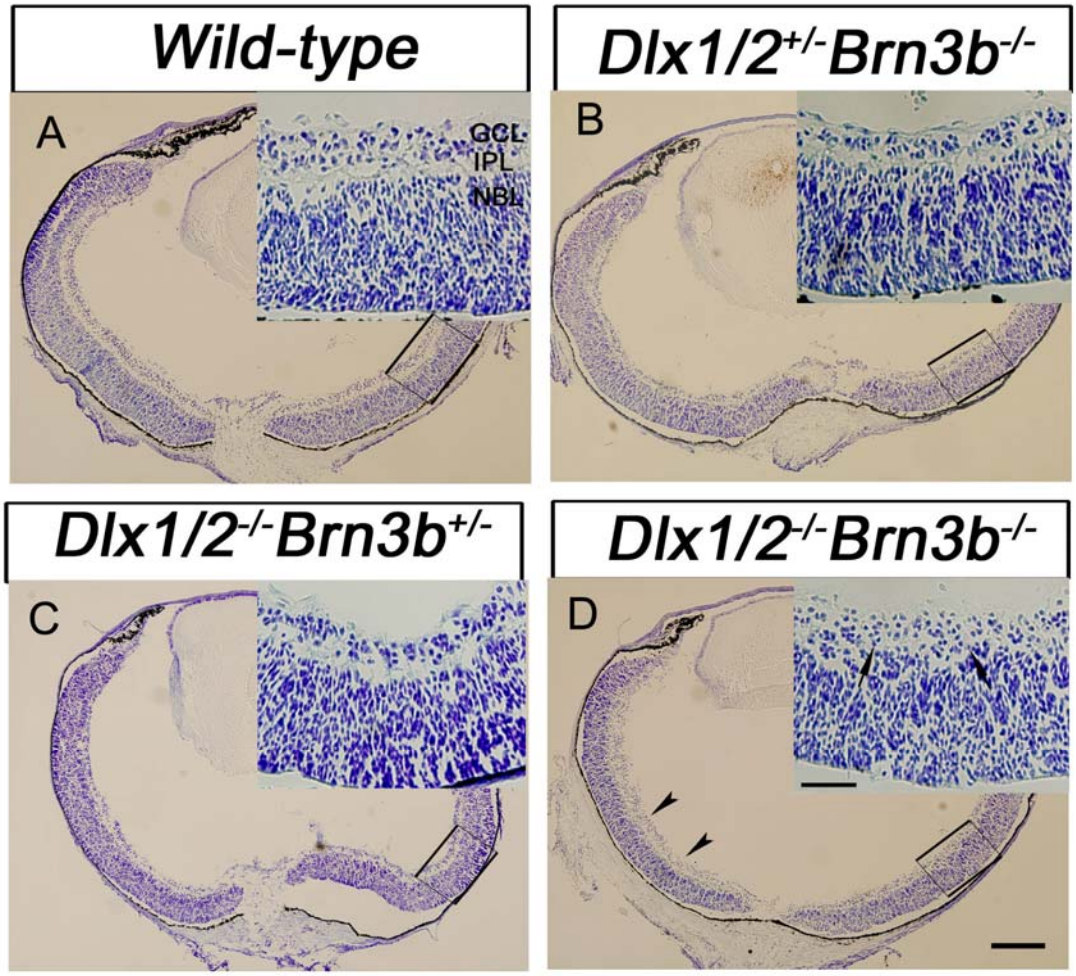
Wild-type
A
GCL
IPL
NBL
Dlx1/2+/-Brn3b-/-
B
Dlx1/2-/-Brn3b+/-
C
Dlx1/2-/-Brn3b-/-
D

Fig. 4 Histological characterization of wild-type, *Dlx*1/*Dlx*2$^{+/-}$*Brn*3b$^{-/-}$, *Dlx*1/*Dlx*2$^{-/-}$*Brn*3b$^{+/-}$, and *Dlx*1/*Dlx*2$^{-/-}$*Brn*3b$^{-/-}$ retinas

(A-D) Cresyl Violet staining of E18.5 retinas shows reduced GCL thickness of the mutant retinas (D). Compared to wild-type (A), the GCL of the *Dlx*1/*Dlx*2$^{+/-}$*Brn*3b$^{-/-}$ single (B), *Dlx*1/*Dlx*2$^{-/-}$*Brn*3b$^{+/-}$ double (C), and *Dlx*1/*Dlx*2$^{-/-}$*Brn*3b$^{-/-}$ triple (D) knockout retinas appear reduced, but no significant difference can be distinguished among these three mutants. An example of the apparent fusion of the GCL and NBL in the triple null retina is demonstrated (D insert, arrow), with no clear IPL shown. Inserts show boxed regions at a higher magnification. GCL, ganglion cell layer; IPL, inner plexiform layer; NBL, neuroblastic layer. Scale bars: 50μm in D; 25μm in insert.

Fig. 5a

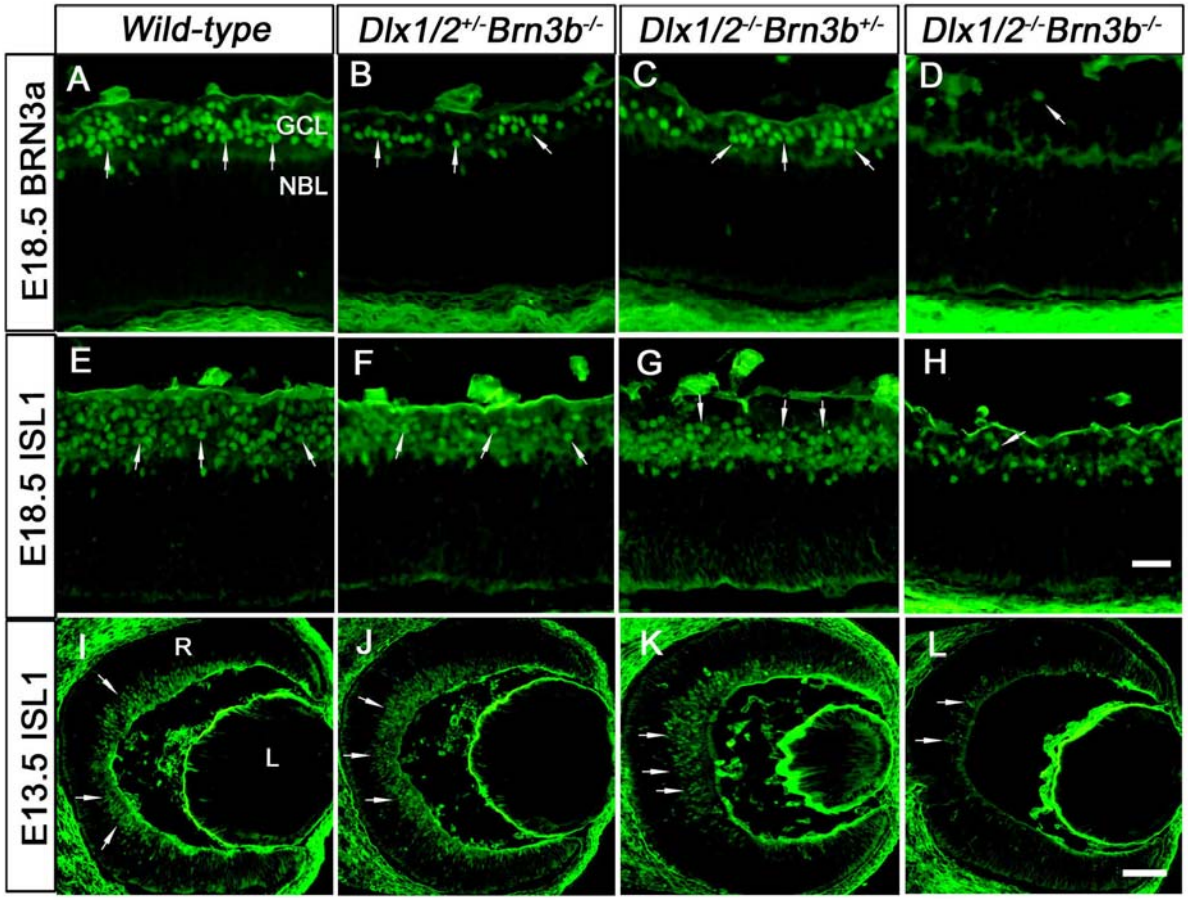
Wild-type
Dlx1/2+/-Brn3b-/-
Dlx1/2-/-Brn3b+/-
Dlx1/2-/-Brn3b-/-
E18.5 BRN3a
E18.5 ISL1
E13.5 ISL1
A
B
C
D
E
F
G
H
I
J
K
L
GCL
NBL
R
L

Fig. 5b

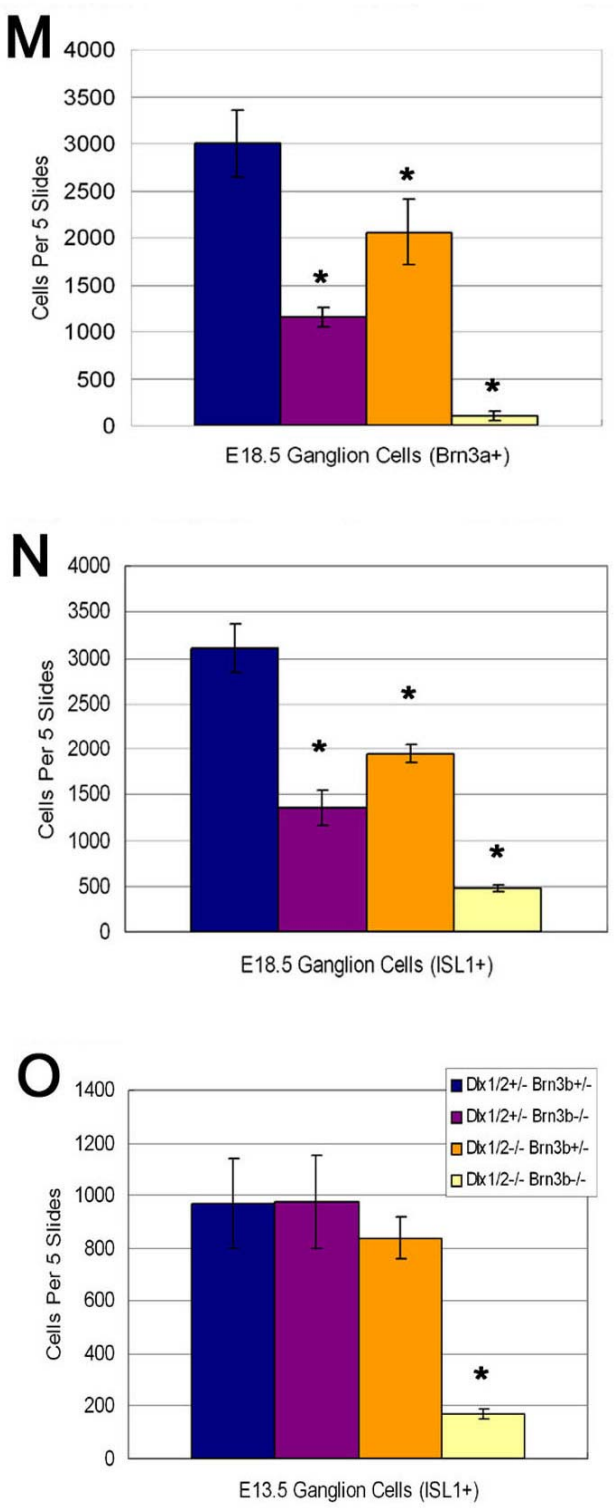
M
4000
3500
3000
2500
2000
1500
1000
500
0
Cells Per 5 Slides
*
*
*
E18.5 Ganglion Cells (Brn3a+)
N
4000
3500
3000
2500
2000
1500
1000
500
0
Cells Per 5 Slides
*
*
*
E18.5 Ganglion Cells (ISL1+)
O
1400
1200
1000
800
600
400
200
0
Cells Per 5 Slides
Dlx1/2+/- Brn3b+/-
Dlx1/2+/- Brn3b-/-
Dlx1/2-/- Brn3b+/-
Dlx1/2-/- Brn3b-/-
*
E13.5 Ganglion Cells (ISL1+)

Fig. 5 Severe RGC loss in *Dlx*1/*Dlx*2$^{-/-}$*Brn*3b$^{-/-}$ retinas

(A-H) Immunostaining with RGC specific markers BRN3a and ISL1 shows decreased RGC numbers in *Dlx*1/*Dlx*2$^{+/-}$*Brn*3b$^{-/-}$, *Dlx*1/*Dlx*2$^{-/-}$*Brn*3b$^{+/-}$, and *Dlx*1/*Dlx*2$^{-/-}$*Brn*3b$^{-/-}$ retinas at E18.5. However, the RGC loss is more severe in the triple null retinas (D, H arrow). (I-L) Significant loss of ISL1 positive RGC is only observed in *Dlx*1/*Dlx*2$^{-/-}$*Brn*3b$^{-/-}$ retinas at E13.5, but not in *Brn*3b single or *Dlx*1/*Dlx*2 double mutants. (M-N) Although *Dlx*1/*Dlx*2$^{+/-}$*Brn*3b$^{-/-}$ and *Dlx*1/*Dlx*2$^{-/-}$*Brn*3b$^{+/-}$ mutants show reduced number of RGC at E18.5, a much more severe RGC loss is detected in the triple null retinas (95% reduction in BRN3a+ cells and 84% reduction in ISL1+ cells). (O) At E13.5, an 81% ISL1+ RGC loss only occurs in *Dlx*1/*Dlx*2$^{-/-}$*Brn*3b$^{-/-}$ retinas. Histograms represent the mean ± SD, n=4, *p<0.01. R, Retina; L, Lens; GCL, ganglion cell layer; NBL, neuroblastic layer. Scale bars: 20μm in H (applies to A-H); 50μm in L.

Fig. 6

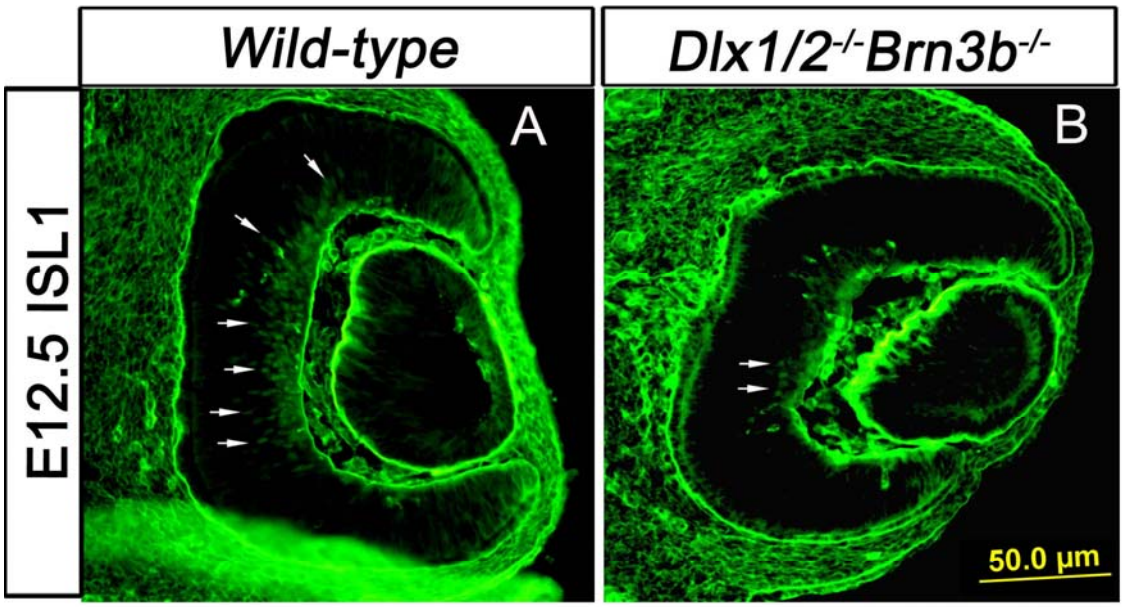

Fig. 6 RGC loss occurs in E12.5 *Dlx*1/*Dlx*2$^{-/-}$*Brn*3b$^{-/-}$ retinas

Immunostaining with a RGC specific marker ISL1 shows early born RGCs are located at the inner central retina of both wild-type and *Dlx*1/*Dlx*2$^{-/-}$*Brn*3b$^{-/-}$ eyes at E12.5 (A, B arrows). Compared to the wild-type retina, RGC number in *Dlx*1/*Dlx*2$^{-/-}$*Brn*3b$^{-/-}$ retina is reduced (A, B). Scale bar: 50μm.

4.3 Cell fate switch from ganglion to amacrine cell in the *Dlx*1*Dlx*2/*Brn*3b null retina

Since GCL cellularity was only modestly affected in *Dlx*1/*Dlx*2/*Brn*3b triple null retinas despite a near absence of RGC, we determined the number of amacrine, horizontal and cone cells, which have highly overlapping birthdates with RGC. Antibodies to PAX6 and Syntaxin were used as amacrine cell markers (Barnstable, Hofstein et al. 1985; Belecky-Adams, Tomarev et al. 1997). We counted PAX6 immunopositive cells located in the inner NBL as amacrine cells. No significant difference was observed between wild-type, *Brn*3b single, *Dlx*1/*Dlx*2 double and *Dlx*1/*Dlx*2/*Brn*3b triple knockout retinas (Fig. 7 A-D, Q). In the GCL, PAX6 is expressed in both RGC and displaced amacrine cells at E18.5 (Belecky-Adams, Tomarev et al. 1997; Inoue, Hojo et al. 2002; de Melo, Qiu et al. 2003). We observed notable reductions of PAX6+ cells in the GCL of *Brn*3b single and *Dlx*1/*Dlx*2 double knockout eyes (Fig. 7 B, C). This reduced PAX6 expression in the GCL is due to RGC loss (Gan, Xiang et al. 1996; de Melo, Du et al. 2005). However, in the triple null GCL, there was only a minimal reduction in PAX6 expressing cells (Fig. 7 D), supporting the presence of more displaced amacrine cells in the triple null GCL, thereby reducing the severity of total cell loss in the combined mutant retina. Syntaxin is a pan-amacrine cell marker and is present in the cell body and dendrites of all amacrine cells, but not RGCs (Barnstable, Hofstein et al. 1985). DAPI was used as a counterstain to facilitate quantification of cells expressing syntaxin and confirmed that the total cell number of the triple null GCL was not reduced to as great an extent as

we had predicted (Fig 7 H). Notably, a significant 1.8 fold increase of syntaxin+ cells was observed in the triple null GCL (1761±122) compared with wild-type controls (930±72) ($t=8.18$, $p<0.01$, $n=4$) (Fig. 7 E-H, R). The amount of syntaxin+ cells in *Brn*3b single and *Dlx*1/*Dlx*2 double knockout GCL were not significantly altered.

For horizontal cells, we used antibodies to NF165 and PROX1 as cell specific markers (Dyer, Livesey et al. 2003). No aberrantly positioned horizontal cells were observed. Quantification of NF165 immunoreactivity was used to determine horizontal cell number. A significant reduction was not observed in the triple null retinas (Fig. 7 I-L, S). Although the majority of cone photoreceptors are born before birth in mice, the well-accepted cell markers for cones, VSX1, cone opsin and peanut agglutinin (PNA) are not clearly detected until P5 (Chow, Snow et al. 2001). Therefore, we detected cone cells in E18.5 retinas with an antibody to recoverin, a calcium-binding protein expressed by cones and cone bipolar cells from E17.5 (Milam, Dacey et al. 1993). Our results did not identify any abnormalities in recoverin+ cells. Recoverin expressing cells were positioned correctly in the outer, peripheral regions of wild type and mutant retinas (Fig. 7 M-P); moreover, cell quantification did not identify any significant differences between wild-type and mutants (Fig. 7 T). Taken together, these results suggest that the combined absence of *Dlx*1/*Dlx*2 and *Brn3b* gene function switches the cell fate of a ganglion cell to that of a dislocated amacrine cell in the GCL, but does not affect the amacrine cells localized to the INL, horizontal, or cone cell differentiation.

Fig. 7a

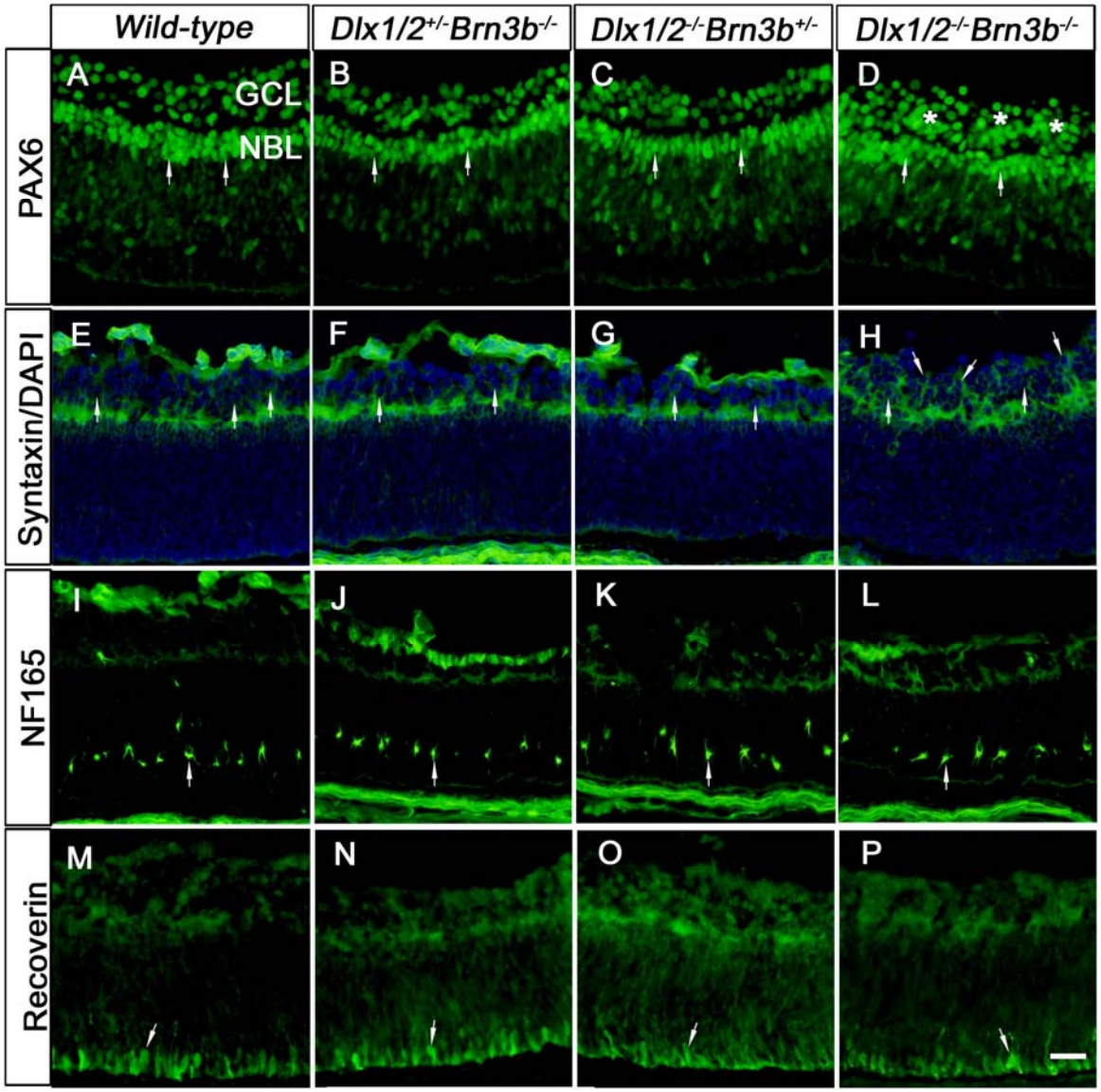
Wild-type
Dlx1/2+/-Brn3b-/-
Dlx1/2-/-Brn3b+/-
Dlx1/2-/-Brn3b-/-
PAX6
Syntaxin/DAPI
NF165
Recoverin
A
B
C
D
E
F
G
H
I
J
K
L
M
N
O
P
GCL
NBL

Fig. 7b

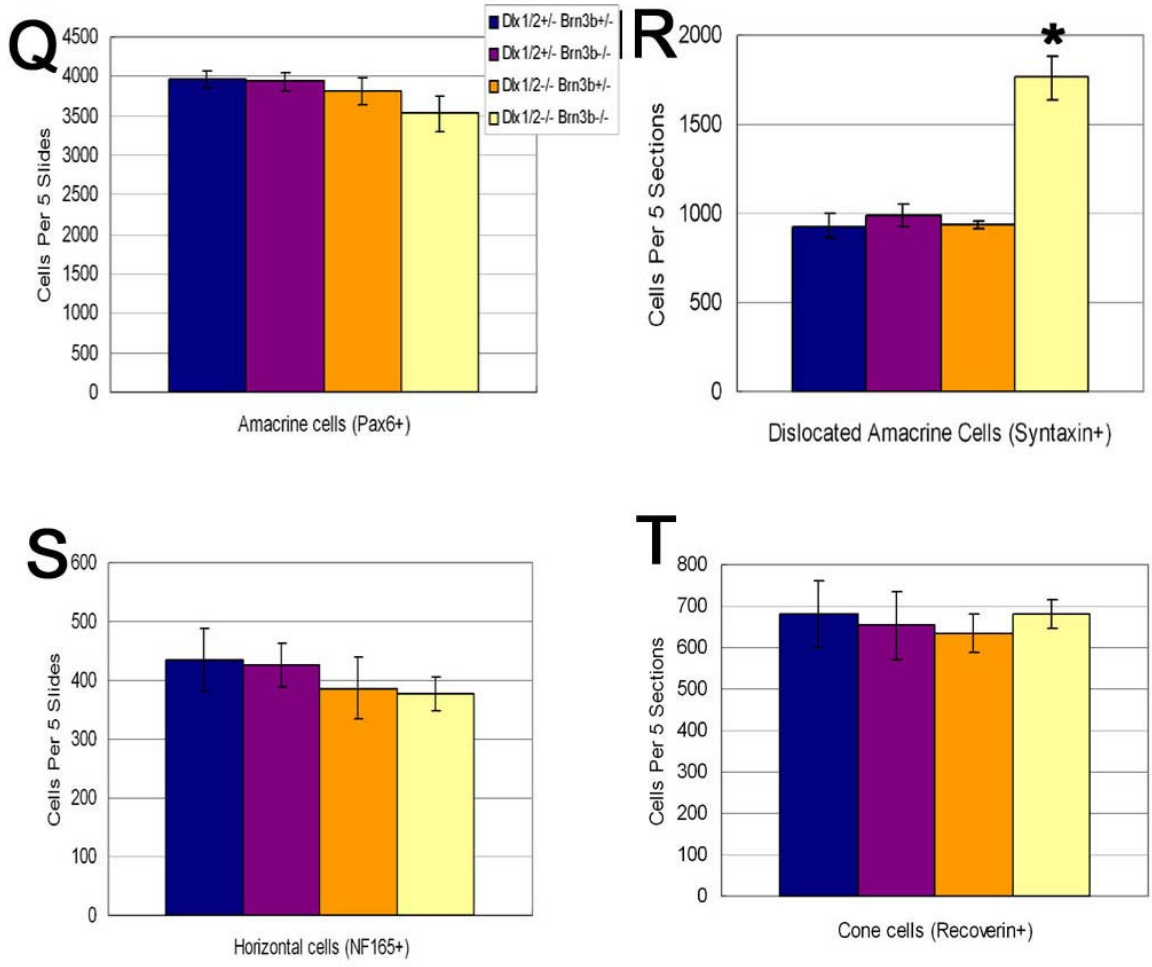
Q
Dlx1/2+/- Brn3b+/-
Dlx1/2+/- Brn3b-/-
Dlx1/2-/- Brn3b+/-
Dlx1/2-/- Brn3b-/-
Cells Per 5 Slides
4500
4000
3500
3000
2500
2000
1500
1000
500
0
Amacrine cells (Pax6+)
R
*
Cells Per 5 Sections
2000
1500
1000
500
0
Dislocated Amacrine Cells (Syntaxin+)
S
Cells Per 5 Slides
600
500
400
300
200
100
0
Horizontal cells (NF165+)
T
Cells Per 5 Sections
800
700
600
500
400
300
200
100
0
Cone cells (Recoverin+)

Fig. 7 Increased amacrine cells are located in the *Dlx*1/*Dlx*2$^{-/-}$*Brn*3b$^{-/-}$ GCL.

(A-D, Q) No significant differences in PAX6 expressing amacrine cells are identified in the inner NBL among the different mutants (arrow, Q). However, more PAX6+ cells are evident in the GCL of the *Dlx*1/*Dlx*2$^{-/-}$*Brn*3b$^{-/-}$ retina (D, asterisks). (E-H, R) Syntaxin immunostaining reveals increased number of displaced amacrine cells in the GCL of the *Dlx*1/*Dlx*2$^{-/-}$*Brn*3b$^{-/-}$ retina (H, arrow). Quantification of syntaxin immunoreactive cells shows a 1.8 fold increase of amacrine cells in the triple null GCL (R). (I-L, S) The horizontal cell marker NF165 is expressed in normal number (S) and position in the triple null retina (arrow). (M-P, T) Recoverin expression is not significantly different between the mutants and wild-type, supporting the conclusion that cone cell differentiation is not affected. Histograms represent the mean ± SD, n=4, *: $p<0.01$. GCL, ganglion cell layer; NBL, neuroblastic layer. Scale bar: 20μm

To further confirm this model, we performed birth-dating experiments by labelling progenitor cells with a single BrdU injection in pregnant animals at E12.5, E13.5 or E16.5 gestational ages. Since retinal progenitors require 16-24 hours to progress through S phase to G1/G0, and because we were obligated to harvest the mutant embryos at E18.5 before they die at birth, we did not perform BrdU labeling at E17.5, or E18.0. BrdU expressing cells are those in their final S phase at the time of BrdU injection, and are therefore marked on the date they were born. Most of the E12.5 and E13.5 birth-dated cells were located in the GCL, with no differences in quantity or spatial expression between *Dlx*1/*Dlx*2/*Brn*3b triple mutants and wild-type controls (Fig. 8 A, B, E, F; data not shown). Few E16.5 birth-dated cells migrated to the GCL, with most remaining in the NBL (Fig. 8 C, D, G, H). The numbers of BrdU expressing cells in the GCL did not show any difference between wild-type and triple mutant sections in the E12.5, E13.5 and E16.5 birth-dated retinas (Fig. 8 I). These results suggest that the absence of *Dlx*1/*Dlx*2/*Brn*3b did not affect the early migration of retinal progenitors to the GCL. Next, we used antibodies to BRN3a (RGC) and syntaxin (amacrine) to determine the identity of these birth-dated cells. Strikingly, very few cells were co-labeled by BRN3a and BrdU in E12.5 birth-dated triple null retinas (14±1 of mutants versus 199±10 of wild-type, $t=24.6$, $p<0.005$, $n=4$; Fig. 8 A, B, J). However, more cells were co-labeled with syntaxin and BrdU in the GCL of these E12.5 birth-dated triple null retinas, as compared with wild-type controls (Fig. 8 E, F, K). These results suggest that in *Dlx*1/*Dlx*2/*Brn*3b null retinas, most of the retinal progenitors, which exit mitosis at E12.5 migrate to the GCL, adopt an

amacrine rather than a RGC cell fate in this cell layer. Similar results were observed in E13.5, as well as E16.5 birth-dated mutants (Fig. 8 C, D, G, H, J, K; data not shown). Therefore, we conclude that the absence of *Dlx*1/*Dlx*2/*Brn*3b results in a cell fate switch from ganglion to displaced amacrine cells.

Fig. 8a

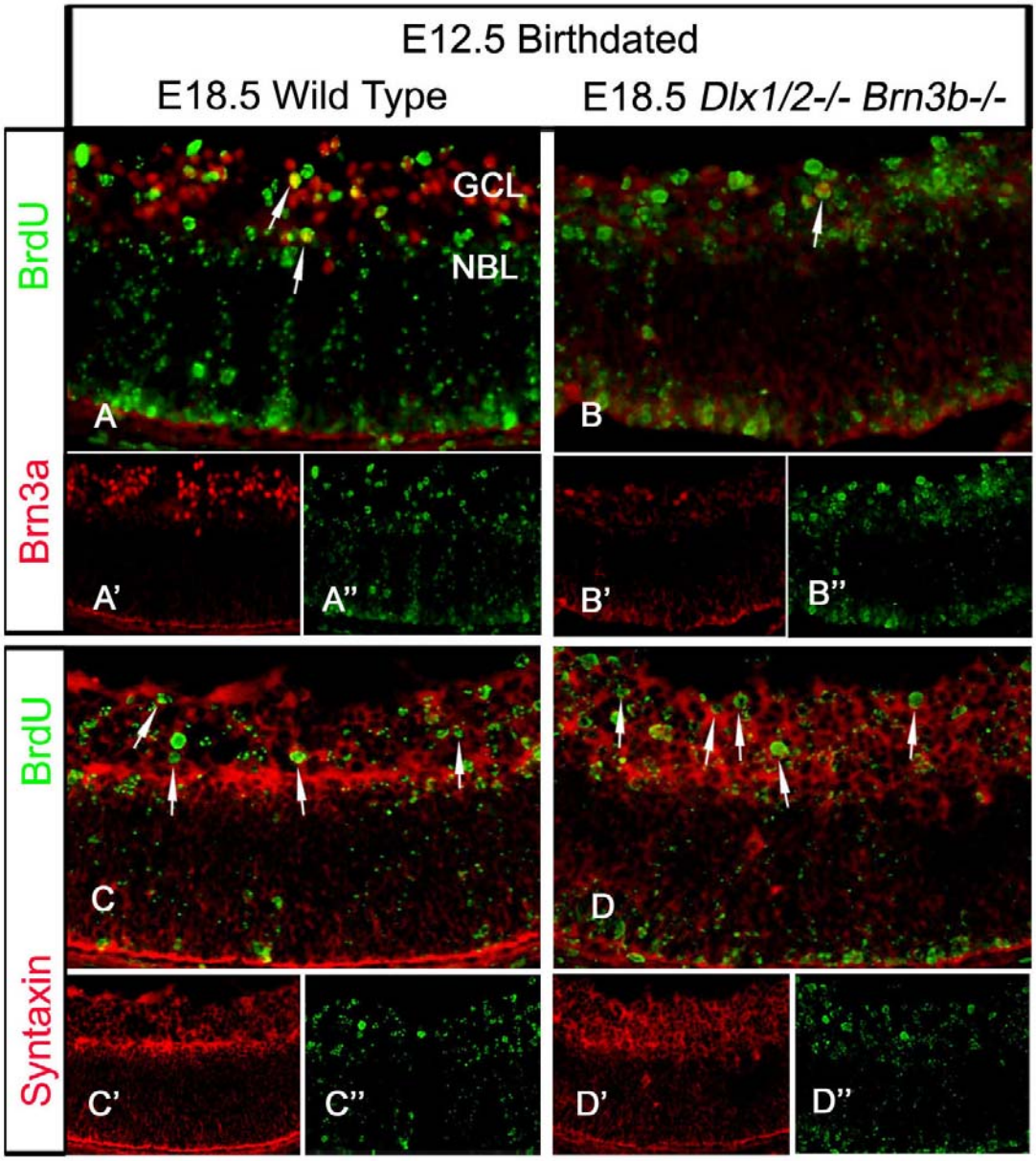
E12.5 Birthdated
E18.5 Wild Type
E18.5 Dlx1/2-/- Brn3b-/-
BrdU
Brn3a
GCL
NBL
A
B
A'
A''
B'
B''
BrdU
Syntaxin
C
D
C'
C''
D'
D''

Fig. 8b

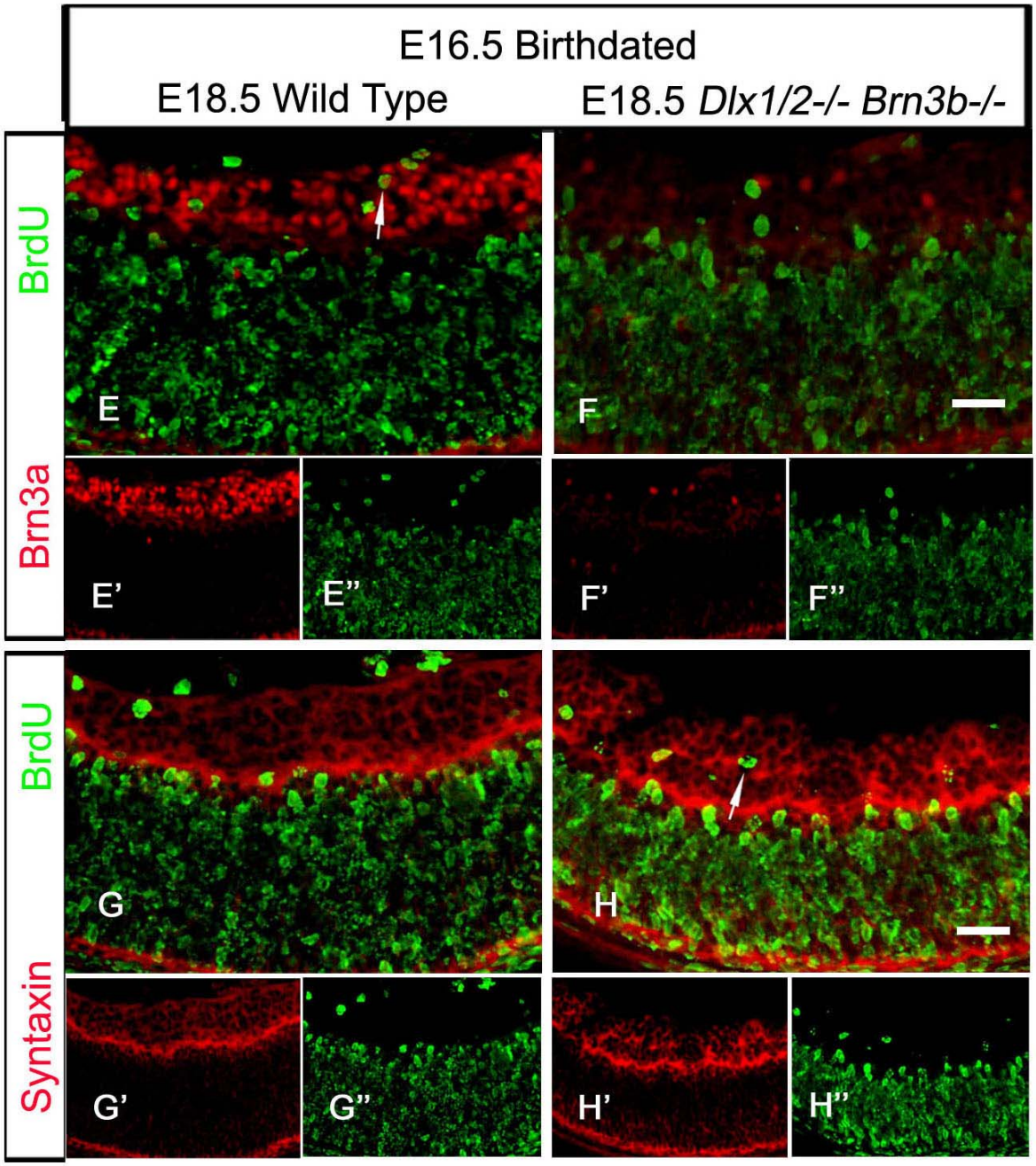
E16.5 Birthdated
E18.5 Wild Type
E18.5 Dlx1/2-/- Brn3b-/-
BrdU
Brn3a
E
F
E'
E''
F'
F''
BrdU
Syntaxin
G
H
G'
G''
H'
H''

Fig. 8c

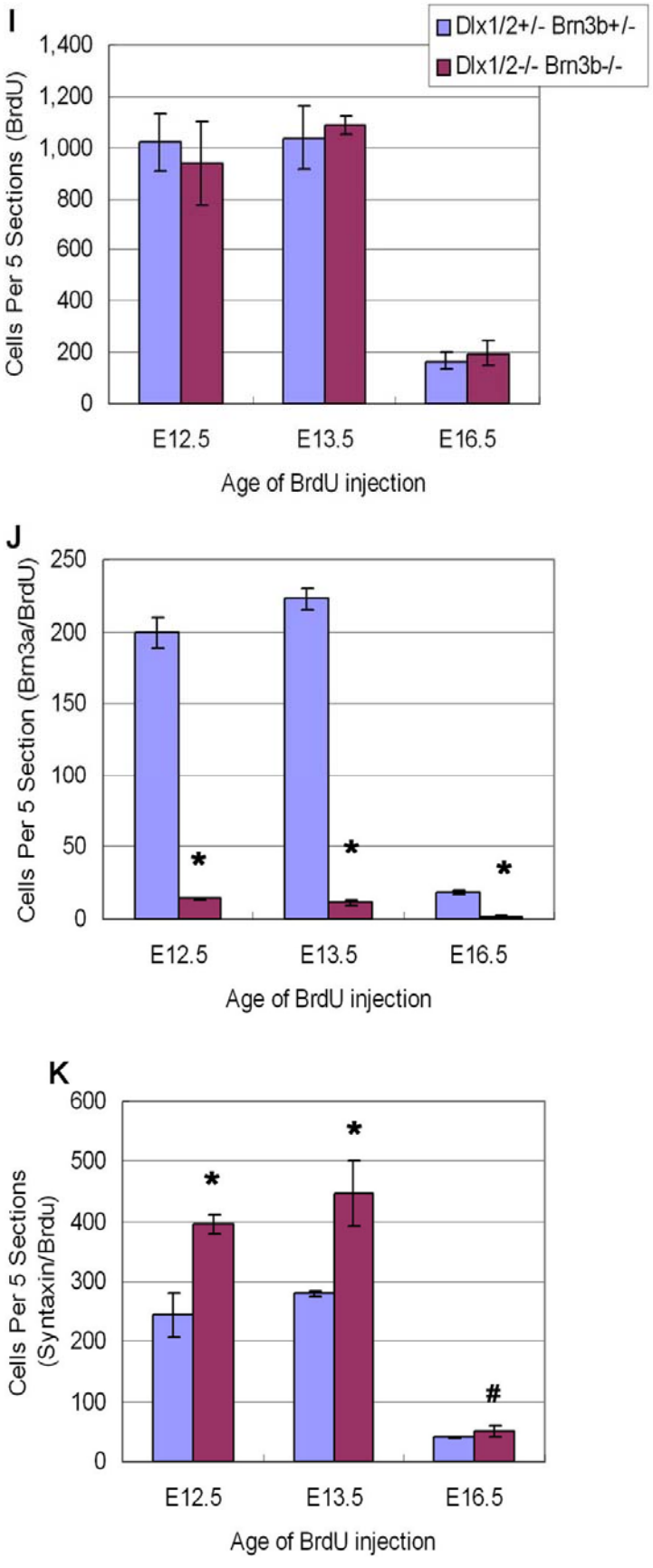
I
Dlx1/2+/- Brn3b+/-
Dlx1/2-/- Brn3b-/-
Cells Per 5 Sections (BrdU)
1,400
1,200
1,000
800
600
400
200
0
E12.5
E13.5
E16.5
Age of BrdU injection
J
Cells Per 5 Section (Brn3a/BrdU)
250
200
150
100
50
0
*
*
*
E12.5
E13.5
E16.5
Age of BrdU injection
K
Cells Per 5 Sections (Syntaxin/Brdu)
600
500
400
300
200
100
0
*
*
#
E12.5
E13.5
E16.5
Age of BrdU injection

Fig. 8 More retinal progenitors adopt a displaced amacrine cell fate in the *Dlx*1/*Dlx*2$^{-/-}$*Brn*3b$^{-/-}$ mutants

(A-D) BrdU pulse labeling at E12.5 and co-expression with BRN3a or Syntaxin reveal that in the *Dlx*1/*Dlx*2$^{-/-}$*Brn*3b$^{-/-}$ retina, few cells are identified as RGC (A, B, arrow), whereas more cells differentiate as amacrine cells and migrate to the GCL (C, D, arrow). Most of the E12.5 BrdU pulse labeled cells are located in the GCL (B'', D''), indicating that deletion of *Dlx*1/*Dlx*2 and *Brn*3b does not affect retinal progenitor cell (RPC) migration. (E-F, G-H) BrdU pulses at E16.5 identify more displaced amacrine cells in the triple null retina as well, although most of the BrdU+ cells remain in the NBL. (I-K) Quantification of E12.5, E13.5 and E16.5 birth-dated cells identify similar quantities of BrdU+ cells located in the GCL of wild-type and *Dlx*1/*Dlx*2$^{-/-}$*Brn*3b$^{-/-}$ retinas (I). During all the embryonic stages tested, RPC of the *Dlx*1/*Dlx*2$^{-/-}$*Brn*3b$^{-/-}$ retina prefer an amacrine cell fate in GCL, rather than RGC (J, K). Histograms represent the mean ± SD, n=4, *: $p<0.005$, #: $p<0.05$. GCL, ganglion cell layer; NBL, neuroblastic layer. Scale bar: 20μm

4.4 The displaced amacrine cells found in *Dlx*1/*Dlx*2/*Brn*3b null retina GCL are cholinergic amacrine cells

To further determine the identity of those amacrine cells displaced to GCL of *Dlx*1/*Dlx*2/*Brn*3b null retinas, we studied postnatal retinas by culturing E18.5 *Dlx*1/*Dlx*2/*Brn*3b null and wild-type retinas for 7 days *in vitro* (DIV7). Although amacrine cells can be divided into more than 30 subtypes, GABAergic and glycinergic amacrine cells are the two major types, representing almost 90% of the total amacrine population (MacNeil and Masland 1998; Voinescu, Kay et al. 2009). The two glutamic acid decarboxylase (GAD) isoforms, GAD65 and GAD67, are highly expressed in the IPL of both wild-type and *Dlx*1/*Dlx*2/*Brn*3b triple null DIV7 retinas. Both GAD67 and GAD65 expressing cell are detected in the GCLs of both wild-type and *Dlx*1/*Dlx*2/*Brn*3b triple null retinas, with no obvious differences detected. Cholinergic amacrine cells (choline acetyltransferase, ChAT expressing) are starburst amacrine cells, and are an early-born subset of GABAergic amacrine cells during retinal development (Voinescu, Kay et al. 2009). ChAT-expressing cells are distributed in a mirror-symmetric way in wild-type retinas (Fig. 9 E). Compared to the wild-type littermates, more ChAT-positive cells are observed in the GCL of *Dlx*1/*Dlx*2/*Brn*3b null retina (98.4±9.7 versus 59.5±3.4, $t=7.53$, $P<0.01$, $n=4$) (Fig. 9, F). These results suggest that the displaced amacrine cells in *Dlx*1/*Dlx*2/*Brn*3b null retinas are GABAergic amacrines, in particular, a population of double GABAergic/cholinergic amacrine cells. Glycine transporter (GlyT1) is used as a glycinergic amacrine cell marker. GlyT1 is localized primarily to the cells in the INL

of both wild-type and *Dlx*1/*Dlx*2/*Brn*3b null retinas (Fig. 9, G, H), with no difference observed between those two genotypes.

Fig. 9

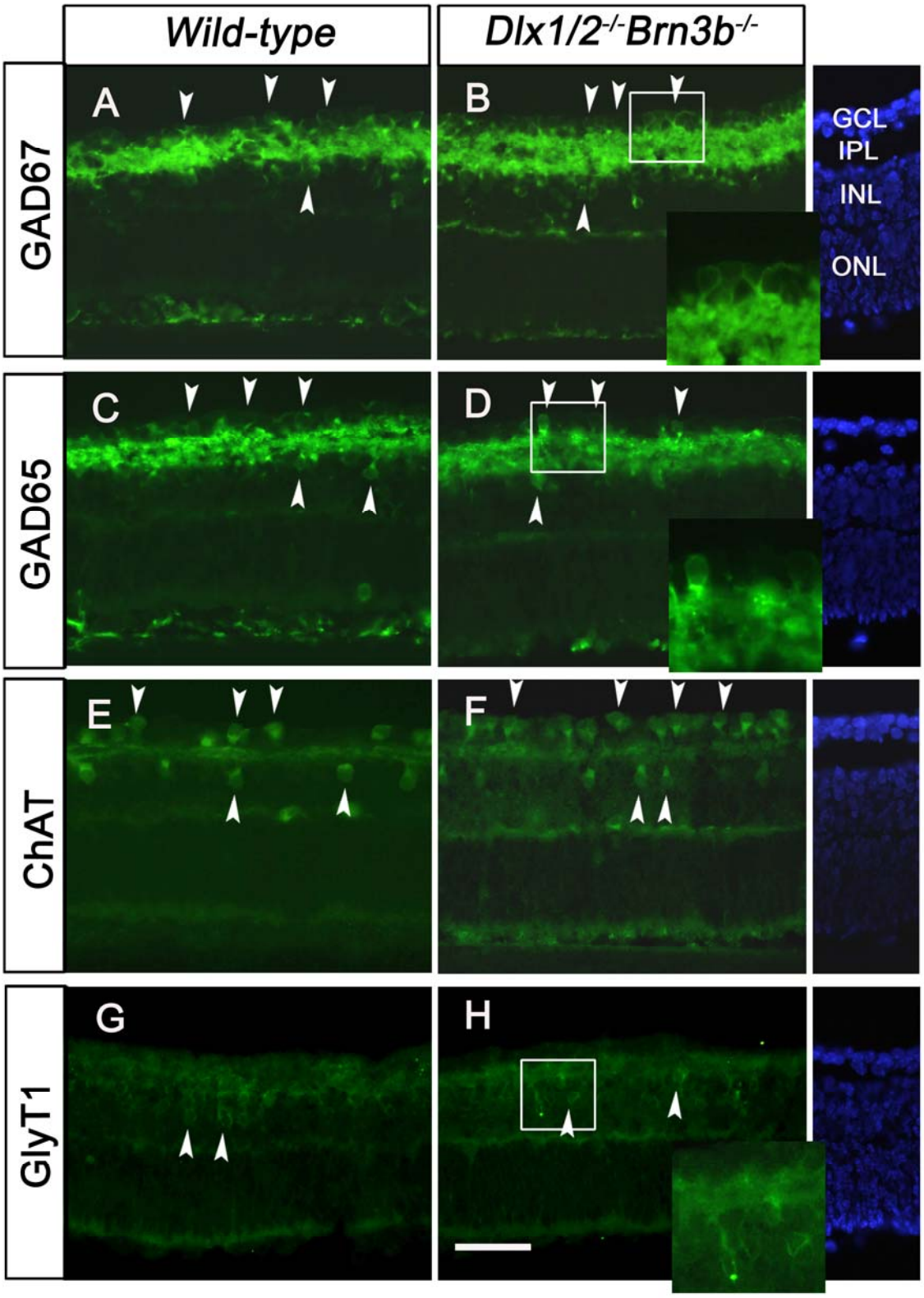
Wild-type
Dlx1/2-/-Brn3b-/-
GAD67
GAD65
ChAT
GlyT1
A
B
C
D
E
F
G
H
GCL
IPL
INL
ONL

Fig. 9 More cholinergic amacrine cells are located in the GCL of *Dlx*1/*Dlx*2/*Brn*3b null retinal explants. (A-D) Both GAD65 and GAD67 are highly expressed in the IPL, as well as the GCL and inner layer of the INL of both wild-type and *Dlx*1/*Dlx*2/*Brn*3b triple null DIV7 retinas (A-D arrow heads). (E-F) More ChAT-expressing cells are located in the GCL of the *Dlx*1/*Dlx*2/*Brn*3b null retina, than in the wild-type retina (E, F arrow heads). (G, H) GlyT1 expression is restricted to the cells in the INL, but not to the GCL, of both wild-type and *Dlx*1/*Dlx*2/*Brn*3b null retinas (G, H arrow heads). GCL, ganglion cell layer; IPL, inner plexiform layer; INL, inner nuclear layer; ONL, out nuclear layer; Scale bar: 20μm

4.5 RGC axon pathfinding defects occur at the optic chiasm in *Dlx*1/*Dlx*2/*Brn*3b mutants

RGC axons form the optic nerves and innervate specific CNS targets. To determine whether the triple gene deletion affects RGC axonal guidance, we used anterograde diI labelling of RGC axons at E18.5. First, we observed a dramatically reduced optic nerve thickness in the *Dlx*1/*Dlx*2/*Brn*3b triple null embryos, confirming the significant reduction of RGCs in the GCL (Fig. 10 D, D'). RGC axons are tightly bundled in the optic nerve and extend to the optic chiasm, where a majority of RGC axons cross the midline and project contralaterally, with a small proportion of axons projecting to ipsilateral targets, as shown in the diI labeled wild-type controls (Fig 10 A). In the *Brn*3b single knockout mice (*Dlx*1/*Dlx*2$^{+/-}$*Brn*3b$^{-/-}$), a larger proportion of RGC axons were observed to aberrantly project into ipsilateral optic tracts, with some of the axons abnormally deviated at the midline of the diencephalon and projecting dorsally (Erkman, Yates et al. 2000). No axonal pathfinding defects were identified at the optic chiasm in the *Dlx*1/*Dlx*2 double knockout mice (*Dlx*1/*Dlx*2$^{-/-}$*Brn*3b$^{+/-}$). Although RGC axonal pathfinding defects were observed in the *Brn*3b knockout mice, half of the mutants had a normal optic chiasm, with tightly bundled axons in the optic nerve and optic tract (Fig. 10 B, E). However, in the triple mutants, all of the examined embryos showed abnormal optic chiasms (Fig. 10 D, E). In most cases, the majority of RGC axons appeared to stall at the midline and failed to extend either contralaterally or ipsilaterally. Of axons which crossed the midline, a large proportion aberrantly projected dorsally to the hypothalamus, instead of to the optic tracts. One

of the more notable defects in the triple mutants was that post-chiasm, all the axons were bundled very loosely. In some cases, a proportion of axons exited the optic nerve bundle prior to reaching the midline (Fig. 10 D, D'). Of interest, unlike the increased proportion of aberrant ipsilateral projections in the *Brn*3b single mutants, very few axons were detected to project ipsilaterally in the *Dlx*1/*Dlx*2/*Brn*3b triple null mutants, with most axons crossing the midline. These findings support a genetic interaction between *Brn*3b and the *Dlx*1/*Dlx*2 transcription factors for RGC axonal pathfinding.

Furthermore, we explored the two central visual targets. The axons from all four genotypes reached the two central targets, the LGN and the SC. Compared to the strong fluorescent signal in the wild-type LGN, a weak but very clear signal was detected in the *Brn*3b single and the *Dlx*1/*Dlx*2/*Brn*3b triple null mutants at the LGN, consistent with the dramatic RGC loss and thin optic nerves (Fig. 11 C, E). As observed in the wild-type LGN, the axons maintain a very strict boundary from the telencephalon in *Dlx*1/*Dlx*2/*Brn*3b triple null mutants, with no obvious aberrant axonal projection in LGN. Similar results were observed at the level of the SC, that the *Dlx*1/*Dlx*2/*Brn*3b triple null mutants show fewer RGC axons projections, but no obvious pathfinding errors (Fig. 11 F-I). This result is different from the previous studies in the *Brn*3b single knock-out mouse, which show aberrant RGC axonal projections at all pathfinding choices (Erkman, Yates et al. 2000).

Fig. 10

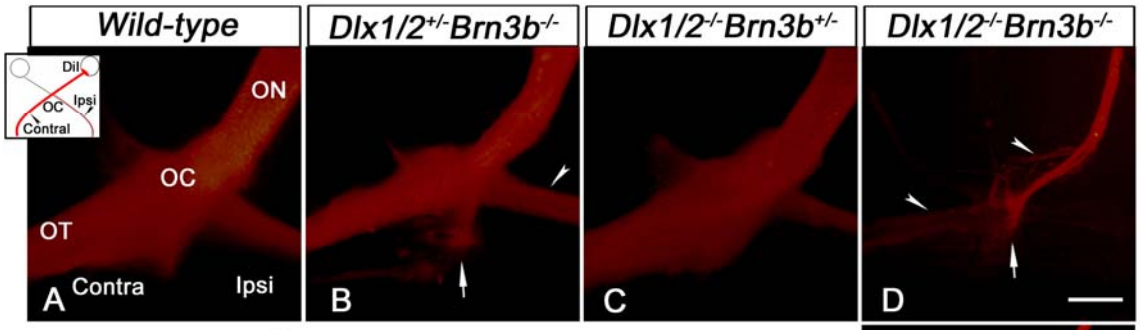

E	Aberrant axon guidance at OC
Wild-type	0/6
Dlx1/2$^{+/-}$ Brn3b$^{-/-}$	2/5
Dlx1/2$^{-/-}$ Brn3b$^{+/-}$	0/5
Dlx1/2$^{-/-}$ Brn3b$^{-/-}$	5/5

Fig. 10 Combined disruptions of *Dlx*1/*Dlx*2 and *Brn*3b result in severe RGC axonal guidance defects at the optic chiasm.

(A-D) Anterograde diI labeling of E18.5 RGC axons in wild-type, *Dlx*1/*Dlx*2$^{+/-}$*Brn*3b$^{-/-}$, *Dlx*1/*Dlx*2$^{-/-}$*Brn*3b$^{+/-}$ and *Dlx*1/*Dlx*2$^{-/-}$*Brn*3b$^{-/-}$ mutants. Aberrant ipsilateral projections were found in *Brn*3b single null mice (B, arrowhead), with some axons projecting dorsally to the hypothalamus (B, arrow). However, no obvious axonal guidance defects were observed at the optic chiasm of *Dlx*1/*Dlx*2 double mutants (C). Of significance, the *Dlx*1/*Dlx*2/*Brn*3b triple null mice feature dramatically reduced optic nerve thickness (D, D'). Severe axonal guidance defects in the triple null mice included de-fasciculated axons in the ON and OT (D, D', arrowheads) and aberrant dorsal projections to the hypothalamus (D, D', arrows). No ipsilateral projections were observed in the *Dlx*1/*Dlx*2$^{-/-}$*Brn*3b$^{-/-}$ mutants. (E) All of the examined triple knockout embryos demonstrated RGC axonal guidance defects. ON, optic nerve; OC, optic chiasm; OT, optic tract; Ipsi, ipsilateral projection; Contra, contralateral projection. Scale bar: 100μm.

Fig. 11

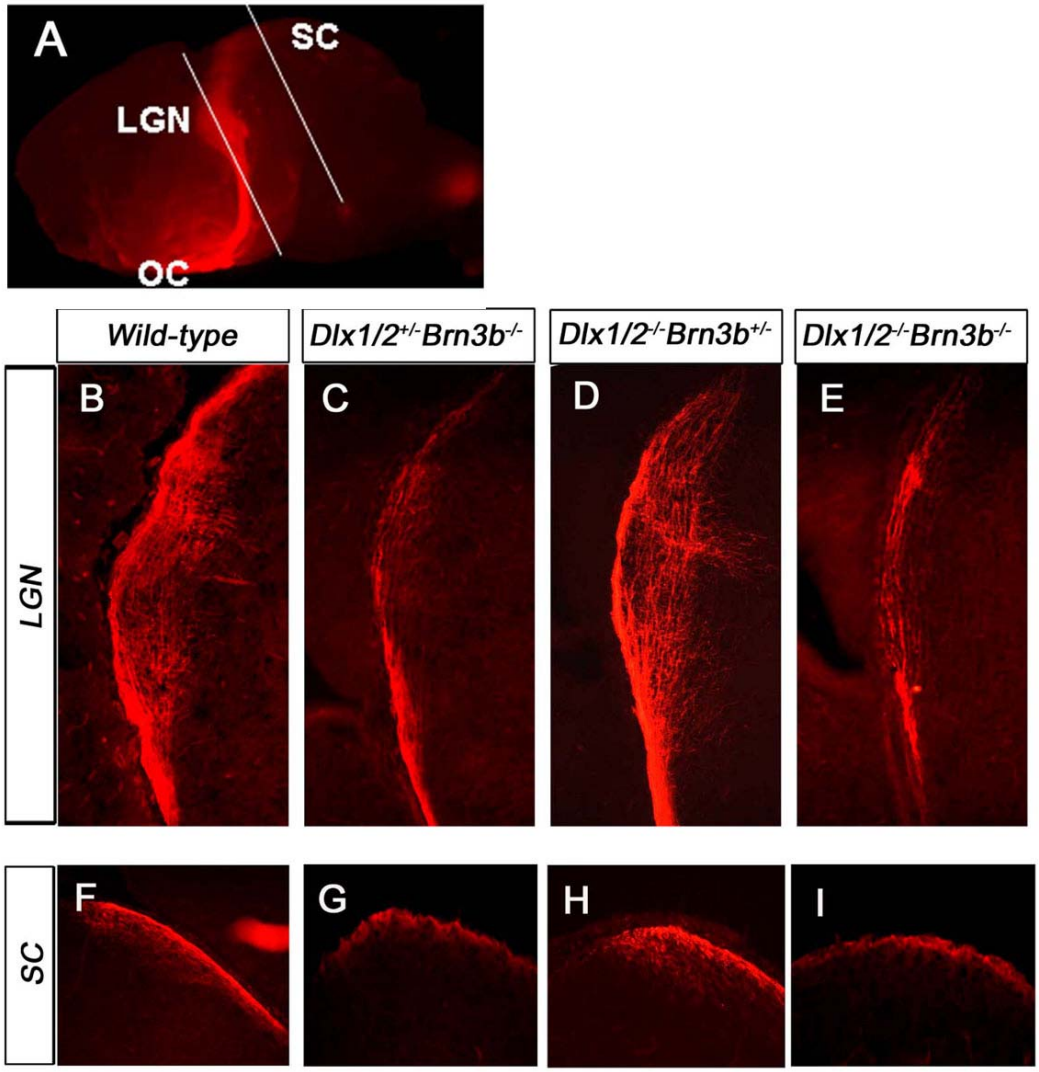
A
SC
LGN
OC
Wild-type
Dlx1/2+/-Brn3b-/-
Dlx1/2-/-Brn3b+/-
Dlx1/2-/-Brn3b-/-
B
C
D
E
LGN
F
G
H
I
SC

Fig. 11 Loss of *Dlx*1/*Dlx*2 and *Brn*3b has no effect on RGC innervation of the LGN and SC

(A) Lateral view of the optic tract of an E18.5 wild-type mouse (telencephalon removed). The optic chiasm is located at the ventral midline of the diencephalon. Two lines represent the section planes for LGN and SC. (B-E) Labeled RGC axons at the lateral geniculate nucleus (LGN). In comparison with the wild-type LGN, the *Dlx*1/*Dlx*2$^{-/-}$*Brn*3b$^{-/-}$ mutant LGN is reduced (E). No axons penetrate into the telencephalon in either one of the phenotypes. (F-I) RGC axons project to the superior colliculus (SC), with no obvious errors found in either one of the phenotypes.

4.6 Increased apoptosis and abnormal cell division in *Dlx1/Dlx2/Brn3b* triple null retina

To test the effects of the triple gene deletion on retinal cell death, we used an antibody to cleaved caspase-3 to quantify apoptosis. At E13.5, the triple null mutants had a significant 4 fold increase in apoptotic cells, compared to the wild-type littermates (70.5±11 of mutants versus 15.5±7 of wild-type, $t=8.37$, $p<0.01$, $n=4$; Fig. 12 A, B, G). However, for E16.5 and E18.5 triple mutants, the number of cleaved caspase-3 positive cells was similar to wild-type (Fig. 12 G). In the triple mutants at E13.5, we observed that the majority of the caspase-3+ cells were confined to the inner retina, where the prospective RGCs are located. Unlike the *Brn*3b single knockouts or *Dlx*1/*Dlx*2 double knockouts (Gan, Wang et al. 1999; de Melo, Du et al. 2005), enhanced apoptosis later than E13.5 was not detected in the *Dlx*1/*Dlx*2/*Brn*3b triple mutants.

To assess cellular proliferation in the triple null mice, we used an antibody to phosphohistone H3 (PH3) to detect M-phase cells and BrdU pulse labeling for S-phase cells. At E13.5, no differences were identified between wild-type and triple mutants. At E16.5, the triple mutant retinas displayed a significant reduction (46%) in M-phase cells as compared to wild-type (Fig. 12 D, H). This reduction of M-phase cells was also observed in E18.5 mutant retinas, with a 41% decrease in PH3+ cells (Fig. 12 H). We observed a similar trend of BrdU labelled cells in the triple mutants, with fewer S-phase cells detected in E16.5 and E18.5 mutants (data not shown). These data suggest that the absence of *Dlx*1/*Dlx*2/*Brn*3b gene function might disturb cell

cycle progression in the retinal progenitor cell population. To further explore this hypothesis, we performed propidium iodide (PI) staining and cell cycle analysis using flow cytometry. In concordance with our prior results, in the triple knockout retinas at E16.5 and E18.5, there were reduced proportions of cells in S or G2/M phases, with more cells remaining at G1/G0, when compared to wild-type littermates (Fig. 12 E, F). Taken together, we conclude that *Dlx*1/*Dlx*2 and *Brn*3b together are functioning in maintaining retinal progenitor cell proliferation and cell cycle progression.

Fig. 12

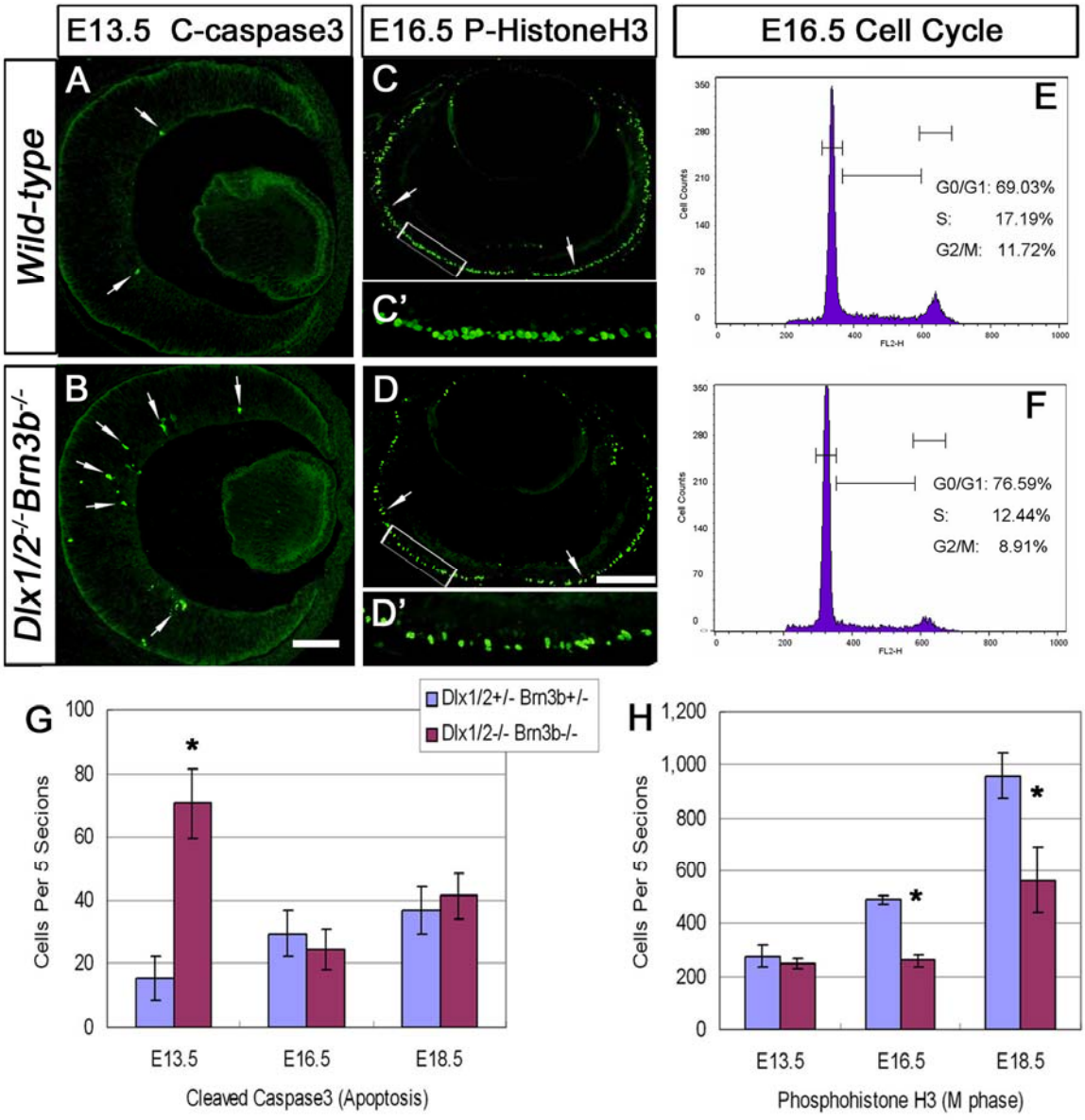
E13.5 C-caspase3
E16.5 P-HistoneH3
E16.5 Cell Cycle
Wild-type
Dlx1/2-/-Brn3b-/-
A
B
C
C'
D
D'
E
F
G0/G1: 69.03%
S: 17.19%
G2/M: 11.72%
G0/G1: 76.59%
S: 12.44%
G2/M: 8.91%
Cell Counts
FL2-H
G
H
Dlx1/2+/- Brn3b+/-
Dlx1/2-/- Brn3b-/-
Cells Per 5 Secions
E13.5
E16.5
E18.5
Cleaved Caspase3 (Apoptosis)
Phosphohistone H3 (M phase)

Fig. 12 Combined losses of *Dlx*1/*Dlx*2 and *Brn*3b result in enhanced apoptosis and abnormal cell proliferation

(A, B, G) Immunostaining of cleaved-caspase-3 shows a 4-fold increase of apoptotic cells in E13.5 *Dlx*1/*Dlx*2$^{-/-}$*Brn*3b$^{-/-}$ retinas (B, G). There is no significant difference in the number of apoptotic cells at E16.5 and E18.5 (G). (C-D, H) Anti-phosphone-histone H3 labeling and quantification revealed decreased numbers of M-phase cells at E16.5 and E18.5 in *Dlx*1/*Dlx*2/*Brn*3b triple null retinas (D, D', H). However, this reduction of M-phase cells was not detected at E13.5 (H). C' and D' show higher magnification of the boxed regions in C and D, respectively. (E, F) Cell cycle analysis shows lower percentages of S-phase and G2/M phase cells at E16.5 in the *Dlx*1/*Dlx*2$^{-/-}$*Brn*3b$^{-/-}$ retinas. Histograms represent the mean ± SD, n=4, *: $p<0.01$. Scale bars: 50μm in B; 25μm in D.

4.7 *Math5* and *NeuroD* expression are unaffected by the deletion of *Dlx1/Dlx2* and *Brn3b*

Previous studies have established *Math5*, a bHLH proneural gene that is expressed early in retina development, as a master control gene in RGC fate commitment. Loss of *Math5* function results in massive RGC loss and an increase of amacrine cells as well as cone photoreceptor cells (Brown, Kanekar et al. 1998; Brown, Patel et al. 2001; Liu, Mo et al. 2001; Wang, Kim et al. 2001). Interestingly, the increased amacrine cells in the *Math5* mutant retinas are dislocated into the GCL, similar to the phenotype that we observed in the *Dlx*1/*Dlx*2/*Brn*3b triple null retinas. *Math5* promotes RGC cell fate by regulating a network of downstream RGC-differentiation genes, which include *Brn3a* and *Brn3b*. We considered whether the RGC loss and amacrine cell fate shift in the *Dlx*1/*Dlx*2/*Brn*3b triple null retinas was through a similar *Math5* regulatory pathway. Unlike the well established regulatory relationship between *Math5* and *Brn3b*, whether *Dlx1* and/or *Dlx2* are part of the *Math5* transcriptional network remains unclear. To explore the relationship between *Dlx1/Dlx2* and *Math5*, we first studied their gene expression patterns in the developing retina. Combined ISH and IF were performed on mouse retinas at different developmental stages. *Math5* mRNA and DLX2 protein co-express in the early developing retina, but not at late embryonic stages (Fig 13). At E11.5, both *Math5* and *Dlx2* are expressed by cells located in the central retinal region. By E13.5, more *Dlx2* single positive cells are detected in the inner central retina, where the differentiated RGCs are located. *Math5* mRNA is expressed throughout the retina at

this stage, with absence in the inner central region (Fig 13 D-F). *Math5* expression is dramatically down-regulated after E16.5, and is restricted to the proliferating region at the ciliary margin at E18.5 (Fig 13 G, J). *Dlx2* is expressed strongly in the inner NBL and GCL in later embryonic stages. Few double *Math5/Dlx2* positive cells are detected at this developmental stage in the retina.

We further tested if *Dlx2* expression is altered in the *Math5* mutant retina. Dual IF experiments with BRN3b and DLX2 antibodies were performed on retinas of *Math5* mutants and wild-type littermates. As expected, a thinner GCL was noticed in *Math5*$^{-/-}$ retinas, and BRN3b expression was severely reduced in the E16.5 *Math5*$^{-/-}$ retina (Fig. 14 E, H) (Brown, Patel et al. 2001; Wang, Kim et al. 2001). Unlike the dramatically reduced BRN3b expression that we observed, the reduction of DLX2 expression was subtle in the E16.5 *Math5*$^{-/-}$ retina. DLX2 was expressed strongly in the remaining cells of the GCL in the *Math5*$^{-/-}$ retina (Fig. 14 F). Interestingly, the few BRN3b positive cells remaining in the GCL of the *Math5*$^{-/-}$ retina all expressed DLX2 (Fig. 14 G). These data suggest that in the absence of *Math5*, DLX2 is functioning to promote or maintain *Brn3b* expression in the developing retina. DLX2 expression, however, is not significantly affected by the absence of *Math5*. Similar results were observed in the E15.5 *Math5*$^{-/-}$ retina (data not shown, unpublished observations, Dr. Nadean Brown).

Finally, we explored whether *Math5* expression is altered in the absence of *Brn3b*, *Dlx1/Dlx2*, or all three genes. Using *in situ* hybridization, we studied *Math* mRNA levels at E13.5, when *Math5* is robustly expressed throughout the retina.

Math5 expression was readily detected in the wild-type, *Brn3b* single mutant, *Dlx1/Dlx2* double mutant and *Dlx*1/*Dlx*2/*Brn*3b triple mutant retinas. No obvious difference was found amongst these four genotypes (Fig. 15 A-D). Taken together, these data suggest that *Math5* is genetically located upstream of the *Brn3b* pathway, but is parallel to the *Dlx1/Dlx2* pathway in RGC development (Fig. 35).

A second bHLH proneural gene, *NeuroD*, is shown to play a role in amacrine cell development. Loss of *NeuroD* function in retinal explants results in delayed amacrine cell differentiation. There are no detectable amacrine cells in the *ath3/neuroD* double knockout mouse. Mis-expression of *NeuroD* promotes amacrine cell production (Morrow, Furukawa et al. 1999; Inoue, Hojo et al. 2002). Here we also considered whether *NeuroD* was promoting the amacrine cell fate shift observed in our *Dlx*1/*Dlx*2/*Brn*3b triple null model. Unexpectedly, the distribution and numbers of the *NeuroD* expressing cells remain similar in the wild-type and *Dlx*1/*Dlx*2/*Brn*3b triple null retina at E18.5 (Fig. 15 E, H). Despite the increased displaced amacrine cells in the GCL of the triple null retina, *NeuroD* expression was not detected in that layer (Fig. 15 H). Interestingly, a subtle decrease of *NeuroD* expression was observed in the *Brn3b* single mutant retina, but the significance of this finding awaits further clarification (Fig. 15 F). These data suggest that the loss of *Dlx*1/*Dlx*2 and *Brn*3b has no effect on *NeuroD* expression, and increased amacrine cell differentiation in the *Dlx*1/*Dlx*2/*Brn*3b triple null retina is not due to *NeuroD* upregulation. Our findings are consistent with *NeuroD*'s place upstream of *Dlx*1/2 and *Brn*3b in parallel and non-overlapping genetic pathways.

Fig. 13

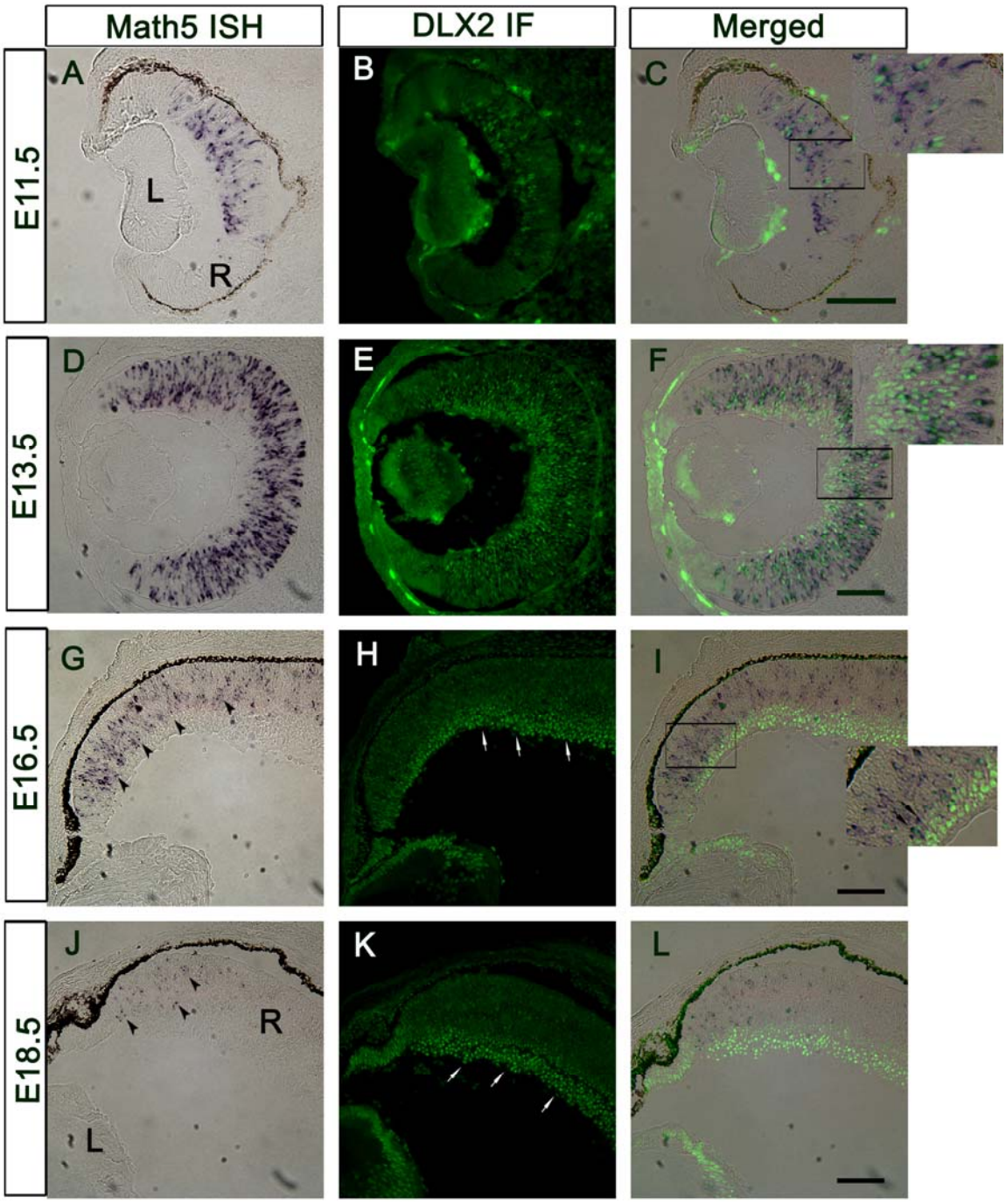
Math5 ISH
DLX2 IF
Merged
E11.5
E13.5
E16.5
E18.5
A
B
C
D
E
F
G
H
I
J
K
L
L
R
R
L

Fig. 13 Combined *in situ* hybridization/immunofluorescence shows that *Math5* mRNA and DLX2 protein are co-expressed in early developing retina, but not in late embryonic stages.

(A-C) Both *Math5* mRNA and DLX2 protein are expressed in the central region of E11.5 retina. (D-F) at E13.5, *Math5* mRNA is expressed throughout the retina, except the inner central region. At this stage, the *Math5*/DLX2 double positive cells are located in the middle layer of retina. DLX2 single positive cells are readily detected in the inner central retina. Math5 single expressing cells, however, are restricted to the outermost proliferating zone of retina. (G-I) *Math5* expression is dramatically down-regulated at E16.5 (G, arrow heads). DLX2 is strongly expressed in the GCL and inner NBL (H, arrows). Double positive cells with *Math5*/DLX2 are still detectable in the NBL (I insert, arrows). (H-L) At E18.5, *Math5* is confined to the region closed to ciliary margin (J, arrow heads). DLX2 expression is restricted in the GCL and inner NBL (K, arrows), without double positive cells. R, Retina; L, Lens; GCL, ganglion cell layer; NBL, neuroblast layer. Scale bar: 100μm

Fig. 14

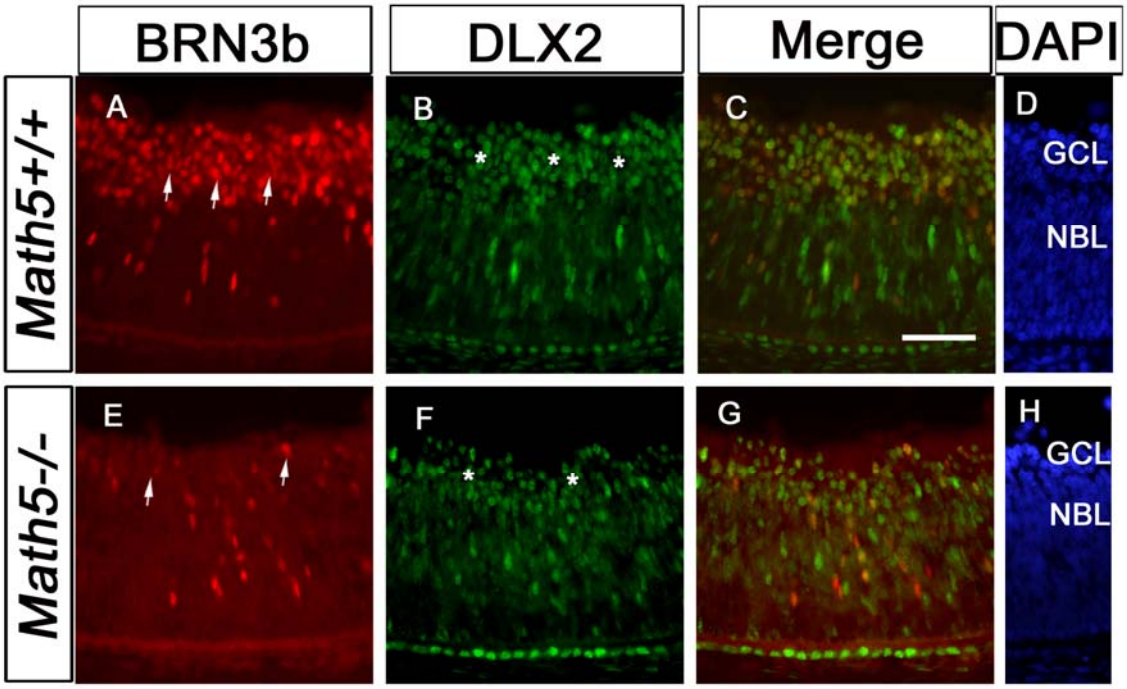

Fig. 14 BRN3b, but not DLX2, expression is significantly reduced in *Math5* null retinas at E16.5.

(A, E) BRN3b is strongly expressed in the GCL of wild-type retina, but is dramatically reduced in the *Math5*$^{-/-}$ retina at E16.5. Few cells are still detectable in the *Math5* null GCL (E, arrows). A reduced thickness in the GCL is noticed in the *Math5*$^{-/-}$ retina (D, H). Almost all the cells remaining in the *Math5*$^{-/-}$ retina GCL are DLX2 positive (F, stars). With no single BRN3b-positive cells detected in the *Math5*$^{-/-}$ retina GCL, most of the BRN3b positive cells co-express DLX2 (G). GCL, ganglion cell layer; NBL, neuroblast layer. Scale bar: 100μm.

Fig. 15

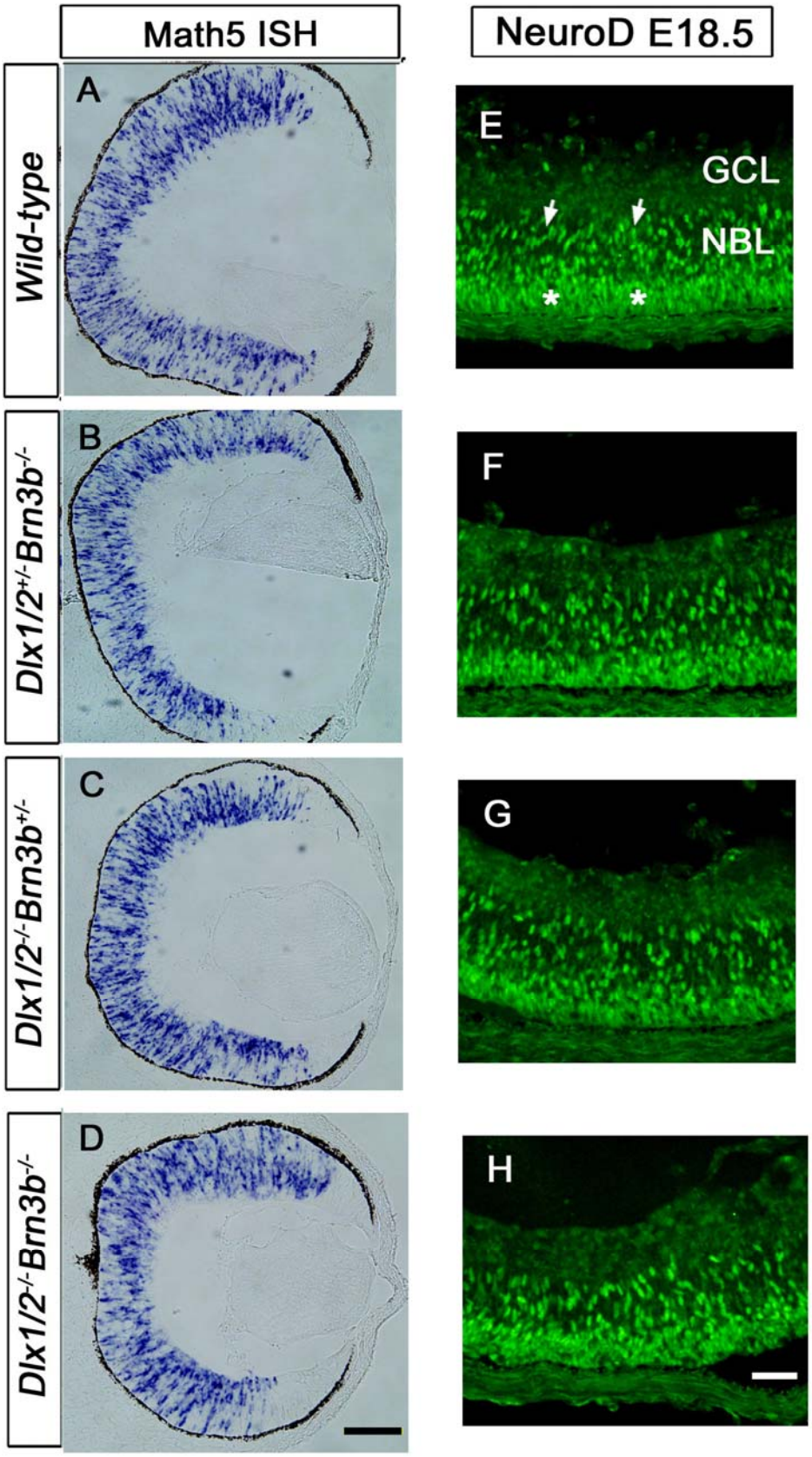
Math5 ISH
NeuroD E18.5
Wild-type
Dlx1/2+/-Brn3b-/-
Dlx1/2-/-Brn3b+/-
Dlx1/2-/-Brn3b-/-
A
B
C
D
E
F
G
H
GCL
NBL

Fig. 15 *Math*5 and NeuroD expression are not affected by the combined deletion of *Dlx*1/*Dlx*2 and *Brn*3b.

(A-D) Digoxigenin *in situ* hybridization on E13.5 sections shows that *Math*5 is expressed throughout the proliferating zone of the developing retina, except for the ciliary margin. No difference was detected between wild-type, *Dlx*1/*Dlx*2$^{+/-}$*Brn*3b$^{-/-}$ single, *Dlx*1/*Dlx*2$^{-/-}$*Brn*3b$^{+/-}$ double and *Dlx*1/*Dlx*2$^{-/-}$*Brn*3b$^{-/-}$ triple mutants. (E-H) Immunofluorescence of NeuroD on E18.5 retinas showed two populations of NeuroD expressing cells. NeuroD expression is detected in the outermost NBL (stars in E). Scattered NeuroD positive cells are also detected in the innermost NBL (arrows in E). NeuroD expressing cells are not observed in the GCL at this developmental stage. In terms of cell distribution and cell numbers, no significant difference is observed between wild-type and *Dlx1/Dlx2*$^{-/-}$*Brn3b*$^{-/-}$ mutants. GCL, ganglion cell layer; NBL, neuroblast layer. Scale bars: 40μm in D; 20μm in H.

4.8 Deletion of *Dlx*1/2 and *Brn*3b increases *Crx* homeobox gene expression

As previously reported, there was increased *Crx* RNA expression in the *Dlx*1/*Dlx*2 double mutant, and a 1.4 fold increase of *Crx* expression in *Brn*3b null retinas (de Melo, Du et al. 2005; Qiu, Jiang et al. 2008). Here, we examined the expression of *Crx* RNA in the *Dlx*1/*Dlx*2/*Brn*3b triple mutant, and found that both *Crx* expression was expanded and increased when compared to wild-type, *Brn*3b single and *Dlx*1/*Dlx*2 double mutants (Fig. 16 A-D). We also observed ectopic *Crx* expressing cells located in the inner retinas of these mutants (Fig. 16 D). Intriguingly, this data suggests that *Dlx*1/*Dlx*2 and *Brn*3b may repress *Crx* expression in the embryonic retina. However, it is also possible that the observed increased *Crx* expression represents a default state.

Fig. 16

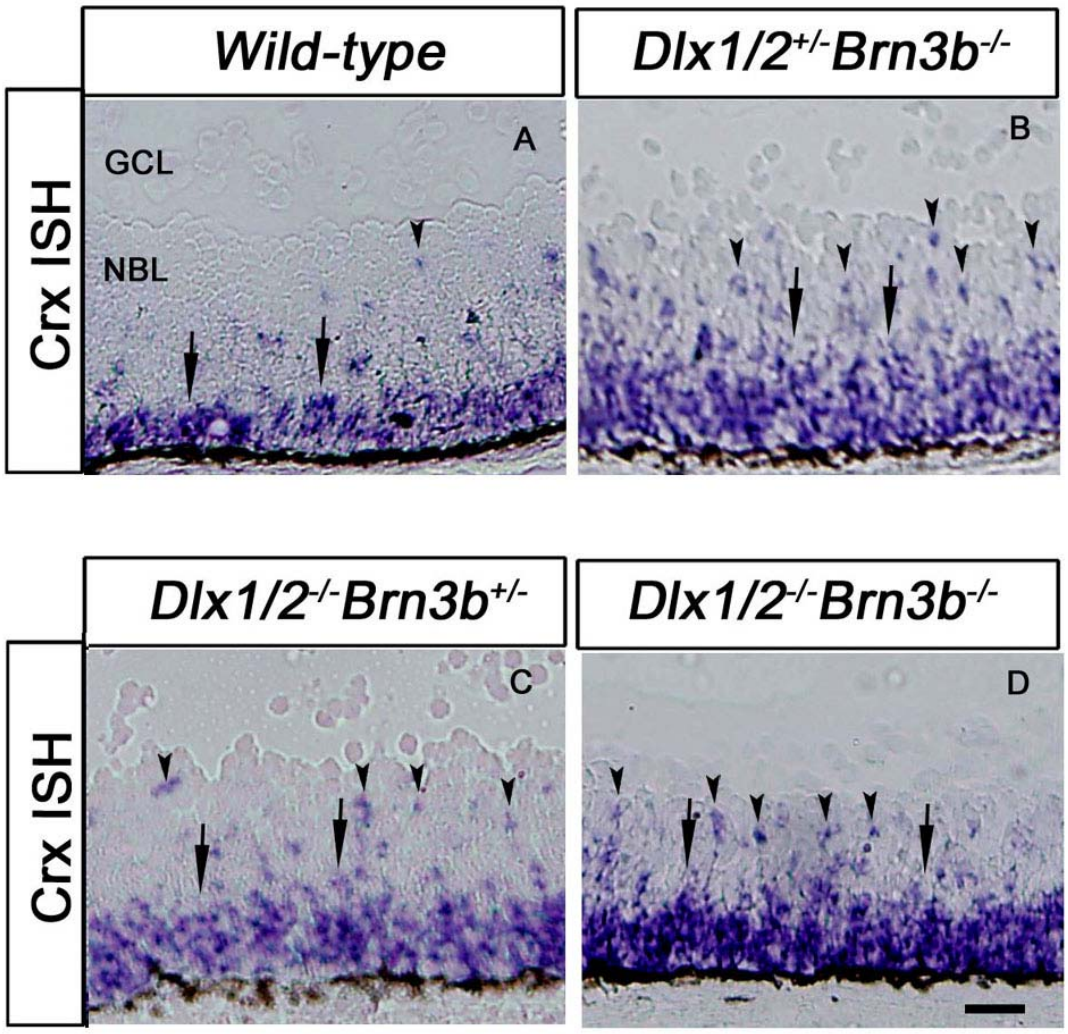
Wild-type
Dlx1/2+/-Brn3b-/-
Crx ISH
GCL
NBL
A
B
Dlx1/2-/-Brn3b+/-
Dlx1/2-/-Brn3b-/-
Crx ISH
C
D

Fig. 16 *Crx* homeobox gene expression is up-regulated by loss of either *Dlx*1/*Dlx*2 or *Brn*3b function.

(A) Using digoxigenin *in situ* RNA hybridization, *Crx* RNA was predominantly detected in the outer NBL of wild-type E18.5 retina (arrow), with only a few *Crx*-expressing cells in the inner NBL (arrowhead). (B, C) *Crx* expression is increased in the *Brn*3b single mutant (B, arrow) and *Dlx*1/*Dlx*2 double mutant (C, arrow). More ectopic *Crx* RNA expression is evident in the central and inner NBL (B, C, arrowheads). (D) In the *Dlx*1/*Dlx*2$^{-/-}$*Brn*3b$^{-/-}$ retina, there is increased *Crx* expression (arrow) as well as more ectopic expression in the inner NBL (arrowheads). GCL, ganglion cell layer; NBL, neuroblastic layer. Scale bar: 20μm.

4.9 DLX1 and DLX2 proteins regulate *Brn*3b by binding to specific homeodomain-DNA motifs of the *Brn*3b promoter *in vivo*

DLX2 is first expressed in the E11.5 retina, from the apical surface which is adjacent to the ophthalmic ventricular surface, to the basal retina. However, BRN3b is only detected in the inner, central retina. As development proceeds, more BRN3b cells also co-express DLX2, and at E16.5 and later time-points, all BRN3b positive cells co-express DLX2 (Fig. 3). Given the temporal and spatial patterns of expression of DLX2 and BRN3b, we postulated that DLX1 and/or DLX2 directly regulate *Brn*3b transcription during retinogenesis. To determine whether DLX1 and/or DLX2 regulate *Brn*3b transcription by interacting with genomic DNA sequences within the *Brn*3b gene locus, we used chromatin immunoprecipitation (ChIP) of embryonic retina and specific DLX1 or DLX2 antibodies to detect DLX proteins localized to the *Brn*3b promoter region *in vivo*, in combination with electrophoretic mobility shift assays (EMSA) to detect specific DLX protein- *Brn*3b promoter DNA sequence complexes *in vitro*. For the ChIP assays, we selected candidate binding regions based on groups of putative TAAT/ATTA homeodomain consensus DNA-binding motifs. We studied 6 kb of genomic DNA upstream of the *Brn*3b translational initiation codon, and focused on a 2.5 kb TAAT/ATTA rich region, located in the *Brn*3b promoter 2,263 bp upstream of the start codon. The ChIP assay was performed by using PFA cross-linked cells prepared from E16.5 retina and hindbrain (used as a negative control since this tissue does not express any members of the *Dlx* gene family)(Zhou, Le et al. 2004; de Melo, Zhou et al. 2008). For PCR analysis after immunoprecipitation with anti-DLX1

or DLX2 antibodies, we designed 7 pairs of oligonucleotide primers to encompass this 2.5 kb candidate TAAT/ATTA rich region, and designated the fragments as 3bP1 - 7, respectively (Table 5). Notably, only site 3bP4 was amplified by PCR of both DLX1 and DLX2 antibody immunoprecipitated DNA following reversal of cross-linking, indicating that both DLX1 and DLX2 occupy the *Brn*3b promoter region 3bP4 in the E16.5 retina (Fig. 17 B). No evidence was found for either DLX1 or DLX2 binding to the other 6 sites of this promoter region (data not shown). ChIP assays performed with E16.5 hindbrain negative control tissues, or the control immunoprecipitation without primary antibodies did not identify any binding (Fig. 17 B). Hence, these results suggest that either DLX1 and/or DLX2 are localized to the *Brn*3b promoter, specifically at the site 3bP4, *in vivo*.

To confirm DLX1 or DLX2 binding specificity to *Brn*3b promoter site 3bP4 DNA, we performed EMSA. We incubated radiolabeled 3bP4 oligonucleotide fragments with recombinant DLX1 or DLX2 proteins, and observed two specific protein-DNA band shifts (de Melo, Zhou et al. 2008), as DLX1-3bP4 and DLX2-3bP4 complexes (Fig. 17 C, lanes 2, 7). These bands were competitively inhibited by excess unlabeled or "cold" 3bP4 probe (Fig. 17 C, lanes 3, 8), and were "supershifted" by addition of specific DLX1 or DLX2 antibodies (Fig. 17 C, lanes 4, 9). An irrelevant antibody was used as a control antibody in this supershift assay, and we did not observe any supershifted band of these protein-DNA complexes (Fig. 17 C, lanes 5, 10).

Fig. 17a

A Mouse Brn3b Gene Structure

MGI_102524_Pou4f2 : chr8:81329081-81332724

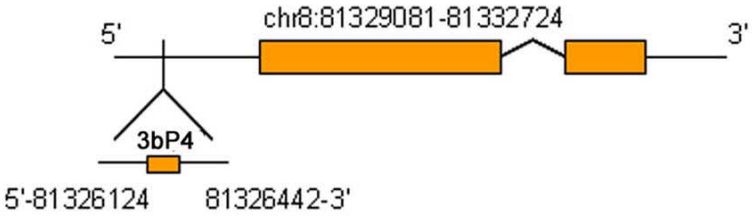

3bP4

MGI_102524 chr8: 81326124 - 81326442

GTTCAGCAGACTGTTGCCACAATAGTGTTTGGGCAAGTCCTCAGGGCTGCTTTTGACTTTACAT

CTAATTAGACACCTAATGAAAGGGAAGAATCCTTCCCCATGCGGTTTCCCTCCTTGGTATCTTT

TGTGCCTTTATTTATACACATAAACACACTACTTAGGAGTTGAAATACCACAAAGTTTTTTCTCTT

TCTGTACCTCACTCCCTGTAACAGTCTGGGGGAATTAGGTGGAGGAAAACATTTGTCTTCCTGA

TGTTTCCTACTCTGCTCAGAATTTCTTTGGGCATGTGGTCCTTCCTCACTCAACACTGAG

B

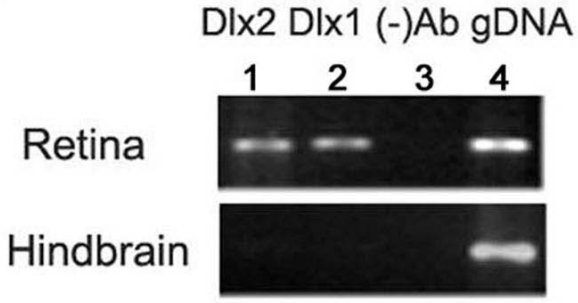

Fig. 17b

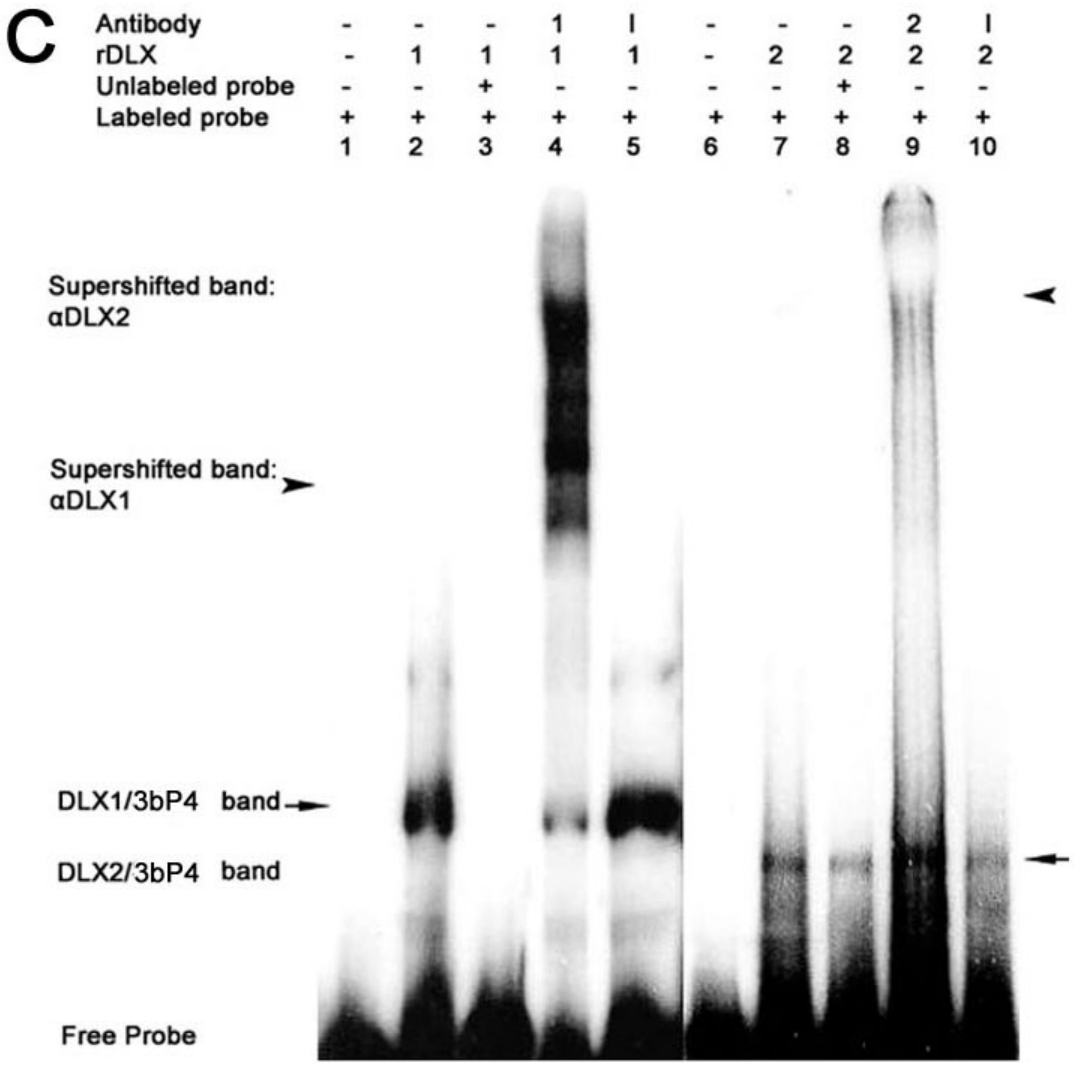
C
Antibody - - - 1 I - - - 2 I
rDLX - 1 1 1 1 - 2 2 2 2
Unlabeled probe - - + - - - - + - -
Labeled probe + + + + + + + + + +
1 2 3 4 5 6 7 8 9 10
Supershifted band: αDLX2
Supershifted band: αDLX1
DLX1/3bP4 band
DLX2/3bP4 band
Free Probe

Fig. 17 DLX1 and DLX2 proteins bind to the *Brn3b* promoter region.

(A) The *Brn*3b gene is located on mouse chromosome 8, and putative DLX homeodomain DNA binding sites (TAAT/ATTA) are located within the 5'-promoter region (denoted 3bP4) (A, underlined). (B) Chromatin immunoprecipitation (ChIP) assays using E16.5 retina and DLX1 and DLX2 antibodies followed by PCR identified specific *Brn*3b promoter DNA sequences (lane 1, 2). E16.5 hindbrain was used as negative control because this tissue does not express DLX1 or DLX2 proteins. Control immunoprecipitation was performed without primary antibodies and demonstrated no bands (lane 3). Genomic DNA was used as positive input (lane 4). (C) Using recombinant (r) DLX1 and DLX2 proteins, electrophoretic mobility shift assays (EMSA) demonstrated direct and specific *in vitro* binding of DLX1 and DLX2 proteins to the *Brn*3b promoter region (3bP4) identified by ChIP *in situ*. Radiolabeled 3bP4 oligonucleotides, when incubated alone migrate as free probe (lane 1, 6). rDLX1 or rDLX2 proteins form complexes with labeled 3bP4 probe and are shifted (lane 2, 7 arrows, respectively). Specific antibody to DLX1 or DLX2 was incubated with rDLX1 or rDLX2 proteins and labeled 3bP4 probe, and form a supershifted band (lane 4, 9 arrowheads, respectively). Excess unlabeled probe was used for cold competition (lane 3, 8). Antibody to mouse IgG was used as an irrelevant antibody and no supershift was observed (lane 5, 10).

To provide further evidence that DLX1 and DLX2 regulate transcription of *Brn*3b through its promoter site 3bP4, we performed transient co-transfection and site-directed mutagenesis assays. A plasmid expressing *Dlx*1 or *Dlx*2 was co-transfected into HEK293 cells with a vector in which the *Brn*3b 3bP4 promoter region drives expression of the luciferase reporter gene. DLX1 co-transfection resulted in a 2.1 fold increase of luciferase activity, whereas co-transfection with DLX2 induced a 2.5 fold increase (Fig. 18 A). Mutations of any of the three candidate TAAT/ATTA binding motifs within the 3bP4 promoter region significantly reduced the activation of luciferase activity by DLX1 and DLX2 *in vitro*, indicating that DLX1 or DLX2 activation of 3bP4 promoter expression may occur via any one of the three binding sites. Hence, we concluded that DLX1 and DLX2 proteins directly activate *Brn*3b transcription through its promoter site 3bP4 *in vitro*. In addition, we performed co-transfection with both *Dlx*1 and *Dlx*2 expression vectors and found that *Dlx*1 and *Dlx*2 had no synergistic function in regulating the 3b4 promoter. Co-transfection of both *Dlx*1 and *Dlx*2 results in transcriptional activity similar to *Dlx*2 single transfection in the reporter gene assay (Fig 18 B).

Fig. 18

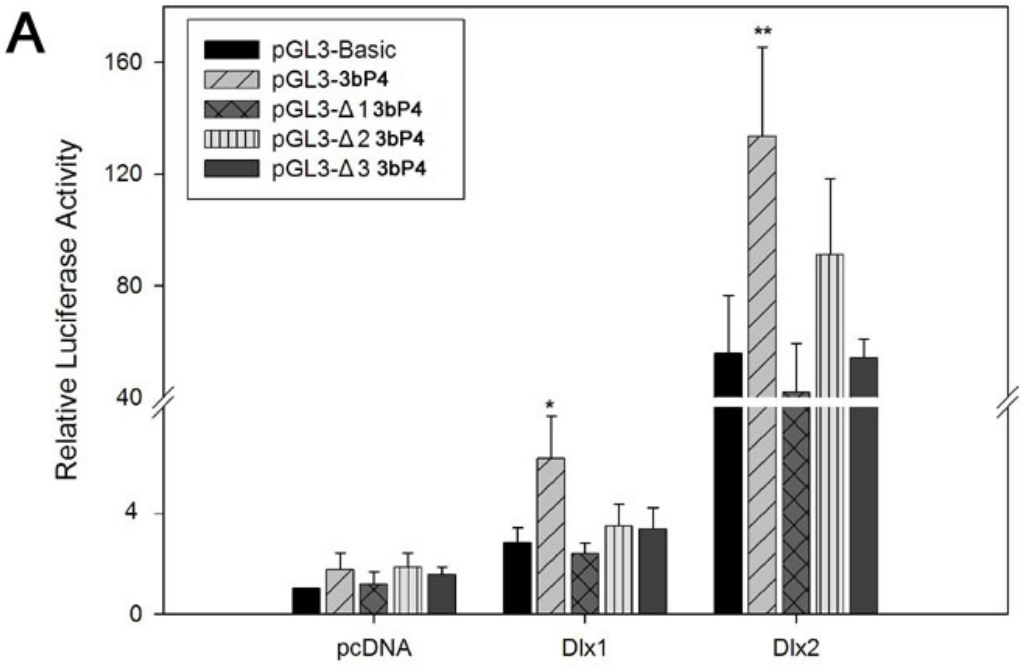
A
pGL3-Basic
pGL3-3bP4
pGL3-Δ1 3bP4
pGL3-Δ2 3bP4
pGL3-Δ3 3bP4
Relative Luciferase Activity
160
120
80
40
4
0
*
**
pcDNA
Dlx1
Dlx2

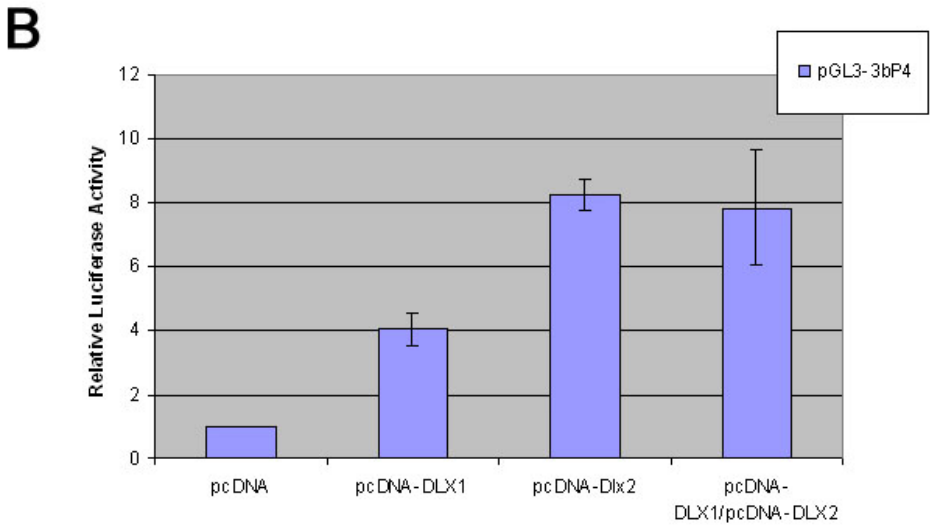
B
pGL3-3bP4
Relative Luciferase Activity
12
10
8
6
4
2
0
pcDNA
pcDNA-DLX1
pcDNA-Dlx2
pcDNA-DLX1/pcDNA-DLX2

Fig. 18 DLX1 and DLX2 activate *Brn*3b transcription *in vitro*.

(A) Reporter gene assays reveal that co-transfection of either DLX1 or DLX2 with the *Brn*3b promoter region 3bP4 reporter construct activated luciferase activity. Mutations of any of the three candidate TAAT/ATTA binding motifs significantly reduced the activation of reporter gene activity by DLX1 and DLX2. (B) *Dlx*1 and *Dlx*2 had no synergistic function in regulating 3b4 promoter, yielding similar transcriptional activity as *Dlx*2 single transfection in the luciferase assay. *: $P<0.05$, **: $P<0.01$

4.10 Mis-expression of *Dlx*2 *in utero* results in ectopic BRN3b expression *in vivo*

Gain-of-function assays in retinal explants are compromised by the loss of trophic support of RGCs due to transection of the optic nerves during tissue dissection and specimen preparation (de Melo, Zhou et al. 2008). To circumvent this problem, we proceeded to ectopically express *Dlx*2 in the intact embryo. E14.5 retinas were electroporated *in utero* with pCIG2-mCherry-*Dlx*2 (Fig. 19 A-G) and pCIG2-mCherry control plasmids (H-J), and harvested at E18. In pCIG2-mCherry-*Dlx*2 electroporated retinas, mCherry epifluorescence reflects ectopic DLX2 expression in the outer NBL (arrows in Fig. 19 C, D) which promoted ectopic BRN3b expression in the outer portion of the NBL (arrows in Fig. 19 F, G). Endogenous DLX2 and BRN3b expression were also detected in the GCL and INL (stars in Fig. 19 C, D, F, G, I, J). No ectopic BRN3b was detected in the control electroporated retina NBL (Fig. 19 I, J). Similar results were obtained from an additional three experimental and two control electroporated retinas.

To distinguish endogenous DLX2 or BRN3b expression from exogenous expression, cell counting was performed on the mCherry positive cells located ectopically in the outer NBL, but not the GCL. Cell numbers were obtained by counting mCherry positive cells, DLX2/mCherry double positive cells, and BRN3b/mCherry double positive cells. About 84% mCherry positive cells express DLX2 in pCIG2-mCherry-*Dlx*2 electroporated retina. ~12% mCherry positive cells co-express BRN3b in pCIG2-mCherry-*Dlx*2 electroporated retinal region, but not in pCIG2-mCherry transfected retina (Fig. 19 K). When combined with our transient

transfection assays *in vitro*, these *in utero* misexpression experiments support the hypothesis that *Dlx*2 gene function promotes for *Brn*3b expression in the embryonic retina *in vivo*.

Fig. 19

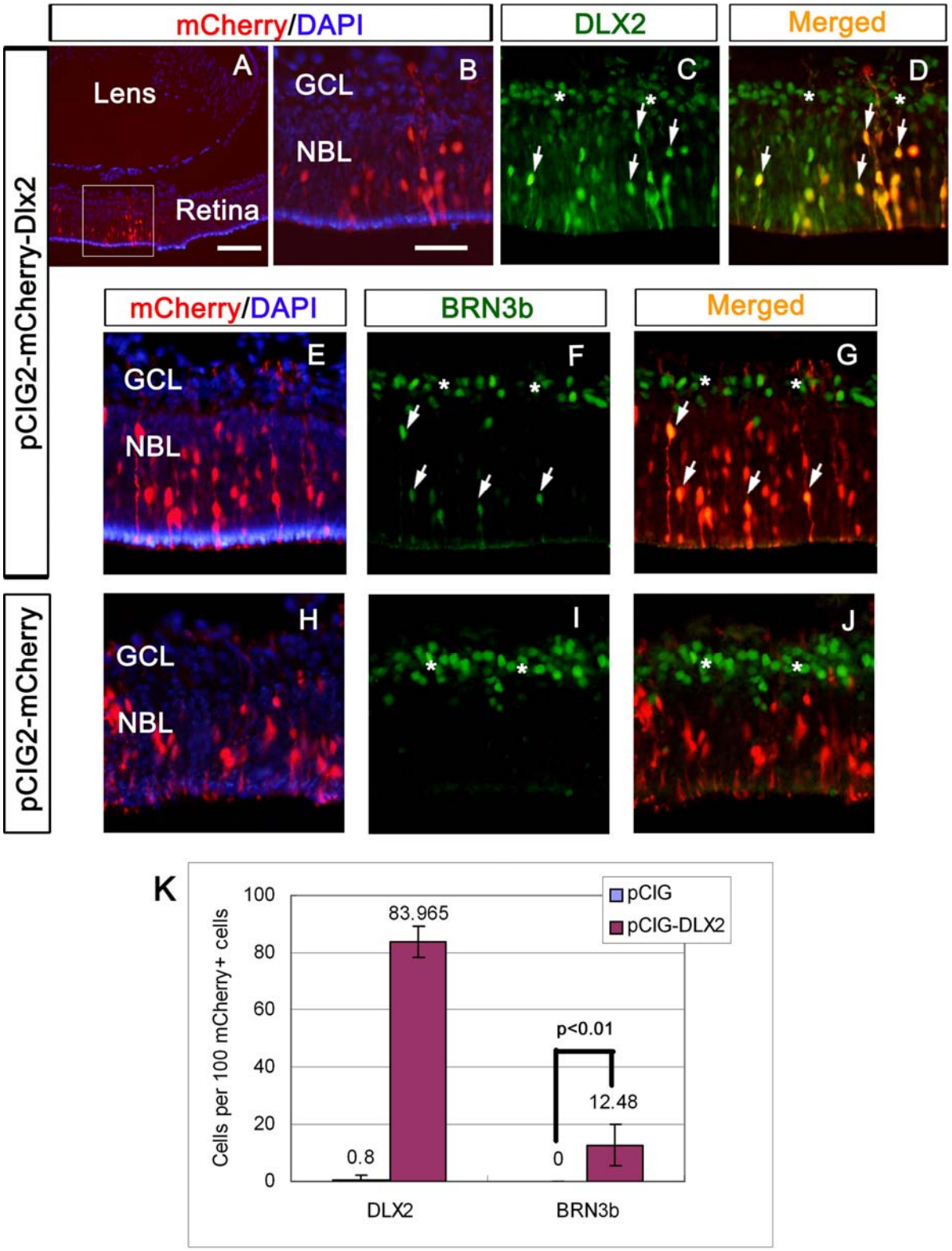
mCherry/DAPI
DLX2
Merged
pCIG2-mCherry-Dlx2
A
Lens
Retina
B
GCL
NBL
C
D
mCherry/DAPI
BRN3b
Merged
E
GCL
NBL
F
G
pCIG2-mCherry
H
GCL
NBL
I
J
K
Cells per 100 mCherry+ cells
100
80
60
40
20
0
83.965
0.8
p<0.01
12.48
0
pCIG
pCIG-DLX2
DLX2
BRN3b

Fig. 19 *In utero* electroporation of *Dlx*2 results in ectopic BRN3b expression *in vivo*.

E14.5 retinas were electroporated with pCIG2-mCherry-Dlx2 (A-G) and pCIG2-mCherry control plasmids (H-J), and harvested at E18. Endogenous DLX2 and BRN3b expression were also detected in the GCL and INL (stars in C, D, F, G, I, J). Immunostaining shows that the DLX2 antibody recognizes the mCherry epifluorescence in pCIG2-mCherry-*Dlx*2 electroporated retinas, but not the control electroporated areas (arrows in C, D). Double positive cells expressing both mCherry and BRN3b were found in the DLX2 electroporated area in the outer layer of the NBL (arrows in F, G). No ectopic BRN3b expression was detected in the control electroporated retina NBL (I, J). Cell counting was performed on the mCherry positive cells located in outer NBL. In the pCIG2-mCherry-Dlx2 electroporated retina, 84% mCherry positive cells are also DLX2 positive cells. Within this area, 12% mCherry positive cells co-express BRN3b (K). GCL, ganglion cell layer; NBL, neuroblastic layer. Scale bars: 50μm in A; 20μm in B (applies to B-J).

4.11 *Brn3b* expression is decreased by knockdown of *Dlx*2 expression in primary embryonic retinal cultures

Furthermore, to determine if *Brn3b* expression is reduced by decreased DLX2 expression, we transfected primary cell cultures of wild-type E14.5 retina with small interfering RNAs (siRNA) targeting the *Dlx*2 coding sequence, and a scrambled control siRNA (de Melo, Zhou et al. 2008). The transfection of *Dlx*2 siRNA showed an efficient knockdown of *Dlx*2 mRNA, with a concomitant decreased level of expression of *Brn*3b mRNA, compared to the transfection of control siRNA and untreated retinal cells (Fig. 20). Taken together with the RGC phenotype of the *Dlx*1/*Dlx*2 double knockout (de Melo, Du et al. 2005), these knockdown experiments support that *Dlx*2 gene functions in promoting *Brn*3b expression *in vivo*.

Fig. 20

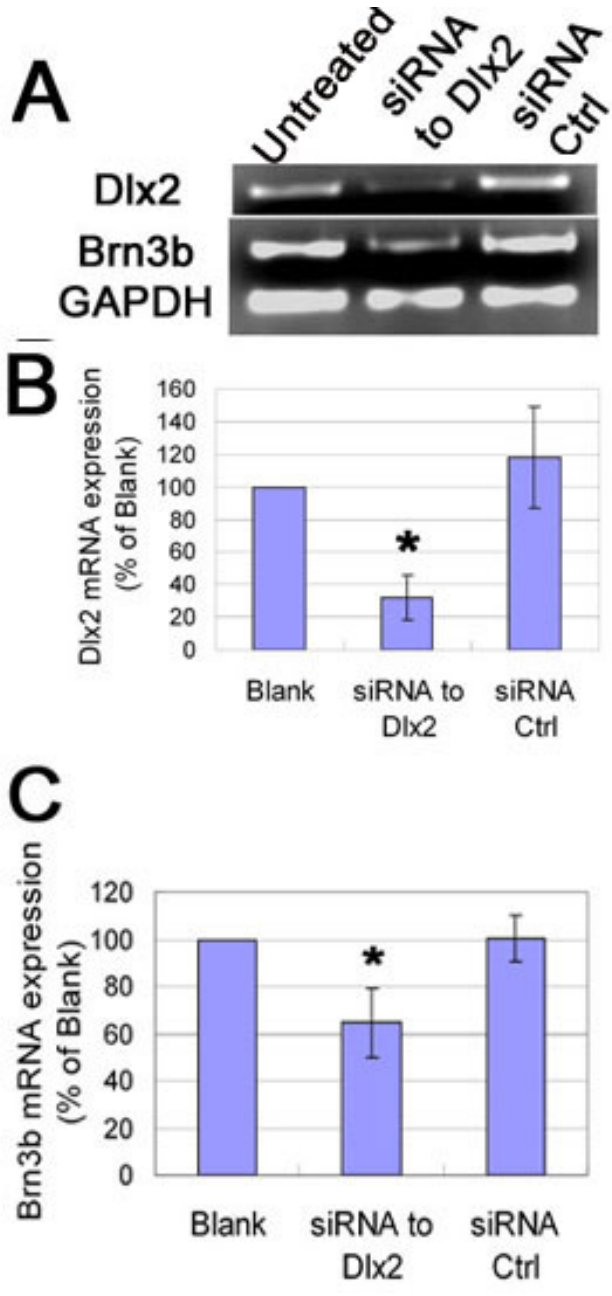
A
Untreated
siRNA to Dlx2
siRNA Ctrl
Dlx2
Brn3b
GAPDH
B
Dlx2 mRNA expression (% of Blank)
160
140
120
100
80
60
40
20
0
*
Blank
siRNA to Dlx2
siRNA Ctrl
C
Brn3b mRNA expression (% of Blank)
120
100
80
60
40
20
0
*
Blank
siRNA to Dlx2
siRNA Ctrl

Fig. 20 Knockdown of *Dlx*2 expression in primary embryonic retinal cultures at E14.5 results in decreased *Brn*3b expression.

(A) RT-PCR shows reduced expression of *Dlx*2 and *Brn*3b mRNA in the *Dlx*2 siRNA transfected cells, compared to the untreated and control siRNA transfected cells. (B, C) Quantitative real-time RT-PCR demonstrated an efficient knockdown of *Dlx*2 expression using specific siRNA to the *Dlx*2 coding sequence, but not with control siRNA. The knockdown of *Dlx*2 results in a significant reduction of *Brn*3b expression. (* $p<0.05$)

4.12 *Brn3b* represses DLX2 expression transiently, but not through directly binding to the *Dlx*1/*Dlx*2 cis-regulatory sequences

A regulatory loop between *Dlx*1/*Dlx*2 and *Brn*3b has been proposed. Previous studies have shown that *Brn*3b represses *Dlx*1 and *Dlx*2 expression in the embryonic retina (Mu, Fu et al. 2005; Qiu, Jiang et al. 2008). However, we found that the negative regulation of BRN3b on *Dlx2* expression is transient. Compared to wild-type littermates, *Brn3b* null retinas showed increased *Dlx2* expression at E13.5. Cell counting confirmed this finding by revealing a 1.5 fold increase of DLX2 positive cells in E13.5 *Brn*3b-null retina compared to wild-type (Fig. 21 C, D, and G). No significant difference was detected between wild-type and *Brn*3b mutants at E11.5 and E16.5. These data suggests a transient regulation of BRN3b on *Dlx2* expression.

Next, we considered how this regulation might occur at the molecular level. BRN3b functions as a transcription factor by directly binding to consensus *Pou*4f2 DNA-binding sites located in promoter regions of target genes [5'-(A/G)TTAATGAG(C/T)-3'] (Xiang, Zhou et al. 1995). We studied four currently known *cis*-acting elements of the *Dlx*1/*Dlx*2 bigenic cluster including two intergenic enhancers, *I12b* and *I12a*, and two upstream regulatory elements (URE), *URE1* and *URE2* (Ghanem, Jarinova et al. 2003; Ghanem, Yu et al. 2007). Two putative binding sites were identified in *URE2*, and one site in *I12b*. Interestingly, two putative *Pou*4f2 binding sites were also found in exon-3 of *Dlx*1 and in exon-2 of *Dlx*2 (Fig. 22 A). ChIP was subsequently performed, using Eomesodermin (*Eomes*), a confirmed direct transcriptional target of BRN3b, as a positive control. However, except for *Eomes,* no

other target regions were amplified by the PCR (Fig. 22 B). We conclude that BRN3b negatively regulates *Dlx2* expression via mechanisms other than direct BRN3B protein-*Dlx*1/*Dlx*2 *cis*-regulatory region DNA binding.

Fig. 21

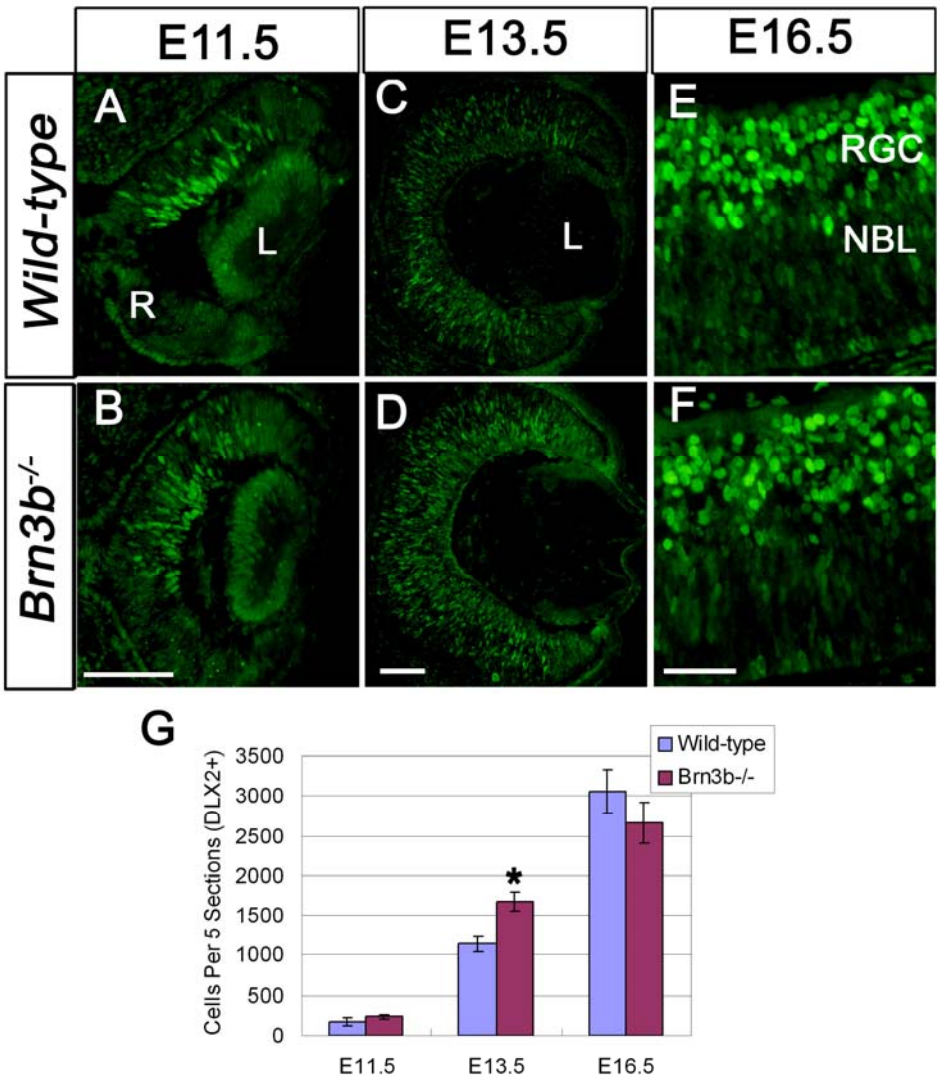
E11.5
E13.5
E16.5
Wild-type
Brn3b-/-
A
B
C
D
E
F
L
R
RGC
NBL
G
Wild-type
Brn3b-/-
Cells Per 5 Sections (DLX2+)
3500
3000
2500
2000
1500
1000
500
0
*
E11.5
E13.5
E16.5

Fig. 21 *Brn*3b transiently represses DLX2 expression at E13.5.

(A-F) Retinal sections from wild-type and *Brn*3b$^{-/-}$ mice were immunostained with DLX2 antibody at E11.5, E13.5 and E16.5. There is a significant increase of DLX2 expression in *Brn*3b-null retinas at E13.5, but not at E11.5 or E16.5. (G) Quantification of DLX2 positive cells reveals a 1.5 fold increase in E13.5 *Brn*3b-null retina compared to wild-type. No significant difference was detected between wild-type and *Brn*3b mutants at E11.5 and E16.5. R, Retina; L, Lens; GCL, ganglion cell layer; NBL, neuroblastic layer. Scale bar: 50μm.

Fig. 22

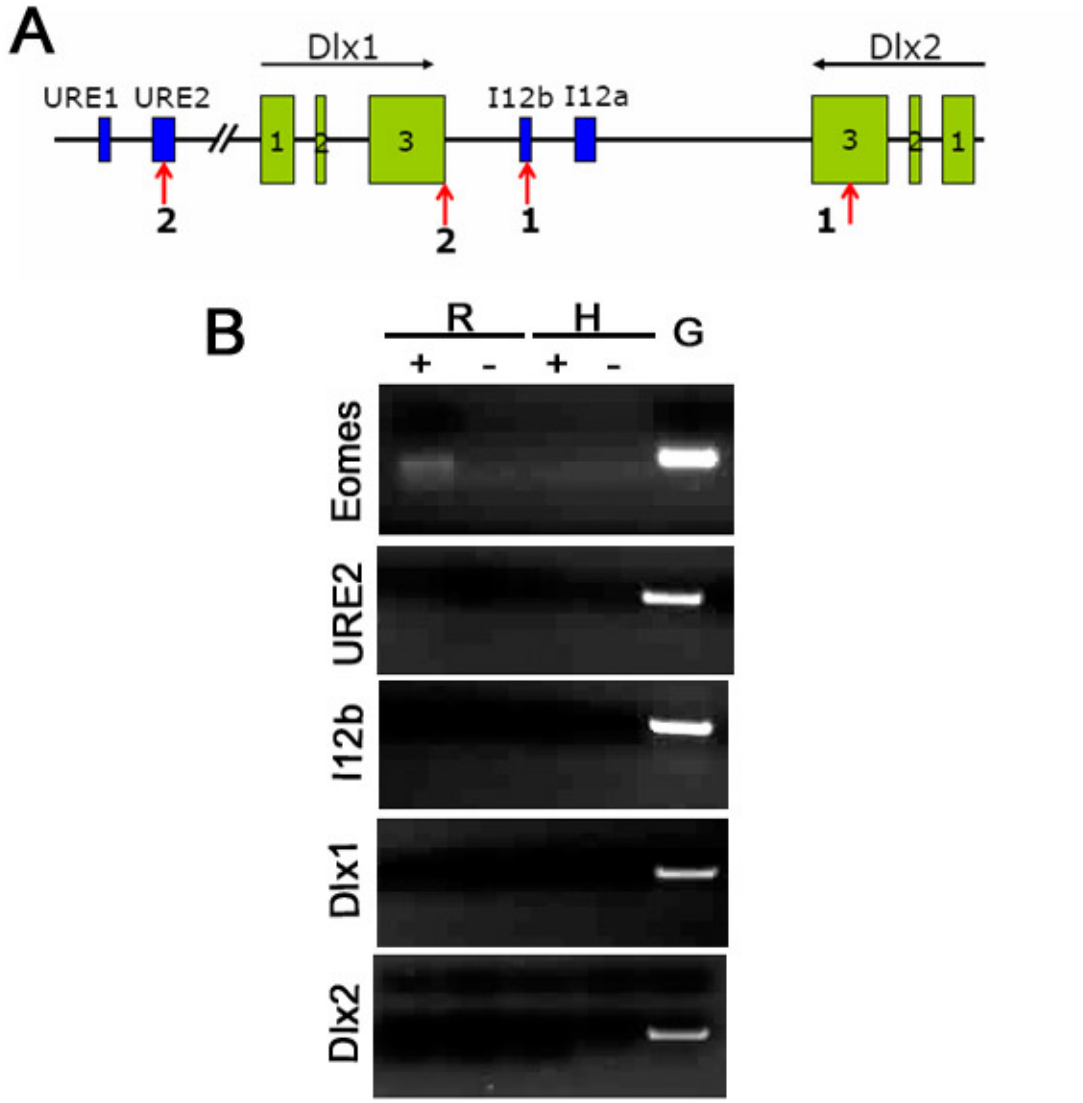
A
Dlx1
Dlx2
URE1 URE2
I12b I12a
1
2
3
2
1
2
3
2
1
B
R
H
G
+ - + -
Eomes
URE2
I12b
Dlx1
Dlx2

Fig. 22 BRN3b does not bind to *Dlx*1/*Dlx*2 cis-regulatory sequences *in situ*.

(A) A schematic diagram shows the genomic organization of the mouse *Dlx1/Dlx2* bigene cluster. Both *Dlx1* and *Dlx2* genes contain three exons. Two *cis*-acting regulators, *I12a* and *I12b*, are located between the *Dlx1* and *Dlx2* genes. Two conserved enhancer elements, URE1 and URE2, are found in the 5' flanking region of *Dlx1* (Poitras, Ghanem et al. 2007). Four candidate consensus BRN3b DNA binding motifs are found in the *cis*-regulatory elements and exons. Arrows indicate the positions of these putative BRN3b binding motifs, and numbers underneath the arrows represent the number of these motifs located in that region. (B) Chromatin immunoprecipitation (ChIP) assays using E16.5 retina and BRN3b antibody followed by PCR identified the previously characterized BRN3b transcriptional target *Eomes*. However, BRN3b protein fails to bind either of the putative binding sites located at the *Dlx1* and *Dlx2* genes locus. E16.5 hindbrain was used as a negative control. Control immunoprecipitations were performed without primary antibodies and resulted in no bands. Genomic DNA was used as positive input. R, Retina; H, hindbrain; G, genomic DNA; +, with BRN3b antibody; -, without BRN3b antibody.

4.13 *Dlx2* and *Brn3a* expression in the developing mouse retina

DLX*2* is expressed prior to *Brn3a* expression in the developing retina (Fig. 23). By E12.5, DLX2 expression is detected throughout the developing retina, from the apical surface to the inner basal retina. However, no BRN3a expression can be identified in the retina at this stage (Fig. 23 A-C). This pattern is different from the DLX2/BRN3b co-expression pattern observed in the early developing retina (Fig. 3). Retina cells begin to express BRN3a after E13.5, which is two days after the initiation of DLX2 and DLX1 expression (data not shown) (Quina, Pak et al. 2005). As development proceeds, both DLX2 and BRN3a expressing cells are restricted to the inner retina. In the GCL, BRN3a expressing cells represent a sub-population of DLX2 positive cells. At E16.5 and P0, almost all BRN3a positive cells co-express DLX2, whereas some DLX2 single positive cells clearly exist (Fig. 23 D-I). This temporal and spatial expression pattern of DLX2 and BRN3a suggests that in addition to *Brn*3b, DLX2 may also regulate *Brn3a* transcription during retinal development.

Fig. 23

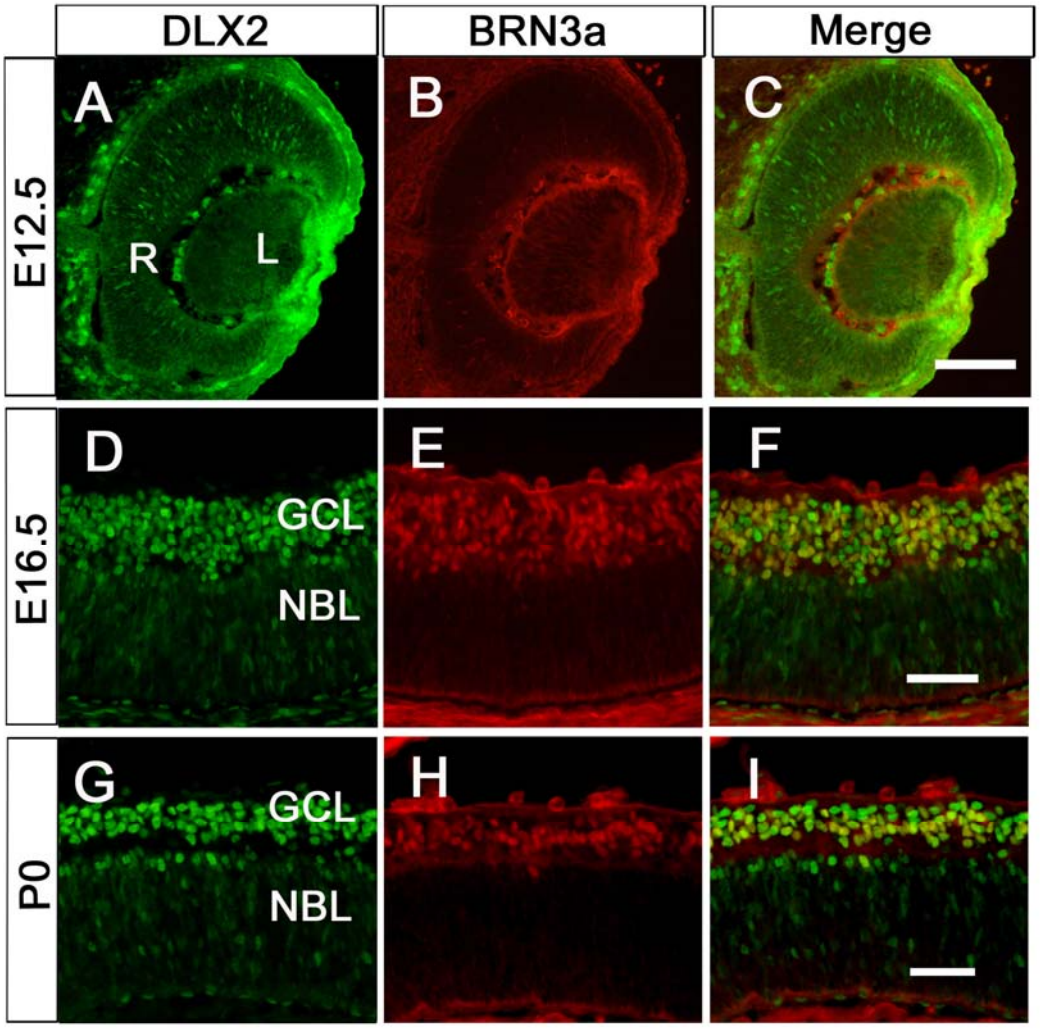

Fig. 23 DLX2 expression precedes BRN3a expression in the developing mouse retina

(A-C) At E12.5, DLX2 but not BRN3a expression can be detected in the retina. (D-F) At E16.5, BRN3a expression is restricted to the GCL, whereas DLX2 expression is in the GCL and inner NBL. Most of the BRN3a expressing cells are DLX2 co-positive cells. (G-I) A similar expression pattern is observed in the P0 retina. DLX2 expression is primarily localized to the GCL and inner NBL, whereas BRN3a is expressed only in the GCL. Some DLX2 single positive cells are distinguished in the GCL and inner NBL, but no BRN3A single positive cells are observed. R, Retina; L, Lens; GCL, ganglion cell layer; NBL, neuroblastic layer. Scale bars: 50μm in C; 25μm in F and I.

4.14 *Brn3a* expression is altered with either *Dlx1/Dlx2* loss of function or *Dlx2* mis-expression in the developing retina

To determine whether *Brn3a* transcription is under the direct regulation of DLX1 and/or DLX2, we first assessed the expression of BRN3a in the *Dlx1/Dlx2* double knock-out mouse retinas. The BRN3a-specific antibody was used for immunofluorescent studies. Compared to the wild-type littermates, the *Dlx1/Dlx2* mutant retinas have a reduced number of BRN3a-positive cell numbers at E18.5 (Fig. 24 A, B). A semi-quantitative western blot assay confirmed this observation. Protein was harvested from the *Dlx1/Dlx2* double mutant and wild-type littermate retinas at E18.5. With equivalent total protein input, the *Dlx1/Dlx2* mutant retinas showed marked reduction of BRN3a protein, in comparision to the beta-actin loading control (Fig. 24 C). Furthermore, quantitative RT-PCR assays were used to examine *Brn3a* transcript levels in both mutant and wild-type retinas. Not surprisingly, a significant reduction of *Brn3a* mRNA level was detected in the *Dlx1/Dlx2* double null retinas, in comparison to their wild-type littermates (Fig. 24 D). Taken together, these data support that DLX1 or/and DLX2 function is necessary to regulate and/or maintain *Brn3a* expression in the developing retina.

To further determine whether DLX2 is sufficient to regulate *Brn3a* expression in the embryonic retina, we ectopically expressed DLX2 *in vivo*. As described in section 4.10, *in utero* electroporation was performed on E14.5 wild-type retinas, using pCIG2-EGFP-*Dlx*2 and pCIG2-EGFP control plasmid (Fig. 25). Embryos were harvested at E18. In the pCIG2-EGFP-*Dlx*2 electroporated retinas, EGFP

epifluorescence identified ectopic DLX2 expression in the outer NBL (arrows in Fig. 25 B and C). This mis-expression of DLX2 was consistent with ectopic BRN3a expression in the NBL (arrows in Fig. 25 H and I). No ectopic BRN3a expression was observed in the control retina. Endogenous DLX2 and BRN3a expression were detected in the GCL and inner INL (stars in Fig. 25). Taken together, our data suggest that DLX2 regulates *Brn3a* expression in the developing retina.

Fig. 24

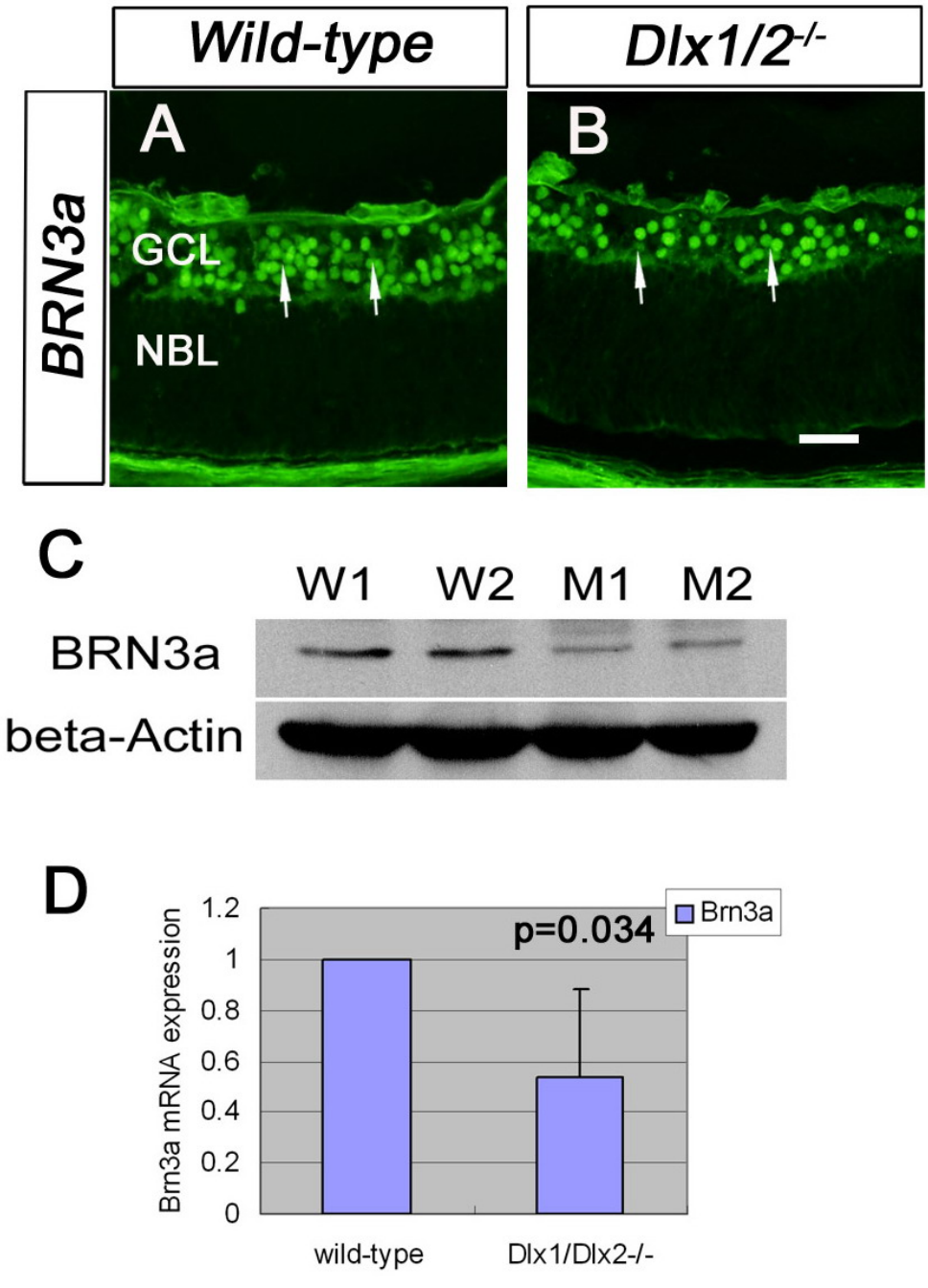
Wild-type
Dlx1/2-/-
BRN3a
A
B
GCL
NBL
C
W1
W2
M1
M2
BRN3a
beta-Actin
D
Brn3a mRNA expression
1.2
1
0.8
0.6
0.4
0.2
0
p=0.034
Brn3a
wild-type
Dlx1/Dlx2-/-

Fig. 24 BRN3a expression is reduced in the *Dlx1/Dlx2* double null retina

(A and B) BRN3a antibody was used for immunofluorescence assays on E18.5 retina sections. BRN3a positive cells are restricted to the GCL of both wild-type and *Dlx1/Dlx2* double null retinas (arrows). Compared to the wild-type, a significant reduction of the number of BRN3a expressing cells was shown in the *Dlx1/Dlx2* mutant retina. (C) Protein from E18.5 retinas was used for Western blot assays. Protein was extracted from the retinas of wild-type and *Dlx1/Dlx2* mutant embryos, and was loaded separately (representative samples: W1, W2, M1, and M2, respectively). Beta-actin was used as an internal control. The *Dlx1/Dlx2* double null retinas showed consistent reduction of BRN3a protein level. (D) Using E18.5 total retina RNA, quantitative RT-PCR revealed a significant reduction of *Brn3a* mRNA level in the *Dlx1/Dlx2* double null retinas, in comparison to the wild-type littermates. GCL, ganglion cell layer; NBL, neuroblastic layer. Scale bar: 25μm.

Fig. 25

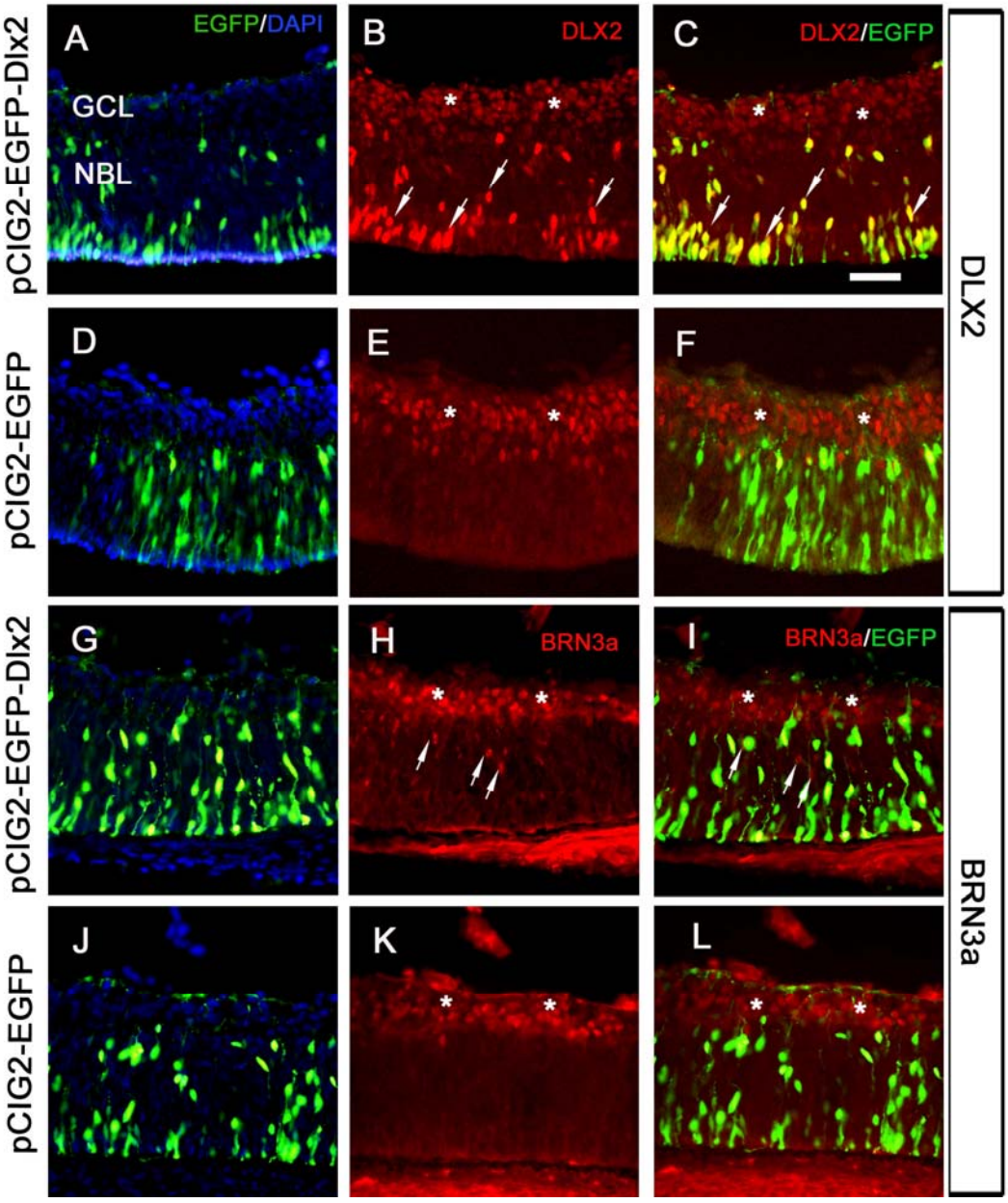
pCIG2-EGFP-Dlx2
pCIG2-EGFP
pCIG2-EGFP-Dlx2
pCIG2-EGFP
A
EGFP/DAPI
GCL
NBL
B
DLX2
C
DLX2/EGFP
D
E
F
G
H
BRN3a
I
BRN3a/EGFP
J
K
L
DLX2
BRN3a

Fig. 25 *In utero* electroporation of *Dlx*2 results in ectopic *Brn*3a expression *in vivo*.

E14.5 retinas were electroporated with pCIG2-EGFP-*Dlx*2 (A-C, G-I) and pCIG2-EGFP control plasmid (D-F, J-L), and harvested at E18. (A-F) DLX2 antibody was used for immunostaining. Endogenous DLX2 expressing cells were identified in the GCL and inner INL (stars in B, C, E, and F). EGFP epifluorescence replicates the ectopically expressed DLX2 protein in pCIG2-EGFP-*Dlx*2 electroporated retinas, but not the control electroporated areas (arrows in B, C). (G-L) BRN3a antibody was used for immunostaining. Endogenous BRN3a expressing cells were restricted in the GCL (stars in H, I, K, and J). Few ectopic BRN3a expressing cells were detected in the NBL of the DLX2 electroporated retina (arrows in H and I), but not the control electroporated retina (K, L). GCL, ganglion cell layer; NBL, neuroblastic layer. Scale bars: 20μm.

4.15 DLX2 but not DLX1 regulates *Brn3a* in the mouse retinogenesis.

Our previous studies established that both DLX1 and DLX2 proteins regulate *Brn3*b transcription by direct interaction with specific HD-DNA binding motifs located in the *Brn3*b promoter (section 4.9). We then explored whether this was the case for *Brn3*a expression. We studied ~ 6 kb of genomic DNA sequence upstream of the *Brn*3a translational initiation codon, and focused on 6 regions with putative TAAT/ATTA homeodomain DNA binding motifs. ChIP assays were performed using chromatin from E16.5 retina tissues, with antibodies specific to DLX1 or DLX2 proteins. Six pairs of oligonucleotide primers were designed for the PCR analysis after immunoprecipitation. These PCR primers were designed to encompass the six TAAT/ATTA rich regions, namely 3A1 - 6 (Table 5). Two promoter regions, 3A-1 and 3A-3, were amplified by PCR. Interestingly, both 3A-1 and 3A-3 regions were amplified from DLX2 antibody immunoprecipitated DNA. DLX1 antibody failed to precipitate all of the six candidate regions (Fig. 26 B). E16.5 hindbrain was used as negative control tissues due to the complete absence of DLX1 and DLX2 expression. A second immunoprecipitation control was performed by not adding primary antibodies. The negative controls did not reveal any binding. These results suggest that only DLX2, but not DLX1, is localized to two of the identified *Brn*3a promoter regions, 3A-1 and 3A-3, *in vivo*.

Electrophoretic mobility shift assays (EMSA) were performed to test the binding specificity of DLX2 to the *Brn*3a promoter DNA sequences *in vitro*. Radioactive ^{32}P was used to label the two ChIP amplified oligonucleotide fragments,

3A-1 and 3A-3, respectively. The radiolabelled 3A-1 and 3A-3 probes were incubated with DLX2 recombinant protein, and two specific protein-DNA complexes were formed and resulted as two shifted bands on the EMSA autoradiograph (Fig. 26 C, arrows). The formation of these DLX2-DNA complexes was competitively inhibited by adding excess unlabelled probes (Fig. 26C, lanes 3 and 8). Addition of the specific DLX2 antibody resulted in the formation of DLX2 antibody-protein-DNA complexes, which are "supershifted" bands compared to the protein-DNA bands (Fig. 26C, arrowheads). No "supershifted" band was observed when an irrelevant antibody was used, confirming the specificity of the DLX2 antibody-protein-DNA interaction.

To investigate whether DLX2 regulates *Brn3a* transcription through interactions with the two promoter regions 3A-1 and 3A-3, we performed transient co-transfection assays in cultured cell lines. A reporter vector with a luciferase reporter gene downstream to either the *Brn*3a 3A-1 or 3A-3 promoter sequences was cloned and co-transfected with a DLX2- expressing plasmid into HEK293 cells. The co-transfection of DLX2 and region 3A-1 resulted in a 3-fold increase of luciferase activity, whereas co-transfection of DLX2 and region 3A-3 did not demonstrate significant activation of reporter gene expression (Fig. 27). Co-transfection assays performed in the retinoblastoma Y79 cell line showed similar results (data not shown). These results were somewhat surprising. Both promoter regions 3A-1 and 3A-3 were specifically bound to DLX2 protein *in vitro*, but only the DLX2-3A-1 interaction actively promoted reporter gene transcription. One explanation is that the transcriptional regulation of the 3A-3 region may depend on a broader genetic context.

The identified 3A-3 region might function as an enhancer element, but not as a promoter. A second explanation is that other co-activators might be required for DLX2 to regulate transcription via these 3A-1 or 3A-3 elements. The HEK293 or Y79 cells might express one of the co-activators specific to the 3A-1 region, but not the 3A-3 region. Finally, we have not confirmed that DLX2 binds directly to the 3A-3 region *in situ* using nuclear extracts for EMSA as well as other assays *in vivo*.

Fig. 26

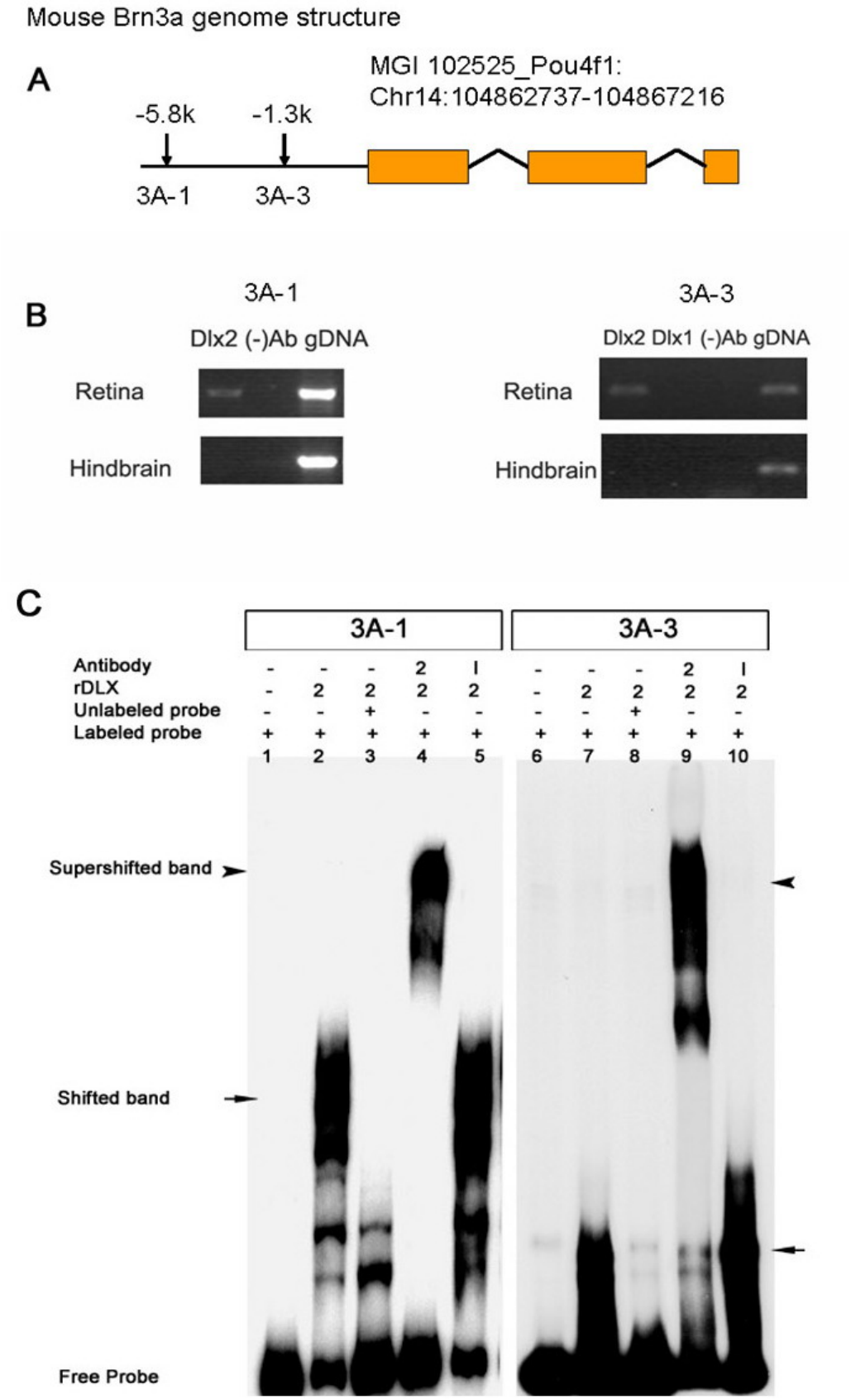
Mouse Brn3a genome structure
A
MGI 102525_Pou4f1:
Chr14:104862737-104867216
-5.8k
-1.3k
3A-1
3A-3
B
3A-1
Dlx2 (-)Ab gDNA
Retina
Hindbrain
3A-3
Dlx2 Dlx1 (-)Ab gDNA
Retina
Hindbrain
C
3A-1
3A-3
Antibody
rDLX
Unlabeled probe
Labeled probe
1 2 3 4 5 6 7 8 9 10
Supershifted band
Shifted band
Free Probe

Fig. 26 DLX2 but not DLX1 protein binds to the *Brn3a* promoter region.

(A) The mouse *Brn3a* genome structure. The *Brn*3a gene is located on mouse chromosome 14. Two promoter regions with putative DLX homeodomain DNA binding sites (TAAT/ATTA) are identified as 3A-1 and 3A-3, and are located 5.8 kb and 1.3 kb, respectively, upstream of the *Brn*3a translational initiation codon (arrows). (B) Chromatin immunoprecipitation (ChIP) assays were performed using E16.5 retina tissues. PCR analysis identified two candidate *Brn3a* promoter regions from DLX2 antibody-precipitated DNA, but not DLX1 antibody-precipitated DNA. A Control immunoprecipitation was performed without primary antibodies and demonstrated no non-specific bands. Genomic DNA was used as positive input. E16.5 hindbrain was used as a negative control. (C) Electrophoretic mobility shift assays (EMSA) confirm the direct and specific DLX2 protein-DNA interaction *in vitro*. Radiolabeled 3A-1 and 3A-3 oligonucleotides migrate as free probes when incubated alone (lane 1, 6). Recombinant(r) DLX2 protein form complexes with labeled 3A-1 and 3A-3 probes and are shifted (lane 2, 7 arrows, respectively). DLX2-specific antibody was incubated with rDLX2 protein and labeled 3A-1 and 3A-3 probe, and formed supershifted bands (lane 4, 9 arrowheads, respectively). Excess unlabeled 3A-1 and 3A-3 probes were added to compete with the labeled probes for rDLX2 protein, and shifted bands were eliminated (lane 3, 8). Antibody to mouse IgG was used as an irrelevant (I) antibody control and no supershift was observed (lane 5, 10).

Fig. 27

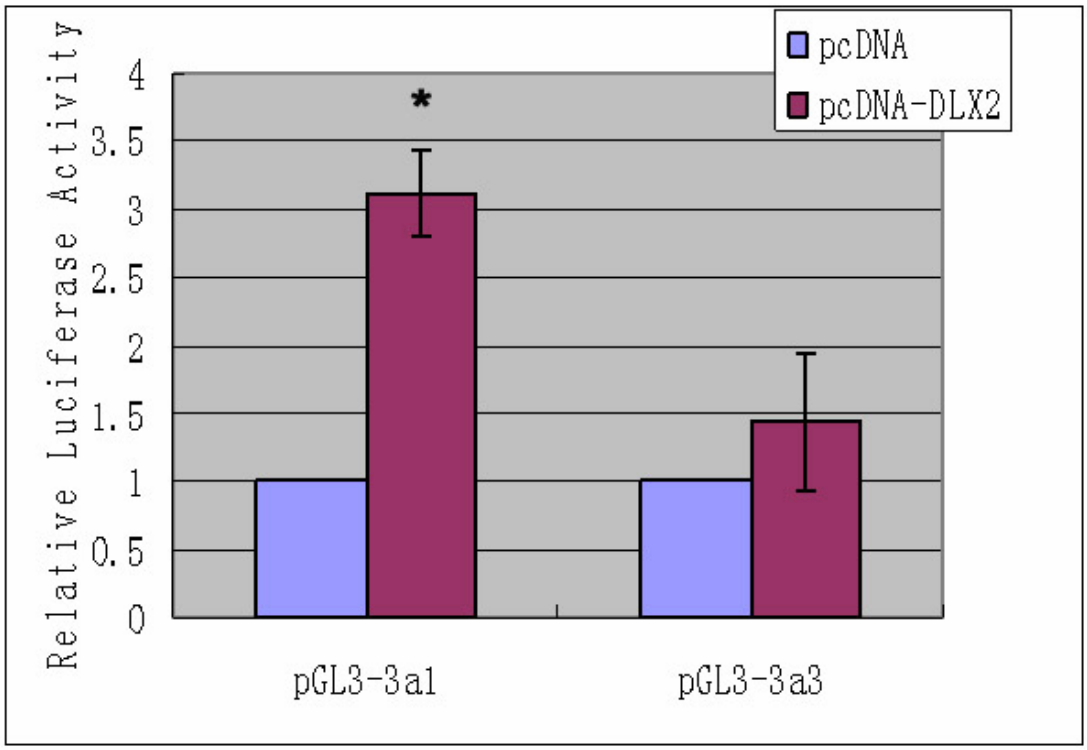
Relative Luciferase Activity
0
0.5
1
1.5
2
2.5
3
3.5
4
*
pcDNA
pcDNA-DLX2
pGL3-3a1
pGL3-3a3

Fig. 27 DLX2 activates the promoter region 3A-1, but not region 3A-3 transcription *in vitro*.

Reporter gene assays were performed by co-transfection of DLX2 with either *Brn*3a promoter region 3A-1, or promoter region 3A-3. The co-transfection of DLX2 with the *Brn*3a promoter region 3A-1 significantly increased luciferase reporter activity 3-fold. However, co-transfection of DLX2 with the *Brn*3a promoter region 3A-3 yielded no significant activation. *: $P<0.01$.

4.16 Both DLX2 and BRN3b proteins bind to the *Brn3a* promoter region 3A-1 *in vitro*

To further investigate the possibility of other co-activators specific to the *Brn3a* promoter region 3A-1, we interrogated this 3A-1 sequence *in silico* and found that 3A-1 indeed is a conserved regulatory region containing multiple binding sites for other transcription factors. In addition to the HD DNA binding sites (TAAT/ATTA), there are putative POU4 binding sites (G/ATTAATGAT/C) and octamer sites (ATATGCAT) (Fig. 28 A) (Trieu, Ma et al. 2003; Mao, Kiyama et al. 2008). Previous studies showed that *Brn3a* is a downstream target of *Brn3b* in retinogenesis, and there is reduced *Brn3a* expression in *Brn3b* mutants (Erkman, McEvilly et al. 1996). With the POU4 binding sites identified in the 3A-1 region, it was reasonable to propose that BRN3b acts as a co-activator of DLX2 and regulates *Brn*3a transcription through interacting with the 3A-1 promoter region.

To test this hypothesis, we first did an EMSA to detect the direct binding of BRN3b to region 3A-1 *in vitro*. The 286bp 3A-1 region contains 8 putative HD (DLX2) DNA binding sites and 4 putative POU3 binding sites. To determine which one, or all, of them are actual binding sites, we divided this 286bp DNA sequence into 4 sub-regions or motifs. Each sub-region contains 2 or 3 DLX binding sites, and 1 or 2 POU binding sites (Fig. 28 A). These sub-regions were labelled with ^{32}P, and incubated with recombinant DLX2 or BRN3b proteins. Of the four motifs that we studied, only sub-regions 2 and 3 formed DNA-protein complexes with DLX2, and two shifted bands were subsequently observed on the EMSA autoradiograph (Fig. 28

B Lanes 4 and 6; Fig. 29 B arrows). Incubation of Motifs 1 and 4 with DLX2 protein failed to form specific shifted band. Interestingly, BRN3b recognizes and binds to the same binding regions (sub-regions 2 and 3) of the 3A-1 promoter regions, as does DLX2 (Fig. 28 B lanes 12 and 14).

The binding specificity of the DLX2-motif2 and DLX2-motif3 was further investigated. By adding excess unlabeled probes, the shifted bands were competitively inhibited (Fig. 29 B lanes 3, 10). Addition of specific DLX2 antibody, but not irrelevant antibody, was able to form antibody-protein-DNA complexes, resulting in "supershifted" bands (Fig. 29 B, arrowheads). Furthermore, mutagenesis was introduced into the putative binding sites of motifs 2 and 3, respectively. Mutation of candidate binding site sequences interfered with protein-DNA complex formation, suggesting that these consensus binding sites are required for DLX2 recognition and binding to DNA (Fig. 29 B, lanes 7 and 14). Taken together, these data suggest that both DLX2 and BRN3b bind to the *Brn3a* promoter region 3A-1, specifically on motif2 and motif3. However, whether DLX2 and BRN3b act as transcriptional co-activators remains to be clarified. Furthermore, it will be necessary to confirm by ChIP-reChIP assay of developing retina whether both DLX2 and BRN3b co-occupy region 3A-1 *in vivo*.

Fig. 28

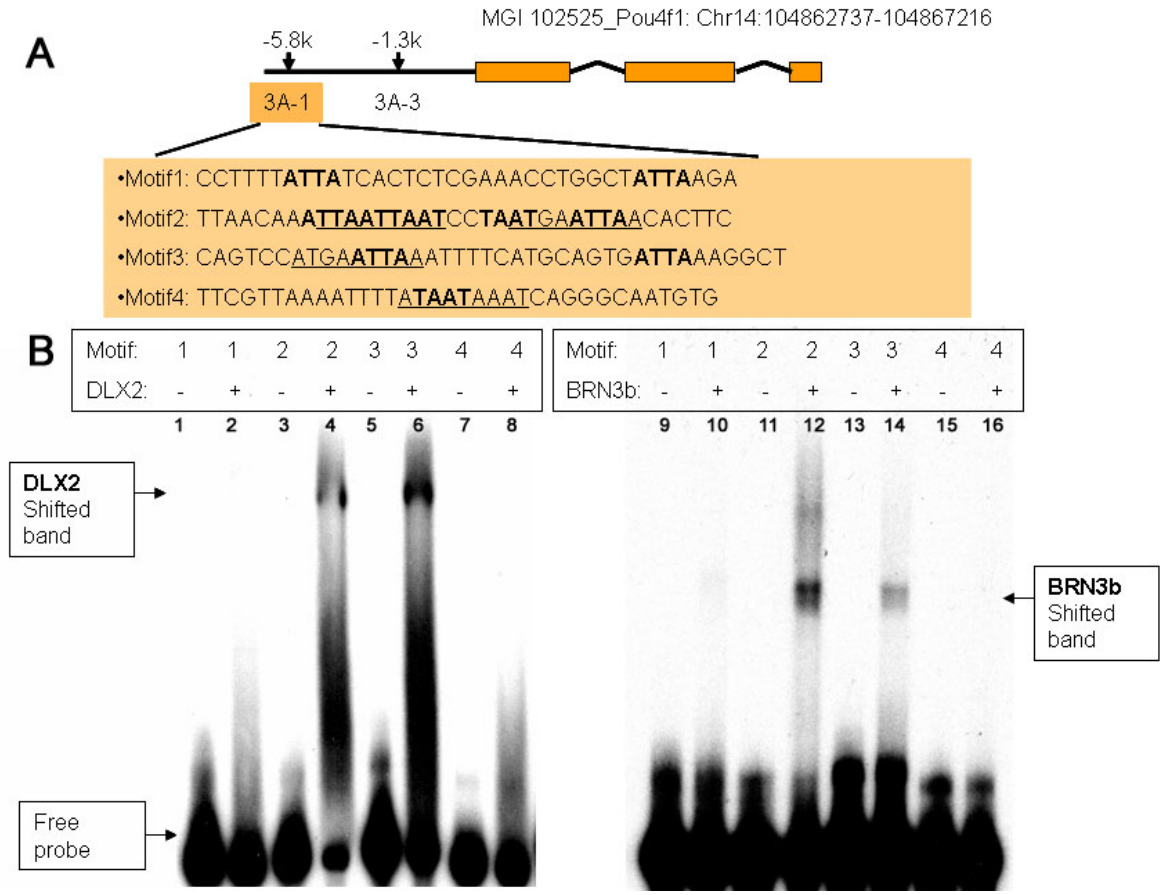
A
MGI 102525_Pou4f1: Chr14:104862737-104867216
-5.8k
-1.3k
3A-1
3A-3
•Motif1: CCTTTTATTATCACTCTCGAAACCTGGCTATTAAGA
•Motif2: TTAACAAATTAATTAATCCTAATGAATTAACACTTC
•Motif3: CAGTCCATGAATTAAATTTTCATGCAGTGATTAAAGGCT
•Motif4: TTCGTTAAAATTTTATAATAAATCAGGGCAATGTG
B
Motif: 1 1 2 2 3 3 4 4
DLX2: - + - + - + - +
1 2 3 4 5 6 7 8
Motif: 1 1 2 2 3 3 4 4
BRN3b: - + - + - + - +
9 10 11 12 13 14 15 16
DLX2 Shifted band
BRN3b Shifted band
Free probe

Fig. 28 Both DLX2 and BRN3b bind directly to the same promoter sub-regions of 3A-1 *in vitro*

(A) The 3A-1 promoter region was arbitrarily divided into four binding sub-regions or motifs, motifs 1-4. Each motif contains 2 or 3 DLX binding sites, and 1 or 2 POU binding sites (bold sequences are HD binding sites, and underlined sequences are POU4 binding sites). (B) Electrophoretic mobility shift assays (EMSA) confirm that both DLX2 and BRN3b form protein-DNA complexes with 3A-1 region *in vitro*. Radiolabeled motif 1, 2, 3 and 4 oligonucleotides migrate as free probes when incubated alone (lane 1 to 16). Recombinant DLX2 protein forms specific protein-DNA complexes with labeled motif 2 and motif 3 probes and are shifted (lane 4 and 6). Recombinant BRN3b protein binds to the same motif 2 and 3. Similar shifted bands are shown (lane 12 and 14).

Fig. 29

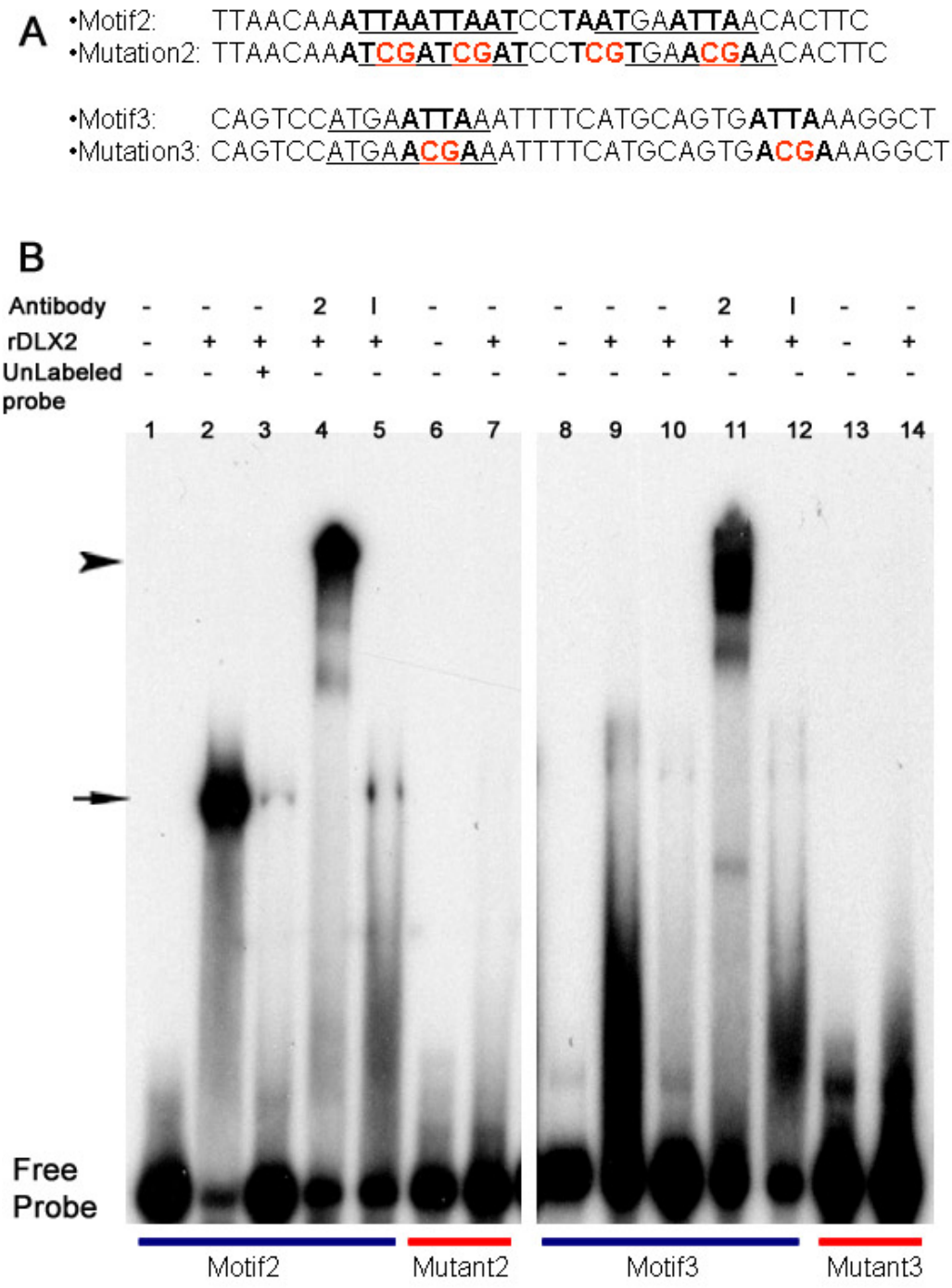
A
•Motif2: TTAACAAATTAATTAATCCTAATGAATTAACACTTC
•Mutation2: TTAACAATCGATCGATCCTCGTGAACGAACACTTC
•Motif3: CAGTCCATGAATTAAATTTTCATGCAGTGATTAAAGGCT
•Mutation3: CAGTCCATGAACGAAATTTTCATGCAGTGACGAAAGGCT
B
Antibody - - - 2 I - - - - - 2 I - -
rDLX2 - + + + + - + - + + + + - +
UnLabeled probe - - + - - - - - - - - - - -
1 2 3 4 5 6 7 8 9 10 11 12 13 14
Free Probe
Motif2
Mutant2
Motif3
Mutant3

Fig. 29 Binding motifs 2 and 3 are required for specific DLX2 protein-DNA interactions

(A) Mutagenesis is introduced into the putative HD and POU4 binding sites on motif 2 and motif 3. Bold sequences are HD binding sites, and underlined sequences are POU4 binding sites. Mutagenesis was used to alter both HD and POU4 binding sequences (Red). (B) Electrophoretic mobility shift assays (EMSA) confirm that the consensus binding sites are required for the direct and specific DLX2 protein-DNA interaction *in vitro*. Radiolabeled motif2 and motif3 are incubated with recombinant(r) DLX2 protein, and the resulting DLX2-DNA complexes are shown as shifted bands (arrows, lanes 2 and 9, respectively). The complex formation is inhibited by addition of excess unlabeled motif 2 and motif 3 probes (lanes 3 and 10). Specific DLX2 antibody is incubated with rDLX2 protein and labeled motif 2 or motif 3 probes, and form supershifted bands (arrowheads, lane 4, 11, respectively). Addition of the antibody to mouse IgG does not result in supershifted band (lane 5, 12). The mutagenesis of the binding sites eliminates the DLX2-DNA binding completely, in both motif 2 and motif 3 (lanes 7 and 14).

4.17 *Dlx1/Dlx2/Brn3a* triple null retinas have a phenotype similar to *Dlx1/Dlx2* double null retinas

We have previously demonstrated that *Dlx1/Dlx2* and *Brn3b* function in parallel and in cross-regulatory pathways in regulating RGC genesis. Absence of *Dlx1/Dlx2* and *Brn3b* genes leads to much more severe retinal phenotypes than mutations of either gene alone. The retinal phenotypes include significant RGC loss, increased amacrine cell differentiation, aberrant RGC axonal central projection, and cell cycle defects (4.2-4.6). *Brn3a* and *Brn3b* share a largely overlapping pattern of expression in the developing RGCs, with *Brn3a* as the predominant factor in postnatal retinas (Quina, Pak et al. 2005). Although the *Brn*3a mutant mouse showed no obvious retinal defects at birth, conditional deletion of *Brn3a* alters RGC dendritic stratification in the adult retina (Badea, Cahill et al. 2009). Knock-in of *Brn3a* in the *Brn3b* locus is able to rescue the RGC loss observed in *Brn3b* null mice (Pan, Yang et al. 2005).

Here we tested whether *Dlx1/Dlx2* and *Brn3a* play a combinatorial role in prenatal retinal development, similar to *Dlx1/Dlx2* and *Brn3b* in RGC genesis and differentiation. To test this hypothesis, we generated *Dlx*1/*Dlx*2/*Brn*3a triple knockout mice. As expected, the *Dlx*1/*Dlx*2/*Brn*3a triple null mice die shortly after birth. These triple mutant animals have grossly normal eyes at this stage, with a well developed lens, iris, cornea and RPE at E18.5. Histology studies showed that the retinas have a well organized laminar structure (data not shown). The triple null retinas have a modestly reduced GCL, which is indistinguishable from the *Dlx1/Dlx2* double mutant

retinas. Immunostaining was performed to assess retina neuronal differentiation at E18.5. Antibodies to BRN3b and ISL1 were used as RGC markers. As expected, the majority of the BRN3b and ISL1 positive cells were located in the GCL of all phenotypes. There were a reduced number of ganglion cells in both *Dlx1/Dlx2* double knockout and *Dlx1/Dlx2/Brn3a* triple mutant retinas, but not in the *Brn3a* single mutant retinas (Fig. 30 A-H). However, in terms of RGC loss, cell counting results did not yield statistically significant differences between *Dlx1/2* double null and *Dlx1/Dlx2/Brn3a* triple null retinas (Fig. 30 I). E13.5 and E15.5 retinas were also analysed and similar results were observed as at E18.5 (data not shown). Other early differentiated retina neuronal classes were studied, including amacrine and horizontal cells, but no significant difference was observed between wild-type, *Brn*3a single, *Dlx*1/*Dlx*2 double and *Dlx*1/*Dlx*2/*Brn*3a triple null retinas (Fig. 31). Taken together, the *Dlx*1/*Dlx*2/*Brn*3a triple null retinas have similar retinal defects to that observed in the *Dlx*1/*Dlx*2 double mutants, suggesting that *Dlx1/Dlx2* and *Brn3a* do not have combinatorial roles in embryonic retina development.

Furthermore, we used anterograde diI tracing to detect any possible RGC axonal pathfinding defects at E18.5. The tightly bundled optic nerves were observed in all four genotypes, including wild-type, *Brn3*a single mutant, *Dlx1/Dlx2* double mutant, and *Dlx1/Dlx2/Brn3a* triple mutant mice. No obvious aberrant axonal pathfinding from the optic nerve was observed. With the majority of the axons projecting contra-laterally, the optic chiasms were well formed morphologically in all the samples studied. The optic tracts continued their journey to central targets post-

optic chiasm. These data suggest that deletion of both *Dlx1/Dlx2* and *Brn3a* did not lead to any obvious RGC axonal projection defects at any of the major pathfinding choices, including the optic nerve, optic chiasm, optic tract and the two central targets (Fig. 32, data not shown).

Fig. 30

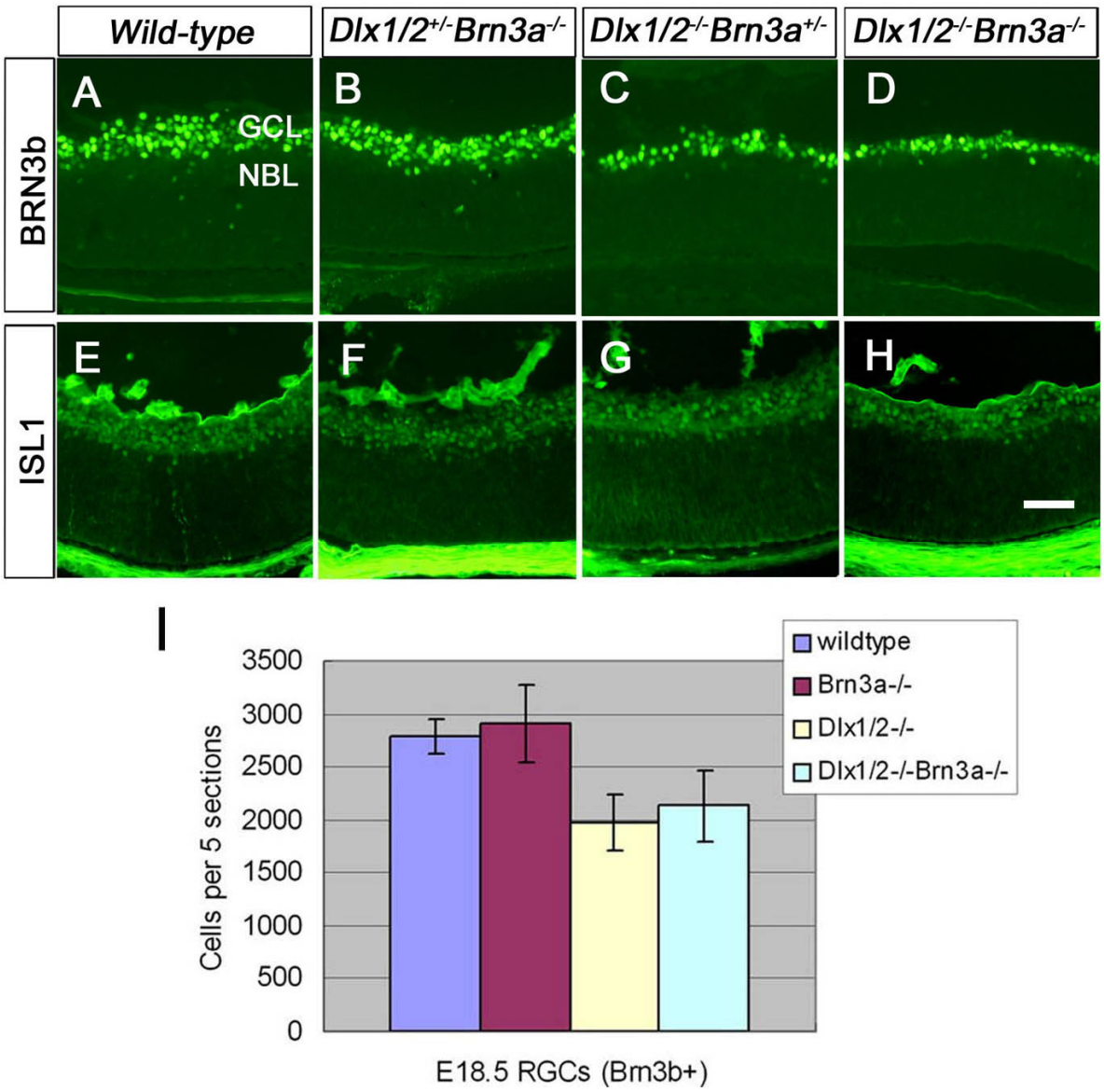
Wild-type
Dlx1/2+/-Brn3a-/-
Dlx1/2-/-Brn3a+/-
Dlx1/2-/-Brn3a-/-
BRN3b
ISL1
A
B
C
D
E
F
G
H
GCL
NBL
wildtype
Brn3a-/-
Dlx1/2-/-
Dlx1/2-/-Brn3a-/-
Cells per 5 sections
3500
3000
2500
2000
1500
1000
500
0
E18.5 RGCs (Brn3b+)

Fig. 30 *Dlx1/Dlx2/Brn3a* triple null and *Dlx1/Dlx2* double null retinas have similar RGC loss at E18.5

(A-H) Antibodies to BRN3b and ISL1 were used as RGC specific markers in immunostaining. Decreased RGC numbers (both BRN3b positive and ISL1 positive cells) were observed in *Dlx*1/*Dlx*2$^{-/-}$*Brn*3a$^{+/-}$ and *Dlx*1/*Dlx*2$^{-/-}$*Brn*3a$^{-/-}$ retinas at E18.5 (C, D, G, and H). (I) Quantification of BRN3b positive cells showed significant reduction of RGCs in both *Dlx1/Dlx2* double and *Dlx1/Dlx2/Brn3a* triple null retinas. However, there is no statistical difference observed between these two genotypes. GCL, ganglion cell layer; NBL, neuroblastic layer. Scale bars: 20μm.

Fig. 31

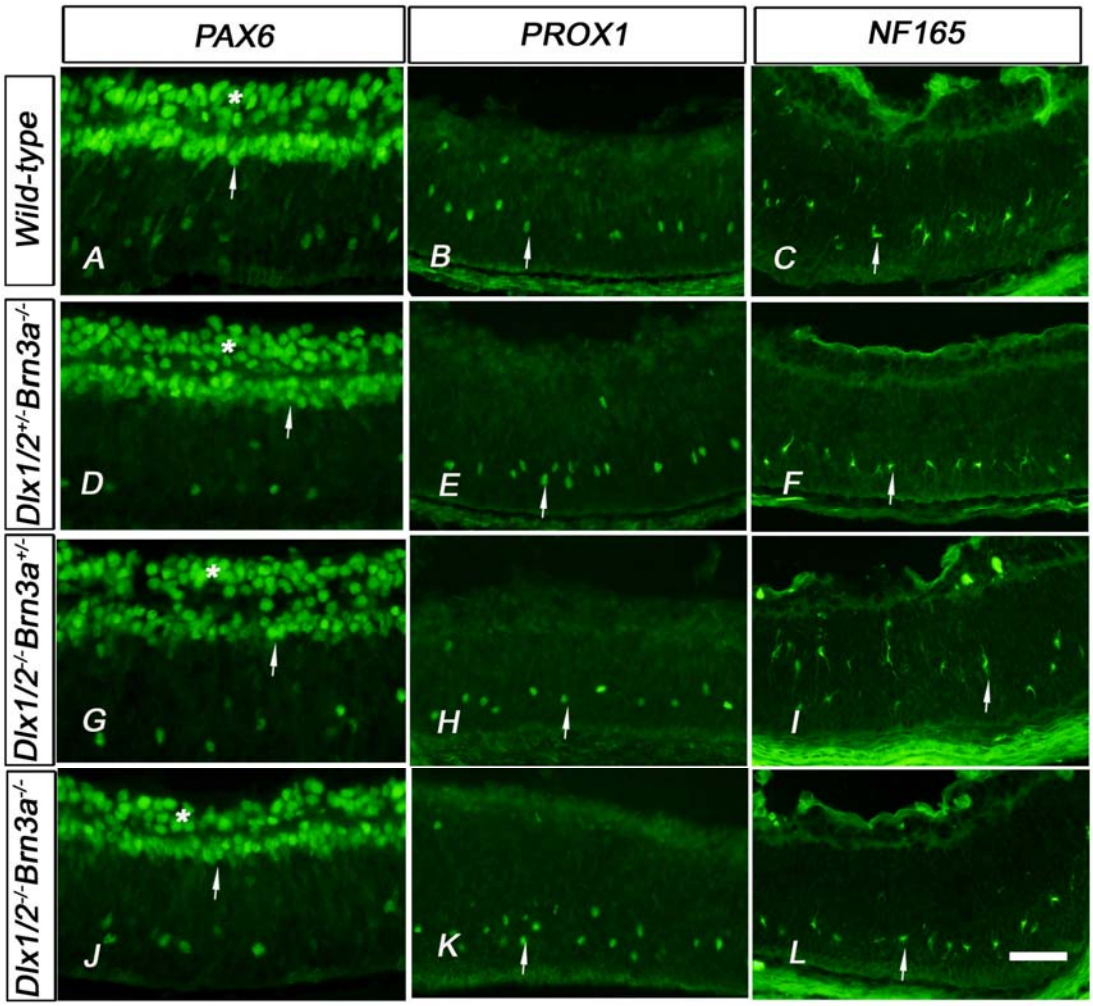
PAX6
PROX1
NF165
Wild-type
Dlx1/2+/-Brn3a-/-
Dlx1/2-/-Brn3a+/-
Dlx1/2-/-Brn3a-/-
A
B
C
D
E
F
G
H
I
J
K
L

Fig. 31 No other early differentiated retina neuronal classes are affected in the *Dlx1/Dlx2/Brn3a* triple null retinas

(A-L) Antibodies to PAX6, PROX1, and NF165 were used as amacrine (PAX6) and horizontal cell (PROX1, NF165) markers, respectively. PAX6 expressing amacrine cells are located in the inner NBL, and significant differences were not observed among the different mutants (stars in A, D, G, and J). Both PROX1 and NF165 expressing cells are located in the outer NBL, and there were no obvious differences observed between all four genotypes, suggesting horizontal cells are not affected (arrows in B, E, H, K and C, F, I, L). GCL, ganglion cell layer; NBL, neuroblastic layer. Scale bar: 20μm

Fig. 32

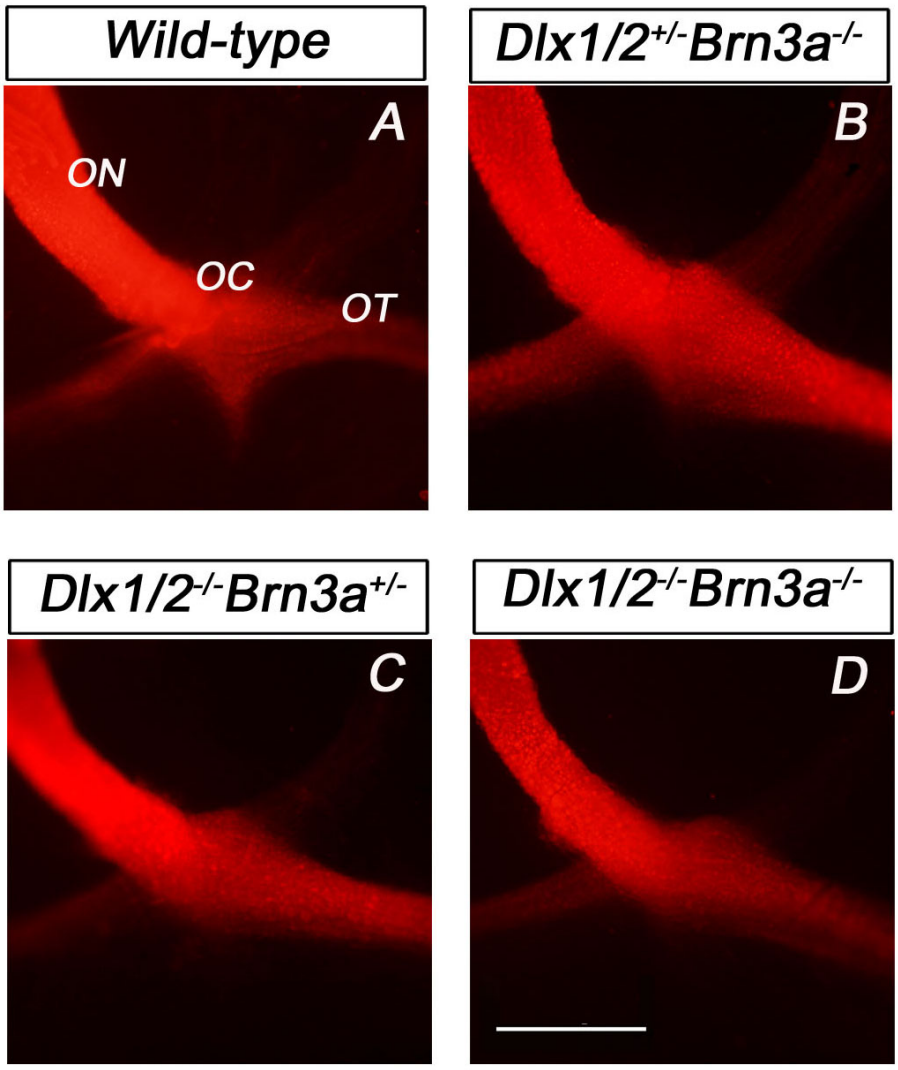

Fig. 32 No obvious RGC axonal guidance defects are observed in the *Dlx*1/*Dlx*2/*Brn*3a triple null mutants.

Anterograde diI labeling was used for RGC axonal projection studies at E18.5. The thickness of optic nerves was reduced in both *Dlx1/Dlx2* double and *Dlx1/Dlx2/Brn3a* triple null mice (C, D). No obvious axonal guidance defects were observed at the optic nerve, optic chiasm and optic tract from wild-type, *Dlx*1/*Dlx*2$^{+/-}$*Brn*3a$^{-/-}$, *Dlx*1/*Dlx*2$^{-/-}$*Brn*3a$^{+/-}$ and *Dlx*1/*Dlx*2$^{-/-}$*Brn*3a$^{-/-}$ mutants. ON, optic nerve; OC, optic chiasm; OT, optic tract; Scale bar: 200μm.

4.18 MicroRNA-124 is co-expressed with DLX2 in embryonic and adult retinas

Previously we have identified *Brn3a* and *Brn3b* as two novel transcriptional targets of DLX1 and DLX2. Other DLX1/DLX2 targets that have also been characterized by our lab or other research groups include *TrkB*, *Crx*, *Otx2*, and *Olig2* (Pinto V and Eisenstat D, unpublished data) (de Melo, Zhou et al. 2008). Not much is known about the upstream regulation of the *Dlx1/Dlx2* genes, except studies on several *cis*-acting elements of the *Dlx1/Dlx2* bigenic cluster, including two intergenic enhancers, *I12b* and *I12a*, and two upstream regulatory elements (URE), *URE1* and *URE2* (Du G and Eisenstat D, unpublished data) (Hamilton, Woo et al. 2005; Poitras, Ghanem et al. 2007).

MicroRNAs (miRNAs) are endogenous, small, non-coding, regulatory RNAs, ~ 22 nts in size (Carthew and Sontheimer 2009). miRNAs bind to target sites in the 3'-untranslated region (3'-UTR) of mRNAs and negatively regulate gene expression post-transcriptionally, especially in development and tumorigenesis. It is shown that most mammalian mRNAs are conserved targets of one or more miRNAs (Friedman, Farh et al. 2009). We considered whether *Dlx1* and *Dlx2* are also regulated by one or more miRNAs, especially during retinogenesis.

Using *TargetScan,* a well accepted miRNA target prediction tool, we first analysed the *Dlx2* 3'-UTR for putative miRNA binding seeds *in silico* (Bartel 2009). We found that within the 1kb *Dlx2* 3'-UTR, there are multiple conserved sites for miRNAs, among which four sites are broadly conserved among all vertebrates. Those sites are target seeds for miR-124, 129, 216a and 216b, respectively (Fig. 33).

miR-124 is specifically expressed in the developing CNS and the neural retina (Karali, Peluso et al. 2007; Landgraf, Rusu et al. 2007). *Dlx2* was reported as being a target of miR-124 in adult subventricular zone (SVZ) neurogenesis (Cheng, Pastrana et al. 2009). By performing combined DLX2 immunohistochemistry (IHC) with *in situ* RNA hybridization (ISH) using an LNA-modified miR-124 probe (Exiqon), we demonstrated that DLX2 and miR124 are co-expressed in the same retinal cell population from E13.5 to P14 (Fig. 34). MicroRNAs and their transcription factor targets usually interact in a double-negative feedback loop (Johnston, Chang et al. 2005; Xu, Papagiannakopoulos et al. 2009). Using luciferase reporter assays, we also observed a negative regulation of DLX2 on miR124 transcription (data not shown). Taken together, these data suggest an interesting regulatory loop between *Dlx2* and miR124 during retinogenesis. However, further work is required to thoroughly investigate these cross-regulatory interactions between this microRNA and other miRNAs and the *Dlx*1/*Dlx*2 bigenic cluster.

Fig. 33

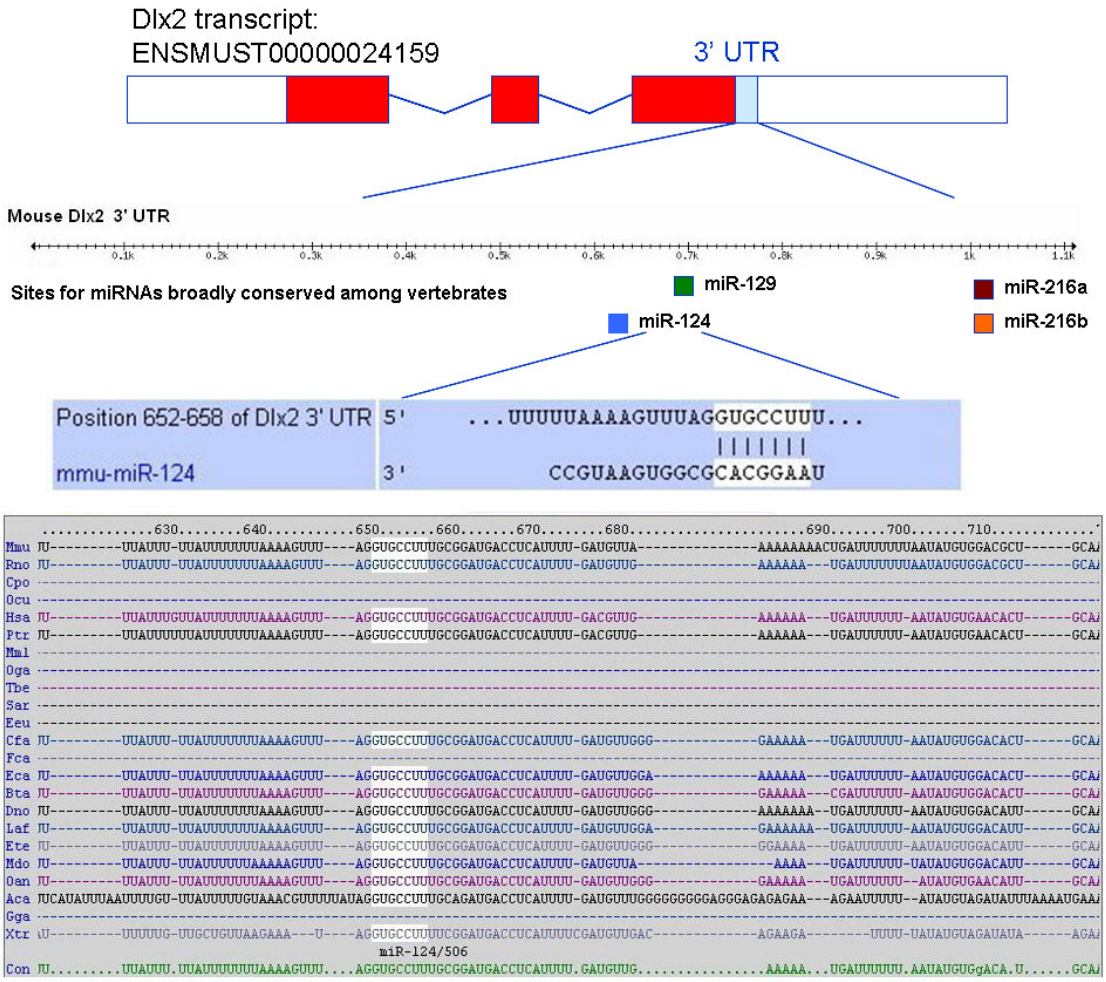
Dlx2 transcript:
ENSMUST00000024159
3' UTR
Mouse Dlx2 3' UTR
Sites for miRNAs broadly conserved among vertebrates
miR-129
miR-124
miR-216a
miR-216b
Position 652-658 of Dlx2 3' UTR
5' ...UUUUUAAAAGUUUAGGUGCCUUU...
mmu-miR-124
3' CCGUAAGUGGCGCACGGAAU
miR-124/506

Fig. 33 Conserved *miR124* target site is located at the Dlx2 3'-UTR

Four broadly conserved microRNAs, miR-124, miR-129 and miR216a/b, are predicted to target the 3'-UTR of *Dlx2* (*TargetScan*) (Bartel 2009). Sequence alignments show the match of miR-124 and its target site on *Dlx2* 3'-UTR. The putative miR-124 binding site is well conserved among vertebrates.

Fig. 34

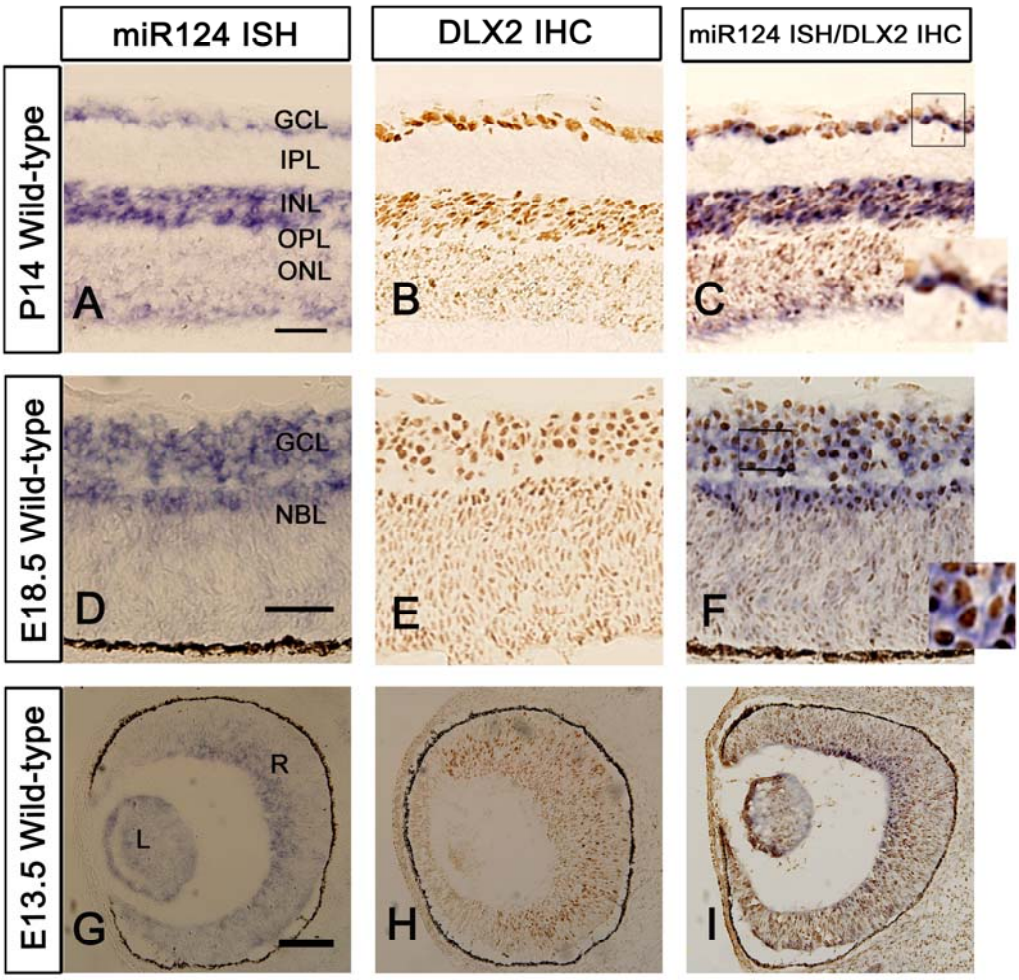
miR124 ISH
DLX2 IHC
miR124 ISH/DLX2 IHC
P14 Wild-type
E18.5 Wild-type
E13.5 Wild-type
GCL
IPL
INL
OPL
ONL
NBL
R
L
A
B
C
D
E
F
G
H
I

Fig. 34 *miR124* is co-expressed with DLX2 in embryonic and adult mouse retina

DLX2 antibody and LNA-modified miR-124 probe were used for combined immunohistochemistry (IHC) and *in situ* RNA hybridization (ISH). (A-C) At P14, miR-124 is expressed in the GCL and INL, where DLX2 expression is detected. Weak miR-124 expression is also identified in the outer ONL at this stage. (D-F) miR-124 is expressed in the GCL and inner NBL of E18.5 retina. DLX2 is co-expressed with miR-124 in these two layers. DLX2 is expressed in the nuclei and miR-124 is located in the cytoplasm (box in F). (G-I) At E13.5, miR-124 is expressed more centrally in the retina, whereas DLX2 expression is more dispersed. Co-expression was detected in the central retina (I). GCL: ganglion cell layer; IPL, inner plexiform layer; INL, inner nuclear layer; OPL, outer plexiform layer; ONL, outer nuclear layer; NBL: neuroblastic layer; L: lens; R: retina; Scale bars: 25μm in A and C; 50μm in G.

Chapter 5 Discussion and Future Directions

5.1 *Dlx*1/*Dlx*2 and *Brn*3b play combinatorial roles in retinal ganglion cell development

During retinogenesis, external cues and transcriptional regulation control the identity of retinal cell types (Livesey and Cepko 2001). The coordinated activities of several TFs are required for the differentiation of specific retinal cell types. The combinatorial roles of homeodomain (HD) and bHLH TFs have been extensively studied. For example, the homeobox gene *Chx*10 (*Vsx*2) and bHLH genes *Mash*1 (*Ascl*1)/*Neurod*4 (*Math*3) co-regulate bipolar cell genesis and the homeobox gene *Crx* and bHLH gene *Neurod*1 induce photoreceptor development (Morrow, Furukawa et al. 1999; Hatakeyama, Tomita et al. 2001). Herein, we report combinatorial roles of the homeobox genes *Dlx*1/*Dlx*2 and the class IV POU domain-containing gene *Brn*3b in retinal cell fate specification. We have demonstrated more severe retinal abnormalities in the *Dlx*1/*Dlx*2/*Brn*3b triple null mice than for either the *Dlx*1/*Dlx*2 double mutants or the *Brn*3b single knockouts. We detected a near complete loss of retinal ganglion cells (RGCs) in the triple null retinas from E12.5 to E18.5. Based on previous studies, neither *Dlx*1/*Dlx*2 nor *Brn*3b is necessary for the initiation of RGC differentiation (Gan, Wang et al. 1999; de Melo, Du et al. 2005). Expression of TFs positioned upstream of *Dlx*1/*Dlx*2 or *Brn*3b, such as *Math5* and *Chx10*, is required for the competence of retinal progenitors to initiate expression of *Brn*3b and *Dlx*1/*Dlx*2 for terminal differentiation, maturation and survival of RGC (Wang, Kim et al. 2001;

Yang, Ding et al. 2003). The observed 70-80% loss of RGCs in *Brn*3b single mutant mice only occurs at E15.5 or later stages, whereas 33% loss of RGCs in the *Dlx*1/*Dlx*2 double KO mice is only detected by E18.5 (Gan, Wang et al. 1999; de Melo, Du et al. 2005). Unlike these "late" RGC losses, we found that the combined disruption of *Dlx*1/*Dlx*2 and *Brn*3b resulted in a dramatic reduction of RGCs by E12.5, supporting a combined and possibly a synergistic role for these homeobox genes in early RGC differentiation. Although the majority of the E12.5 and E13.5 birth-dated retinal cells were correctly positioned in the GCL, very few expressed RGC differentiation markers in the triple null retinas (Fig. 8). Hence, without affecting early migration of retinal progenitors to the nascent GCL, combined loss of *Dlx*1/*Dlx*2 and *Brn*3b function severely impaired RGC genesis, differentiation and survival.

Using a retina-specific KO of the LIM HD gene *Isl*1, *Isl*1/*Brn*3b double null mice were generated. The authors observed severe RGC loss but normal RGC genesis before E13.5, and with *Brn*3b, *Isl*1 was shown to define a distinct, yet overlapping RGC sub-population under the regulation of MATH5 (Mu, Fu et al. 2008; Pan, Deng et al. 2008). An almost complete loss of RGC as well as severe losses of other retinal cell types resulted from the *Math5*/*Brn*3b double null mice (Moshiri, Gonzalez et al. 2008). We propose that *Math5*-*Brn*3b/*Isl*1 and *Dlx*1/*Dlx*2-*Brn*3b regulate two parallel transcriptional pathways for RGC differentiation (Fig. 35). In this model, the deletion of both *Isl*1 and *Brn*3b would not affect the competence of retinal progenitors to become RGC, since *Dlx*1 and *Dlx*2 would still be available for promoting RGC differentiation. However, deletion of *Dlx*1/*Dlx*2 and *Brn*3b would block the two

dominant pathways for RGC differentiation and survival. The few remaining RGC in *Dlx*1/*Dlx*2/*Brn*3b compound mutants could be derived from the small population of *Isl*1 expressing progenitors, which are distinct from those expressing *Brn*3b (Moshiri, Gonzalez et al. 2008). It is important to note that the apoptosis induced by *Brn*3b deletion occurs after E16.5 and continues postnatally; this postnatal cell death contributes to the loss of mature ganglion cell numbers (Erkman, McEvilly et al. 1996; Gan, Xiang et al. 1996; Gan, Wang et al. 1999) whereas it remains unknown whether there is postnatal RGC death in the *Dlx*1/*Dlx*2 KO since these mutants die at P0. Our model (Fig. 35) would predict a complete loss of RGC in *Dlx*1/*Dlx*2/*Math5* compound mutants.

5.2 Early born amacrine cells share the same retinal bi-potential precursor cells with RGCs

In addition to the early RGC loss, we found a ~ 2-fold increase in dislocated amacrine cells in the E18.5 *Dlx*1/*Dlx*2/*Brn*3b null GCL; thereby GCL cellularity was only modestly reduced. This cell fate switch was demonstrated throughout all embryonic stages examined, supported by the BrdU birth-dating experiments. This cell fate shift was unexpected, since no other retinal cell type other than RGC are affected by deletion of either *Dlx*1/*Dlx*2, or *Brn*3b (Erkman, McEvilly et al. 1996; Gan, Xiang et al. 1996; de Melo, Du et al. 2005). However, a similar phenotype has been reported in *Math5* mutant mice, with an increase of starburst amacrine cells in the GCL (Wang, Kim et al. 2001) as well as increased cones, bipolar and Müller cells

(Brown, Patel et al. 2001; Wang, Kim et al. 2001). *Math5* is expressed in retinal progenitors during or immediately after the last cell division, promoting RGC specification by driving exit from the cell cycle, and repressing non-RGC specifying TFs (Brown, Kanekar et al. 1998; Brown, Patel et al. 2001; Le, Wroblewski et al. 2006; Mu, Fu et al. 2008). The amacrine cell fate shift in the *Dlx*1/*Dlx*2/*Brn*3b null retinas might result from a different mechanism than from the one observed in *Math5* mutant retinas. There was preserved expression of *Math5* in the *Brn*3b, *Dlx*1/*Dlx*2 and triple KO mice (Fig. 15). One possible explanation is that retinal progenitor cells accumulate more than one competency by expressing "early" factors, such as *Math5*, *Neurod*1, *Chx10*, or *Mash*1. Using lineage tracing, *Math5* expression is associated with multiple retinal neuronal types, including RGC, photoreceptors, horizontal, and amacrine cells (Yang, Ding et al. 2003). Cells with restricted developmental potential migrate properly and are further specified to differentiate under the regulation of "late" factors. In this case, both *Dlx*1/*Dlx*2 and *Brn*3b act as the "late" factors and are responsible for the terminal differentiation of RGCs (refer to model, Fig. 35). Without *Dlx*1/*Dlx*2 and *Brn*3b, precursor cells restricted to RGC and amacrine cell fates migrate to the GCL correctly but are unable to terminally differentiate into RGC and either undergo apoptosis or differentiate into amacrine cells.

A relationship of amacrine birthdates and soma position has been observed (Voinescu, Kay et al. 2009). Cholinergic (ChAT expressing) amacrine cells are among the earliest born amacrine cells, and tend to migrate and occupy the GCL and inner layer of INL. Glycinergic amacrine cells are late born cells and are confined to the

INL. The upregulation of ChAT, but not GlyT1, in *Dlx*1/*Dlx*2/*Brn*3b null retinas suggests that the loss of *Dlx*1/*Dlx*2 and *Brn*3b resulted in an increase of early born amacrine cells, but not late born amacrine cells. The early born amacrine cells, but not the late born amacrine cells, may share the same progenitor pool with RGCs. It is possible that the amacrine pathway is the default pathway of those ganglion/amacrine precursors that migrated to the GCL. Without *Math5/Brn3b*, or *Dlx1/Dlx2*, the precursors are unable to differentiate to RGCs, and instead adopt an amacrine cell fate .

Other observations support the hypothesis that RGC and amacrine cells arise from bi-potential precursors. For example, in *Neurod*1-*Neurod*4 double mutants, amacrine cells were severely decreased, whereas RGC were increased, localized to the GCL and aberrantly in the INL; *Foxn*4$^{-/-}$ retinas showed a dramatic loss of amacrine cells and dislocated RGCs within the INL instead of the GCL (Inoue, Hojo et al. 2002; Li, Mo et al. 2004). Recent studies have demonstrated that a *Neurod*1 knock-in at the *Math5* locus re-established RGC gene expression (*Isl*1 and *Brn*3b), RGC specification and optic nerve formation, without the over-production of amacrine cells (Mao, Wang et al. 2008). Retinal progenitor cell (RPC) single cell gene-expression profiles showed significant levels of *Math5*, *Neurog*2 (*Ngn*2) and *Neurod*1 in individual RPCs isolated from the same developmental time point (Trimarchi, Stadler et al. 2008). Hence, "early" factors, including *Math5* and *Neurod*1, advance RPC to more narrowly defined but overlapping competencies, whereas, "late" factors, such as *Dlx*1/*Dlx*2 and *Brn*3b, promote these restricted-potential RPC

towards more specialized retinal neuron cell fates.

5.3 RGCs are required for retinal cell differentiation and proliferation

RGCs normally secrete various signalling molecules, including Shh, VEGF and GDF11 (Kim, Wu et al. 2005; Wang, Dakubo et al. 2005). Therefore the observed increase in dislocated amacrine cells in the GCL of the *Dlx*1/*Dlx*2/*Brn*3b triple KO could be the indirect influence of the dramatic RGC loss and the consequent decrease of these signalling molecules, and subsequent removal of inhibition of amacrine cell differentiation. However, the role of these extrinsic cues on amacrine cell genesis remains to be elucidated. These putative changes in the external milieu could also explain the cell cycle disruption observed in the triple null retinas. Fewer mitotic cells were detected in the proliferation zone of the triple null retinas, with a higher proportion of cells remaining in the G_1/G_0 phase. Shh is expressed as mitogen for retinal precursor cells, and Shh regulation of downstream molecules, such as Gli1, Ccnd1 and Cdc25b, controls proliferation of retinal precursors (Mu, Fu et al. 2005; Wang, Dakubo et al. 2005). No cell cycle disruption was observed in either the *Dlx*1/*Dlx*2 double or *Brn*3b single mutants (Gan, Xiang et al. 1996; de Melo, Du et al. 2005). This further supports a synergistic role of *Dlx*1/*Dlx*2 and *Brn*3b in retinogenesis.

5.4 *Dlx1/Dlx2* and *Brn3b* function in parallel but cooperative regulatory genetic pathways

By E16.5, when DLX2 is mainly restricted to the GCL and INL, BRN3b positive cells are a subset of the DLX2 positive cell population. This spatio-temporal relationship between DLX2 and BRN3b expression suggested that DLX2 and/or DLX1 could regulate a second, later phase of *Brn*3b expression during retinal development. We demonstrated that both DLX1 and DLX2 bind to a specific *Brn*3b promoter region *in situ* and activate its expression *in vitro*. In addition, we identified three candidate functional binding sites located within the *Brn*3b promoter. Moreover, siRNA-mediated knockdown of *Dlx*2 in primary embryonic retina cultures resulted in decreased expression of *Brn*3b consistent with reduced BRN3b expression in the *Dlx*1/*Dlx*2 double knockout mouse retina (de Melo, Du et al. 2005). Finally, ectopic expression of BRN3b occurred following *in utero* retinal electroporation of *Dlx*2. These observations strongly support the direct regulation by DLX1 and DLX2 of *Brn*3b transcription *in vivo*. Taken together, both *Dlx*1 and *Dlx*2 promote *Brn*3b expression during retinal development.

Interestingly, the absence of *Dlx*1/*Dlx*2 in the embryonic forebrain resulted in reduced expression of *Oct*6/SCIP (*Pou*3f1) and *Brn*-4 (*Pou*3f4), two class III POU HD factors, in the developing SVZ (Anderson, Qiu et al. 1997). This observation suggests that DLX1/DLX2 may directly regulate other POU HD transcription factors besides *Brn*3b, such as *Brn*3a (*Pou*4f1) or *Brn*3c (*Pou*4f3) in the developing retina and thus further explain the severe retinal phenotype observed in the *Dlx*1/*Dlx*2/*Brn*3b

triple null mice. Hence, loss of *Dlx*1 and/or *Dlx*2 function could reduce transcription of all *Brn*3 genes in the retina, therefore blocking the functional redundancy of *Brn*3 gene family members (Pan, Yang et al. 2005). This was supported by our discovery that DLX2 binds to specific regions of the Brn3a promoter and activates its expression *in vitro* and *in utero*.

Previous loss-of-function and microarray profiling studies support the hypothesis that *Brn*3b negatively regulates *Dlx*1 and *Dlx*2 expression in the embryonic retina (Mu, Fu et al. 2005; Qiu, Jiang et al. 2008). However, little is known about this regulation at the molecular level. We also observed a transient increase in DLX2 expression at E13.5 but not at E11.5 or E16.5 in the *Brn*3b single KO retina. Since apoptosis of RGCs occur in *Brn*3b mutants at ~E15.5, the initial increase in DLX2 expression could be lost due to the ensuing RGC cell death. Another possibility is that repression of *Dlx*2 by BRN3b occurs at E13.5-E14.5, during the peak of early-born RGCs differentiation regulated by *Math5*-*Brn*3b. This repression is removed with diminishing *Math5* expression after E16.5 (Brown, Kanekar et al. 1998).

Using ChIP assays of E16.5 retinal tissue, we tested whether this negative regulation could be due to occupancy of *Dlx*1/*Dlx*2 regulatory regions by BRN3b. Several *cis*-acting elements of the *Dlx*1/*Dlx*2 bigenic cluster have been characterized, including two intergenic enhancers, I12b and I12a, and two upstream regulatory elements (URE), URE1 and URE2 (Ghanem, Jarinova et al. 2003; Ghanem, Yu et al. 2007). These four *cis*-regulatory elements were examined for consensus *Pou*4f2

DNA-binding sites [5'-(A/G)TTAATGAG(C/T)-3'] (Xiang, Zhou et al. 1995), and we found two putative binding sites in URE2 and one site was identified in I12b. In subsequent ChIP assays we could not detect occupancy by BRN3b at any of these *Dlx*1/*Dlx*2 *cis*-regulatory regions, although we replicated binding to the Eomesodermin (*Eomes*) promoter, an established direct target of BRN3b (Mao, Kiyama et al. 2008). It therefore seems more likely that the repression of *Dlx*1/*Dlx*2 expression by BRN3b is mediated by protein-protein interactions, or via other mechanisms, rather than through transcriptional regulation.

Taken together, the mutual regulatory interactions between *Dlx*1/*Dlx*2 and *Brn*3b and the more severe phenotype observed in the triple null retinas suggests that *Dlx*1/*Dlx*2-*Brn*3b and *Math5*-*Brn*3b are two parallel but cross-regulatory genetic pathways in retinogenesis (Fig. 35). *Math5* is the predominant regulator of early *Brn*3b expression. However, after E16, concurrent with the significant decrease of *Math5* expression (Brown, Kanekar et al. 1998), *Dlx*1 and *Dlx*2 are playing important roles in *Brn*3b expression, and more importantly, in the RGC differentiation and survival. This may explain the requirement for *Dlx*1 and *Dlx*2 function for late born RGC, and why significant RGC loss in the *Dlx*1/*Dlx*2 null retina was only observed after E16.5 (de Melo, Du et al. 2005). Characterization of the transcriptomes of *Dlx*1 and *Dlx*2 as well as other homeobox genes, and their regulation by micro-RNAs, will further contribute to our understanding of the role of these transcription factors in retinal development.

Fig. 35

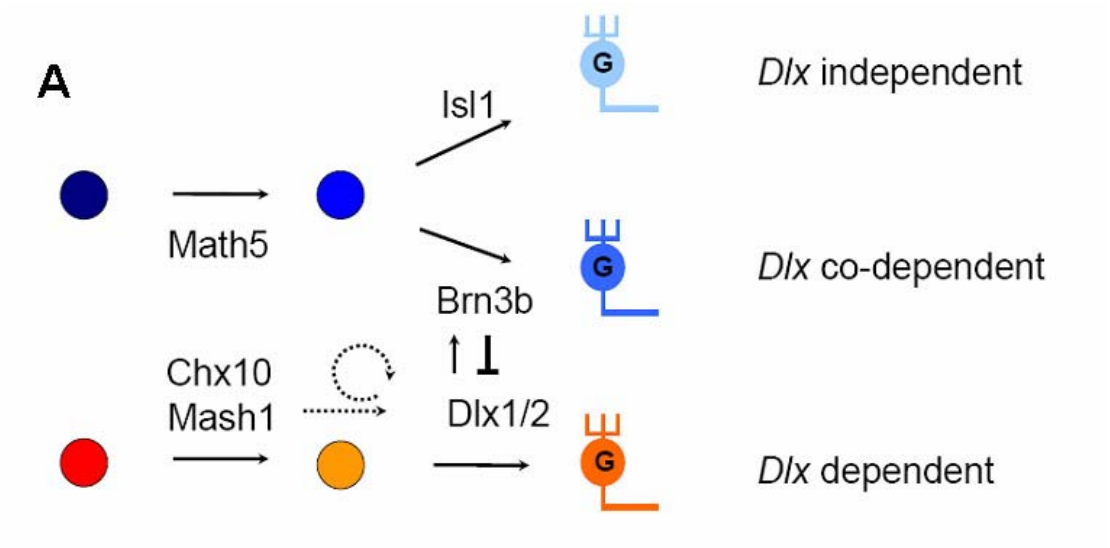
A
Isl1
Math5
Brn3b
Chx10
Mash1
Dlx1/2
G
G
G
Dlx independent
Dlx co-dependent
Dlx dependent

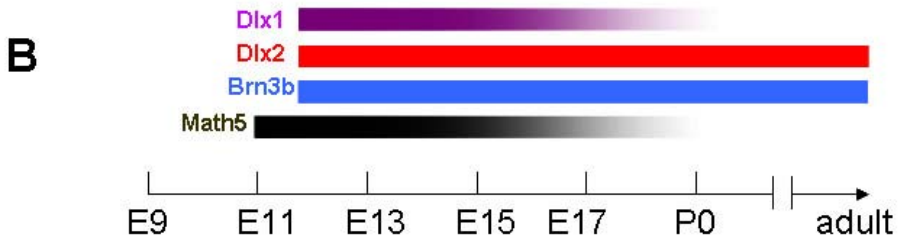
B
Dlx1
Dlx2
Brn3b
Math5
E9
E11
E13
E15
E17
P0
adult

Fig. 35 *Dlx*1/*Dlx*2-*Brn*3b and *Math*5 (*Atoh*7)-*Brn*3b/*Isl*1 are two parallel but cross-regulatory pathways in RGC development

(A) Multi-potential retinal progenitors gain limited competence by expressing "early" factors, such as *Math*5 (*Atoh*7) or *Chx*10 (*Vsx*2). *Dlx*1/*Dlx*2 and *Brn*3b function in the terminal differentiation and survival of RGC. The *Math*5-*Brn*3b/*Isl*1 pathway determines the majority of early-born RGC, whereas *Dlx*1/*Dlx*2-*Brn*3b regulates a group of late-born RGCs. Both DLX1 and DLX2 regulate *Brn*3b gene expression, whereas BRN3b transiently represses *Dlx*1/*Dlx*2. *Dlx*1/*Dlx*2 and *Brn3b* may function in the terminal differentiation of distinct populations of RGCs. (B) *Math5* expression in the retina starts at E11, which is prior to the expression of *Brn3b*, *Dlx1*, and *Dlx2*. After E17, however, *Math5* expression is decreased dramatically. No *Math5* is detected in the adult mouse retina. *Brn3b*, *Dlx1* and *Dlx2* are first identified at E11.5. Both *Dlx2* and *Brn3b* remain robust expression throughout the adulthood, whereas *Dlx1* expressed is down-regulated postnatally. Solid lines, established regulation; broken lines, proposed regulation.

5.5 DLX2 but not DLX1 regulates *Brn3a* expression in the retinogenesis

In the developing retina, *Dlx2* expression precedes *Brn3a* expression by ~ 2 gestational days. By E16.5, most BRN3a positive cells are restricted to the ganglion cell layer, and co-express DLX2. In the *Dlx1/Dlx2* double knockout mice, there is a significant reduction of *Brn3a* expression, at both the mRNA and protein level, Moreover, the mis-expression of DLX2 in developing retina is sufficient to promote ectopic *Brn3a* expression the NBL. These observations support the regulation of *Brn3a* expression by DLX2 during retinogenesis.

Both DLX1 and DLX2 bind directly to the promoter of *Brn3b* and regulate its transcription. However, this is not the case in *Brn3a* expression. Using ChIP assays, we demonstrated that DLX2 but not DLX1 binds to the *Brn3a* promoter *in situ*. Two candidate *Brn3a* promoter regions were immunoprecipitated by the DLX2 antibody, but not by the DLX1 antibody. Both regions contain consensus HD binding sites, and show direct and specific binding to the DLX2 protein. Despite their overlapping expression patterns and redundant functions in forebrain and retina development, both DLX2 and DLX1 have their own unique functions. *Brn3a* could be one of the DLX2 specific transcriptional targets. Other DLX2 specific transcription targets have been identified in the developing retina, including *TrkB*, *Crx* and *Otx2* (de Melo, Zhou et al. 2008) (Pinto V and Eisenstat D, unpublished observations). The *Dlx5/Dlx6* intergenic enhancer (*MI56*) is a direct target of both DLX1 and DLX2 in the developing forebrain. However, only DLX2, but not DLX1 antibody, is able to immunoprecipitate *MI56* from P0 retinas (Zhou, Le et al. 2004). Similar DLX2 specific functions have

been observed previously. For example, *Arx* is a direct target of DLX2 in the developing forebrain and mediates the GABAergic interneuron migration (Colasante, Collombat et al. 2008). DLX2 binds directly to the promoter region of *Msx2* and regulates its expression in the branchial arch development (Diamond, Amen et al. 2006). However, the role of DLX1 in the regulation of either *Arx* or *Msx*2 has not been fully explored.

A second explanation for DLX2 specific binding to the *Brn3a* promoter is the possible dominant role of *Dlx2* as a transcription factor in retinal development. Both DLX1 and DLX2 are expressed in an overlapping fashion in the early developing retina. After E16.5, DLX1 expression is reduced in the retina, and no DLX1 expression is detected postnatally. DLX2 expression is well maintained throughout the embryonic and postnatal stages (de Melo, Qiu et al. 2003). Since the ChIP assays were performed on E16.5 retina tissues, it is possible that the DLX1 antibody is unable to precipitate the small amount of DLX1 protein expressed at this stage. Therefore, *Brn3a* might be a target of DLX1 in the early developing retina, but not at later stages. The transcriptional regulation depends upon the temporal developmental context. The possible dominant role of *Dlx2* in retinal development is supported by the observation that the *Dlx2* single knockout mice show a similar, albeit reduced, RGC loss to the *Dlx1/Dlx2* double knockout retina, whereas the *Dlx1* single mutant retinas are comparable to their wild-type littermates (Globa A and Eisenstat D, unpublished observations).

5.6 *Brn3a* is a downstream target of both DLX2 and BRN3b in the developing retina

Of the two candidate *Brn3a* promoter regions identified by the DLX2 ChIP, only the 3A-1 region and DLX2 co-transfection is able to promote luciferase reporter gene activation. The 3A-1 promoter region is a well conserved regulatory region, which contains both HD DNA binding sites and POU4 DNA binding sites. EMSA assays demonstrate that both DLX2 and BRN3b bind directly and specifically to this 3A-1 region, on the same binding motifs *in vitro*. Mutagenesis of these putative binding sites eliminates the ability of DLX2 to bind the DNA oligonucleotide probes. It is possible that by binding to the 3A-1 promoter region, BRN3b acts as a co-activator for DLX2 and regulates *Brn3a* expression during retinogenesis. This could explain the observed results of the luciferase assays, with only 3A-1 but not 3A-3 co-transfection with DLX2 activating reporter gene transcription *in vitro*. We did co-transfection assays in two different cell lines, human embryonic kidney (HEK) 293 and the retinoblastoma cell line Y79. Interestingly, there is endogenous *Brn3b* expression detected in HEK293 cells and adult mouse kidney (Wagner, Wagner et al. 2003). Y79 retinoblastoma cells, on the other hand, have strong *Brn-2* (POU3F2) expression, which can be repressed by Rb restoration (Cobrinik, Francis et al. 2006). All of the POU domain factors recognize and bind to similar DNA sequences (Turner 1996; Phillips and Luisi 2000). It is possible that the *Brn3b* endogenously expressed in the HEK293 cells and the *Brn2* expressed in the Y79 cells both function as co-activators with DLX2 and promote luciferase reporter gene transcription *in vitro*.

To elucidate this combinational role of co-factors, further work needs to be done. For example, co-transfection of DLX2 and BRN3b into a cell line without endogenous POU factors expression could be explored as well as ChIP-reChIP assays demonstrating co-occupancy of region 3A-1 by DLX2 and BRN3b.

BRN3a is also identified to regulate itself (autoregulation) by binding to this same 3A-1 promoter region. Interestingly, opposite transcriptional effects were observed between *in vitro* gene reporter assays and *in vivo* transgenic models. Negative regulation by BRN3a on its own expression was detected using a transgenic mouse model. However, with co-transfection of BRN3a and its promoter region into a cultured cell line, BRN3a significantly activated reporter gene transcription (Trieu, Ma et al. 2003). The different co-factors *in vivo* and *in vitro* are clearly playing different roles in this example.

Unlike the severe RGC loss and axonal guidance defects in the *Dlx1/Dlx2/Brn3b* null mice, *Dlx1/Dlx2/Brn3a* compound knockout mice have a similar retinal phenotype to the *Dlx1/Dlx2* double null model at E18.5 (Fig. 32). Although all three *Brn3* POU-domain transcription factors demonstrated functional equivalence in promoting RGC genesis, *Brn3b* has a more dominant role in RGC development (Liu, Khare et al. 2000; Pan, Yang et al. 2005). No obvious retinal phenotype was observed in the conventional *Brn3a* mutant mice at birth, whereas the conditional *Brn3a* mice showed altered RGC dendritic stratification (Badea, Cahill et al. 2009). In the absence of *Brn3a*, *Brn3b* plays a compensatory role in retinogenesis; therefore the RGC loss found in the *Dlx1/Dlx2/Brn3a* triple null is not as severe as

observed in the *Dlx1/Dlx2/Brn3b* retinas.

5.7 A homeobox genes regulatory network is modulating retinogenesis and optic nerve innervation

To understand the gene regulatory network that controls retinogenesis is one of the central goals of retinal development research. Here we demonstrated a transcriptional regulatory circuitry between homeobox genes *Dlx1/Dlx2* and *Brn3a/Brn3b*. *Dlx1/Dlx2* and *Brn3b* function in parallel but cooperative regulatory pathways to determine RGC cell fate. Both DLX1 and DLX2 promote *Brn3b* expression, whereas BRN3b represses *Dlx1/Dlx2*. *Dlx1/Dlx2* is playing a combinatorial role with *Brn3b* in promoting RGC differentiation. However, only DLX2 and BRN3b regulate *Brn3a* expression during retinogenesis, and no combined role exists between *Dlx1/Dlx2* and *Brn3a*.

Another example of homeobox transcriptional regulatory circuitry is between *Otx2* and *Crx*. Both *Otx2* and *Crx* are functioning to specify photoreceptor cell differentiation. OTX2 regulates *Crx* expression by directly binding to its promoter region. On the other hand, CRX represses *Otx2* transcription. In addition, CRX autoregulates its own expression by activating the *Crx* promoter (Hennig, Peng et al. 2008).

This and other accumulating evidence makes the retinal gene regulatory program a complex transcriptional network. Even the regulatory relations among homeobox genes alone are very complicated (Fig. 36). One gene normally regulates

multiple targets. In addition to *Dlx2*, BRN3b also negatively regulates other homeobox genes including *Crx*, *Otx2*, and *Prox1*, to specify RGC differentiation (Qiu, Jiang et al. 2008). DLX2 also functions as a transcriptional repressor for *Crx* and *Otx2* during photoreceptor differentiation (Pinto V and Eisenstat D, unpublished). In the *Dlx1/Dlx2* double mutant retinas, there is increased *Crx* expression in outer NBL and ectopic *Crx* expression in GCL (Fig. 16) (de Melo, Du et al. 2005).

The HD TFs also cooperate with bHLH factors and regulate retinogenesis. BRN3b negatively regulates *Math3*, *NeuroD1* and *Ngn2* (Qiu, Jiang et al. 2008). CRX activates the expression of *NeuroD1* (Hennig, Peng et al. 2008). An interesting regulatory circuitry between *Dlx1/Dlx2* and *Mash1* is identified during forebrain development. *Mash1* is shown to promote GABAergic interneuron differentiation at both the VZ and SVZ of the telencephalon (Fode, Ma et al. 2000; Yun, Fischman et al. 2002). By directly activating the *Dlx1/Dlx2* intergenic region (*I12b*), MASH1 regulates expression of *Dlx1/Dlx2* in the developing forebrain (Poitras, Ghanem et al. 2007). DLX1/DLX2 represses *Mash1* expression and mediates the LGE development (Yun, Fischman et al. 2002). Recent studies done in Dr. Rubenstein's lab showed that *Dlx1/Dlx2* and *Mash1* function in parallel but cross-regulatory pathways in striatal patterning and differentiation (Long, Cobos et al. 2009; Long, Swan et al. 2009). This is similar to how *Dlx1/Dlx2* and *Brn3b* function in promoting RGC genesis.

In addition to retinogenesis, homeobox genes also play important roles in retinal axonal pathfinding. The mechanism underlying how these HD TFs affect axonal pathfinding is not entirely known. One possibility is that the downstream

targets directly regulated by these HD TFs are responsible for axonal guidance. Examples of this are the repression of *EphB1* by *Isl2*, and *Vax1/Vax2* regulation of *EphB2/EphB3* expression. The roles of the *Dlx* homeobox genes in RGC axonal guidance have not yet been reported. However, in the mouse telencephalon, *Dlx*1 and *Dlx*2 promote the tangential migration of GABAergic interneurons, by repressing axonal growth (Cobos, Borello et al. 2007) and by repressing the expression of Neuropilin-2 (Le, Du et al. 2007). It is possible that the genetic program defining RGC identity also encodes a unique "sensory" network for axons, determining how and where RGC axons respond to the guidance cues en route to CNS targets.

Fig. 36

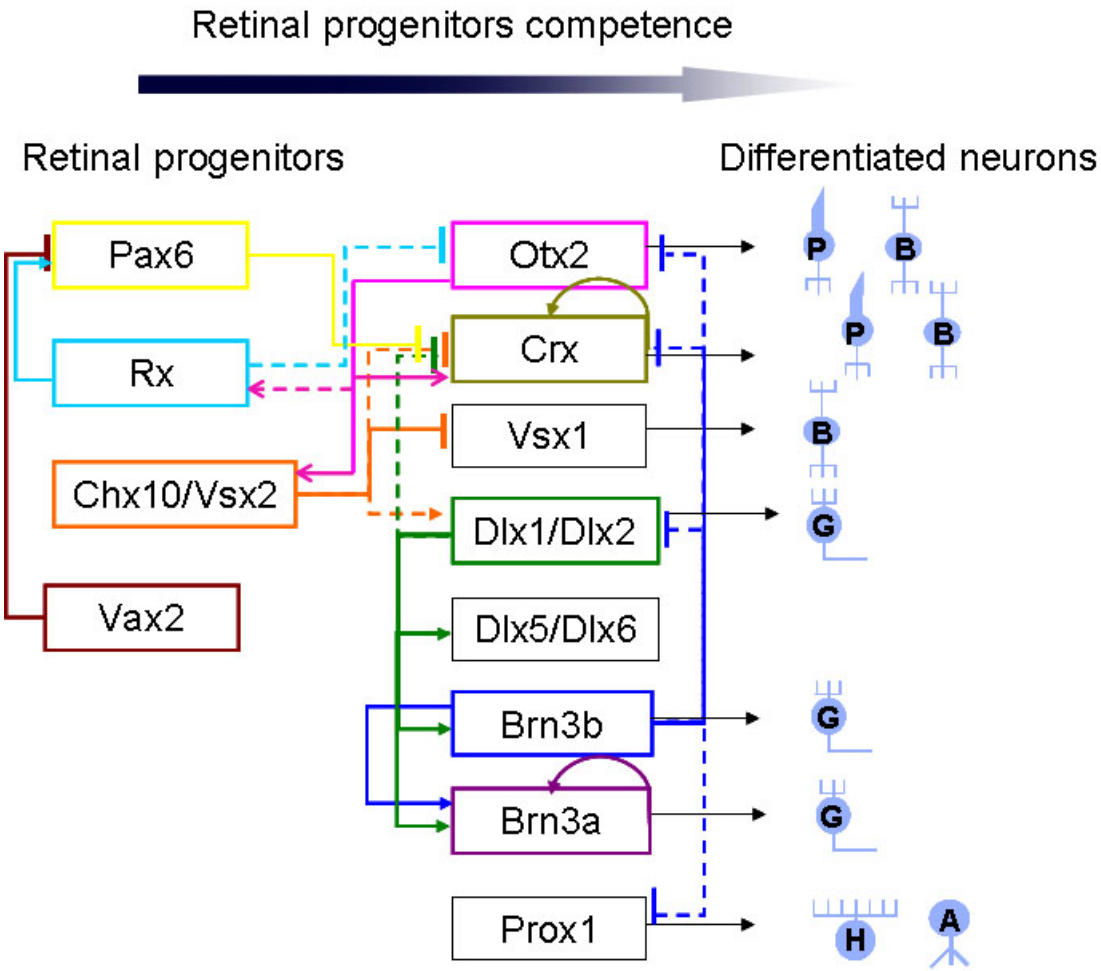
Retinal progenitors competence
Retinal progenitors
Differentiated neurons
Pax6
Rx
Chx10/Vsx2
Vax2
Otx2
Crx
Vsx1
Dlx1/Dlx2
Dlx5/Dlx6
Brn3b
Brn3a
Prox1
P
B
P
B
B
G
G
G
H
A

Fig. 36 HD TFs regulatory interactions during retinogenesis

Homeodomain transcription factors (TFs) act in concert during retinogenesis. *Pax6*, *Rx*, *Chx10/Vsx2* and *Vax2* are expressed early (initiated by E9) in the retinal progenitors of the optic vesicle and are essential for the maintenance of progenitor proliferation and multipotency. The "late" TFs, such as *Dlx1/Dlx2* and *Brn3b* are initiated after E11.5 in postmitotic cells. The "late" TFs promote progenitors to exit cell cycle and differentiate to certain neuronal classes. The regulatory interaction occurs among "early" and "late" TFs. VAX2 represses *Pax6* transcription. Rx promotes *Pax6* expression, but represses *Otx2* expression. OTX2 promotes the transcription of *Chx10*, *Rx* and *Crx*. One TF can act as enhancer as well as repressor. DLX1 and DLX2 activate the transcription of *Dlx5/Dlx6* and *Brn3b*, while DLX2 represses *Crx* expression. The ganglion specific TF, BRN3b, promotes early-born RGC fate by repressing other cell type networks, including *Dlx1/Dlx2* (late-born RGC), *Crx* and *Otx2* (photoreceptor and bipolar neurons). P, photoreceptor; B, bipolar; G, ganglion cell; A, amacrine; H, horizontal; Color code, one color represents one gene and its regulatory functions; solid line, verified direct regulation; dotted line, predicted regulation; →: enhance; -| : repress

5.8 Post-transcriptional regulation of *Dlx* expression and retinogenesis

MicroRNAs (miRNA), a group of endogenous non-coding RNAs, function to "fine-tune" gene expression in the development of multiple organ systems. In the last few years, several research groups have reported miRNA expression and function in the developing and mature retinas of different species. To date, there are about 80 miRNAs identified in the mouse retina, 20 of which appear to be retinal specific (Xu, Witmer et al. 2007). After being transcribed by RNA Polymerase II, the primary miRNAs are processed by *Dicer* and become mature miRNAs. The retinal *Dicer* conditional knockout mice showed disorganization of the retinal laminar structure, general degeneration of all retinal cell types, and decreased ERG amplitudes at one month postnatally (Damiani, Alexander et al. 2008). Mature miRNAs, including miRNA-124 and miRNA-96, are decreased in this model. This study suggests the potential involvement of miRNAs in retinal development and function. Research focussed on specific miRNAs supports this notion. By negatively regulating the expression of *caspase-9* and *apaf1*, miRNA24a represses apoptosis in the *Xenopus* developing retina (Walker and Harland 2009). A group of miRNAs, miRNA-129, -155, -214 and -222, are shown to inhibit *Xotx2* and *Xvsx1* in the *Xenopus* retina and promote bipolar cell generation (Decembrini, Bressan et al. 2009).

Here we demonstrated the expression of miRNA-124 in the embryonic and postnatal mouse retina. miRNA-124 is considered to be a "pro-neuronal" miRNA. miRNA-124 was first cloned from mouse brain tissue in 2002, and has been subsequently identified in the zebrafish retina (Lagos-Quintana, Rauhut et al. 2002;

Wienholds, Kloosterman et al. 2005). Over-expression of miRNA-124 in HeLa cells shifts the mRNA profile to that of a brain-enriched pattern (Lim, Lau et al. 2005). By repressing *Sox9,* miRNA-124 is shown to regulate neural stem cell lineage progression in the subventricular zone of the adult mouse brain (Cheng, Pastrana et al. 2009). *Dlx2* is predicted as a target of miRNA-124, and is repressed by co-transfection with miRNA-124 into HeLa cells *in vitro* (Cheng, Pastrana et al. 2009). In this study, we found co-expression of *Dlx2* and miRNA-124 in both the developing and mature retina. This is somewhat surprising, since most of the miRNAs show mutually exclusive expression patterns with their target genes. One possible explanation is that, instead of a complete shut down of DLX2 translation, miRNA-124 is functioning to "fine-tune" *Dlx2* expression, to homeostatically regulate *Dlx2* expression in the developing retina. A similar co-expression pattern of DLX2 and miRNA-124 is detected in the adult mouse brain (Cheng, Pastrana et al. 2009).

The second well conserved potential miRNA target site located on the *Dlx2* 3'UTR is for miRNA-129. As described previously, miRNA-129 is shown to repress two homeobox genes, *Otx2* and *Vsx1*, in the developing *Xenopus* (Decembrini, Bressan et al. 2009). miRNA-129 is also among a miRNA cluster highly expressed in the retinoblastoma (Zhao, Yang et al. 2009). The third predicted target site is conserved for miRNA-216, which is identified in the human pancreas tissue, and is shown to be a pancreas specific miRNA (Szafranska, Davison et al. 2007; Greither, Grochola et al. 2010). Of interest, *Dlx2* is also expressed in the developing mouse pancreas (Ho A and Eisenstat D, unpublished). Investigation into the potential

interaction of miRNA-129, or miRNA-216 and *Dlx2* could bring insights into both retinal and pancreas development and possibly, tumorigenesis.

5.9 Conclusion and Future directions

In conclusion, studies included in this thesis have demonstrated a regulatory circuitry among *Dlx1/Dlx2* and *Brn3a/Brn3b* during mouse retinal development. By binding directly to the promoter regions, both DLX1 and DLX2 regulate *Brn3b* expression, whereas only DLX2 regulates *Brn3a* expression during retinogenesis. BRN3b transiently represses Dlx2 expression in the E13.5 retina. *Dlx1/Dlx2* and *Brn3b* play a combinatorial role in retinal development and optic nerve pathfinding. Loss of *Dlx1/Dlx2* and *Brn3b* function results in massive RGC loss and severe retinal axonal projection defects at the optic chiasm. A probable retinal progenitor cell fate switch occurs in the *Dlx1/Dlx2/Brn3b* triple null retinas, with increased cholinergic amacrine cells differentiation, which are dislocated into the GCL. *Brn3a* is a downstream target of both DLX2 and BRN3b. No combinatorial role is identified between *Dlx1/Dlx2* and *Brn3a* during embryonic retinal development. Finally, we initiated a study of miRNA-124 expression in the developing and mature retina. DLX2 and miRNA-124 are co-expressed in the mouse retina throughout the embryonic and adult periods. A possible regulatory loop exists between DLX2 and miRNA-124. Further investigation is required to elucidate this mechanism.

Retinogenesis is a complex process, which involves different regulatory factors on many different levels, such as transcriptional and post-transcriptional regulation.

Previous research has revealed many “master” retinal regulator genes, such as *Pax6*, *Rx*, and *Math5*. Some of them are responsible for early eye initiation, and some for specifying certain retinal cell types. However, retinal development will never be explained by a simple “one gene to one cell type” level of regulation. An integrated view of all the regulators is the final goal of all developmental biology research. Elegant studies showed that CHX10 regulates the transcription of the miRNA183 cluster, which in turn represses *Mitf* by post-transcriptional modulation (Xu 2009). This is an excellent example for a model of regulatory integration. It is of interest to determine a global regulatory network controlling the retinal development. Such work will contribute greatly to our understanding of retinogenesis, and eventually the pathogenesis of developmental ocular diseases.

References

Akagi, T., T. Inoue, et al. (2004). "Requirement of multiple basic helix-loop-helix genes for retinal neuronal subtype specification." J Biol Chem **279**(27): 28492-28498.

Anderson, S., M. Mione, et al. (1999). "Differential origins of neocortical projection and local circuit neurons: role of Dlx genes in neocortical interneuronogenesis." Cereb Cortex **9**(6): 646-654.

Anderson, S. A., D. D. Eisenstat, et al. (1997). "Interneuron migration from basal forebrain to neocortex: dependence on Dlx genes." Science **278**(5337): 474-476.

Anderson, S. A., M. Qiu, et al. (1997). "Mutations of the homeobox genes Dlx-1 and Dlx-2 disrupt the striatal subventricular zone and differentiation of late born striatal neurons." Neuron **19**(1): 27-37.

Badea, T. C., H. Cahill, et al. (2009). "Distinct roles of transcription factors brn3a and brn3b in controlling the development, morphology, and function of retinal ganglion cells." Neuron **61**(6): 852-864.

Bailey, T. J., H. El-Hodiri, et al. (2004). "Regulation of vertebrate eye development by Rx genes." Int J Dev Biol **48**(8-9): 761-770.

Barbieri, A. M., V. Broccoli, et al. (2002). "Vax2 inactivation in mouse determines alteration of the eye dorsal-ventral axis, misrouting of the optic fibres and eye coloboma." Development **129**(3): 805-813.

Barbieri, A. M., G. Lupo, et al. (1999). "A homeobox gene, vax2, controls the patterning of the eye dorsoventral axis." Proc Natl Acad Sci U S A **96**(19): 10729-10734.

Barnstable, C. J., R. Hofstein, et al. (1985). "A marker of early amacrine cell development in rat retina." Brain Res **352**(2): 286-290.

Bartel, D. P. (2009). "MicroRNAs: target recognition and regulatory functions." Cell **136**(2): 215-233.

Belecky-Adams, T., S. Tomarev, et al. (1997). "Pax-6, Prox 1, and Chx10 homeobox gene expression correlates with phenotypic fate of retinal precursor cells." Invest Ophthalmol Vis Sci **38**(7): 1293-1303.

Bertrand, N., D. S. Castro, et al. (2002). "Proneural genes and the specification of neural cell types." Nat Rev Neurosci **3**(7): 517-530.

Bertuzzi, S., R. Hindges, et al. (1999). "The homeodomain protein vax1 is required for axon guidance and major tract formation in the developing forebrain." Genes Dev **13**(23): 3092-3105.

Birgbauer, E., C. A. Cowan, et al. (2000). "Kinase independent function of EphB receptors in retinal axon pathfinding to the optic disc from dorsal but not ventral retina." Development **127**(6): 1231-1241.

Boije, H., P. H. Edqvist, et al. (2009). "Horizontal cell progenitors arrest in G2-phase and undergo terminal mitosis on the vitreal side of the chick retina." Dev Biol **330**(1): 105-113.

Brittis, P. A., D. R. Canning, et al. (1992). "Chondroitin sulfate as a regulator of neuronal patterning in the retina." Science **255**(5045): 733-736.

Brittis, P. A., V. Lemmon, et al. (1995). "Unique changes of ganglion cell growth cone behavior following cell adhesion molecule perturbations: a time-lapse study of the living retina." Mol Cell Neurosci **6**(5): 433-449.

Brown, N. L., S. Kanekar, et al. (1998). "Math5 encodes a murine basic helix-loop-helix transcription factor expressed during early stages of retinal neurogenesis." Development **125**(23): 4821-4833.

Brown, N. L., S. Patel, et al. (2001). "Math5 is required for retinal ganglion cell and optic nerve formation." Development **128**(13): 2497-2508.

Bulfone, A., F. Wang, et al. (1998). "An olfactory sensory map develops in the absence of normal projection neurons or GABAergic interneurons." Neuron **21**(6): 1273-1282.

Burmeister, M., J. Novak, et al. (1996). "Ocular retardation mouse caused by Chx10 homeobox null allele: impaired retinal progenitor proliferation and bipolar cell

differentiation." Nat Genet **12**(4): 376-384.

Cai, Z., G. S. Feng, et al. (2010). "Temporal requirement of the protein tyrosine phosphatase Shp2 in establishing the neuronal fate in early retinal development." J Neurosci **30**(11): 4110-4119.

Carthew, R. W. and E. J. Sontheimer (2009). "Origins and Mechanisms of miRNAs and siRNAs." Cell **136**(4): 642-655.

Cepko, C. L. (1999). "The roles of intrinsic and extrinsic cues and bHLH genes in the determination of retinal cell fates." Curr Opin Neurobiol **9**(1): 37-46.

Cheng, L. C., E. Pastrana, et al. (2009). "miR-124 regulates adult neurogenesis in the subventricular zone stem cell niche." Nat Neurosci **12**(4): 399-408.

Chow, R. L., C. R. Altmann, et al. (1999). "Pax6 induces ectopic eyes in a vertebrate." Development **126**(19): 4213-4222.

Chow, R. L., B. Snow, et al. (2001). "Vsx1, a rapidly evolving paired-like homeobox gene expressed in cone bipolar cells." Mech Dev **109**(2): 315-322.

Chow, R. L., B. Volgyi, et al. (2004). "Control of late off-center cone bipolar cell differentiation and visual signaling by the homeobox gene Vsx1." Proc Natl Acad Sci U S A **101**(6): 1754-1759.

Clandinin, T. R. and D. A. Feldheim (2009). "Making a visual map: mechanisms and molecules." Curr Opin Neurobiol **19**(2): 174-180.

Clark, A. M., S. Yun, et al. (2008). "Negative regulation of Vsx1 by its paralog Chx10/Vsx2 is conserved in the vertebrate retina." Brain Res **1192**: 99-113.

Cobos, I., U. Borello, et al. (2007). "Dlx transcription factors promote migration through repression of axon and dendrite growth." Neuron **54**(6): 873-888.

Cobos, I., M. E. Calcagnotto, et al. (2005). "Mice lacking Dlx1 show subtype-specific loss of interneurons, reduced inhibition and epilepsy." Nat Neurosci **8**(8): 1059-1068.

Cobrinik, D., R. O. Francis, et al. (2006). "Rb induces a proliferative arrest and curtails Brn-2 expression in retinoblastoma cells." Mol Cancer **5**: 72.

Colasante, G., P. Collombat, et al. (2008). "Arx is a direct target of Dlx2 and thereby contributes to the tangential migration of GABAergic interneurons." J Neurosci **28**(42): 10674-10686.

Damiani, D., J. J. Alexander, et al. (2008). "Dicer inactivation leads to progressive functional and structural degeneration of the mouse retina." J Neurosci **28**(19): 4878-4887.

de Melo, J., G. Du, et al. (2005). "Dlx1 and Dlx2 function is necessary for terminal differentiation and survival of late-born retinal ganglion cells in the developing mouse retina." Development **132**(2): 311-322.

de Melo, J., X. Qiu, et al. (2003). "Dlx1, Dlx2, Pax6, Brn3b, and Chx10 homeobox gene expression defines the retinal ganglion and inner nuclear layers of the developing and adult mouse retina." J Comp Neurol **461**(2): 187-204.

de Melo, J., Q. P. Zhou, et al. (2008). "Dlx2 homeobox gene transcriptional regulation of Trkb neurotrophin receptor expression during mouse retinal development." Nucleic Acids Res **36**(3): 872-884.

Decembrini, S., D. Bressan, et al. (2009). "MicroRNAs couple cell fate and developmental timing in retina." Proc Natl Acad Sci U S A **106**(50): 21179-21184.

Depew, M. J., C. A. Simpson, et al. (2005). "Reassessing the Dlx code: the genetic regulation of branchial arch skeletal pattern and development." J Anat **207**(5): 501-561.

Diamond, E., M. Amen, et al. (2006). "Functional interactions between Dlx2 and lymphoid enhancer factor regulate Msx2." Nucleic Acids Res **34**(20): 5951-5965.

Dorval, K. M., B. P. Bobechko, et al. (2005). "Transcriptional activity of the paired-like homeodomain proteins CHX10 and VSX1." J Biol Chem **280**(11): 10100-10108.

Dunlop, S. A. (1990). "Early development of retinal ganglion cell dendrites in the marsupial Setonix brachyurus, quokka." J Comp Neurol **293**(3): 425-447.

Dyer, M. A. and C. L. Cepko (2001). "p27Kip1 and p57Kip2 regulate proliferation in distinct retinal progenitor cell populations." J Neurosci **21**(12): 4259-4271.

Dyer, M. A., F. J. Livesey, et al. (2003). "Prox1 function controls progenitor cell proliferation and horizontal cell genesis in the mammalian retina." Nat Genet **34**(1): 53-58.

Edqvist, P. H. and F. Hallbook (2004). "Newborn horizontal cells migrate bi-directionally across the neuroepithelium during retinal development." Development **131**(6): 1343-1351.

Eisenstat, D. D., J. K. Liu, et al. (1999). "DLX-1, DLX-2, and DLX-5 expression define distinct stages of basal forebrain differentiation." J Comp Neurol **414**(2): 217-237.

Elshatory, Y., M. Deng, et al. (2007). "Expression of the LIM-homeodomain protein Isl1 in the developing and mature mouse retina." J Comp Neurol **503**(1): 182-197.

Erkman, L., R. J. McEvilly, et al. (1996). "Role of transcription factors Brn-3.1 and Brn-3.2 in auditory and visual system development." Nature **381**(6583): 603-606.

Erkman, L., P. A. Yates, et al. (2000). "A POU domain transcription factor-dependent program regulates axon pathfinding in the vertebrate visual system." Neuron **28**(3): 779-792.

Fabre, P. J., T. Shimogori, et al. (2010). "Segregation of ipsilateral retinal ganglion cell axons at the optic chiasm requires the Shh receptor Boc." J Neurosci **30**(1): 266-275.

Fazeli, A., S. L. Dickinson, et al. (1997). "Phenotype of mice lacking functional Deleted in colorectal cancer (Dcc) gene." Nature **386**(6627): 796-804.

Feldheim, D. A., P. Vanderhaeghen, et al. (1998). "Topographic guidance labels in a sensory projection to the forebrain." Neuron **21**(6): 1303-1313.

Feng, L., Z. H. Xie, et al. (2010). "MATH5 controls the acquisition of multiple retinal cell fates." Mol Brain **3**: 36.

Ferda Percin, E., L. A. Ploder, et al. (2000). "Human microphthalmia associated with mutations in the retinal homeobox gene CHX10." Nat Genet **25**(4): 397-401.

Fode, C., Q. Ma, et al. (2000). "A role for neural determination genes in specifying the dorsoventral identity of telencephalic neurons." Genes Dev **14**(1): 67-80.

Friedman, R. C., K. K. Farh, et al. (2009). "Most mammalian mRNAs are conserved targets of microRNAs." Genome Res **19**(1): 92-105.

Frisen, J., P. A. Yates, et al. (1998). "Ephrin-A5 (AL-1/RAGS) is essential for proper retinal axon guidance and topographic mapping in the mammalian visual system." Neuron **20**(2): 235-243.

Fuhrmann, S. (2010). "Eye morphogenesis and patterning of the optic vesicle." Curr Top Dev Biol **93**: 61-84.

Fujitani, Y., S. Fujitani, et al. (2006). "Ptf1a determines horizontal and amacrine cell fates during mouse retinal development." Development **133**(22): 4439-4450.

Furukawa, T., E. M. Morrow, et al. (1997). "Crx, a novel otx-like homeobox gene, shows photoreceptor-specific expression and regulates photoreceptor differentiation." Cell **91**(4): 531-541.

Furukawa, T., E. M. Morrow, et al. (1999). "Retinopathy and attenuated circadian entrainment in Crx-deficient mice." Nat Genet **23**(4): 466-470.

Gan, L., S. W. Wang, et al. (1999). "POU domain factor Brn-3b is essential for retinal ganglion cell differentiation and survival but not for initial cell fate specification." Dev Biol **210**(2): 469-480.

Gan, L., M. Xiang, et al. (1996). "POU domain factor Brn-3b is required for the development of a large set of retinal ganglion cells." Proc Natl Acad Sci U S A **93**(9): 3920-3925.

Garcia-Frigola, C., M. I. Carreres, et al. (2008). "Zic2 promotes axonal divergence at

the optic chiasm midline by EphB1-dependent and -independent mechanisms." Development **135**(10): 1833-1841.

Garelli, A., N. P. Rotstein, et al. (2006). "Docosahexaenoic acid promotes photoreceptor differentiation without altering Crx expression." Invest Ophthalmol Vis Sci **47**(7): 3017-3027.

Gehring, W. J. and K. Ikeo (1999). "Pax 6: mastering eye morphogenesis and eye evolution." Trends Genet **15**(9): 371-377.

Ghanem, N., O. Jarinova, et al. (2003). "Regulatory roles of conserved intergenic domains in vertebrate Dlx bigene clusters." Genome Res **13**(4): 533-543.

Ghanem, N., M. Yu, et al. (2007). "Distinct cis-regulatory elements from the Dlx1/Dlx2 locus mark different progenitor cell populations in the ganglionic eminences and different subtypes of adult cortical interneurons." J Neurosci **27**(19): 5012-5022.

Godement, P., J. Salaun, et al. (1984). "Prenatal and postnatal development of retinogeniculate and retinocollicular projections in the mouse." J Comp Neurol **230**(4): 552-575.

Godinho, L., J. S. Mumm, et al. (2005). "Targeting of amacrine cell neurites to appropriate synaptic laminae in the developing zebrafish retina." Development **132**(22): 5069-5079.

Goldberg, J. L., M. E. Vargas, et al. (2004). "An oligodendrocyte lineage-specific semaphorin, Sema5A, inhibits axon growth by retinal ganglion cells." J Neurosci **24**(21): 4989-4999.

Green, E. S., J. L. Stubbs, et al. (2003). "Genetic rescue of cell number in a mouse model of microphthalmia: interactions between Chx10 and G1-phase cell cycle regulators." Development **130**(3): 539-552.

Greither, T., L. F. Grochola, et al. (2010). "Elevated expression of microRNAs 155, 203, 210 and 222 in pancreatic tumors is associated with poorer survival." Int J Cancer **126**(1): 73-80.

Hallonet, M., T. Hollemann, et al. (1999). "Vax1, a novel homeobox-containing gene,

directs development of the basal forebrain and visual system." Genes Dev **13**(23): 3106-3114.

Hallonet, M., T. Hollemann, et al. (1998). "Vax1 is a novel homeobox-containing gene expressed in the developing anterior ventral forebrain." Development **125**(14): 2599-2610.

Hamilton, S. P., J. M. Woo, et al. (2005). "Analysis of four DLX homeobox genes in autistic probands." BMC Genet **6**: 52.

Harada, T., C. Harada, et al. (2007). "Molecular regulation of visual system development: more than meets the eye." Genes Dev **21**(4): 367-378.

Hatakeyama, J. and R. Kageyama (2004). "Retinal cell fate determination and bHLH factors." Semin Cell Dev Biol **15**(1): 83-89.

Hatakeyama, J., K. Tomita, et al. (2001). "Roles of homeobox and bHLH genes in specification of a retinal cell type." Development **128**(8): 1313-1322.

Hennig, A. K., G. H. Peng, et al. (2008). "Regulation of photoreceptor gene expression by Crx-associated transcription factor network." Brain Res **1192**: 114-133.

Herrera, E., R. Marcus, et al. (2004). "Foxd1 is required for proper formation of the optic chiasm." Development **131**(22): 5727-5739.

Hill, R. E., J. Favor, et al. (1991). "Mouse small eye results from mutations in a paired-like homeobox-containing gene." Nature **354**(6354): 522-525.

Hindges, R., T. McLaughlin, et al. (2002). "EphB forward signaling controls directional branch extension and arborization required for dorsal-ventral retinotopic mapping." Neuron **35**(3): 475-487.

Horsford, D. J., M. T. Nguyen, et al. (2005). "Chx10 repression of Mitf is required for the maintenance of mammalian neuroretinal identity." Development **132**(1): 177-187.

Inoue, T., M. Hojo, et al. (2002). "Math3 and NeuroD regulate amacrine cell fate

specification in the retina." Development **129**(4): 831-842.

Jeong, J., X. Li, et al. (2008). "Dlx genes pattern mammalian jaw primordium by regulating both lower jaw-specific and upper jaw-specific genetic programs." Development **135**(17): 2905-2916.

Johnston, R. J., Jr., S. Chang, et al. (2005). "MicroRNAs acting in a double-negative feedback loop to control a neuronal cell fate decision." Proc Natl Acad Sci U S A **102**(35): 12449-12454.

Karali, M., I. Peluso, et al. (2007). "Identification and characterization of microRNAs expressed in the mouse eye." Invest Ophthalmol Vis Sci **48**(2): 509-515.

Kim, J., H. H. Wu, et al. (2005). "GDF11 controls the timing of progenitor cell competence in developing retina." Science **308**(5730): 1927-1930.

Kim, J. W. and G. Lemke (2006). "Hedgehog-regulated localization of Vax2 controls eye development." Genes Dev **20**(20): 2833-2847.

Lagos-Quintana, M., R. Rauhut, et al. (2002). "Identification of tissue-specific microRNAs from mouse." Curr Biol **12**(9): 735-739.

Landgraf, P., M. Rusu, et al. (2007). "A mammalian microRNA expression atlas based on small RNA library sequencing." Cell **129**(7): 1401-1414.

Langevin, L. M., P. Mattar, et al. (2007). "Validating in utero electroporation for the rapid analysis of gene regulatory elements in the murine telencephalon." Dev Dyn **236**(5): 1273-1286.

Le, T. N., G. Du, et al. (2007). "Dlx homeobox genes promote cortical interneuron migration from the basal forebrain by direct repression of the semaphorin receptor neuropilin-2." J Biol Chem **282**(26): 19071-19081.

Le, T. T., E. Wroblewski, et al. (2006). "Math5 is required for both early retinal neuron differentiation and cell cycle progression." Dev Biol **295**(2): 764-778.

Levine, E. M. and E. S. Green (2004). "Cell-intrinsic regulators of proliferation in vertebrate retinal progenitors." Semin Cell Dev Biol **15**(1): 63-74.

Levine, E. M., P. F. Hitchcock, et al. (1994). "Restricted expression of a new paired-class homeobox gene in normal and regenerating adult goldfish retina." J Comp Neurol **348**(4): 596-606.

Li, S., Z. Mo, et al. (2004). "Foxn4 controls the genesis of amacrine and horizontal cells by retinal progenitors." Neuron **43**(6): 795-807.

Lim, L. P., N. C. Lau, et al. (2005). "Microarray analysis shows that some microRNAs downregulate large numbers of target mRNAs." Nature **433**(7027): 769-773.

Liu, H., P. Etter, et al. (2008). "NeuroD1 regulates expression of thyroid hormone receptor 2 and cone opsins in the developing mouse retina." J Neurosci **28**(3): 749-756.

Liu, I. S., J. D. Chen, et al. (1994). "Developmental expression of a novel murine homeobox gene (Chx10): evidence for roles in determination of the neuroretina and inner nuclear layer." Neuron **13**(2): 377-393.

Liu, W., S. L. Khare, et al. (2000). "All Brn3 genes can promote retinal ganglion cell differentiation in the chick." Development **127**(15): 3237-3247.

Liu, W., Z. Mo, et al. (2001). "The Ath5 proneural genes function upstream of Brn3 POU domain transcription factor genes to promote retinal ganglion cell development." Proc Natl Acad Sci U S A **98**(4): 1649-1654.

Livesey, F. J. and C. L. Cepko (2001). "Vertebrate neural cell-fate determination: lessons from the retina." Nat Rev Neurosci **2**(2): 109-118.

Livne-Bar, I., M. Pacal, et al. (2006). "Chx10 is required to block photoreceptor differentiation but is dispensable for progenitor proliferation in the postnatal retina." Proc Natl Acad Sci U S A **103**(13): 4988-4993.

Long, J. E., I. Cobos, et al. (2009). "Dlx1&2 and Mash1 transcription factors control MGE and CGE patterning and differentiation through parallel and overlapping pathways." Cereb Cortex **19 Suppl 1**: i96-106.

Long, J. E., S. Garel, et al. (2007). "Dlx-dependent and -independent regulation of olfactory bulb interneuron differentiation." J Neurosci **27**(12): 3230-3243.

Long, J. E., C. Swan, et al. (2009). "Dlx1&2 and Mash1 transcription factors control striatal patterning and differentiation through parallel and overlapping pathways." J Comp Neurol **512**(4): 556-572.

Loosli, F., W. Staub, et al. (2003). "Loss of eyes in zebrafish caused by mutation of chokh/rx3." EMBO Rep **4**(9): 894-899.

Ma, W., R. T. Yan, et al. (2004). "bHLH genes cath5 and cNSCL1 promote bFGF-stimulated RPE cells to transdifferentiate toward retinal ganglion cells." Dev Biol **265**(2): 320-328.

Ma, W., R. T. Yan, et al. (2004). "A role of ath5 in inducing neuroD and the photoreceptor pathway." J Neurosci **24**(32): 7150-7158.

MacNeil, M. A. and R. H. Masland (1998). "Extreme diversity among amacrine cells: implications for function." Neuron **20**(5): 971-982.

Manuel, M., T. Pratt, et al. (2008). "Overexpression of Pax6 results in microphthalmia, retinal dysplasia and defective retinal ganglion cell axon guidance." BMC Dev Biol **8**: 59.

Mao, C. A., T. Kiyama, et al. (2008). "Eomesodermin, a target gene of Pou4f2, is required for retinal ganglion cell and optic nerve development in the mouse." Development **135**(2): 271-280.

Mao, C. A., S. W. Wang, et al. (2008). "Rewiring the retinal ganglion cell gene regulatory network: Neurod1 promotes retinal ganglion cell fate in the absence of Math5." Development **135**(20): 3379-3388.

Marquardt, T., R. Ashery-Padan, et al. (2001). "Pax6 is required for the multipotent state of retinal progenitor cells." Cell **105**(1): 43-55.

Marquardt, T. and P. Gruss (2002). "Generating neuronal diversity in the retina: one for nearly all." Trends Neurosci **25**(1): 32-38.

Masland, R. H. (2001). "The fundamental plan of the retina." Nat Neurosci **4**(9): 877-886.

Mathers, P. H., A. Grinberg, et al. (1997). "The Rx homeobox gene is essential for vertebrate eye development." Nature **387**(6633): 603-607.

Mattar, P., L. M. Langevin, et al. (2008). "Basic helix-loop-helix transcription factors cooperate to specify a cortical projection neuron identity." Mol Cell Biol **28**(5): 1456-1469.

McLoon, S. C. and R. B. Barnes (1989). "Early differentiation of retinal ganglion cells: an axonal protein expressed by premigratory and migrating retinal ganglion cells." J Neurosci **9**(4): 1424-1432.

Milam, A. H., D. M. Dacey, et al. (1993). "Recoverin immunoreactivity in mammalian cone bipolar cells." Vis Neurosci **10**(1): 1-12.

Morcillo, J., J. R. Martinez-Morales, et al. (2006). "Proper patterning of the optic fissure requires the sequential activity of BMP7 and SHH." Development **133**(16): 3179-3190.

Morrow, E. M., T. Furukawa, et al. (1999). "NeuroD regulates multiple functions in the developing neural retina in rodent." Development **126**(1): 23-36.

Moshiri, A., E. Gonzalez, et al. (2008). "Near complete loss of retinal ganglion cells in the math5/brn3b double knockout elicits severe reductions of other cell types during retinal development." Dev Biol **316**(2): 214-227.

Mu, X., X. Fu, et al. (2008). "Gene regulation logic in retinal ganglion cell development: Isl1 defines a critical branch distinct from but overlapping with Pou4f2." Proc Natl Acad Sci U S A **105**(19): 6942-6947.

Mu, X., X. Fu, et al. (2005). "A gene network downstream of transcription factor Math5 regulates retinal progenitor cell competence and ganglion cell fate." Dev Biol **280**(2): 467-481.

Mu, X., X. Fu, et al. (2005). "Ganglion cells are required for normal progenitor- cell proliferation but not cell-fate determination or patterning in the developing mouse retina." Curr Biol **15**(6): 525-530.

Mui, S. H., R. Hindges, et al. (2002). "The homeodomain protein Vax2 patterns the dorsoventral and nasotemporal axes of the eye." Development **129**(3):

797-804.

Mui, S. H., J. W. Kim, et al. (2005). "Vax genes ventralize the embryonic eye." Genes Dev **19**(10): 1249-1259.

Nelson, S. M., L. Park, et al. (2009). "Retinal homeobox 1 is required for retinal neurogenesis and photoreceptor differentiation in embryonic zebrafish." Dev Biol **328**(1): 24-39.

Nguyen, M. and H. Arnheiter (2000). "Signaling and transcriptional regulation in early mammalian eye development: a link between FGF and MITF." Development **127**(16): 3581-3591.

Nishida, A., A. Furukawa, et al. (2003). "Otx2 homeobox gene controls retinal photoreceptor cell fate and pineal gland development." Nat Neurosci **6**(12): 1255-1263.

Ochocinska, M. J. and P. F. Hitchcock (2009). "NeuroD regulates proliferation of photoreceptor progenitors in the retina of the zebrafish." Mech Dev **126**(3-4): 128-141.

Oliver, G., B. Sosa-Pineda, et al. (1993). "Prox 1, a prospero-related homeobox gene expressed during mouse development." Mech Dev **44**(1): 3-16.

Oron-Karni, V., C. Farhy, et al. (2008). "Dual requirement for Pax6 in retinal progenitor cells." Development **135**(24): 4037-4047.

Oster, S. F., M. O. Bodeker, et al. (2003). "Invariant Sema5A inhibition serves an ensheathing function during optic nerve development." Development **130**(4): 775-784.

Pak, W., R. Hindges, et al. (2004). "Magnitude of binocular vision controlled by islet-2 repression of a genetic program that specifies laterality of retinal axon pathfinding." Cell **119**(4): 567-578.

Pan, L., M. Deng, et al. (2008). "ISL1 and BRN3B co-regulate the differentiation of murine retinal ganglion cells." Development **135**(11): 1981-1990.

Pan, L., Z. Yang, et al. (2005). "Functional equivalence of Brn3 POU-domain transcription factors in mouse retinal neurogenesis." Development **132**(4): 703-712.

Pan, Y., R. I. Martinez-De Luna, et al. (2010). "Regulation of photoreceptor gene expression by the retinal homeobox (Rx) gene product." Dev Biol **339**(2): 494-506.

Panganiban, G. and J. L. Rubenstein (2002). "Developmental functions of the Distal-less/Dlx homeobox genes." Development **129**(19): 4371-4386.

Peng, G. H. and S. Chen (2005). "Chromatin immunoprecipitation identifies photoreceptor transcription factor targets in mouse models of retinal degeneration: new findings and challenges." Vis Neurosci **22**(5): 575-586.

Pennesi, M. E., J. H. Cho, et al. (2003). "BETA2/NeuroD1 null mice: a new model for transcription factor-dependent photoreceptor degeneration." J Neurosci **23**(2): 453-461.

Petros, T. J., B. R. Shrestha, et al. (2009). "Specificity and sufficiency of EphB1 in driving the ipsilateral retinal projection." J Neurosci **29**(11): 3463-3474.

Petryniak, M. A., G. B. Potter, et al. (2007). "Dlx1 and Dlx2 control neuronal versus oligodendroglial cell fate acquisition in the developing forebrain." Neuron **55**(3): 417-433.

Phillips, K. and B. Luisi (2000). "The virtuoso of versatility: POU proteins that flex to fit." J Mol Biol **302**(5): 1023-1039.

Pleasure, S. J., S. Anderson, et al. (2000). "Cell migration from the ganglionic eminences is required for the development of hippocampal GABAergic interneurons." Neuron **28**(3): 727-740.

Plump, A. S., L. Erskine, et al. (2002). "Slit1 and Slit2 cooperate to prevent premature midline crossing of retinal axons in the mouse visual system." Neuron **33**(2): 219-232.

Poche, R. A., K. M. Kwan, et al. (2007). "Lim1 is essential for the correct laminar positioning of retinal horizontal cells." J Neurosci **27**(51): 14099-14107.

Poitras, L., N. Ghanem, et al. (2007). "The proneural determinant MASH1 regulates forebrain Dlx1/2 expression through the I12b intergenic enhancer." Development **134**(9): 1755-1765.

Powell, L. M. and A. P. Jarman (2008). "Context dependence of proneural bHLH proteins." Curr Opin Genet Dev **18**(5): 411-417.

Punzo, C., S. Kurata, et al. (2001). "The eyeless homeodomain is dispensable for eye development in Drosophila." Genes Dev **15**(13): 1716-1723.

Purves, D. and S. M. Williams (2001). Neuroscience. Sunderland, Mass., Sinauer Associates.

Qiu, F., H. Jiang, et al. (2008). "A comprehensive negative regulatory program controlled by Brn3b to ensure ganglion cell specification from multipotential retinal precursors." J Neurosci **28**(13): 3392-3403.

Qiu, M., A. Bulfone, et al. (1997). "Role of the Dlx homeobox genes in proximodistal patterning of the branchial arches: mutations of Dlx-1, Dlx-2, and Dlx-1 and -2 alter morphogenesis of proximal skeletal and soft tissue structures derived from the first and second arches." Dev Biol **185**(2): 165-184.

Quina, L. A., W. Pak, et al. (2005). "Brn3a-expressing retinal ganglion cells project specifically to thalamocortical and collicular visual pathways." J Neurosci **25**(50): 11595-11604.

Quiring, R., U. Walldorf, et al. (1994). "Homology of the eyeless gene of Drosophila to the Small eye gene in mice and Aniridia in humans." Science **265**(5173): 785-789.

Rasband, K., M. Hardy, et al. (2003). "Generating X: formation of the optic chiasm." Neuron **39**(6): 885-888.

Reese, B. E. (2011). "Development of the retina and optic pathway." Vision Res **51**(7): 613-632.

Rowan, S. and C. L. Cepko (2004). "Genetic analysis of the homeodomain transcription factor Chx10 in the retina using a novel multifunctional BAC transgenic mouse reporter." Dev Biol **271**(2): 388-402.

Rowan, S., C. M. Chen, et al. (2004). "Transdifferentiation of the retina into pigmented cells in ocular retardation mice defines a new function of the homeodomain gene Chx10." Development **131**(20): 5139-5152.

Samee, N., V. Geoffroy, et al. (2008). "Dlx5, a positive regulator of osteoblastogenesis, is essential for osteoblast-osteoclast coupling." Am J Pathol **173**(3): 773-780.

Schulte, D., T. Furukawa, et al. (1999). "Misexpression of the Emx-related homeobox genes cVax and mVax2 ventralizes the retina and perturbs the retinotectal map." Neuron **24**(3): 541-553.

Schwarz, M., F. Cecconi, et al. (2000). "Spatial specification of mammalian eye territories by reciprocal transcriptional repression of Pax2 and Pax6." Development **127**(20): 4325-4334.

Serafini, T., S. A. Colamarino, et al. (1996). "Netrin-1 is required for commissural axon guidance in the developing vertebrate nervous system." Cell **87**(6): 1001-1014.

Shirasaki, R. and S. L. Pfaff (2002). "Transcriptional codes and the control of neuronal identity." Annu Rev Neurosci **25**: 251-281.

Spira, A., S. Hudy, et al. (1984). "Ectopic photoreceptor cells and cell death in the developing rat retina." Anat Embryol (Berl) **169**(3): 293-301.

Sung, C. H. and J. Z. Chuang (2010). "The cell biology of vision." J Cell Biol **190**(6): 953-963.

Swaroop, A., D. Kim, et al. (2010). "Transcriptional regulation of photoreceptor development and homeostasis in the mammalian retina." Nat Rev Neurosci **11**(8): 563-576.

Szafranska, A. E., T. S. Davison, et al. (2007). "MicroRNA expression alterations are linked to tumorigenesis and non-neoplastic processes in pancreatic ductal adenocarcinoma." Oncogene **26**(30): 4442-4452.

Thompson, H., D. Barker, et al. (2006). "Slits contribute to the guidance of retinal ganglion cell axons in the mammalian optic tract." Dev Biol **296**(2): 476-484.

Tomita, K., M. Ishibashi, et al. (1996). "Mammalian hairy and Enhancer of split homolog 1 regulates differentiation of retinal neurons and is essential for eye morphogenesis." Neuron **16**(4): 723-734.

Torres, M., E. Gomez-Pardo, et al. (1996). "Pax2 contributes to inner ear patterning and optic nerve trajectory." Development **122**(11): 3381-3391.

Trieu, M., A. Ma, et al. (2003). "Direct autoregulation and gene dosage compensation by POU-domain transcription factor Brn3a." Development **130**(1): 111-121.

Trimarchi, J. M., M. B. Stadler, et al. (2008). "Individual retinal progenitor cells display extensive heterogeneity of gene expression." PLoS ONE **3**(2): e1588.

Trousse, F., E. Marti, et al. (2001). "Control of retinal ganglion cell axon growth: a new role for Sonic hedgehog." Development **128**(20): 3927-3936.

Turner, E. E. (1996). "Similar DNA recognition properties of alternatively spliced Drosophila POU factors." Proc Natl Acad Sci U S A **93**(26): 15097-15101.

Vetter, M. L. and N. L. Brown (2001). "The role of basic helix-loop-helix genes in vertebrate retinogenesis." Semin Cell Dev Biol **12**(6): 491-498.

Voinescu, P. E., J. N. Kay, et al. (2009). "Birthdays of retinal amacrine cell subtypes are systematically related to their molecular identity and soma position." J Comp Neurol **517**(5): 737-750.

Voronina, V. A., E. A. Kozhemyakina, et al. (2004). "Mutations in the human RAX homeobox gene in a patient with anophthalmia and sclerocornea." Hum Mol Genet **13**(3): 315-322.

Wagner, K. D., N. Wagner, et al. (2003). "The Wilms' tumor suppressor Wt1 encodes a transcriptional activator of the class IV POU-domain factor Pou4f2 (Brn-3b)." Gene **305**(2): 217-223.

Walker, J. C. and R. M. Harland (2009). "microRNA-24a is required to repress apoptosis in the developing neural retina." Genes Dev **23**(9): 1046-1051.

Wang, S. W., B. S. Kim, et al. (2001). "Requirement for math5 in the development of

retinal ganglion cells." Genes Dev **15**(1): 24-29.

Wang, Y., G. D. Dakubo, et al. (2005). "Retinal ganglion cell-derived sonic hedgehog locally controls proliferation and the timing of RGC development in the embryonic mouse retina." Development **132**(22): 5103-5113.

Wienholds, E., W. P. Kloosterman, et al. (2005). "MicroRNA expression in zebrafish embryonic development." Science **309**(5732): 310-311.

Wigle, J. T., K. Chowdhury, et al. (1999). "Prox1 function is crucial for mouse lens-fibre elongation." Nat Genet **21**(3): 318-322.

Wigle, J. T. and D. D. Eisenstat (2008). "Homeobox genes in vertebrate forebrain development and disease." Clin Genet **73**(3): 212-226.

Williams, S. E., C. A. Mason, et al. (2004). "The optic chiasm as a midline choice point." Curr Opin Neurobiol **14**(1): 51-60.

Wilson, D. S., B. Guenther, et al. (1995). "High resolution crystal structure of a paired (Pax) class cooperative homeodomain dimer on DNA." Cell **82**(5): 709-719.

Xiang, M., L. Gan, et al. (1997). "Essential role of POU-domain factor Brn-3c in auditory and vestibular hair cell development." Proc Natl Acad Sci U S A **94**(17): 9445-9450.

Xiang, M., L. Gan, et al. (1996). "Targeted deletion of the mouse POU domain gene Brn-3a causes selective loss of neurons in the brainstem and trigeminal ganglion, uncoordinated limb movement, and impaired suckling." Proc Natl Acad Sci U S A **93**(21): 11950-11955.

Xiang, M., L. Zhou, et al. (1995). "The Brn-3 family of POU-domain factors: primary structure, binding specificity, and expression in subsets of retinal ganglion cells and somatosensory neurons." J Neurosci **15**(7 Pt 1): 4762-4785.

Xu, N., T. Papagiannakopoulos, et al. (2009). "MicroRNA-145 regulates OCT4, SOX2, and KLF4 and represses pluripotency in human embryonic stem cells." Cell **137**(4): 647-658.

Xu, S. (2009). "microRNA expression in the eyes and their significance in relation to functions." Prog Retin Eye Res **28**(2): 87-116.

Xu, S., P. D. Witmer, et al. (2007). "MicroRNA (miRNA) transcriptome of mouse retina and identification of a sensory organ-specific miRNA cluster." J Biol Chem **282**(34): 25053-25066.

Yan, R. T. and S. Z. Wang (1998). "neuroD induces photoreceptor cell overproduction in vivo and de novo generation in vitro." J Neurobiol **36**(4): 485-496.

Yan, R. T. and S. Z. Wang (2004). "Requirement of neuroD for photoreceptor formation in the chick retina." Invest Ophthalmol Vis Sci **45**(1): 48-58.

Yang, Z., K. Ding, et al. (2003). "Math5 determines the competence state of retinal ganglion cell progenitors." Dev Biol **264**(1): 240-254.

Yun, K., S. Fischman, et al. (2002). "Modulation of the notch signaling by Mash1 and Dlx1/2 regulates sequential specification and differentiation of progenitor cell types in the subcortical telencephalon." Development **129**(21): 5029-5040.

Yun, S., Y. Saijoh, et al. (2009). "Lhx2 links the intrinsic and extrinsic factors that control optic cup formation." Development **136**(23): 3895-3906.

Zerucha, T. and M. Ekker (2000). "Distal-less-related homeobox genes of vertebrates: evolution, function, and regulation." Biochem Cell Biol **78**(5): 593-601.

Zhang, L., P. H. Mathers, et al. (2000). "Function of Rx, but not Pax6, is essential for the formation of retinal progenitor cells in mice." Genesis **28**(3-4): 135-142.

Zhao, J. J., J. Yang, et al. (2009). "Identification of miRNAs associated with tumorigenesis of retinoblastoma by miRNA microarray analysis." Childs Nerv Syst **25**(1): 13-20.

Zhou, Q. P., T. N. Le, et al. (2004). "Identification of a direct Dlx homeodomain target in the developing mouse forebrain and retina by optimization of chromatin immunoprecipitation." Nucleic Acids Res **32**(3): 884-892.

Zuber, M. E., G. Gestri, et al. (2003). "Specification of the vertebrate eye by a network

of eye field transcription factors." Development **130**(21): 5155-5167.